RISK-AWARE CONTROL, DISPATCH AND COORDINATION IN SUSTAINABLE POWER SYSTEMS

ROBERT MIETH

2021

RISK-AWARE CONTROL, DISPATCH AND COORDINATION IN SUSTAINABLE POWER SYSTEMS

Vorglegt von Robert Mieth, MSc., geb. 3. Jan. 1991 in Dresden

der Fakultät IV - Elektrotechnik und Informatik der Technischen Universität Berlin zur Erlangung des akademischen Grades Doktor der Ingenieurwissenschaften (Dr.-Ing.).

Für Opa.
Der Dr. ist für mich, der Ing. ist für dich.

ABSTRACT

A timely transition towards a sustainable carbon-neutral power sector requires modern power systems to host increasing numbers of renewable energy sources (RES) and other non-traditional distributed energy sources (DER). However, the stochastic nature and limited controllability of these resources undermines the efficiency of current power system and market operations and creates new forms of physical and financial risks. Modern and future operational paradigms must internalize and mitigate these risks to ensure availability of sustainable electric power at a socially acceptable cost.

This dissertation proposes uncertainty- and risk-aware decision-making tools for transmission and distribution systems to account for RES and DER stochasticity. The proposed methods leverage mathematically and computationally advantageous properties of a chance-constrained optimal power flow formulation to internalize statistical uncertainty parameters and predefined risk levels into generator dispatch and reserve decisions. As a result, these decisions are immunized against uncertain RES and DER generation at minimal system cost, while avoiding a sub-optimal over- or underestimation of reserve requirements. Additionally, this dissertation explores data-driven and learning-based modifications of the proposed approaches to ensure robustness against estimation errors of uncertainty parameters.

Furthermore, this dissertation shows that convex properties of the proposed chance-constrained framework yield risk-aware price signals that enable an efficient stochastic electricity market design. Specifically, separate energy and reserve prices that capture the expected system state, its inherent uncertainty and the risk acceptance of its participants enable a fully *ex-ante* settlement of the market. The proposed chance-constrained market design overcomes typical shortcomings of scenario-based stochastic market designs related to computational tractability and per-scenario trade-offs and fulfills desirable market properties for all outcomes of the underlying uncertainty. Additionally, this dissertation demonstrates that the volatility of system state-variables can be controlled in this market via suitable variance metrics and how risk-averse behavior and asymmetric information among market participants can be modeled. The proposed market design and prices are analyzed for distribution (retail) and transmission (wholesale) markets.

ZUSAMMENFASSUNG

Die zeitnah notwendige Dekarbonisierung des Stromsektors erfordert signifikante Investitionen in erneuerbare Energieanlagen (EE) und in flexible, dezentrale Energieressourcen (DER). Das stochastische und nur eingeschränkt regelbare Einspeiseverhalten dieser Ressourcen beeinträchtigt jedoch die Wirksamkeit und Effizienz derzeitiger Methoden des Stromnetzbetriebes und des Stromhandels und schafft neue Formen physikalischer und finanzieller Risiken.

Diese Dissertation untersucht stochastische Optimierungsmodelle, die in der Gegenwart volatiler Einspisung von EE und DER einen sicheren und kostengünstigen Betrieb von Verteil- und Übertragungsnetzen gewährleisten. Die vorgeschlagenen Modelle und Lösungsmethoden nutzen dafür mathematisch und numerisch vorteilhafte Eigenschaften stochastischer Optimierung mit probabilistischen Nebenbedingungen (englisch *chance constraints*) aus, um statistische Parameter der EE und DER Einspeisung sowie explizite Risikobewertungen in Planungsentscheidungen über Generatoreinsatz und Reservevorhaltung einzubeziehen. Dadurch werden diese Entscheidungen zu minimalen zusätzlichen Systemkosten immunisiert, während eine suboptimale Über- oder Unterschätzung des Reservebedarfs vermieden wird. Weiterhin untersucht diese Dissertation datengestützte Modifikationen der entwickelten Optimierungsmodelle, um den Effekt eventueller Fehler bei der Schätzung statistischer Parameter abzuschwächen.

Die zunächst für einen risikobewussten Netzbetrieb entwickelten mathematischen Optimierungsprobleme sind konvex und erlauben daher eine markttheoretische Ableitung von Preissignalen zur Entwicklung eines praktikablen stochastischen Strommarktdesigns. Insbesondere kann gezeigt werden, dass separate Energie- und Reservepreise den erwarteten Systemzustand, statistische Informationen über unsichere Parameter und die Risikoakzeptanz der Markteilnehmer transparent abbilden. Dies ermöglicht eine planungssichere Beschaffung der notwendigen Erzeugungs- und Übertragungsresourcen und erhöht somit Versorgungssicherheit und -effizienz. Das vorgeschlagene Marktdesign mit *chance constraints* vermeidet typische Probleme szenariobasierter stochastischer Marktdesigns in Bezug auf Berechnungskomplexität und Transparenz. Die hergeleiteten Preissignale werden im Detail analytisch untersucht und die Erfüllung notwendiger ökonomischer Kriterien bewiesen. Zusätzlich zeigt diese Dissertation, dass die Volatilität bestimmter Systemvariablen durch geeignete Varianzmetriken kontrolliert werden kann und wie risikoaverses Verhalten sowie asymmetrische Informationen unter den Marktteilnehmern modelliert werden können.

The work and results presented in this cumulative dissertation are based on publications [P1]–[P5]. Some additional results, extensions or applications are published in [S1]–[S6].

In all first-authored publications [P1]–[P5] the author of this dissertation led the research effort and preparation of the manuscript. In all second-authored publications [S1]–[S6] the author of this dissertation contributed to the research effort and preparation of the manuscript. All co-authors have agreed that the material and results of these publications may be used in the preparation of this dissertation.[1] References to all primary publications [P1]–[P5] and auxiliary publications [S1]–[S6] are provided throughout the dissertation and are labeled [P#] and [S#], respectively

Publications central to this dissertation:

[P1] **R. Mieth** and Y. Dvorkin, «Data-driven distributionally robust optimal power flow for distribution systems,» *IEEE Control Systems Letters*, vol. 2, no. 3, pp. 363–368, 2018 (cit. on pp. vii, 8, 9, 14, 17, 19, 25, 31, 45, 51, 53, 63, 68, 90, 91, 115, 117, 177).

[P2] **R. Mieth** and Y. Dvorkin, «Online learning for network constrained demand response pricing in distribution systems,» *IEEE Transactions on Smart Grid*, vol. 11, no. 3, pp. 2563–2575, 2019 (cit. on pp. vii, 9, 14, 18, 19, 25, 45, 61, 90, 91, 103, 115, 133, 177).

[P3] **R. Mieth** and Y. Dvorkin, «Distribution electricity pricing under uncertainty,» *IEEE Transactions on Power Systems*, vol. 35, no. 3, pp. 2325–2338, 2019 (cit. on pp. vii, 9, 14, 19, 20, 22–25, 31, 45, 48, 89, 115–117, 129, 130, 132, 133, 177).

[P4] **R. Mieth**, J. Kim, and Y. Dvorkin, «Risk-and variance-aware electricity pricing,» *Electric Power Systems Research*, vol. 189, p. 106 804, 2020 (cit. on pp. vii, 9, 14, 20, 22, 23, 25, 31, 39, 41, 44, 90, 115, 129, 130, 132, 174, 177).

[P5] **R. Mieth**, M. Roveto, and Y. Dvorkin, «Risk Trading in a Chance-Constrained Stochastic Electricity Market,» *IEEE Control Systems Letters*, vol. 5, no. 1, pp. 199–204, 2021 (cit. on pp. vii, 8, 9, 14, 22, 24, 25, 129, 177).

1 The written agreements are available with the author upon request.

Auxiliary publications:

[S1] A. Hassan, **R. Mieth**, M. Chertkov, *et al.*, «Optimal load ensemble control in chance-constrained optimal power flow,» *IEEE Transactions on Smart Grid*, vol. 10, no. 5, pp. 5186–5195, 2018 (cit. on pp. vii, 19, 68, 90, 177).

[S2] A. Hassan, **R. Mieth**, D. Deka, *et al.*, «Stochastic and distributionally robust load ensemble control,» *IEEE Transactions on Power Systems*, 2020 (cit. on pp. vii, 19, 177).

[S3] R. Weinhold and **R. Mieth**, «Fast Security-Constrained Optimal Power Flow through Low-Impact and Redundancy Screening,» *IEEE Transactions on Power Systems*, 2020 (cit. on pp. vii, 164, 177).

[S4] M. Roveto, **R. Mieth**, and Y. Dvorkin, «Co-Optimization of VaR and CVaR for Data-Driven Stochastic Demand Response Auction,» *IEEE Control Systems Letters*, 2020 (cit. on pp. vii, 17, 32, 177).

[S5] J. Kim, **R. Mieth**, and Y. Dvorkin, «Computing a Strategic Decarbonization Pathway: A Chance-Constrained Equilibrium Problem,» *IEEE Transactions on Power Systems*, pp. 1–1, 2020 (cit. on pp. vii, 23, 177).

[S6] C. Gerwin, **R. Mieth**, and Y. Dvorkin, «Compensation Mechanisms for Double Auctions in Peer-to-Peer Local Energy Markets,» *Current Sustainable/Renewable Energy Reports*, pp. 1–11, 2020 (cit. on pp. vii, 20, 172, 177).

ACKNOWLEDGMENTS

This dissertation and all the work and formative experiences that led to its creation were enabled by the guidance, support, trust and friendship of many amazing people.

I am enormously grateful to Jörg Raisch, who trusted and supported me from the very first moment. Thank you for being so open-minded towards my plans and ideas and for always providing fast and helpful feedback

I cannot begin to express my gratitude to Yury Dvorkin, whose mentorship made me a better researcher and, especially, writer. Спасибо, Юрий for welcoming me in your group, for always pushing me (and everyone) to achieve nothing short of perfection, for your guidance on eye level through the intricacies of academia and for teaching me the art of effective presentation and discussion via the Münzenberg-Transformation (hyphen intentional). I hope to be able to reciprocate your support, especially your constant availability for a brief meeting or political anecdote, no matter how busy your schedule, in my future career.

Many (if not most) of the milestones of my early academic life were guided and supported by Christian von Hirschhausen, for which I am deeply thankful. In fact, he introduced me to the world of power system models and taught me all the things they cannot tell us. Thank you, Christian. Now it is time to get the band together and start working.

This work would not have been possible without the generous support of the Rainer Lemoine-Foundation. I would like to express my gratitude to the executive board and the board of trustees of the foundation for placing their trust in me and their offer to join the group of Reiner Lemoine-Fellows. I hope that my work provides the expected step towards a sustainable future. Also, I would like to thank Lutz Plöttner for his congenial attendance to all my requests and questions.

I would like to thank Francisco de Leon for inviting me to come to NYU and enabling everything that came out of this visit. I also thank Ulrike Locherer of TU Berlin for helping me to deal with so much of the university's bureaucracy, Petra Haase of TU Berlin for her support with many "extraordniary" processes and Raquel Thompson of NYU for all the work that she (repeatedly) put into my visa procedures.

I am very grateful to Christian Hans and Lia Strenge, who helped me shaping my freshly-graduate ideas into something that could be called a proposal and withstood a review. I did enjoy working with and learning from you and hope that we collaborate again in the future. I also thank my NYU colleagues, co-authors and friends Jip Kim, Ali Hassan, Samrat Acharya, Anwar Khan and Matt Roveto. I hope we can soon share a cake and other sweets again. In particular I want to thank Richard Weinhold, my friend and "academic twin" for all the shared experiences in modeling, programming, teaching, writing, Bavarian politics, transformer construction and, of course, hiking.

None of this would have been possible without the infinite support of my family and friends. Special thanks go to Sandro, Lennart and Ole for their everlasting companionship.

I am grateful to my parents Kathrin and Jürgen for raising me with all the love and care that I could have wished for and for always making sure that my brother and I had all the freedom and opportunity to learn and grow. Danke Mama und Papa! I also want to thank my brother for all the intense discussions at the dinner table.

I thank my amazing wife Dr. Norah (a real scientist) for all her love, support and for reminding me about what is truly important.

CONTENTS

LIST OF FIGURES

LIST OF TABLES

ACRONYMS

AC	alternating current
ACOPF	AC Optimal Power Flow
ADS	Arrow-Debreu Security
ADMM	alternating direction method of (Lagrangian) multipliers
AGC	automatic generator control
CC-ACOPF	chance-constrained AC optimal power flow
CC-DCOPF	chance-constrained DC optimal power flow
CC-OPF	chance-constrained optimal power flow
cdf	cumulative distribution function
CVaR	conditional-value-at-risk
DC	direct current
DCOPF	DC Optimal Power Flow
DER	distributed energy resource
DLMP	distribution locational marginal price
DR	demand response
DSO	distribution system operator
EENS	expected energy not served
ES	energy storage
EV	electric vehicle
FND	fictitious nodal demand
KKT	Karush-Kuhn-Tucker
LMP	locational marginal price
LOLP	loss of load probability
LSE	least-square estimator
MPEC	mathematical program with equilibrium constraints
OOS	out-of-sample
OPF	optimal power flow
PTDF	power transfer distribution factor
PV	photovoltaic
RES	renewable energy sources
SOC	second-order conic
TSO	transmission system operator
VaR	value-at-risk

NOMENCLATURE

The following notations are shared by Chapters 3–8. Some chapter-specific modifications and additions are introduced within the respective chapters. Appendices A–C slightly modify some notations to present the introduced concepts concisely.

Sets:

$\mathcal{A}_i$	For radial networks: Set of ancestor nodes of node i
$\mathcal{C}_i$	For radial networks: Set of children nodes of node i
$\mathcal{D}_i$	For radial networks: Set of downstream nodes of node i, including i
$\mathcal{G}$	Set of generators
$\mathcal{L}$	Set of network edges (lines)
$\mathcal{N}$	Set of network nodes (buses)
$\mathcal{N}^+$	For radial networks: Set of network nodes without root node.
$\mathcal{P}$	Distributional ambiguity set
$\mathcal{U}$	Set of uncertain (renewable) generators
$\mathbb{R}$	Set of real numbers
$\mathbb{R}_+$	Set of non-negative real numbers

Variables and Parameters:

a_i	Generator cost function parameter (first-order)
b_i	Generator cost function parameter (second-order)
b	Suceptance
$c_{0-2,i}$	Generator cost function parameters (standard form)
e	Vector of ones
f^p	Vector of active power flows, indexed by f^p_{ij}, $ij \in \mathcal{L}$ (in radial systems indexed by f^p_i, $i \in \mathcal{N}^+$)
f^q	Vector of active power flows, indexed by f^q_{ij}, $ij \in \mathcal{L}$ (in radial systems indexed by f^q_i, $i \in \mathcal{N}^+$)
g	Conductance
p	Vector of active net injections, indexed by p_i, $\forall i \in \mathcal{N}$
p_D	Vector of active power demand, indexed by $p_{D,i}$, $i \in \mathcal{N}$
p_G	Vector of controllable active power generation, indexed by $p_{G,i}$, $i \in \mathcal{G}$, limited by $[p^{min}_{G,i}, p^{max}_{G,i}]$

p_U	Vector of uncertain active power generation, indexed by $p_{U,i},\ i \in \mathcal{U}$
q_D	Vector of reactive power demand, indexed by $q_{D,i},\ i \in \mathcal{N}$
q_G	Vector of controllable active power generation, indexed by $q_{G,i},\ i \in \mathcal{G}$, limited by $[q_{G,i}^{min}, q_{G,i}^{max}],\ i$
q_U	Vector of uncertain active power generation, indexed by $q_{U,i},\ i \in \mathcal{U}$
s	Apparent power flow
t	Optimization auxiliary variable
u	Vector of nodal voltage magnitudes squared, indexed by $u_i = v_i^2,\ i \in \mathcal{N}$, limited by $[u_i^{min}, u_i^{max}]$
v	Vector of nodal voltage magnitudes, indexed by $v_i,\ \forall i \in \mathcal{N}$, limited by $[v_i^{min}, v_i^{max}]$
x	Reactance
y	Admittance
z_ϵ	Risk parameter, typically $z_\epsilon := \Phi^{-1}(1-\epsilon)$
A	For radial systems: Flow sensitivity matrix
$B^{(f)}$	Line susceptance matrix
$B^{(n)}$	Bus susceptance matrix
$B^{(p)}$	Power transfer distribution factor matrix
I	Identity matrix
M	Matrix of auxiliary decision variables
R	Matrix of sensitivity factors related to active power
S	Total system uncertainty given by $S^2 := e^\top \Sigma e$
T	Auxiliary matrix of sensitivity factors
X	Matrix of sensitivity factors related to reactive power
α	Vector of balancing participation factors, indexed by $\alpha_i,\ i \in \mathcal{G}$
γ	Vector of factors mapping active to reactive power, indexed by $\gamma_i,\ i \in \mathcal{N}$, given by power factor $\cos\phi_i$ so that $\gamma_i := \sqrt{1-\cos^2\phi_i}/\cos\phi_i$
θ	Vector of voltage angles, indexed by $\theta_i,\ i \in \mathcal{N}$
λ	Typically, dual multiplier of power balance and energy price
π	Price
ρ	Optimization auxiliary variable
χ	Dual multiplier of balancing adequacy constraint and reserve price
ω	Vector of forecast errors / uncertain injections, indexed by ω_i
Σ	Variance-Covariance matrix of ω

Φ	Cumulative distribution function of the standard normal distribution
Ω	Uncertainty space, $\boldsymbol{\omega} \in \Omega$

Operators and Modifiers:

$\hat{\cdot}$	Observed value or estimation based on historical observations
$\bar{\cdot}$	Linearization point or mean
$\cdot_t$	Additional time index
$\check{\cdot}$	Inverse of a matrix
$\cdot^\top$	Transpose of vector or matrix
$\mathrm{conv}(\cdot)$	Convex hull
$\mathrm{diag}(x)$	Diagonal matrix with vector x as entries in the main diagonal
$F(\cdot)$	Power flow equations
$\mathbb{E}(\cdot)$	Expected value
$\mathbb{F}$	Risk measure
$\mathbb{P}(\cdot)$	Probability
$\mathrm{Var}(\cdot)$	Variance
$\mathrm{VaR}_{1-\epsilon}(\cdot)$	$1-\epsilon$ value-at-risk
$\sigma(\cdot)$	Standard deviation
$\Re(x)$	Real part of complex number x
$\Im(x)$	Imaginary part of complex number x
$\lVert\cdot\rVert_2$	2-norm

Part I

INTRODUCTION

1 INTRODUCTION

1.1 THE SUSTAINABLE POWER SYSTEM: CERTAINLY UNCERTAIN

Availability of electric power at an acceptable cost has, in the last century, become a central driver of post-industrialized development, [1], and its sudden shortfall has the potential to shut down entire continents, [2], [3]. In this century, power systems and their institutional and regulatory frameworks, have to maintain and expand the *availability* of electric power, while simultaneously enabling a timely transition towards a *sustainable* carbon-neutral power sector, [4]. This transition, in turn, requires power systems to host more renewable energy sources (RES) and other non-traditional resources, such as flexible loads and battery storages. However, the stochastic nature and limited controllability of these resources challenges the efficiency and reliability of established concepts in power engineering and economics by injecting new forms of exogenous physical *uncertainty*.

Uncertainty of any source exposes power system operations to a variety of *physical* and *financial risks*. Physical risks are related to the inability of the system to serve loads, e.g. due to equipment outage triggered by overload protection systems or destruction, or infeasible voltage and frequency characteristics. Although not every system disturbance leads to load shedding or system collapse, required corrective actions, repair and maintenance can incur severe financial implications to the system and its stakeholders. Further, greater uncertainty can amplify "purely" financial risks, mostly related to more volatile electricity prices and ad hoc out-of-market corrections that may challenge the market's liquidity, efficiency and impedes economic long-term planning, [5], [6].

Current operation and planning procedures have been tuned to high efficiency to mitigate risks from traditional uncertainty, which are of a relatively low magnitude, e.g. imperfect demand forecasts, or low probability, e.g. unplanned equipment outages, [7]. For such uncertainty, automated and distributed frequency and voltage controls, as well as emergency switching and generator re-dispatch, corrects any deviation between the expected and real-time system state. However, necessary temporal control hierarchies (primary, secondary, tertiary control) and their spatial impact (local control, area control, synchronous system) depend on the system operator's generator schedules (dispatch), which are typically obtained from solving an optimal power flow (OPF) problem or its variant, [8]. While the exact OPF can vary between system operators, they are typically *deterministic*, i.e.

ignore stochastic characteristics of renewable and flexible resources, and rely on fixed external reserve margins and security heuristics, [9]. These shortcomings amplify physical and financial risks and obstruct the efficient and reliable accommodation of RES required for the energy transition.

The work in this dissertation aims to provide methods to mitigate and control physical and financial risks in renewable-dominant power systems by internalizing RES uncertainty into (i) central *dispatch* and *control* decisions, and (ii) price-based *coordination* mechanisms, thus rendering them uncertainty- and risk-aware.

- **Risk-aware dispatch and control:** The work in this part presents methods for risk-aware dispatch decisions in transmission and distribution systems. These methods extend established OPF formulations to account for reserves needed to ensure sufficient generation and transmission capacity, as well as compliance with operating limits of system state variables (e.g. voltage magnitudes). By formulating reserve requirements as functions of the available statistical information of the underlying uncertainty and predefined risk-levels and suitable balancing control policies, these requirements become endogenous to the decision-making problem. Thus, potentially over- or under-conservative deterministic reserve requirements are avoided. Additionally, this part deals with situations where only partial information on the uncertainty statistics is available from historical data or some information has to be learned "on the fly" in an online decision-making process. The resulting sets of model formulations and solution techniques aim to support renewable-dominant power system operations by robustifying dispatch decisions against forecast errors at a minimal additional cost.

- **Risk-aware coordination:** The work in this part internalizes the risk-aware OPF formulations described above into electricity markets. Convex properties of these formulations yield efficient risk-aware price signals that incentivize a system-beneficial behavior of all market participants. Here, computing separate energy and reserve prices that capture the expected system state and its inherent uncertainty, respectively, enables a fully *ex-ante* settlement of the market. Additionally, this part proposes an approach to control the volatility of system state-variables and to model risk-averse behavior, as well as asymmetric information, among the market participants. The resulting coordination mechanisms and price analyses for distribution (retail) and transmission (wholesale) markets aim to enable new stochastic electricity market designs that internalize the inherent uncertainty of RES and risk attitudes of market participants and, thus, support the transition towards a sustainable power sector.

1.2 SCOPE AND CHALLENGES

This dissertation focuses on internalizing available statistical information on parameter uncertainty and risk evaluation into short-term decision-making tools. These look-ahead (day-ahead, hour-ahead, minutes-ahead) decision-making processes rely on OPF formulations that capture the *steady-state* physics of the analyzed power system.

1.2.1 *The New Role of Distribution Systems*

In traditional power systems, electrical power is generated in central large-scale power plants. High-voltage transmission systems provide efficient long-distant transportation of the power to load points or load centers, where it is transformed to lower voltage levels. Thus, low-voltage distribution systems haven been designed for the passive role of ensuring power flow from the, so called substation, transformer towards commercial or residential loads. This passive and uni-directional paradigm in distribution systems is challenged by the growing deployment of distributed energy resources (DERs), e.g. rooftop photovoltaic (PV), battery storages, and electric vehicles (EVs), in combination with communication-based digital control systems, e.g. smart meters and smart appliances. For example, power production at the premises of end-consumers may lead to so-called reverse power flows, i.e. from the customer towards the substation, and infeasible voltage profiles [10], [11]. Further, uncontrollable small-scale generation that is directly used to serve customer load, so called behind-the-meter generation, increases the uncertainty and volatility of net demand visible to the system operator. As a result, uncertainty and volatility at the substation increases, too, requiring more reserve and flexibility from the transmission system, [12], and impacting equipment degradation, [13].

On the other hand, and in addition to such benefits to the DER operator as reduced electricity bills or partial autonomy from the utility, DERs also have the potential to provide a broad range of beneficial services to the utility, [12], [14]. Controllable battery storages and flexible demand can actively shape the system load profile and, thus, mitigate the effects of uncontrolled generation from PV and wind, [15]–[17] and peak-load scenarios, [18]. This also includes voltage control and active power loss reduction by leveraging properties of power electronic inverters, [19]–[22], and vehicle-to-grid capabilities of EVs, [14], [23].

However, many advantages of DERs remain unlocked due to the centralized nature in distribution system operations, [12], and their inability to explicitly internalize uncertainty and risk in their dispatch and coordination processes. This dissertation aims to address some challenges related to the uncertain behind-the-meter generation in the presence of controllable DERs by proposing stochastic decision-making and pricing frameworks tailored towards active distribution systems.

1.2.2 *Enabling Distributed Resources*

Leveraging demand-side flexibility is envisioned as one of the central requirements for the successful transition to a RES-dominant power system, [24], [25]. Effective load shaping via demand response (DR) programs can counteract short-term volatility of RES and support both distribution and transmission system operations, [12]. However, existing DR programs mainly target commercial and industrial loads that are relatively homogeneous in size and technical capabilities and, thus, are fairly easy to price and interface with energy managements systems used by utilities [25]. On the other hand, aggregated residential loads also have the potential to participate in load shaping, i.e. by leveraging thermal inertia of cooling and heating systems or incentivizing individual peak-load reduction, [26], [27]. However, aggregation of these small-scale distributed resources is challenged by their heterogeneous characteristics and electricity usage patterns and preferences. Additionally, resource specific load control is obstructed by extensive requirements of communication infrastructure and associated cybersecurity considerations, [28], [29].

Hence, effective deployment of large numbers of small-scale flexible resources requires methods to learn customer preferences and behavior, while relying on passive one-way communication channels, [30]. However, current aggregation and DR deployment strategies, e.g. by commercial DR service providers ("aggregators"), are mainly concerned with optimizing DR remuneration (i.e. profit), while ignoring the physical context in which the individual resources are operated in, [31], [32]. Resulting DR actions may, therefore, be infeasible due to power flow or voltage level violations in the distribution system.

The work in this dissertation addresses the challenges related to deploying flexible resources in distribution systems by studying methods of uncertainty-aware and learning-based distribution system operation. This includes the development of a learning framework that continuously infers statistical information from the behavior of residential DR participants, as well as uncertainty-aware and physics-informed price information that supports efficient DER deployment.

1.2.3 *Uncertainty and Variability at Scale*

In the past, power supply from central large-scale generators via an interconnected transmission system significantly improved the system's cost efficiency and reliability. Large generators can be operated at greater fuel-efficiency and, with the exception of nuclear power plants, [33], are characterized by lower capacity-weighted investment costs, [34]. At the same time, a wide-ranging aggregation of loads through meshed trans-regional transmission networks largely offset demand variations at smaller time scales and their remaining interday trends became fairly predictable, [7], [8].

Investments in RES similarly benefit from the economics of scale. The per-megawatt investment cost for wind turbines drops significantly if they are aggregated in larger wind parks, [35], and the *International Energy Agency* predicts that utility-scale PV investments will outpace those in distributed PV in 2021, [36]. Because the exact generation output from wind and PV depends on random atmospheric events, i.e. turbulent wind speeds and cloud movements, utility-scale RES inject a new level of uncertainty and variability into the transmission system.

These large-scale uncertainty sources in combination with high numbers of intermittent DERs require new means of quantifying and allocating reserve capacities to mitigate resulting physical and financial risks. On the one hand, it is common to internalize potential unplanned outages of generation or transmission system via preventive dispatch decisions (so called N-1 criterion), [37]. On the other hand, current practices to determine reserve requirements related to short-term RES volatility rely on exogenous and ad-hoc policies, [38]. As a result, these reserves are often overly conservative, sub-optimally allocated, or ignorant of the economics of potential reserve providers, [9].

The work in this dissertation aims to address certain challenges of transmission-level uncertainty by discussing risk-aware (AC and DC) OPF formulations that internalize stochastic and spatial information of uncertain RES into reserve quantification and allocation.

1.2.4 *Complex Systems with Complex Markets*

One of the central designations of power systems is to provide reliable universal access to electric power at socially acceptable cost, thus linking operational feasibility to economic adequacy. Practical implementation of this link has, in the past three decades, taken the form of (competitive) *electricity markets*. The market-based coordination of electricity supply, transmission and demand at various time scales has been shown to significantly improve resource efficiency, reliability and transparency, [1], [34], [38], [39]. On the other hand, however, coupling a highly complex and dynamic power system with an equally complex and dynamic economic system, [40], requires careful market design choices to avoid instabilities that may eventually lead to failures, such as the 2000-01 Californian electricity shortage, [41].

Current electricity markets have been designed around traditional, i.e. central, large-scale, controllable, and often high-inertia, forms of electricity generation, [42]. Recent market design developments that acknowledge a shift in the generation-mix towards stochastic RES and emerging means of storage and control have so far been "*primarily incremental in nature*", [38], benefiting mostly from enhanced computational technologies. The market clearing procedures resulting from these incremental changes have brought some efficiency gains, but at the same time suffer from acceptance issues related to intransparent price formation processes, [9], [38].

One of the main challenges of the RES-dominated electricity market is to maintain *resource adequacy*, i.e. create incentives for the provision of flexible energy and reserve capacity such that short term forecast deviations and fluctuations can always be balanced, [42]. This requires an efficient and transparent examination of (potentially unused) reserve capacity that internalizes spatio-temporal stochastic characteristics of the underlying uncertainty. The resulting remuneration of energy and reserve providers must be *incentive compatible* (i.e. encourage system beneficial behavior) and ensure *cost recovery* (i.e. ensure at least a zero profit for all participants), independent of the method and outcome of internalizing stochastic considerations, [9], [43]. Finally, stochastic electricity market efficiency depends on *risk-allocation*, i.e. market participants that are able to mitigate or hedge against risk at least cost should carry the system risk, [42].

The work in this dissertation addresses some challenges related to stochastic electricity markets to enable uncertainty-aware energy and reserve prices that comply with desirable market properties for all outcomes of the uncertainty. Additionally, a risk-market for efficient risk-evaluation and -allocation is proposed and discussed.

1.3 READER'S GUIDE

The chapters of this dissertation are related and reference each other, but are edited such that each chapter can be read and understood independently. The central chapters 3–8 are split among Parts II and III. Part II, consisting of Chapters 3–5, is concerned with optimizing the centrally dispatched power system under uncertainty and Part III, consisting of Chapters 6–8, establishes risk-aware formulations for electricity markets. Chapters 4–8 are based on [P1]–[P5] and each include an illustrative case study with numerical experiments that demonstrate applicability and performance of the proposed methods and formulations.

The content of each chapter is outlined below:

- **Chapter 2** reviews relevant publications on risk-aware dispatch and electricity markets. It introduces and surveys existing methods that address some of the challenges outlined above and provides reference for the contributions of this dissertation.

- **Chapter 3** derives risk-aware OPF formulations for transmission and distribution systems, using chance constraints. Model formulations in subsequent chapters 4–8 extend or modify these models.

- **Chapter 4** proposes a data-driven distributionally robust approach for the operation of an active distribution grid under the uncertainty of behind-the-meter resources. This chapter shows how optimized DER schedules and control policies can be immunized against uncertainty in the probabilistic models of forecast errors obtained from available historical data points. This chapter is based on our work in [P1].

- **Chapter 5** describes an online learning framework that continuously learns the price sensitivity of DR resources in a distribution system, while co-optimizing generation and reserve allocation from controllable DERs. Additionally, this chapter discusses learning performance guarantees and deals with distributional ambiguity of the response model. This chapter is based on our work in [P2].

- **Chapter 6** proposes a stochastic coordination and pricing scheme for DERs in distribution systems. The chapter proves the existence of a competitive equilibrium in the proposed market and comprehensively discusses price components and DER incentives. Further, the previously lossless OPF formulation from Chapter 3 is extended towards linearized losses. This chapter is based on our work in [P3].

- **Chapter 7** generalizes the results from Chapter 6 towards a complete (meshed) AC system formulation and shows how stochastic uncertainty information can be internalized into reserve allocation and pricing. Additionally, this chapter shows how the volatility (variance) of state-variables can be controlled. This chapter is based on our work in [P4].

- **Chapter 8** develops a stochastic electricity market based on Chapters 6 and 7 by incorporating risk-averse attitudes of market participants and the market operator. The chapter proves the existence of interpretable prices and risk allocations for continuous and discrete cases. This chapter is based on our work in [P5].

- **Chapter 9** concludes this dissertation, summarizes its key findings and provides a brief outlook on future research directions.

Additionally, some preliminaries and theory used in this dissertation are reviewed in Appendices A–C:

- **Appendix A** reviews convex and conic optimization theory.
- **Appendix B** derives power flow equations and introduces the notion of optimal power flow (OPF).
- **Appendix C** introduces fundamental concepts and vocabulary of (electricity) markets.

2 LITERATURE REVIEW

This chapter consists of three sections. Section 2.1 surveys current goals and stochastic approaches in power system operation, dispatch and control. The bedrock of this discussion is the chance-constrained optimal power flow (CC-OPF) problem, its solution approaches, modifications and applications. Section 2.2 provides a comprehensive discussion of current approaches and challenges to stochastic electricity markets, pricing under uncertainty and allocation of risk and reserve. Finally, Section 2.3 summarizes the contributions of this dissertation relative to the existing literature and provides a brief impact statement.

2.1 POWER SYSTEM DISPATCH UNDER UNCERTAINTY

Power system operations are primarily driven by two considerations. First, the total system load is at most times lower than the installed generation (and transmission) capacity, so that there exist numerous combinations of generator outputs that satisfy all loads with respect to the system's physical constraints (e.g. transmission capacity and voltage levels). Finding the *optimal* (least cost) combination of generation levels to meet system demand is called the *economic dispatch* problem. Finding an economic dispatch solution that results in physically feasible power flows is called *optimal power flow (OPF)* problem. (See Appendix B and [8], [44].) Second, the system is subject to real-time deviations from the scheduled conditions due to load and weather variations or unplanned equipment outages. To ensure a stable system between dispatch intervals (one hour to 15 minutes), suitable regulation means and fast reserve capacity must be in place to mitigate such variations. These reserve requirements additionally constrain the OPF solution space and thus establish a connection between the reliability of the power system and its economic operation.

2.1.1 *Pursuing System Balance*

The main objective in steady-state power system analyses, in traditional OPF problems, [45]–[49], and in this dissertation, is to match generation and load, i.e. to ensure *power balance*. However, as pointed out in [50], balancing generation and load is an extremely complex task, whose goal is not only economic operation, but also *system stability*. In fact, the idea of a perfect power balance is rather abstract and achieving it impossible, [50], considering that a typical power system includes hundreds to thousands of generators and millions of loads, each subject to individual variations at various time scales. Hence, we follow [51] and call the power system stable if it is able to remain in or return to a state of equilibrium characterized by a *nominal frequency*, acceptable *voltage levels*, and long-term feasible operating conditions for all generation and transmission equipment assets.

Frequency control seeks to manage an active power mismatch, also called (area) control error, [7], [8], [51]. In the presence of generation from conventional generators, immediate small mismatches between the system load and generation are instantaneously balanced via the kinetic energy stored in their high-inertia spinning rotors, [8]. Thus, a generator's electric power injected into the grid may differ from the mechanical power injected into its rotor shaft, leading to a loss of rotational frequency if mechanical power is too low and vice versa.[1] If an observed frequency deviates beyond a predefined threshold, for example, as a result of larger imbalances, the power input of one or multiple generators must be corrected accordingly. In first instance, this correction is achieved via *automatic generator control (AGC)*. While at traditional steam-turbines AGC was achieved via frequency dependent governor systems, modern systems rely on fast digital control signals, [52]. In fact, with increasing amounts of inverter-connected generation resources, such as solar farms or battery storages, also synthetic "inertia" provision from power electronic systems has become a highly discussed topic, [53]–[55].

Following this immediate and local *primary* imbalance response to counteract frequency drifts, slower *secondary* and *tertiary* control units participate in restoring nominal frequency and optimal economic dispatch, respectively, by adapting their power output based on predefined area control participation or explicit operator commands. Table 2.1 shows an overview of this control hierarchy and the reserves associated with the different response time scales. This approach is international common practice, with some modification or alternate definitions for each system operator or regulatory institution, [56].

In high-voltage meshed transmission systems, voltage control schemes, on the other hand, mainly deal with the need to ensure sufficient provision of reactive power. At network nodes (buses) that host generators, voltage is locally controlled by the generator's automatic voltage regulators, [8], [44], [56]. At load buses (substations) or interconnection buses, local voltage and reactive power controls can be implemented via explicit voltage support services from larger loads and DERs, [56], [57], or power-electronic FACTS technology, [58]. However, voltage differences caused by power flows from generation to load buses, are relatively small in high-voltage transmission sys-

1 This relationship is captured in the so called *swing equation* $A\frac{d\omega}{dt} = P_m - P_e$, where P_m and P_e denote mechanical and electrical power, respectively, A is a generator parameter capturing its inertial characteristics, and ω is the generator frequency, [8], [50].

Primary Control: Local and automatic control with a response within seconds. (To stabilize frequency.) **Secondary Control:** Largely automatic, local and area wide control within seconds to minutes. (To recover nominal frequency.) **Tertiary Control:** Operator-driven actions within minutes to hours (To ensure economic and long-term feasible operation).	**Regulation Reserve:** Reserve generation capacity available within seconds to minutes. Called automatically via AGC or fast control signals. **Operation Reserve:** Reserve generation capacity available within minutes to hours. Called semi-automatically or manually.

Table 2.1: Hierarchy of frequency control and related reserves.

tems, [8], [44]. In distribution systems with medium and low voltage levels, on the other hand, reactive *and* active power flows between buses have a higher impact on voltage differences. This effect is amplified by the typically radial structure of distribution systems and must be mitigated by additional local control actions, [59].

2.1.2 *Reserves for Corrective Actions*

Corrective actions to ensure system balance and acceptable voltage levels, require *sufficient* and *deliverable* reserve capacity. Table 2.1 itemizes the non-standardized reserve definitions of different system operators, [56], as two types characterized by their response time and means of activation. Regulation reserves support primary and secondary (frequency) control actions based on predefined policies and are automatically activated by AGC or other control systems to regulate immediate power imbalances that threaten frequency stability. Operation reserves have slower activation times and are subsequently called by secondary and tertiary control systems to return the system to nominal operations, e.g. rectify overloads caused by previous control actions, or restore optimal economic dispatch conditions.

To date, most system operators adopt deterministic criteria to ensure sufficient quantities of regulation and operation reserves, [60], [61]. Most of these policies are ignorant to the stochastic characteristics of loads and RES injections and require reserves as a percentage of generation or peak load, see e.g. [62]. Recently, some system operators have started to procure reserves based on statistical rules such as the e.g., 95-percentile rule in *ERCOT*, [63], the (5+7) rule in *CAISO*, [64], or the "dynamic reserve rating" of the German transmission system operators (TSOs), [65]. However, even if sufficient capacity is available in the system, these reserves may not be deliverable in real time due to adverse locational effects that cause transmission overloads or voltage level violations, [7], [60]. This problem can be overcome by solving uncertainty-aware OPF problems that co-optimize generation set points and reserve allocation by explicitly modeling stochastic resources and corresponding balancing control policies, [P1]–[P5], [7], [66]–[69].

2.1.3 *Stochastic and Robust Approaches*

Consider an OPF with uncertain parameters (e.g. RES injections) formulated as a generic optimization problem:

$$\min_{x} \quad f_0(x, \boldsymbol{\omega}) \tag{2.1a}$$

$$\text{s.t.} \quad f_i(x, \boldsymbol{\omega}) = 0 \qquad i = 1, ..., n \tag{2.1b}$$

$$f_i(x, \boldsymbol{\omega}) \leqslant 0 \qquad i = n+1, ..., m, \tag{2.1c}$$

where $x \in \mathbb{R}^d$ is the vector of decision variables (e.g. generation levels) and $\boldsymbol{\omega} \in \Omega$ is the random vector corresponding to uncertain parameters. Objective (2.1a) seeks to minimize, e.g., costs or system losses with respect to the underlying model of power system physics, enforced as equality constraints in (2.1b), and system limits, enforced as inequality constraints in (2.1c). Noticeably, due to their dependency on $\boldsymbol{\omega}$, functions $f_i(x, \boldsymbol{\omega})$, $i = 0, ..., m$, become random variables, thus obstructing direct methods of solving (2.1), [70].

A broad strand of literature proposed scenario-based stochastic programming to solve OPF problems in the form of (2.1), [43], [67], [71]–[79].[2] Here, an optimal decision x^* is obtained by decomposing uncertainty space Ω into a finite set of discrete scenarios $\{\omega^s\}_{s\in\mathcal{S}}$ and minimizing the total probability-weighted cost of all scenarios. Additionally, scenario-based stochastic programming typically models a two-stage process that introduces corrective actions as additional decision variables u^s, which can be chosen after outcome ω^s has been observed, [80], [81]. First-stage decisions x (e.g. generator outputs and reserve capacity) are shared by all scenarios and second-stage decisions u^s (e.g. deployment of reserves) are scenario-specific. A scenario-based stochastic programming modification of (2.1) can be written as:

$$\min_{x,\{u^s\}} \quad \sum_s \mathbb{P}[\omega^s] f_0(x, u^s, \omega^s) \tag{2.2a}$$

$$\text{s.t. } \forall s: \quad f_i(x, u^s, \omega^s) = 0 \qquad i = 1, ..., n, \tag{2.2b}$$

$$f_i(x, u^s, \omega^s) \leqslant 0 \qquad i = n+1, ..., m, \tag{2.2c}$$

where $\mathbb{P}[\omega^s]$ denotes the probability of scenario ω^s. Generation and reserve schedules obtained from solving stochastic OPF have been shown to robustify system operation against uncertain RES injection, while also reducing long-run cost of operations, [77], [79]. Noticeably, solving (2.2) for every ω^s quickly becomes computationally demanding if many scenarios are considered or the studied system is large, [82]. Thus, most practical scenario-based OPF studies require intricate scenario reduction techniques, [83]–[85], and iterative solution methods such as Bender's Decomposition, [76], [79], [86].

Instead of solving (2.2), *robust* programming seeks to immunize the decision against the *worst-case* outcome chosen from a predefined *uncertainty set* $\mathcal{U}$:

$$\min_x \sup_{\omega \in \mathcal{U}} \quad f_0(x, \omega) \tag{2.3a}$$

$$\text{s.t.} \quad f_i(x, \omega) = 0 \qquad i = 1, ..., n, \tag{2.3b}$$

$$f_i(x, \omega) \leqslant 0 \qquad i = n+1, ..., m. \tag{2.3c}$$

Because the robust approach in (2.3) does not require probabilistic information but only relies on the range of variation of $\boldsymbol{\omega}$ captured in $\mathcal{U}$, [89], computational effort is reduced at the cost of a more conservative (and thus more expensive) solution. The inner maximization problem in (2.3a), however, may require specialized solution methods, [79], or problem-specific reformulations depending on the exact definition of $\mathcal{U}$, [76].

Both approaches in (2.2) and (2.3) aim to internalize the range (variability) of $\boldsymbol{\omega}$ into the decision making process. However, if decision x^* is not immunized against all potential outcomes $\boldsymbol{\omega}$, which may lead to a prohibitively large cost, then there remains a non-zero probability that operational constraints and system cost will exceed their acceptable limits. We consider the severity of these violations weighted

2 Notably, scenario-based stochastic programming has been studied extensively in the context of the stochastic *unit commitment* problem, [74]–[79], [87], i.e. a mixed-integer modification of the OPF problem that assigns a discrete *on* or *off* status for each generator via binary variables for higher modeling fidelity. As this dissertation primarily studies risk-aware extensions to (AC) power flow formulations and leverages convex properties of the resulting formulations, all generators are assumed pre-committed, i.e. available for dispatch. Furthermore, the non-convex mixed-integer unit commitment problem can be convexified by solving the initial commitment problem and then fixing all binary variables to solve the OPF and dispatch the committed generators, [88].

by the likelihood of their occurrence as *risk*. By defining suitable *risk-metrics* $\mathbb{F}_i$, [90], we can modify (2.1) to shape decision-inherent risk such that it becomes acceptable:

$$\min_{x} \quad \mathbb{F}_0[f_0(x, \omega)] \tag{2.4a}$$

$$\text{s.t.} \quad \mathbb{F}_i[f_i(x, \omega)] \leqslant 0 \qquad i = 1, ..., m. \tag{2.4b}$$

The central idea of this approach is to solve a *deterministic* problem that internalizes risk into its decision making process, as opposed to solving a stochastic problem with multiple scenarios and probability weights, thus overcoming the computational complexity of the latter. Solving the risk-aware OPF as in (2.4) has mainly been enabled by the seminal work in [7]. Here, the expected cost of system operation ($\mathbb{F}_0 \equiv \mathbb{E}$) are minimized under the condition that the probability of constraint violations does not exceed a predefined limit ϵ_i. Such constraints can be enforced by limiting the ϵ-Value-at-Risk (VaR_ϵ) such that $\mathbb{F}_i \equiv \text{VaR}_{\epsilon_i}$, see e.g. [91], and are called *chance constraints.*

2.1.4 *The Risk-Aware Chance-Constrained Optimal Power Flow*

Chance-constrained programming, i.e. optimization with probabilistic constraints of the form:

$$\mathbb{P}[f_i(x, \omega) \leqslant 0] \geqslant 1 - \epsilon_i, \tag{2.5}$$

was originally introduced by Charnes and Cooper in 1959, [92], and further refined in [93], [94]. Early adaptations for solving OPF under uncertainty have been reported in [95]–[97], but all of these works required complex iterative solution approaches or approximations. The work in [95] highlights the connection of the chance-constrained OPF problem to loss-of-load probability, an established power system design metric, and iteratively co-optimizes generator and reserve schedules until the probability of load shedding is below the target value. Here, the chance-constrained power balance is evaluated *ex post* via Monte-Carlo sampling. Similar sampling-based solution approaches were proposed in [96] to avoid transmission line overloads in the presence of uncertainty from load and wind generation and in [98] to mitigate random effects from demand response (DR). Departing from sample-based probability evaluation, [97] develops a back-mapping approach to solve an AC Optimal Power Flow (ACOPF) problem with uncertainty and corrective control. Although the authors linearize the power flow equations around the expected value of the uncertain vector, the explicit analytical solution of the underlying probability distribution function renders the resulting problem highly non-convex and computationally demanding.

Further progress was enabled by the development of tractable formulations of risk metrics, including *value-at-risk* and *conditional value-at-risk*, [91], [99], which can be used to formulate and approximate chance constraints, [S4]. Building on the approximations proposed in [100], the work in [101] employs convex chance constraint relaxations to co-optimize an OPF problem with causal balancing control policies $u(x,\omega)$ that are "tuned" by x at decision time and then automatically ensure the system balance based on the realization of ω. Notably, this approach is closely related to AGC or other (automatic) primary and secondary control actions as outlined in Section 2.1.1 above. By defining a suitable control policy and assuming normally distributed forecast errors, [7] proposed a tractable and exact reformulation of the linearized CC-OPF for transmission systems (CC-DCOPF) using convex second-order conic (SOC) constraints.

The basic structure of the CC-OPF is given as:

$$\min_{x} \quad \mathbb{E}[f_0(x,u(x,\omega),\omega)] \tag{2.6a}$$

$$\text{s.t.} \quad f_i(x,u(x,\omega),\omega)=0 \qquad i=1,\dots,n,\ \forall\omega \tag{2.6b}$$

$$\mathrm{VaR}_{\epsilon_i}[f_i(x,u(x,\omega),\omega)] \leqslant 0 \qquad i=n+1,\dots,m, \tag{2.6c}$$

where objective (2.6a) minimizes expected cost (i.e. $\mathbb{F}_0 \equiv \mathbb{E}$), power balance (2.6b) is ensured for all ω through $u(x,\omega)$, and chance constraints (2.6c) are enforced by setting $\mathbb{F}_i \equiv \mathrm{VaR}_{\epsilon_i}$, $i=n+1,\dots,m$, which is equivalent to (2.5). Detailed formulations and derivations are presented in Chapter 3. Balancing control policies $u(x,\omega)$ are defined using *participation factors* that determine the contribution of each resource to correct the system control error. This concept is common in power system operations and, effectively, represents a distributed droop-controlled correction of power imbalances, [44], [89].

The computational tractability of the CC-DCOPF enabled further improvements and extensions of risk-aware dispatch. Instead of a system-wide control policy, [102] proposed participation factors that are sensitive to the source of the imbalance in the network. Non-linear and piecewise linear balancing participation that captures additional reserve physics are proposed in [103], and [104] proposes balancing participation with heterogeneous response times.

The original chance-constrained DC optimal power flow (CC-DCOPF) from [7] assumes exact knowledge of the parameters of the underlying (normal) distribution. This assumption might not hold in reality. A data-robust modification that internalizes potential errors of the estimated mean and variance of the normal distribution was outlined in [7] and further developed in [105] using a predefined uncertainty set (or uncertainty "budget"), and in [P1] using confidence bounds on the estimation accuracy. Similar to [101], the work in [106] shows how chance constraints can be conservatively approximated, and thus robustified, if some distributional parameters are unknown. Distributionally robust CC-OPF formulations that only rely on estimated moments of the underlying distribution parameters (e.g. mean and variance) and do not make a specific assumption on distribution density functions have been studied in [P2], [107].

To guarantee energy and reserve deliverability, the resulting dispatch decision must be feasible with respect to alternating current (AC) power flow physics. However, ACOPF is already NP-hard in its deterministic form, [108], and non-linear AC-power flow equations obstruct deriving a feasible formulation of (2.6b) and (2.6c), [68]. Thus, the success of a chance-constrained AC optimal power flow (CC-ACOPF) formulation hinges on finding suitable relaxations to these equations. While [109], [110] rely on a convex relaxation at the cost of guaranteeing robustness, [111] proposes a conservative inner approximation. Alternatively, the work in [68], [112] successfully derive tractable CC-ACOPF formulations by linearizing power flow equations around an expected point of operation and deriving sensitivity mappings between the system state-variables and an uncertain random vector. Additionally, [68] extends the fist-stage ACOPF solution with statistics-informed reserve requirements and derives an exact SOC relaxation of the otherwise non-convex chance constraint on apparent power flows.

2.1.5 *Risk-Aware Distribution System Operation*

Historically, power transmission and distributions systems have been operated separately by transmission system operators (TSOs) and distribution system operators (DSOs), respectively. Although both systems are interdependent and can be coordinated, [113], the operational priorities, and thus challenges when confronted with uncertainty, vary. The TSO mainly aims to continuously maintain nodal power balances while avoiding transmission overloads. The DSO, on the other hand, is more focused on complying with nodal voltage limits in distribution systems, on minimizing power losses and on following the pre-defined power exchanges with the TSO. These operational paradigms are under pressure handling the constantly increasing volatility of power generation from rising numbers of DERs and aging infrastructure, [114]. Reliability and safety concerns raised with regard to DER intermittency and stochasticity, may limit techno-economic benefits of these resources, obstructing a timely transition towards a carbon-free generation mix. Notably, uncertainty-aware OPF for distribution systems to schedule available resources and means of control, requires comprehensive AC power flow analyses to capture the impact of uncertain DER injections on voltage levels and losses.

While the CC-ACOPF formulations in [68], [109]–[112] rely on some assumptions specific to the operation of transmission systems, e.g. meshed topology or bus specific control paradigms, see also Section 3.3.2, the work in [69] proposes a distribution system-centric approach to the CC-ACOPF that relies on a generic linear mapping between bus injections and voltage levels. Additionally, the chance constraints in [69] are relaxed using a conditional value-at-risk metric, to enable sampling-based and distributed solution methods. The typically *radial* topology of distribution feeders enable exact SOC (branch flow model) and approximate linear (LinDistFlow) reformulations of the AC power flow equations, while maintaining explicit expressions for voltage and reactive power, see [115], [116] and Appendix B.5. Leveraging the LinDistFlow formulation for a convex radial CC-ACOPF formulation, [P1]–[P3] propose risk-aware operation paradigms for distribution systems that accommodate data uncertainty, [P1], co-optimization of DR and DER dispatch policies, [P2], and a loss factor extension, [P3]. Additional work in [S1] leverages the convexity of the proposed CC-ACOPF formulation to co-optimize flexible loads via the alternating direction method of (Lagrangian) multipliers (ADMM). A distributionally robust extension is provided in [S2].

2.2 STOCHASTIC ELECTRICITY MARKETS

The fundamental requirement for cost efficient and reliable power system operation is the availability of necessary resources that can provide generation and control services at an acceptable cost. Restructuring of the electricity sector in Europe and the U.S. in the past decades aimed to enable supply-side competition to establish a cost-regulating framework. Reliability and security requirements are enforced as externalities of grid operations and engineering, [34]. However, the efficiency of unbundled grid and market operations is threatened by increasing short-term volatility and uncertainty injected by RES and DERs. As outlined in Section 2.1.1 above, reliable system operations require the procurement of fast reserve capacity for frequency and voltage control actions to continuously match supply and demand, while maintaining system stability. However, [1] noted in 2008, preceding the mainstream discussion of RES intermittency, that "*the high value of ramp rate on the supply side has no counterpart on the demand side, because customers care only about whether power is on or off.*" In the past, this discrepancy was attenuated by the wide-range aggregation of loads with idiosyncratic volatility, which lead to relatively smooth and predictable load profiles that could be handled by conventional generators, [8], [117]. With increasing injections from stochastic RES, however, the necessary short-term flexibility similarly increases while, at the same time, the overall share of controllable spinning generation in the generation mix declines, [12]. Therefore, procuring and evaluating generation and reserve capacity from electricity markets requires engineering-informed market designs that internalize RES uncertainty and stochasticity, while maintaining required properties of efficient electricity markets, [P3], [P4], [9], [43], [67], [73].

2.2.1 *Pursuing Efficiency*

Trading electricity as a commodity is complicated by its physical characteristics, e.g. continuous balance of supply and demand, network-bound transmission governed by Kirchhoff's laws and high availability requirements due to its public significance. Therefore, and building on the pre-existing experiences of vertically-integrated power system operations, electricity trading took the form of auction-type (pool) markets, [34], [118]. Here, generators submit their price and capacity bids during a bidding phase and the market operator clears these bids in a pricing phase based on complementary demand bids or forecasts and with respect to system requirements, such as transmission and security constraints, [118], [119]. Finally, prices obtained from this *market-clearing* (i.e. matching supply and demand) determine the payments made by consumers (or, more precisely, commercial retailers) and the remunerations paid to generators.

To ensure that this approach fulfills its intended purpose, i.e. maintain reliable electricity supply at socially acceptable cost, it must comply with a set of axiomatic properties. A central requirement is market *efficiency*. Market efficiency has several aspects that are captured in *social welfare*, which is defined as the difference between the total social value ("utility") of consuming a certain quantity of electric energy and the total cost of supplying this quantity. A market is said to be efficient if it maximizes welfare, [34]. If the required quantity is independent of the cost ("inelastic"), i.e. not serving parts of the load is virtually infinitely expensive, welfare maximization is equivalent to cost minimization, [118].

A cost-minimizing market clearing constrained by system requirements and technical capabilities of generators resembles the OPF problem as discussed in Section 2.1 and Appendix B.3. However, whether or not this market-clearing is efficient depends on the pricing process and the resulting producer and consumer payments. Thus, the following additional requirements must be met, [S6], [9], [34], [117], [118]:

1. *Incentive Compatibility*: Producers (or, in the presence of elastic demand, all market participants), have to be encouraged to bid truthfully, i.e. according to their real production cost (or value of consumption).

2. *Cost Recovery*: The payments made to each individual producer must at least cover their cost of production. This is also a substantial requirement to ensure long-term resource adequacy, i.e.

that sufficient production capacity remains in the market and necessary investments are incentivized.

3. *Revenue Adequacy*: The payments collected from consumers must be sufficient to provide cost recovering payments to producers.

A suitable pricing mechanism that has been widely adapted in modern electricity markets builds on *competitive equilibrium theory* and has been proposed in the 1988 edition of [120]. Here, assuming perfect competition, i.e. no market participant is large enough to cause price changes, efficient electricity prices are equal to the *marginal cost* of supply at each bus in the network and emerge as the dual multipliers of the OPF constraints. These prices are called locational marginal prices (LMPs). Derivations and additional discussions on marginal-cost-based pricing are provided in Appendix C.

Due to the heterogeneous planning timescales of different types of generators, most electricity markets are cascaded with various clearing horizons. Common periods are day-ahead, hour-ahead and minutes-ahead ("real time"), [12]. For each planning period, co-optimization of generation and reserve dispatch must rely on demand and RES forecasts. Although these forecasts become more refined and accurate closer to real-time, they will never be perfect. While dispatch and reserve decisions can be robustified against forecast errors with the methods discussed in previous Section 2.1, whether or not they allow an efficient market clearing requires further discussion.

2.2.2 *Challenges in Stochastic Electricity Markets*

A lack of fundamental theory on efficient pricing in stochastic market designs may be one of the reasons why real-world market operators keep relying on deterministic solutions. As noted in [38], [121], [122], current approaches extend the existing market designs with new complex reserve products, such as CAISO's *Flex Ramp*, [123], or ancillary services. These products seek to replicate a stochastic market solution. Robust approaches, on the other hand, guarantee a safe system operation but are unsuitable for market clearing considerations because the actual outcome will almost never be the worst case. Instead, a large strand of literature has studied the scenario-based stochastic programming approach as a means to design stochastic electricity markets, [43], [72], [73], [124], [125].

Recall the generic scenario-based stochastic OPF problem in (2.2), which is shown below with additional dual multipliers in parentheses:

$$\min_{x,\{u^s\}} \quad \sum_s \mathbb{P}[\omega^s] f_0(x, u^s, \omega^s) \tag{2.7a}$$

$$\text{s.t. } \forall s:$$

$$(\lambda_i^s): \quad f_i(x, u^s, \omega^s) = 0 \qquad i = 1, \ldots, n, \tag{2.7b}$$

$$(\delta_i^s): \quad f_i(x, u^s, \omega^s) \leqslant 0 \qquad i = n+1, \ldots, m. \tag{2.7c}$$

The multi-stage nature of stochastic programming naturally resembles multi-stage market clearing procedures at multiple time scales. As discussed in Section 2.1.3, dispatch and reserve decisions derived from stochastic programming allocate generation and reserve capacity more cost-effectively, thus optimizing welfare from a market clearing perspective, [126]. Pricing information can be obtained from an aggregation of dual multipliers obtained from fixed first-stage constraints and probability-weighted scenario specific constraints, e.g. $\sum_i \mathbb{P}[\omega^s]\lambda_i^s$, $\sum_i \mathbb{P}[\omega^s]\delta_i^s$. The resulting payments are cost recovering and revenue adequate *in expectation*, [73], [83], [126], but not necessarily in the individual scenarios. The stochastic market clearing in [43] proposes remedial actions via corrective payments at the price of overall higher cost and deviating from the market equilibrium. In [125] cost recovery and revenue adequacy is achieved, while retaining an equilibrium by abandoning price calculations in the day-ahead phase and settle all trades at the real-time market clearing.

Although the proposals in [43], [125] address some of the market-theoretic caveats of scenario-based stochastic programming, some shortcomings that obstruct a real-world implementation remain. As discussed in Section 2.1.3, the computational tractability of stochastic programming depends on scenario-construction and -reduction techniques. In turn, these techniques will also alter the exact market outcome. Removing the decision-making authority over these parameters from the market participants may reduce transparency and, thus, acceptance of the market design, [9], [38], [117]. Further, purely *ex-post* uplift payments or price settlements expose generators to additional uncertainty, and thus risks, even if cost recovery is ensured.

2.2.3 *The Chance-Constrained Electricity Market*

Risk-aware CC-OPF offers compelling advantages as a market-clearing mechanism and has been proposed as such in [P3]–[P5], [9], [127].

Recall generic CC-OPF (2.6), shown below with dual multipliers in parentheses:

$$\min_{x} \quad \mathbb{E}[f_0(x, u(x, \omega), \omega)] \tag{2.8a}$$

$$\text{s.t.}$$

$$(\lambda_i): \quad f_i(x, u(x, \omega), \omega) = 0 \qquad i = 1, ..., n, \ \forall \omega \tag{2.8b}$$

$$(\delta_i): \quad \mathrm{VaR}_{\epsilon_i}[f_i(x, u(x, \omega), \omega)] \leqslant 0 \qquad i = n+1, ..., m. \tag{2.8c}$$

Because (2.8) solves a risk-aware *deterministic* problem, each constraint yields exactly one dual multiplier. These duals, in turn, naturally internalize risk adjustments of the primal problem. The first proof that prices obtained from these duals yield a competitive equilibrium was provided in [127]. Additionally, by explicitly enforcing constraints on balancing control policies $u(x, \omega)$ such that the system is balanced for all ω, it is possible to derive a marginal-cost-based price for reserve without requiring external reserve requirements. A stochastic electricity market based on chance-constrained market clearing was first proposed in [9]. Instead of per-scenario solutions, the energy and reserve prices derived from the CC-OPF capture all possible uncertainty realizations via an applied risk metric, which guarantees cost recovery and revenue adequacy for convex markets, [9], [128], as well as minimizes the uplift for non-convex[3] markets [9].

The work in [9], [127], however, neglected any constraints related to physical power flows, an important feature for practical implementation. The work in [P3], [P4] proposes a chance-constrained electricity market with comprehensive models of the physical power flow for wholesale (transmission) and retail (distribution) markets, respectively. Here, SOC programming ensures problem convexity and, thus, allows marginal-cost-based pricing from dual multipliers. A qualitative analyses of the resulting LMPs shows that energy prices are only implicitly depending on system uncertainty and risk evaluation. Reserve prices, on the other hand, include explicit terms related to forecast error statistics and the decision-maker's risk perception.

A long-term equilibrium perspective was considered in [S5]. Here, strategic investors seek to optimally expand installed capacity of controllable generation and RES to meet regulatory sustainability targets. Although the resulting mathematical program with equilibrium constraints (MPEC) remains challenging to solve, the chance-constrained approach enabled an internalization of RES stochasticity. As a result, investment in flexible resources where evaluated higher, thus increasing the RES hosting capability of the system.

All electricity market designs in [P3], [P4], [9], [43], [72], [73], [124], [125], as well as the formulation shown in (2.8), minimize *expected cost*. Thus, while internalizing the physical risk of constraint violations, they are *neutral* towards financial risk and neglect the possibil-

3 See Box 5 on page 173 for a brief discussion of non-convexities in electricity markets.

ity of financial markets to hedge against such risk. While explicitly modeling financial risk through *risk-averse* objective functions is common in the fields of stochastic optimization and finance, [81], it has only recently gained attention in power system operations and electricity markets. To a large extent, this was enabled by the theoretical work in [129], [130], which demonstrated the existence of a competitive equilibrium in risk trading. Here, too, efficient prices emerge as the dual multipliers on the market-clearing constraints of the traded financial products. Motivated by [129], [130] multi-stage scenario-based stochastic electricity market with risk-averse competitive equilibrium was proposed in [131]. The work in [132] demonstrated that different risk perceptions of market participants provide an incentive to act strategically, thus causing suboptimal market outcomes, which can be avoided in risk-complete electricity markets. A risk-averse and risk-complete chance-constrained electricity marked was studied in [P5]. Here it was shown that, similar to an optimal allocation of generation and reserve capacity, the optimal allocation of financial risk can decrease the ultimate system operating cost. At the same time, the advantages of the chance-constrained market-clearing are retained.

2.2.4 *Distribution Marginal Pricing*

Proliferation of DERs in low-voltage distribution systems and the subsequent growth of independent, small-scale energy producers has weakened a correlation between wholesale electricity prices and distribution electricity retail rates (tariffs), thus distorting economic signals experienced by end-users [133]. To overcome these distortions, distribution locational marginal prices (DLMPs) have been proposed to incentivize optimal operation and DER investments in low-voltage distribution systems, [23], [134]–[138], and to facilitate the coordination between the transmission and distribution systems, [12], [139]–[141].

However, the physics of low-voltage distribution systems, i.e. low-inertia systems with increasing numbers of power-electronically interfaced resources and non-negligible active and reactive power losses, amplify the stochasticity of distributed RES. Therefore, [P3] proposes a chance-constrained market framework for distribution systems and derives suitable risk- and uncertainty-aware DLMPs. These DLMPs capture balancing and reactive power regulation incentives to control the risk of voltage level violations.

2.3 CONTRIBUTIONS AND IMPACT

The work in this dissertation contributes to the academic literature on uncertainty- and risk-aware power system operation and electricity market designs.

2.3.1 *Chance-Constrained Optimal Power Flow*

Part II studies risk-aware dispatch decisions using tractable reformulations of the CC-OPF problem. Chapter 3 summarizes the models of [P1]–[P5], [7], [68] and presents tractable meshed CC-DCOPF, meshed CC-ACOPF and radial CC-ACOPF formulations in unified notations. The presented meshed CC-ACOPF and CC-DCOPF are adapted from [7] and [P4], [68] respectively. The radial CC-ACOPF formulation has been introduced in our work in [P1]–[P3].

Realizing the new and future role of distribution system operations in sustainable power systems, Chapters 4 and 5 take the perspective of distribution system operators (DSOs) and address challenges related to the stochastic behind-the-meter RES generation. For this purpose, Chapter 4 abandons the assumption of perfect knowledge of the statistical parameters of the underlying uncertainty from Chapter 3. Instead, we use a data-driven approach to robustify the radial CC-ACOPF against inaccuracies that occur when relying on finite historical data to estimate the variance of the underlying distribution. As a result, out-of-sample robustness is improved. In Chapter 5 data acquisition and system operation is coupled in an online learning process. Here, we assume that price-sensitive loads react to incentive signals broadcast by the DSO. However, the exact reaction is unknown and iterative negotiations are obstructed by lacking two-way communication infrastructure. As a result, the DSO must learn price-sensitivity parameters and dynamically adjust the broadcast incentive signals. Chapter 5 modifies a network-agnostic online learning approach as proposed in [31], [32] to additionally internalize operational risks using the chance-constrained framework. As a result, we show that price signals that neglect network physics cause under- or over-voltage issues that can be avoided with the proposed approach.

2.3.2 *Risk-Aware Locational Electricity Pricing*

Part III extends the network-agnostic chance-constrained electricity market from [9] to consider DLMPs, AC-complete LMPs and risk trading. First, continuing the analyses of distribution systems from Chapters 4 and 5, Chapter 6 leverages the mathematical properties of the proposed radial CC-ACOPF to derive efficient DLMPs and reserve prices using convex duality theory. Additionally, we propose an extension of the radial CC-ACOPF to explicitly consider network losses, an important feature for practical DLMP analyses given their typically non-neglectable impact on distribution system operation. A comprehensive analyses of energy and reserve price components enables a detailed evaluation of RES stochasticity and the allocation of flexible capacity in the system, and we show that these prices can constitute a competitive equilibrium.

In Chapter 7 we derive and analyze risk-aware energy and reserve prices for an AC-complete wholesale market clearing using the CC-ACOPF formulation for meshed transmission systems from Chapter 3. Additionally, as suggested in [142], we explicitly consider the variance of system state variables in the objective of the CC-ACOPF via a suitable variance metric. In turn, prices derived from the the resulting variance-aware CC-ACOPF are augmented by additional terms that capture a trade-off between generation flexibility and state variable variance.

Finally, realizing the shortcomings of assuming strictly risk-neutral market participants and system operators in Chapters 6 and 7 and in [9], Chapter 8 proposes a risk-complete chance-constrained electricity market. First, we modify the CC-DCOPF-based market clearing such that market participants are risk-averse. We show that an equilibrium market-clearing can be achieved if risk is evaluated via coherent risk metrics and the market is risk-complete, i.e. participants can trade financial products to hedge against their perceived financial risk. To enable risk trading we introduce a generic financial security product, a so called Arrow-Debreu Security (ADS), that is cleared alongside the standard energy and reserve products. After proofing existence and efficiency of the resulting market clearing for a continuous probability space of the underlying uncertainty, we show that the same results hold for a discretized probability space. While the proposed discretization enables practical risk contracts, the model preserves the continuity of chance constraints.

2.3.3 *Impact Statement*

Besides its contributions to the academic literature, this dissertation should provide some insights to researchers and practitioners working on the sustainable transformation of the power sector:

- Researchers can benefit from the open-source code and data published alongside all proposed methods.
- Distribution system operators can use the proposed methods of uncertainty-aware operation and pricing to improve their short- and long-term planning through an improved evaluation of the expected system state with minimal data requirements.
- Electricity market operators and policymakers may be interested in the proposed approach of internalizing RES uncertainty

and reserve requirements by solving a risk-adjusted deterministic problem instead of a probabilistic problem. Further, the proposed reserve pricing scheme can provide insights for practical data-informed reserve products.

- Power system planners can use the derived decomposition of energy and reserve prices to relate system requirements to uncertainty-statistics with spatial resolution.
- Financial engineers and market theorists may be interested in the proposed connections between power system operation and risk theory.

Part II

RISK-AWARE CONTROL AND DISPATCH

3 CHANCE-CONSTRAINED OPTIMAL POWER FLOW

This chapter derives the CC-DCOPF and CC-ACOPF formulations that form the basis for the results and discussions in subsequent Chapters 4–8. The presented CC-DCOPF extends [7] towards correlated uncertainties, similar to [102]. Derivations of the CC-ACOPF for transmission and radial distribution systems follow [P4], [68] and [P1], [P3], respectively. Some fundamentals on modeling power flows that are required for the derivations in this chapter are summarized in Appendix B.

3.1 PRELIMINARIES

Although the three formulations – CC-DCOPF, radial CC-ACOPF, and meshed CC-ACOPF – require some individual notations and assumptions, those that are shared by all are introduced here following [P4], [68]. Consider an electricity network with n nodes collected in set $\mathcal{N}$ and l lines collected in set $\mathcal{L}$. Further consider set $\mathcal{G}$ of generators and set $\mathcal{U}$ of renewable generators (e.g. wind or commercial solar farms). For simplicity of notation, assume that each node hosts one conventional and one renewable generator, such that $|\mathcal{G}| = |\mathcal{U}| = |\mathcal{N}| = n$. A node with none or multiple generators can be modeled by fixing the generator output limit to zero or by aggregating their injections, respectively. Neither will affect the resulting CC-OPF.

Let vector $p_G \in \mathbb{R}^n$ indexed as $p_{G,i}$, vector $p_D \in \mathbb{R}^n$ indexed as $p_{D,i}$ and vector $p_U \in \mathbb{R}^n$ indexed as $p_{U,i}$ denote the total active power output of conventional generators, the total active power demand and the active power injections from renewable generation at every node. The corresponding reactive power injections are denoted q_G, q_D, q_U and the resulting vectors of net active and reactive power injections are thus given by:

$$p = p_G - p_D + p_U \tag{3.1}$$

$$q = q_G - q_D + q_U. \tag{3.2}$$

Note, that no uncertain component has yet been introduced. The range of admissible active and reactive power generation is $[p_G^{min}, p_G^{max}]$ and $[q_G^{min}, q_G^{max}]$ respectively. Assume that there is no curtailment of renewable generation and that all loads p_D are fixed. These assumptions can be relaxed later. We denote $v \in \mathbb{R}^n$ and $\theta \in \mathbb{R}^n$, indexed as v_i and θ_i, as the vectors of voltage magnitudes and voltage angles. The range of feasible voltage magnitudes is given as $v \in [v^{min}, v^{max}]$.

Each line in $\mathcal{L}$ is a tuple ij denoting its connected nodes $i, j \in \mathcal{N}$. For simplicity, assume a single line between two nodes. Vectors f^p and f^q indexed as f^p_{ij} and f^q_{ij} denote the active and reactive power flows from node i to node j.

At the time of solving the OPF problem, active power injection p_U of uncertain RES is a *forecast* value and the injection in real-time (*ex post*, i.e. after the OPF decision has been made), will likely differ. The real-time deviations from the forecast renewable active power generation p_U is the random vector $\boldsymbol{\omega} \in \Omega$, indexed by $\boldsymbol{\omega}_i$, so that the real-time injection from uncertain renewable sources is given by

$$p_U(\boldsymbol{\omega}) = p_U + \boldsymbol{\omega}. \tag{3.3}$$

Assuming a forecast that is not systematically flawed, the expected value of $\boldsymbol{\omega}$ is $\mathbb{E}[\boldsymbol{\omega}] = 0$ and its variance-covariance matrix is given by $\mathrm{Var}[\boldsymbol{\omega}] = \Sigma$. The space of all possible outcomes of $\boldsymbol{\omega}$ is Ω and, if not otherwise mentioned, $\Omega \equiv \mathbb{R}^n$. Further, assume that the probability distribution of $\boldsymbol{\omega}$ can be modeled by a *normal distribution*. See Box 1 for some additional discussion. Note that random variables are typed in **bold** font.

The cost of active power generation are modeled via a standard *quadratic cost function*, [7], [9], [44], of the form:

$$c_i(p_{G,i}) = c_{2i} p^2_{G,i} + c_{1i} p_{G,i} + c_{0i}, \tag{3.4}$$

where c_{2i}, c_{1i}, and c_{0i} are generator specific parameters.

Box 1 – On centered normal distribution

For most of the formulations, we assume that uncertainty from RES and load forecast errors can be modeled as a centered normal distribution, i.e. $\boldsymbol{\omega} \sim N(0, \Sigma)$. The assumption of zero-mean errors is common in the relevant literature, e.g. [7], [68], [69], [143], [144]. In most cases, as well as in our case, this can be justified by the fact that a non-zero mean error is relatively small as compared to standard deviation values, [145], and it can also be easily incorporated into the formulation by a simple affine transformation. For example, in our formulation a non-zero mean forecast error, i.e. $\mathbb{E}[\boldsymbol{\omega}] = \mu \neq 0$, can be considered by adding it to the forecast value, i.e. $p_U + \mu$. Similarly, one can corroborate the assumption that the error is following a Gaussian distribution. It has been shown in [144], [145] that misfits between empirical and assumed distribution can be compensated by adjustments of the parameters of the normal Gaussian distribution. Thus, the practical advantages of a Gaussian distribution can be exploited without a major loss of generality towards other unimodal distributions. Also, in [145] it has been shown based on empirical data that a Gaussian distribution is a feasible assumption for net load injection forecast errors. Skew corrections may be accounted for by treating the risk-levels (ϵ) of upper and lower constraints asymmetrically. However, such corrections must be conservative to guarantee the required confidence level, [S4], [106].

3.2 CHANCE-CONSTRAINED DCOPF

The non-linear non-convex AC power flow equations often obstruct a straightforward solution of the OPF problem, i.e. the optimization of an objective that is constrained by state variables of the physical power flow. In typical steady-state transmission system analyses, reactive power flows, voltage magnitudes and losses are neglected and the AC power flow equations are replaced by a set of linear equations that approximate active power flows and voltage angles. See Appendix B.4 and [7], [8], [51]. Solving an OPF with this set of linear equations is called DC Optimal Power Flow (DCOPF). To derive the CC-DCOPF formulation, this section recalls the generic DCOPF, formulates uncertain RES injections and the respective system response, and shows how the DCOPF can be modified into a tractable CC-DCOPF. The derivations presented in this section will also provide the basis for the subsequent CC-ACOPF formulations.

3.2.1 *Problem Formulation*

Consider the deterministic DCOPF:

$$\begin{aligned}
\min \quad & c(p_G) && && (3.5a)\\
\text{s.t.} \quad & B^{(n)}\theta = p && && (3.5b)\\
& B^{(f)}\theta = f^p && && (3.5c)\\
& p_{G,i}^{\min} \leqslant p_{G,i} \leqslant p_{G,i}^{\max} && \forall i \in \mathcal{G} && (3.5d)\\
& -f_{ij}^{p,\max} \leqslant f_{ij}^{p} \leqslant f_{ij}^{p,\max} && \forall ij \in \mathcal{L}, && (3.5e)
\end{aligned}$$

where objective (3.5a) minimizes the total cost of electricity supply, i.e. $c(p_G) = \sum_{i \in \mathcal{G}} c_i(p_{G,i})$. Eq. (3.5b) relates the vector of nodal (active) power injections p, as given in (3.1), and voltage angle vector θ via node susceptance matrix $B^{(n)} \in \mathbb{R}^{n \times n}$. Similarly, Eq. (3.5c) relates the vector of (active) power flows f^p and θ via flow susceptance matrix $B^{(f)} \in \mathbb{R}^{l \times n}$. Constraints (3.5d) and (3.5e) enforce the predefined limits of active power generation and active power flow. Problem (3.5) can be solved as a linear program if nodal injections p, and thus flows f^p, are known, i.e. the problem is deterministic.

When, in real-time, renewable injection $p_U(\omega)$ deviates from forecast p_U, as modeled in 3.3, the system needs to restore power balance. Thus, generators will adapt their output following a predefined balancing control policy so that the real-time active power generation is $p_G(\omega)$. Hence, also the relevant state variables become uncertain ($\theta(\omega)$, $f^P(\omega)$), since they depend on forecast error ω and the chosen balancing policy. Given the uncertainty introduced by ω and the corresponding system response, the uncertainty-aware modification of (3.5) is given as:

$$\min \quad \mathbb{E}[c(p_G(\omega))] \tag{3.6a}$$

$$\text{s.t.} \quad B^{(n)}\theta(\omega) = p(\omega) \qquad \forall\omega \tag{3.6b}$$

$$B^{(f)}\theta(\omega) = f^p(\omega) \qquad \forall\omega \tag{3.6c}$$

$$\mathbb{P}[p_{G,i}^{\min} \leqslant p_{G,i}(\omega) \leqslant p_{G,i}^{\max}] \geqslant 1 - 2\epsilon_{p,i} \qquad \forall i \in \mathcal{G} \tag{3.6d}$$

$$\mathbb{P}[-f_{ij}^{p,\max} \leqslant f^p(\omega)_{ij} \leqslant f_{ij}^{p,\max}] \geqslant 1 - 2\epsilon_{f,ij}, \qquad \forall ij \in \mathcal{L}, \tag{3.6e}$$

where objective (3.6a) now minimizes expected cost, equality constraints (3.6b) and (3.6c) must hold for all ω. *Chance constraints* (3.6d) and (3.6e) enforce that generator outputs and flows do not exceed their operational limits with a probability of at least $(1 - \epsilon_p)$ and $(1 - \epsilon_f)$, respectively. Box 2 provides additional discussion on the interpretation of chance constraints. To overcome the infinite dimensionality of problem (3.6) and derive tractable expressions for (3.6d) and (3.6e), we first define a suitable system response model.

Box 2 – On chance constraints as soft constraints.

Constraints that guarantee variables to not exceed given limits with high probability naturally imply a low probability of the variable exceeding this limit. Yet, many constraints in power system models are related to thermal equipment limits with thermodynamic time constants that are larger than the optimization or control horizon.

A transmission line that exceeds its thermal rating will not immediately fail. Rather, it will heat up, sag and eventually trip if the overload persists, [7]. Modeling and optimizing the exact relationship between (stochastic) power injections, line currents and tripping likelihood is possible in approximation, but computationally demanding, [146]. Instead, by enforcing a minimum constraint compliance probability, chance constraints effectively limit the ratio between overload and non-overload time instances without explicitly having to include thermodynamic models.

A similar argument can be made for generators. Limits on power output levels are defined by long-term thermal *and* economic considerations, [34]. Generation limits submitted to power system or market operators are likely more closely related to the economics of fuel efficiency and long term equipment durability. Singular short-term deviations are therefore unlikely to immediately cause generator failures. If a generator requires a strict limitation of its power output, alternative modeling approaches such as excluding it from providing balancing reserve ($\alpha_i = 0$), additional "worst case reserves", [103] or modeling a piecewise linear response, [103], [147], are possible.

Voltage magnitudes are not related to thermodynamic behavior, but related to system stability and power quality. Here, a band of ± 0.05 p.u is typically within normal operations. Short term voltage fluctuations into wider bands might impact the operation of some appliances, but are not necessarily an immediate threat to system stability if suitable reserves are available for corrective action, [50]. See also Section 2.1.1 above.

Finally, note that some constraints that arise in power systems are not suitable to be modeled "softly". For example, energy storage models typically provide a credible state-of-charge with strict physical limitations. Enforcing probabilistic constraints on energy storages, especially over a multi-period horizon, where deviations from forecast net injections carry over to subsequent time steps via a change in SOC, will not accurately capture its true behavior. Instead, a robust approach as in [148] is necessary. (See also discussion in Section 9.2.)

3.2.2 *System Response*

To address the infinite dimensionality of (3.6) we assume an *affine balancing control policy*, i.e. all controllable resources react proportionally to the total system imbalance following AGC settings or system operator commands. See Section 2.1.1 above. Thus, $p_G(\omega)$ is defined in terms of *balancing participation factors* α so that

$$p_G(\omega) = p_G - \alpha e^\top \omega, \tag{3.7}$$

where vector $\alpha \in \mathbb{R}^n_+$ is indexed by α_i and e is the vector of ones with appropriate dimensions.

The resulting vector of nodal active power injections is therefore

$$\begin{aligned} p(\omega) &= p_G(\omega) - p_D + p_U(\omega) \\ &= p_G - \alpha e^\top \omega - p_D + p_U + \omega. \end{aligned} \tag{3.8}$$

Lemma 3.1 (Based on [7, Lemma 2.1])**.** *For any deviation $\omega \in \Omega$ of the forecast renewable injection as per (3.3) and given the affine balancing policy (3.7), system active power is balanced if and only if (i) active power is balanced* in expectation *and (ii)* $e^\top \alpha = 1$.

Proof. System balance requires:

$$e^\top p(\omega) = e^\top(p_G - \alpha e^\top \omega - p_D + p_U + \omega) = 0 \qquad \forall \omega \in \Omega, \tag{3.9}$$

which immediately leads to

$$e^\top(p_G - p_D + p_U) = (e^\top \alpha - 1) e^\top \omega \qquad \forall \omega \in \Omega. \tag{3.10}$$

Condition (3.10) only holds for all ω if

(i) $e^\top(p_G - p_D + p_U) = \mathbb{E}[e^\top p(\omega)] = 0$, and

(ii) $e^\top \alpha = 1$.

Note that (i) uses $\mathbb{E}[\omega] = 0$. □

Now, consider a change of active power flow as a response to uncertain injections $p_U(\omega)$ and control law (3.7). Let matrix $B^{(p)} \in \mathbb{R}^{l \times n}$ define a mapping – called power transfer distribution factor (PTDF) matrix (see Appendix B.4) – between nodal net injections p and power flows f^p such that

$$\begin{aligned} f^P(\omega) = B^{(p)}p(\omega) &= B^{(p)}(p_G - \alpha e^\top \omega - p_D + p_U + \omega) \\ &= B^{(p)}(p_G - p_D + p_U) + B^{(p)}(\omega - \alpha e^\top \omega) \\ &= f^P + B^{(p)}(\omega - \alpha e^\top \omega). \end{aligned} \tag{3.11}$$

Note that it is also possible to compute uncertain voltage angles $\theta(\omega)$ (relative to a reference bus), but (i) this offers no computational advantage for the CC-DCOPF compared to the PTDF-based method presented here and (ii) the exact knowledge of θ is of minor importance for planning stages using the DCOPF.

3.2.3 *Tractable Reformulation*

We now derive a tractable formulation of chance constraints (3.6d) and (3.6e). First, note that violating the the upper or the lower constraint limits are mutually exclusive events so that each of the two-sided chance constraints (3.6d) and (3.6e) can be split into two one-sided chance constraints. Because the modeled ω follows a normal – and thus symmetric – distribution, and the assumed balancing control is symmetric, too, we can write:

$$\begin{aligned} &\mathbb{P}[p_{G,i}^{\min} \leqslant p_{G,i}(\omega) \leqslant p_{G,i}^{\max}] \geqslant 1 - 2\epsilon_{p,i} \\ &\qquad \Leftrightarrow \quad \begin{cases} \mathbb{P}[p_{G,i}(\omega) \leqslant p_{G,i}^{\max}] \geqslant 1 - \epsilon_{p,i} \\ \mathbb{P}[p_{G,i}^{\min} \leqslant p_{G,i}(\omega)] \geqslant 1 - \epsilon_{p,i}, \end{cases} \end{aligned} \tag{3.12}$$

and

$$\begin{aligned} &\mathbb{P}[-f_{ij}^{p,\max} \leqslant f_{ij}^{p}(\omega) \leqslant f_{ij}^{p,\max}] \geqslant 1 - 2\epsilon_{f,ij} \\ &\qquad \Leftrightarrow \quad \begin{cases} \mathbb{P}[f_{ij}^{p}(\omega) \leqslant f_{ij}^{p,\max}] \geqslant 1 - \epsilon_{f,ij} \\ \mathbb{P}[-f_{ij}^{p,\max} \leqslant f_{ij}^{p}(\omega)] \geqslant 1 - \epsilon_{f,ij}. \end{cases} \end{aligned} \tag{3.13}$$

Each of the one-sided chance constraints in (3.12) and (3.13) can be addressed by constraining the value-at-risk (VaR) of the uncertain state variables, [81], [91].

Definition 3.1 ([81, Section 5]). *The* $(1-\epsilon)$*-value-at-risk* $\mathrm{VaR}_{1-\epsilon}$*, or* $(1-\epsilon)$*-quantile, of a random variable* $\mathbf{X}$ *with cumulative distribution function (cdf)* $F_{\mathbf{X}}(z)$ *is defined as:*

$$\mathrm{VaR}_{1-\epsilon}(\mathbf{X}) = \inf\{z \mid F_{\mathbf{X}}(z) \geqslant 1 - \epsilon\}. \tag{3.14}$$

Lemma 3.2. *Let* $\mathbf{X}$ *be a normally distributed random variable. Then:*

$$\mathrm{VaR}_{1-\epsilon}(\mathbf{X}) = \mathbb{E}[\mathbf{X}] + \Phi^{-1}(1-\epsilon)\sigma(\mathbf{X}), \tag{3.15}$$

where Φ^{-1} *denotes the inverse standard normal cdf and* $\sigma(\mathbf{X})$ *the standard deviation of random variable* $\mathbf{X}$*.*

Proof. For any normally distributed variable $\mathbf{X}$ with $\mathbb{E}[\mathbf{X}] = \mu$ and $\sigma(\mathbf{X}) = \sigma$ the inverse cdf F_X^{-1} exists and is defined as:

$$F_X^{-1}(z) = \mu + \sigma \operatorname{erf}^{-1}(2z-1), \tag{3.16}$$

where $\operatorname{erf}^{-1}(2z-1) = \Phi^{-1}(z)$, i.e. the inverse cdf of the *standard* normal distribution. Per definition, $F_X^{-1}(z)$ returns the value that $\mathbf{X}$ will not exceed with probability z. Because any normal distribution is atomless, i.e. there are no jumps in the cdf, it holds that, [91]:

$$\mathrm{VaR}_{1-\epsilon}(\mathbf{X}) = F_X^{-1}(1-\epsilon) = \mathbb{E}[\mathbf{X}] + \Phi^{-1}(1-\epsilon)\sigma(\mathbf{X}). \tag{3.17}$$

□

Corollary 3.1. *Let* $\mathbf{X}$ *be a random variable and* $c \in \mathbb{R}$ *a constant. Enforcing a probability of* X *not exceeding* c *is equivalent to constraining* $\mathrm{VaR}(X)$*:*

$$\mathbb{P}[X \leqslant c] \geqslant 1-\epsilon \quad \Leftrightarrow \quad \mathrm{VaR}_{1-\epsilon}(X) \leqslant c.$$

The reformulation of (3.12) and (3.13) therefore requires expressions $\mathbb{E}[p_{G,i}(\boldsymbol{\omega})]$, $\mathbb{E}[f^p_{ij}(\boldsymbol{\omega})]$, $\sigma(p_{G,i}(\boldsymbol{\omega}))$, and $\sigma(f^p_{ij}(\boldsymbol{\omega}))$. Expectations $\mathbb{E}[f^p_{ij}(\boldsymbol{\omega})]$ and $\sigma(p_{G,i}(\boldsymbol{\omega}))$ follow directly from from (3.7) and (3.11) using $\mathbb{E}[\boldsymbol{\omega}] = 0$:

$$\mathbb{E}[p_{G,i}(\boldsymbol{\omega})] = p_{G,i} \tag{3.18}$$
$$\mathbb{E}[f^p_{ij}(\boldsymbol{\omega})] = f^p_{ij}. \tag{3.19}$$

Standard deviations $\sigma(p_{G,i}(\boldsymbol{\omega}))$ and $\sigma(f^p_{ij}(\boldsymbol{\omega}))$ can be calculated noting that for any random vector $\mathbf{X}$ with covariance matrix Σ_X and constant vectors b, c, it holds that $\sigma(b + c^\top X) = \sqrt{\mathrm{Var}[b + c^\top X]}$ and $\mathrm{Var}[b + c^\top X] = c^\top \Sigma_X c = \left\| c^\top \Sigma_X^{1/2} \right\|_2^2$. Here, $\|\cdot\|_2$ denotes the 2-norm and superscript $\cdot^{1/2}$ denotes a decomposition such that for any matrix $A = A^{1/2}A^{1/2}$. Note that covariance matrices are symmetric and positive semidefinite per definition and, thus, such a decomposition always exists and is unique. It follows that:

$$\sigma(p_{G,i}(\boldsymbol{\omega})) = \alpha_i \sqrt{e^\top \Sigma e} \tag{3.20}$$
$$\sigma(f^p_{ij}(\boldsymbol{\omega})) = \left\| B^{(p)}_{ij} (I - \alpha e^\top) \Sigma^{1/2} \right\|_2, \tag{3.21}$$

where $B^{(p)}_{ij}$ denotes the row vector of the row in $B^{(p)}$ that corresponds to line ij and I is the identity matrix with appropriate dimensions. See Section B.4 for the derivation of $B^{(p)}$.

Expected cost $\mathbb{E}[c(p_G(\omega))]$ in the objective function can be reformulated by first using the quadratic cost model from (3.4) and generator response (3.7):

$$\begin{aligned} c(p_G(\omega)) &= \sum_{i\in\mathcal{G}} c_i(p_{G,i}(\omega)) \\ &= \sum_{i\in\mathcal{G}} [c_{2i}(p_{G,i}(\omega))^2 + c_{1i}p_{G,i}(\omega) + c_{0i}] \\ &= \sum_{i\in\mathcal{G}} [c_{2i}(p_{G,i} - \alpha_i e^\top \omega)^2 + c_{1i}(p_{G,i} - \alpha_i e^\top \omega) + c_{0i}] \\ &= \sum_{i\in\mathcal{G}} [c_i(p_{G,i}) + c_{2i}\alpha_i^2(e^\top \omega)^2 - (p_{G,i} + c_{1i})e^\top \omega]. \end{aligned} \tag{3.22}$$

Next, we apply the expectancy operator and get:

$$\begin{aligned} \mathbb{E}[c(p_G(\omega))] &= \mathbb{E}\sum_{i\in\mathcal{G}} [c_i(p_{G,i}) + c_{2i}\alpha_i^2(e^\top \omega)^2 - (p_{G,i} + c_{1i})e^\top \omega] \\ &= \sum_{i\in\mathcal{G}} [c_i(p_{G,i}) + c_{2i}\alpha_i^2\,\mathbb{E}(e^\top \omega)^2 - (p_{G,i} + c_{1i})\,\mathbb{E}\,e^\top \omega] \\ &\overset{\text{A}}{=} \sum_{i\in\mathcal{G}} [c_i(p_{G,i}) + c_{2i}\alpha_i^2(e^\top \Sigma e)]. \end{aligned} \tag{3.23}$$

For reformulation A in (3.23) we used the fact that for any random variable $\mathrm{Var}[\mathbf{X}] = \mathbb{E}[X^2] - \mathbb{E}[X]^2$, as well as $\mathbb{E}[\omega] = 0$ and $\mathrm{Var}[e^\top \omega] = e^\top \Sigma e$. Note that the reformulated expected cost in (3.23) are now (i) deterministic, (ii) a quadratic function of the committed generation levels p_G and balancing participation factors α_i, and (iii) depending on the total forecast variance $e^\top \Sigma e$, which we denote as S^2.

Using Lemma 3.1, Lemma 3.2, Corollary 3.1 and (3.18)–(3.21) and (3.23) we get the following tractable CC-DCOPF:

$$\begin{aligned} \min \quad & \sum_{i\in\mathcal{G}} [c_i(p_{G,i}) + c_{2i}\alpha^2 S^2] && && (3.24a) \\ \text{s.t.} \quad & B^{(n)}\theta = p_G - p_D + p_U && && (3.24b) \\ & B^{(f)}\theta = f^p && && (3.24c) \\ & e^\top \alpha = 1 && && (3.24d) \\ & p_{G,i} + z_{\epsilon_p}\alpha_i S \leqslant p_{G,i}^{\max} && \forall i \in \mathcal{G} && (3.24e) \\ & -p_{G,i} + z_{\epsilon_p}\alpha_i S \leqslant -p_{G,i}^{\min} && \forall i \in \mathcal{G} && (3.24f) \\ & f_{ij}^p + z_{\epsilon_f} t_{ij} \leqslant f_{ij}^{p,\max} && \forall ij \in \mathcal{L} && (3.24g) \\ & -f_{ij}^p + z_{\epsilon_f} t_{ij} \leqslant f_{ij}^{p,\max} && \forall ij \in \mathcal{L} && (3.24h) \\ & \left\| B_{ij}^{(p)}(I - \alpha e^\top)\Sigma_\omega^{1/2} \right\|_2 \leqslant t_{ij} && \forall ij \in \mathcal{L}, && (3.24i) \end{aligned}$$

where we have defined $z_\epsilon := \Phi(1-\epsilon)$ and $S^2 := e^\top \Sigma e$. Reformulations (3.24e) and (3.24f) of generator chance-constraints (3.6d) are *affine*. Notably term $z_{\epsilon_p} \alpha_i S$ captures the amount of generator reserve capacity as a function of the participation factor, the risk-level ϵ_p and the total uncertainty S. Equation (3.24i) expresses the standard deviation of flows in its SOC form and auxiliary variable t_{ij} relates this standard deviation to the deterministic reformulations (3.24g) and (3.24h) of flow chance-constraints (3.6e). The epigraph relaxation in (3.24i) is exact given the convexity of the SOC expression. Given an objective function that is convex in the decision variables, the resulting problem is conic convex and can be solved efficiently by modern off-the-shelf solvers. See Appendix A for more details on conic optimization and the epigraph relaxation.

3.3 CHANCE-CONSTRAINED ACOPF FOR TRANSMISSION SYSTEMS

We now drop the DCOPF assumptions and explicitly model reactive power flows f^q, voltage angles θ, voltage magnitudes v and losses. This formulation is tailored towards high-voltage transmission systems and was first introduced in [68] and adapted in [P4].

3.3.1 *Problem Formulation*

In the presence of losses, first note that $f^p_{ij} \neq f^p_{ji}$ and $f^q_{ij} \neq f^q_{ji}$ and the apparent power flow limit is denoted by s^{max}_{ij}. We summarize the physical relationship between p, q, f^p, f^q, v and θ as

$$F(p, q, v, \theta) = 0, \tag{3.25}$$

where $F(p, q, v, \theta)$ are the non-linear, non-convex AC power flow equations (B.22). See Appendix B for the detailed derivation. Note that (3.25) also implicitly enforces the power balances. We retain the model of uncertain active power injections $p_U(\boldsymbol{\omega})$ from (3.3). The corresponding uncertain reactive power $q_U(\boldsymbol{\omega})$ is linked to the active power generation through a constant power factor $\cos\phi_i$, i.e. $q_{U,i}(\boldsymbol{\omega}) = q_{U,i} + \gamma_i \boldsymbol{\omega}_i$, where $\gamma_i := \sqrt{1-\cos^2\phi_i}/\cos\phi_i$ and can either be optimized or fixed in advance, e.g to capture the system operator's voltage control strategies. Vector $\gamma \in \mathbb{R}^n$ collects all $\gamma_i, i \in \mathcal{U}$.

Again, any deviation $\boldsymbol{\omega}$ from forecast p_U will cause a specific system response as the combination of explicit control actions to restore power balance and implicit physical reactions. We therefore require a tractable reformulation of the following CC-ACOPF:

$$
\begin{aligned}
\min \quad & \mathbb{E}[c(p_G(\omega))] && && \text{(3.26a)}\\
\text{s.t.} \quad & F(p(\omega), q(\omega), v(\omega), \theta(\omega)) = 0 && \forall \omega && \text{(3.26b)}\\
& \mathbb{P}[p_{G,i}^{\min} \leqslant p_{G,i}(\omega) \leqslant p_{G,i}^{\max}] \geqslant 1 - 2\epsilon_p && \forall i \in \mathcal{G} && \text{(3.26c)}\\
& \mathbb{P}[q_{G,i}^{\min} \leqslant q_{G,i}(\omega) \leqslant q_{G,i}^{\max}] \geqslant 1 - 2\epsilon_p && \forall i \in \mathcal{G} && \text{(3.26d)}\\
& \mathbb{P}[v_i^{\min} \leqslant v_i(\omega) \leqslant v_i^{\max}] \geqslant 1 - 2\epsilon_v && \forall i \in \mathcal{N} && \text{(3.26e)}\\
& \mathbb{P}[(f_{ij}^p(\omega))^2 + (f_{ij}^q(\omega))^2 \leqslant (s_{ij}^{\max})^2] \geqslant 1 - 2\epsilon_f && \forall ij \in \mathcal{L}. && \text{(3.26f)}
\end{aligned}
$$

3.3.2 *System Response*

The active power response $p_G(\omega)$ of each generator is, as in Section 3.2 above, given by participation factors α that represent the relative amount of the system-wide forecast error ($e^\top \omega$) each generator has to compensate for: $p_G(\omega) = p_G - \alpha e^\top \omega$. Again $e^\top \alpha = 1$ is required to balance the system for all ω.

The response of reactive power generation $q_{G,i}(\omega)$, voltage magnitudes $v_i(\omega)$ and voltage angles $\theta_i(\omega)$ is determined by the type of node i. In transmission systems, node types PQ, PV or θV determine which values can be assumed as controlled, i.e. can be modeled as a free decision variable. See Appendix B.3. We denote the set of PQ and PV nodes as $\mathcal{N}^{PQ}, \mathcal{N}^{PV} \subset \mathcal{N}$ and index reference (θV) node as $i = \mathrm{ref}$. At PV nodes $v_i(\omega) = v_i$, $\forall i \in \mathcal{N}^{PV}$ is controlled and $q_{G,i}(\omega)$, $\theta_i(\omega)$, $\forall i \in \mathcal{N}^{PV}$ are implicitly determined by power flow equations $F(p, q, v, \theta)$. Similarly, at PQ nodes $q_{G,i}(\omega) = q_{G,i}$, $\forall i \in \mathcal{N}^{PQ}$ is controlled and $v_i(\omega)$, $\theta_i(\omega)$, $\forall i \in \mathcal{N}^{PQ}$ are implicitly determined by power flow equations $F(p, q, v, \theta)$. Finally, at the θV node $v_{\mathrm{ref}}(\omega) = v_{\mathrm{ref}}$ and $\theta_{\mathrm{ref}}(\omega) = 0$. Thus, active and reactive power response at the θV node is also determined implicitly by power flow equations $F(p, q, v, \theta)$. The resulting active and reactive power flows are implicitly given by $f_{ij}^p(\omega) = f_{ij}^p(v(\omega), \theta(\omega))$ and $f_{ij}^q(\omega) = f_{ij}^q(v(\omega), \theta(\omega))$.

As the implicit system responses are governed by the AC power flow equations in (3.25), a solution can not be obtained directly. Therefore, we use the forecast operating point to linearize $F(p, q, v, \theta) = 0$ using Taylor's theorem as proposed in [68]. Let $(\overline{p}, \overline{q}, \overline{f}^p, \overline{f}^q, \overline{v}, \overline{\theta})$ be the linearization result, then the nodal power injections and line flows are:

$$p_i = \overline{p}_i + J_i^{p,v}(\overline{v},\overline{\theta})v + J_i^{p,\theta}(\overline{v},\overline{\theta})\theta \tag{3.27}$$

$$q_i = \overline{q}_i + J_i^{q,v}(\overline{v},\overline{\theta})v + J_i^{q,\theta}(\overline{v},\overline{\theta})\theta \tag{3.28}$$

$$f_{ij}^p = \overline{f}_{ij}^p + J_{ij}^{fp,v}(\overline{v},\overline{\theta})v + J_{ij}^{fp,\theta}(\overline{v},\overline{\theta})\theta \tag{3.29}$$

$$f_{ij}^q = \overline{f}_{ij}^q + J_{ij}^{fq,v}(\overline{v},\overline{\theta})v + J_{ij}^{fq,\theta}(\overline{v},\overline{\theta})\theta, \tag{3.30}$$

where $J_i^{p,v}, J_i^{p,\theta}, J_i^{q,v}, J_i^{q,\theta}, J_{ij}^{fp}, J_{ij}^{fp,\theta}, J_{ij}^{fq,v}, J_{ij}^{fq,\theta}$ are components of the Jacobian matrix J of F at point $(\overline{p},\overline{q},\overline{f}^p,\overline{f}^q,\overline{v},\overline{\theta})$, i.e. row-vectors of sensitivity factors describing the change of active and reactive nodal injections as functions of v and θ.

Proposition 3.1. *Given the linearized power flow equations (3.27)–(3.30) around the forecast operation point, the implicit system response to forecast deviation $\boldsymbol{\omega}$ can be expressed as an affine relationship:*

$$q_{G,i}(\boldsymbol{\omega}) = q_{G,i} + [R_i^q(I-\alpha e^\top) + X_i^q \operatorname{diag}(\gamma)]\boldsymbol{\omega} \tag{3.31}$$

$$v_i(\boldsymbol{\omega}) = v_i + [R_i^v(I-\alpha e^\top) + X_i^v \operatorname{diag}(\gamma)]\boldsymbol{\omega} \tag{3.32}$$

$$f_{ij}^p(\boldsymbol{\omega}) = f_{ij}^p + [R_{ij}^{fp}(I-\alpha e^\top) + X_{ij}^{fp} \operatorname{diag}(\gamma)]\boldsymbol{\omega} \tag{3.33}$$

$$f_{ij}^q(\boldsymbol{\omega}) = f_{ij}^q + [R_{ij}^{fq}(I-\alpha e^\top) + X_{ij}^{fq} \operatorname{diag}(\gamma)]\boldsymbol{\omega}, \tag{3.34}$$

where row-vectors R_i^q, R_i^v, R_{ij}^{fp}, R_{ij}^{fq} map adjustments of the respective variables to active power changes, row-vectors X_i^q, X_i^v, X_{ij}^{fp}, X_{ij}^{fq} map adjustments of the respective variables to reactive power changes and I is the identity matrix.

Proof. (As presented in [P4, Appendix A]) Rewrite (3.27) and (3.28) in the following form:

$$\begin{bmatrix} p(\boldsymbol{\omega}) \\ q(\boldsymbol{\omega}) \end{bmatrix} - \begin{bmatrix} \overline{p} \\ \overline{q} \end{bmatrix} = \begin{bmatrix} J^{p,v} & J^{p,\theta} \\ J^{q,v} & J^{q,\theta} \end{bmatrix} \begin{bmatrix} v(\boldsymbol{\omega}) \\ \theta(\boldsymbol{\omega}) \end{bmatrix} = J \begin{bmatrix} v(\boldsymbol{\omega}) \\ \theta(\boldsymbol{\omega}) \end{bmatrix}, \tag{3.35}$$

where the rows of matrices $J^\diamond$ are equal to sensitivity vectors $J_i^\diamond$ for $i \in \mathcal{N}$ and $\diamond = \{(p,v);(p,\theta);(q,v);(q,\theta)\}$. First, we sort the rows of the terms in (3.35) by node types and introduce superscripts PQ, PV, θV to indicate the node type:

$$\begin{bmatrix} \begin{bmatrix} p^{PQ}(\boldsymbol{\omega}) \\ p^{PV}(\boldsymbol{\omega}) \\ q^{PQ}(\boldsymbol{\omega}) \end{bmatrix} \\ \begin{bmatrix} p^{\theta V}(\boldsymbol{\omega}) \\ q^{PV}(\boldsymbol{\omega}) \\ q^{\theta V}(\boldsymbol{\omega}) \end{bmatrix} \end{bmatrix} - \begin{bmatrix} \begin{bmatrix} \overline{p}^{PQ} \\ \overline{p}^{PV} \\ \overline{q}^{PQ} \end{bmatrix} \\ \begin{bmatrix} \overline{p}^{\theta V} \\ \overline{q}^{PV} \\ \overline{q}^{\theta V} \end{bmatrix} \end{bmatrix} = \begin{bmatrix} J^A & J^B \\ J^C & J^D \end{bmatrix} \begin{bmatrix} \begin{bmatrix} v^{PQ}(\boldsymbol{\omega}) \\ \theta^{PQ}(\boldsymbol{\omega}) \\ \theta^{PV}(\boldsymbol{\omega}) \end{bmatrix} \\ \begin{bmatrix} v^{PV}(\boldsymbol{\omega}) \\ v^{\theta V}(\boldsymbol{\omega}) \\ \theta^{\theta V}(\boldsymbol{\omega}) \end{bmatrix} \end{bmatrix}, \tag{3.36}$$

where J^{A-D} denote the blocks of re-arranged matrix J from (3.35). Quantities $p^{PQ}(\omega), p^{PV}(\omega), q^{PQ}(\omega)$ are explicitly given by the uncertain generation and the respective system responses such that:

$$\begin{bmatrix} p^{PQ}(\omega) \\ p^{PV}(\omega) \\ q^{PQ}(\omega) \end{bmatrix} - \begin{bmatrix} \overline{p}^{PQ} \\ \overline{p}^{PV} \\ \overline{q}^{PQ} \end{bmatrix} = \begin{bmatrix} p_G^{PQ} \\ p_G^{PV} \\ q_G^{PQ} \end{bmatrix} + \begin{bmatrix} (\omega + \alpha e^\top \omega)^{PQ} \\ (\omega + \alpha e^\top \omega)^{PV} \\ (\operatorname{diag}(\gamma)\omega)^{PQ} \end{bmatrix}. \tag{3.37}$$

Notably, p_U and p_D are not part of the right-hand side of (3.37) because they are fixed parameters. Further, $v^{PV}(\omega) = v^{PV}$, $v^{\theta V}(\omega) = v^{PV}$, and $\theta^{\theta V}(\omega) = \theta^{\theta V}$ due to their node type. We use this relationship and (3.36) and (3.37) to compute the reactions of the uncontrolled variables to uncertainty ω:

$$\begin{bmatrix} v^{PQ}(\omega) \\ \theta^{PQ}(\omega) \\ \theta^{PV}(\omega) \end{bmatrix} - \begin{bmatrix} v^{PQ} \\ \theta^{PQ} \\ \theta^{PV} \end{bmatrix} = (J^A)^{-1} \begin{bmatrix} (\omega + \alpha e^\top \omega)^{PQ} \\ (\omega + \alpha e^\top \omega)^{PV} \\ (\operatorname{diag}(\gamma)\omega)^{PQ} \end{bmatrix}. \tag{3.38}$$

Note that although $v^{PQ}, \theta^{PQ}, \theta^{PV}$ implicitly depend on the AC power flow equations, these variables are endogenous to the model and not subject to uncertainty. Similarly, we get:

$$\begin{bmatrix} p^{\theta V}(\omega) \\ q^{PV}(\omega) \\ q^{\theta V}(\omega) \end{bmatrix} - \begin{bmatrix} p^{\theta V} \\ q^{PV} \\ q^{\theta V} \end{bmatrix} - \begin{bmatrix} \overline{p}^{\theta V} \\ \overline{p}^{PV} \\ \overline{q}^{\theta V} \end{bmatrix} = J^C (J^A)^{-1} \begin{bmatrix} (\omega + \alpha e^\top \omega)^{PQ} \\ (\omega + \alpha e^\top \omega)^{PV} \\ (\operatorname{diag}(\gamma)\omega)^{PQ} \end{bmatrix}. \tag{3.39}$$

Using (3.38), we obtain (3.32) by separating matrix $(J^A)^{-1}$. Similarly, we obtain (3.31) from separating matrix $J^C(J^A)^{-1}$ from (3.39). In analogy, (3.33) and (3.34) can be obtained by noting that $p_i = \sum_{j:ij \in \mathcal{L}} f_{ij}^p$ and $q_i = \sum_{j:ij \in \mathcal{L}} f_{ij}^q$ and combining the sensitivity factors respectively. □

Note that sensitivity vectors $R_i^q, X_i^q, R_i^v, X_i^v, R_{ij}^{f^p}, X_{ij}^{f^p}, R_{ij}^{f^q}, X_{ij}^{f^q}$ can be zero, if i is a PV or PQ node, and depend on the linearization point.

3.3.3 *Tractable Reformulation*

The linear response model of Proposition 3.1 and Lemma 3.2 allow a tractable reformulation of chance constraints (3.26c)–(3.26e), due to the linear dependence of $p_G(\omega)$, $q_G(\omega)$ and $v(\omega)$ to random vector ω. While $f_{ij}^p(\omega)$ and $f_{ij}^q(\omega)$ are in itself also linearly dependent on ω, uncertain apparent power $s_{ij}(\omega) \coloneqq \sqrt{(f_{ij}^p(\omega))^2 + (f_{ij}^q(\omega))^2}$ implies a quadratic dependence that disallows the use of Lemma 3.2. While there exists no tractable direct reformulation of chance constraint (3.26f), it can be replaced by an inner approximation.

Lemma 3.3 (Adapted from [149, Lemmata 5, 17]). *Let the set defined by a quadratic chance constraint be given as*

$$\mathcal{H}_\epsilon = \{(x, a, y, b, k) : \mathbb{P}[(x^\top \omega + a)^2 + (y^\top \omega + b)^2 \leqslant c] \geqslant 1 - \epsilon\},$$

where $x, y \in \mathbb{R}^n$ and $a, b, c \in \mathbb{R}$ are decision variables and ω follows a multivariate Gaussian distribution. For $\epsilon < 1/2$ and fixed $\beta \in (0, 1)$ let

$$\mathcal{G}_{\epsilon,\beta} = \left\{ \begin{array}{c|l} (x, a, y, b, & \mathbb{P}[|x^\top \omega + a| \leqslant t_1] \geqslant 1 - \beta\epsilon \\ & \mathbb{P}[|y^\top \omega + b| \leqslant t_2] \geqslant 1 - (1 - \beta)\epsilon \\ c, t_1, t_2) & t_1^2 + t_2^2 \leqslant c \end{array} \right\},$$

where $t_1, t_2 \in \mathbb{R}$. The projection $\mathcal{G}^{proj}_{\epsilon,\beta}$ of set $\mathcal{G}_{\epsilon,\beta}$ onto variables (a, b, c, d, k) is convex and $\mathcal{G}^{proj}_{\epsilon,\beta} \subseteq \mathcal{H}_\epsilon$, i.e. $\mathcal{G}^{proj}_{\epsilon,\beta}$ is an inner approximation of $\mathcal{H}_\epsilon$.

Proof. Let $t_{xa} = x^\top \omega + a$ and $t_{yb} = y^\top \omega + b$ then $\mathbb{P}[t_{xa}^2 + t_{yb}^2 \leqslant k] \geqslant \mathbb{P}[(t_{xa}^2 \leqslant t_1^2) \cup (t_{yb}^2 \leqslant t_2^2)]$ and we get

$$\begin{aligned} \mathbb{P}[(t_{xa}^2 \leqslant t_1^2) \cup (t_{yb}^2 \leqslant t_2^2)] \geqslant & \mathbb{P}[t_{xa}^2 \leqslant t_1^2] + \mathbb{P}[t_{yb}^2 \leqslant t_2^2] \\ \geqslant & 1 - \beta\epsilon + 1 - (1 - \beta)\epsilon - 1 \\ = & 1 - \epsilon. \end{aligned}$$

Convexity follows from the fact that $\mathbb{P}[|x^\top \omega + a| \leqslant t_1] \geqslant 1 - \epsilon$ if and only if $\mathbb{P}[-t_1 - a \leqslant x^\top \omega \leqslant t_1 - a] \geqslant 1 - \epsilon$ (analogously for y, b, t_2) and that $t_1^2 + t_2^2 \leqslant c$ is a convex quadratic constraint. □

A chance constraint of the form $\mathbb{P}[|x^\top \omega| + a \leqslant c]$ is a special case of the *joint two-sided* chance constraint $\mathbb{P}[c_l \leqslant x^\top \omega \leqslant c_u]$. Normally, we can deal with these constraints by invoking physical arguments as in Section 3.2 above. However, these arguments are infeasible for the application of Lemma 3.3.

Lemma 3.4 (Adapted from [149, Lemma 16]). *Let $\omega \sim N(\mu, \Sigma)$ be a multivariate Gaussian random vector with mean μ and covariance matrix Σ. Further, let $0 < \epsilon \leqslant 1/2$ and $\Sigma^{1/2}(\Sigma^{1/2})^\top = \Sigma$. Then chance constraint $\mathbb{P}[c^{min} \leqslant x^\top \omega \leqslant c^{max}] \geqslant 1 - \epsilon$ can be* outer approximated *by*

$$\begin{aligned} & c^{min} - \mu^\top x \leqslant -z_\epsilon \sigma(x^\top \omega) \\ & c^{max} - \mu^\top x \leqslant z_\epsilon \sigma(x^\top \omega) \\ & c^{min} - c^{max} \leqslant -2 z_{\epsilon/2} \sigma(x^\top \omega), \end{aligned}$$

where $z_\epsilon := \Phi(1 - \epsilon)$. This approximation is equivalent to ensuring

$$\mathbb{P}[c^{min} \leqslant x^\top \omega \leqslant c^{max}] \geqslant 1 - 1.25\epsilon.$$

Proof. See[149, Lemma 16]. □

Using Lemma 3.3 we introduce auxiliary variables $a_{ij}^{f^p}$ and $a_{ij}^{f^p}$, and rewrite (3.26f) as, [P4], [68]:

$$\mathbb{P}[|f_{ij}^{p}| \leqslant a_{ij}^{f^p}] \geqslant 1 - \frac{\epsilon_f}{2} \qquad \forall ij \in \mathcal{L} \tag{3.40a}$$

$$\mathbb{P}[|f_{ij}^{q}| \leqslant a_{ij}^{f^q}] \geqslant 1 - \frac{\epsilon_f}{2} \qquad \forall ij \in \mathcal{L} \tag{3.40b}$$

$$(a_{ij}^{f^p})^2 + (a_{ij}^{f^q})^2 \leqslant s_{ij}^2 \qquad \forall ij \in \mathcal{L}. \tag{3.40c}$$

Constraint (3.40c) is a convex quadratic constraint and constraints (3.40a) and (3.40b) are reformulated using Lemma 3.4, [P4], [68]:

$$f_{ij}^{f^\diamond} + \Phi(1 - \frac{\epsilon_f}{2.5})\sigma(f_{ij}^{\diamond}(\boldsymbol{\omega})) \leqslant a_{ij}^{f^\diamond} \qquad \forall ij \in \mathcal{L} \tag{3.41a}$$

$$-f_{ij}^{\diamond} + \Phi(1 - \frac{\epsilon_f}{2.5})\sigma(f_{ij}^{\diamond}(\boldsymbol{\omega})) \leqslant a_{ij}^{f^\diamond} \qquad \forall ij \in \mathcal{L} \tag{3.41b}$$

$$\Phi(1 - \frac{\epsilon_f}{5})\sigma(f_{ij}^{\diamond}(\boldsymbol{\omega})) \leqslant a_{ij}^{f^\diamond} \qquad \forall ij \in \mathcal{L}, \tag{3.41c}$$

for both $\diamond = p$ and $\diamond = q$. This approximation ensures feasibility of the constraints with desired confidence $1 - \epsilon_f$ and the conservatism of the approximation can be tuned by adapting the divisor (i.e. 2.5 and 5), [68], [149].

The resulting tractable CC-ACOPF is, [P4]:

$$\min \quad \sum_{i \in \mathcal{G}} [c_i(p_{G,i}) + c_{2i}\alpha^2 S^2] \tag{3.42a}$$

$$\text{s.t.} \quad (3.27)\text{–}(3.30) \tag{3.42b}$$

$$\sum_{i \in \mathcal{G}} \alpha_i = 1 \tag{3.42c}$$

$$p_{G,i} + \alpha_i z_{\epsilon_p} S \leqslant p_{G,i}^{max} \qquad \forall i \in \mathcal{G} \tag{3.42d}$$

$$-p_{G,i} + \alpha_i z_{\epsilon_p} S \leqslant -p_{G,i}^{min} \qquad \forall i \in \mathcal{G} \tag{3.42e}$$

$$q_{G,i} + z_{\epsilon_q} t_i^q \leqslant q_{G,i}^{max} \qquad \forall i \in \mathcal{G} \tag{3.42f}$$

$$-q_{G,i} + z_{\epsilon_q} t_i^q \leqslant -q_{G,i}^{min} \qquad \forall i \in \mathcal{G} \tag{3.42g}$$

$$\left\| (R_i^q(I - \alpha e^\top) + X_i^q \operatorname{diag}(\gamma))\Sigma^{1/2} \right\|_2 \leqslant t_i^q \qquad \forall i \in \mathcal{G} \tag{3.42h}$$

$$v_i + z_{\epsilon_v} t_i^v \leqslant v_i^{max} \qquad \forall i \in \mathcal{N} \tag{3.42i}$$

$$-v_i + z_{\epsilon_v} t_i^v \leqslant -v_i^{min} \qquad \forall i \in \mathcal{N} \tag{3.42j}$$

$$\left\| (R_i^v(I - \alpha e^\top) + X_i^v \operatorname{diag}(\gamma))\Sigma^{1/2} \right\|_2 \leqslant t_i^v \qquad \forall i \in \mathcal{G} \tag{3.42k}$$

$\diamond = p, q :$

$$(a_{ij}^{f^\diamond})^2 + (a_{ij}^{f^\diamond})^2 \leqslant (s_{ij}^{max})^2 \qquad \forall ij \in \mathcal{L} \tag{3.42l}$$

$$-a_{ij}^{f^\diamond} + z_{\epsilon_f/2.5} t_{ij}^{f^p} \leqslant f_{ij}^{p} \qquad \forall ij \in \mathcal{L} \tag{3.42m}$$

$$-a_{ij}^{f^\diamond} + z_{\epsilon_f/2.5} t_{ij}^{f^\diamond} \leqslant -f_{ij}^{\diamond} \qquad \forall ij \in \mathcal{L} \tag{3.42n}$$

$$z_{\epsilon_f/5} t_{ij}^{f^\diamond} \leqslant a_{ij}^{f^\diamond} \qquad \forall ij \in \mathcal{L} \tag{3.42o}$$

$$\left\| (R_i^{f^\diamond}(I - \alpha e^\top) + X_i^{f^\diamond} \operatorname{diag}(\gamma))\Sigma^{1/2} \right\|_2 \leqslant t_i^{f^\diamond} \qquad \forall ij \in \mathcal{L}, \tag{3.42p}$$

where we have, as in Section 3.2 above, defined $z_\epsilon := \Phi(1-\epsilon)$ and $S^2 := e^\top \Sigma e$. Objective (3.42a) minimizes the expected generation cost as derived in (3.23). Eq. (3.27)–(3.30) are the active and reactive power balances and flows based on the linearized AC power flow equations. Eq. (3.42c) is the balancing reserve adequacy constraint and (3.42d)–(3.42o) are the deterministic reformulation of chance constraints (3.26c)–(3.26e). Constraints (3.42d) and (3.42e) limit the active power production $p_{G,i}$ and the amount of reserve $\alpha_i z_{\epsilon_p} S$ provided by each generator. Constraints (3.42m)–(3.42o) are the deterministic reformulation of chance constraint (3.26f) using the inner approximation as derived in (3.40) and (3.41) above.

The standard deviation of reactive power outputs, voltage levels and flows resulting from the uncertainty and the system response is given by the SOC constraints (3.42h), (3.42k) and (3.42p). The derivation of these expressions follows analogously to (3.21) on page 37. Given the convexity of the SOC constraints, auxiliary variables t_i^q, t_i^v, t_{ij}^{fp}, t_{ij}^{fq} relate these standard deviations to the reactive output limits (3.42f) and (3.42g), voltage bounds (3.42i) and (3.42j) and flow limits (3.42m)–(3.42o).

3.4 CHANCE-CONSTRAINED ACOPF FOR DISTRIBUTION SYSTEMS

This section presents an CC-ACOPF for radial distribution networks as proposed in [P1]–[P3].

3.4.1 *Problem Formulation*

In the following, we consider a generic low-voltage distribution system with controllable DERs and uncontrollable (behind-the-meter) stochastic generation resources. Therefore, instead of modelling uncertain injection $p_U(\boldsymbol{\omega})$ separately, we fix $p_U = 0$ and write uncertain net demand as

$$\begin{aligned} p_D(\boldsymbol{\omega}) &= p_D - p_U(\boldsymbol{\omega}) \\ &= p_D - (p_U + \boldsymbol{\omega}) \\ &\overset{p_U=0}{=} p_D - \boldsymbol{\omega}, \end{aligned} \tag{3.43}$$

so that p_D aggregates forecast demand and renewable generation. For the distinction between forecast errors in active and reactive power components of the nodal net load injections, there are two reasonable treatment methods, [P1]:

(i) The uncertain nodal injections result from an unpredictable combination of various appliances leading to an equally unpredictable power factor at the bus. If the modeled variance in active and reactive power demand is sufficiently small so that the realized power factor is physically consistent, the random errors can be treated independently such that $p_{D,i}(\omega_i) = p_{D,i} - \omega_i$ and $q_{D,i}(\omega) = q_{D,i} - \omega_i^q$ and $\mathrm{Cov}(\omega_i, \omega_i^q) \approx 0$, $\forall i$.

(ii) The uncertain nodal injections result from the unpredictable utilization of large appliances with a constant power factor. In this case, as in Section 3.3 above, the corresponding uncertain reactive net demand $q_D(\omega)$ is linked to the active net demand through a constant power factor $\cos\phi_i$, i.e.

$$q_{D,i}(\omega) = q_{D,i} - \gamma_i \omega_i, \tag{3.44}$$

where $\gamma_i := \sqrt{1-\cos^2\phi_i}/\cos\phi_i$ can either be optimized or fixed in advance.

For the sake of generality, the following formulations will be based on option (i) and we note that option (ii) can be recovered by defining $\omega_i^q := \gamma_i \omega_i$. We denote Σ_q as the covariance matrix of $\omega^q = [\omega_i^q,\ i \in \mathcal{N}]$ and highlight that $\Sigma_q = \mathrm{diag}(\gamma)\Sigma\,\mathrm{diag}(\gamma)$ when $\omega_i^g := \gamma_i \omega_i$.

As in Section 3.3 for a given power flow and system response model the resulting CC-ACOPF aims to enforce

$$\mathbb{P}[p_{G,i}^{\min} \leqslant p_{G,i}(\omega^{p,q}) \leqslant p_{G,i}^{\max}] \geqslant 1 - 2\epsilon_p \qquad \forall i \in \mathcal{G} \tag{3.45a}$$

$$\mathbb{P}[q_{G,i}^{\min} \leqslant q_{G,i}(\omega^{p,q}) \leqslant q_{G,i}^{\max}] \geqslant 1 - 2\epsilon_q \qquad \forall i \in \mathcal{G} \tag{3.45b}$$

$$\mathbb{P}[v_i^{\min} \leqslant v_i(\omega^{p,q}) \leqslant v_i^{\max}] \geqslant 1 - 2\epsilon_v \qquad \forall i \in \mathcal{N} \tag{3.45c}$$

$$\mathbb{P}[(f_{ij}^p(\omega^{p,q}))^2 + (f_{ij}^q(\omega^{p,q}))^2 \leqslant (s_{ij}^{\max})^2] \geqslant 1 - 2\epsilon_f \quad \forall ij \in \mathcal{L}, \tag{3.45d}$$

where $\omega^{p,q}$ denotes dependency on uncertain active and reactive net demand ω and ω^q. Clearly, the same model and reformulations that have been presented in Section 3.3 can be applied here. However, the radial structure of distribution networks allows a convex relaxation and linearization of power flow equations $F(p, q, v, \theta) = 0$. Here, we use the linear approximation of the *branch-flow model* (*LinDistFlow* to find a suitable system response model. See Section B.5 for derivations of the branch flow and LinDistFlow models.

3.4.2 *System Response*

Consider a distribution system as a radial network given by tree graph $\Gamma(\mathcal{N}, \mathcal{L})$, as in Figure 3.1. We define a *root node* with index $i = 0$ as the substation, i.e. an infinite power source with fixed voltage magnitude v_0. Set $\mathcal{N}^+ := \mathcal{N} \setminus \{0\}$ collects all non-root nodes. Each node is associated with a set of ancestor (or parent) nodes $\mathcal{A}_i$, a set of children nodes $\mathcal{C}_i$ and a set of downstream nodes $\mathcal{D}_i$ (including i). Since Γ is radial, it is $|\mathcal{A}_i| = 1, i \in \mathcal{N}^+$ and all lines $l \in \mathcal{L}$ are indexed by $\mathcal{N}^+$. Each node $i \in \mathcal{N}$ is characterized by its active and reactive net power demand ($p_{D,i}$ and $q_{D,i}$), i.e. the difference between the nodal load and behind-the-meter DER output, and voltage magnitude $v_i \in [v_i^{min}, v_i^{max}]$. To use linear operators, we introduce $u_i = v_i^2$ limited by $u_i^{min} = (v_i^{min})^2$ and $u_i^{max} = (v_i^{max})^2$. In addition to controllable power output $p_{G,i}^P \in [p_{G,i}^{min}, p_{G,i}^{max}]$, we model the controllable reactive power output as $q_{G,i}^P \in [q_{G,i}^{min}, q_{G,i}^{max}]$. Active and reactive power flows on edge i with resistance r_i, reactance x_i and apparent power limit s_i^{max} are given by f_i^P and f_i^Q. Vectors $r = [r_i,\ i \in \mathcal{N}^+]^\top$ and $x = [x_i,\ i \in \mathcal{N}^+]^\top$ collect all resistances and reactances.

All controllable DERs are small-scale generators with given production costs and constant generation limits. As above in (3.7), all controllable generators follow the balancing policy

$$p_{G,i}(\omega) = p_{G,i} - \alpha_i e^\top \omega. \tag{3.46}$$

The same policy is enforced for reactive power balancing as

$$q_{G,i}(\omega^q) = q_{G,i} - \alpha_i e^\top \omega^q. \tag{3.47}$$

Note that we do not distinguish between the participation in active and reactive balancing but use a single α_i for both of these actions.

Leveraging the radial network topology, the *LinDistFlow* formulation allows the following linear recursive approximation of $F(p, q, v, \theta) = 0$ as per (B.35):

$$p_{G,0} - \sum_{j \in \mathcal{C}_0} f_j^p = 0 \tag{3.48a}$$

$$q_{G,0} - \sum_{j \in \mathcal{C}_0} f_j^q = 0 \tag{3.48b}$$

$$f_i^p + p_{G,i} - \sum_{j \in \mathcal{C}_i} f_j^p = p_{D,i} \qquad \forall i \in \mathcal{N}^+ \tag{3.48c}$$

$$f_i^q + q_{G,i} - \sum_{j \in \mathcal{C}_i} f_j^q = q_{D,i} \qquad \forall i \in \mathcal{N}^+ \tag{3.48d}$$

$$u_i + 2(r_i f_i^p + x_i f_i^q) = u_{\mathcal{A}_i} \qquad \forall i \in \mathcal{N}^+. \tag{3.48e}$$

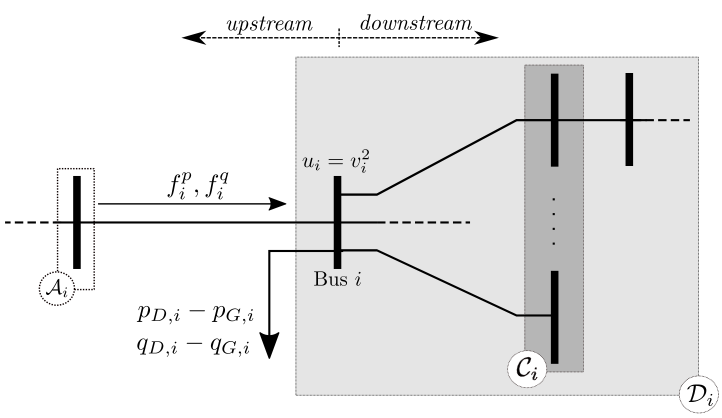

Figure 3.1: Power flow notations in a radial network.

Note that due to the linearization, second- and higher-order terms, and thus power losses, are neglected. A useful correction of this simplification has been proposed in [P3] as reported in Chapter 6.

We find a more compact matrix representation of (3.48c)–(3.48e) by defining the following mappings:

$$A \mid A_{ij} = \begin{cases} 1, & \text{if edge } i \text{ is part of the path} \\ & \text{from root node } 0 \text{ to node } j \\ 0, & \text{otherwise} \end{cases} \quad \forall i,j \in \mathcal{N}^+ \tag{3.49}$$

$$R = A^\top \operatorname{diag}(r) A \tag{3.50}$$

$$X = A^\top \operatorname{diag}(x) A. \tag{3.51}$$

Using the uncertainty models for active and reactive net demand (3.43) and (3.44), active and reactive balancing policies (3.46) and (3.47) and mappings (3.49)–(3.51) we get the system response for each bus $i \in \mathcal{N}^+$:

$$f_i^p(\boldsymbol{\omega}) = A_i p(\boldsymbol{\omega}) = f_i^p + A_i(e - \alpha e^\top)\boldsymbol{\omega} \tag{3.52}$$

$$f_i^q(\boldsymbol{\omega}^q) = A_i q(\boldsymbol{\omega}^q) = f_i^q + A_i(e - \alpha e^\top \boldsymbol{\omega}^q)\boldsymbol{\omega} \tag{3.53}$$

$$\begin{aligned} u_i(\boldsymbol{\omega}^{p,q}) &= 2(R_i p(\boldsymbol{\omega}) + X_i q(\boldsymbol{\omega}^q)) \\ &= u_i - 2R_i(I - \alpha e^\top)\boldsymbol{\omega} - 2X_i(I - \alpha e^\top)\boldsymbol{\omega}^q \\ &= u_i - 2T_i(\alpha)\boldsymbol{\omega}^{p,q}, \end{aligned} \tag{3.54}$$

where $p(\boldsymbol{\omega}) = p_G(\boldsymbol{\omega}) - p_D(\boldsymbol{\omega})$, $q(\boldsymbol{\omega}^q) = q_G(\boldsymbol{\omega}^q) - q_D(\boldsymbol{\omega}^q)$, $T_i(\alpha) := [R_i(I - \alpha e^\top)\ X_i(I - \alpha e^\top)]$, $\boldsymbol{\omega}^{p,q} := [\boldsymbol{\omega}\ \boldsymbol{\omega}^q]^\top$, and A_i, R_i, X_i denote the row vectors corresponding to the i-th row of the respective matrix.

3.4.3 *Tractable Reformulation*

Given linear balancing policies (3.46) and (3.47) generation chance constraints (3.45a) and (3.45b) can be directly reformulated using Corollary 3.1. The same reformulation applies for voltage chance constraints (3.45c) given the linear system response in (3.54) and using covariance matrix:

$$\Sigma_{p,q} = \begin{bmatrix} \Sigma & 0 \\ 0 & \Sigma_q \end{bmatrix}. \tag{3.55}$$

Note that $\Sigma_{p,q}$ can be extended to also capture cross-correlation between $\boldsymbol{\omega}$ and $\boldsymbol{\omega}_q$.

For the reformulation of apparent power flow constraint (3.45d) the results from Lemmas 3.3 and 3.4 can be used. Alternatively, instead of inner-approximating the chance constraint itself, we can also linearize the apparent power flow constraint $(f_i^p)^2 + (f_i^q)^2 \leqslant (\overline{s}_i)^2$ through a twelve-sided polygon:

$$a_{1,c} f_i^P(\boldsymbol{\omega}) + a_{2,c} f_i^Q(\boldsymbol{\omega}_q) + a_{3,c} s_i^{\max} \leqslant 0 \quad c = 1 \ldots 12, \tag{3.56}$$

where $a_{1,c}$, $a_{2,c}$ and $a_{3,c}$ are coefficients[1] of the set of the linearized constraints, [150]. This approach is common in distribution system analyses and has been used to model reactive power limits of power electronic inverter systems in the context of distribution system operations, [150]. Recalling that $\boldsymbol{\omega}$ and $\boldsymbol{\omega}^q$ are independent, it holds that

$$\begin{aligned} &\mathbb{P}[a_{1,c}f_i^P(\boldsymbol{\omega}) + a_{2,c}f_i^Q(\boldsymbol{\omega}_q) + a_{3,c}s_i^{\max} \leqslant 0] \geqslant 1-\epsilon_f \\ &\Leftrightarrow \\ &a_{1,c}(f_i^p + z_{\epsilon_f}t_i^{f^p}) + a_{2,c}(f_i^q + z_{\epsilon_f}t_i^{f^q}) + a_{3,c}s_i^{\max} \leqslant 0, \end{aligned} \tag{3.57}$$

where $t_i^{f^p}$ and $t_i^{f^q}$ refer to the standard deviation of active and reactive power flows and are enforced as:

$$t_i^{f^p} \geqslant \left\| A_i(I - \alpha e^\top)\Sigma^{1/2} \right\|_2 \tag{3.58}$$

$$t_i^{f^q} \geqslant \left\| A_i(I - \alpha e^\top)\Sigma_q^{1/2} \right\|_2 . \tag{3.59}$$

As polyhedral reformulation (3.56) is an inner approximation, the desired confidence level $1-\epsilon_f$ will be maintained by reformulation (3.57). Note that enforcing constraint (3.57) for each side c of the polyhedron slightly overestimates the violation probability when two of the linear constraints are binding, i.e. the optimal solution of the OPF problem lies in the corner of the polyhedron. This leads to a more conservative solution, but maintains the desired level of security.

The complete tractable radial CC-ACOPF is now given as:

$$\min \quad \sum_{i\in\mathcal{G}} [c_i(p_{G,i}) + c_{2i}\alpha^2 S^2] \tag{3.60a}$$

s.t. (3.58), (3.59) and (3.48a)–(3.48e)

$$\sum_{i\in\mathcal{G}} \alpha_i = 1 \tag{3.60b}$$

$$p_{G,i} + z_{\epsilon_p} S\alpha_i \leqslant p_{G,i}^{\max} \qquad \forall i \in \mathcal{G} \tag{3.60c}$$

$$-p_{G,i} + z_{\epsilon_p} S\alpha_i \leqslant -p_{G,i}^{\min} \qquad \forall i \in \mathcal{G} \tag{3.60d}$$

$$q_{G,i} + z_{\epsilon_q} S_q\alpha_i \leqslant q_{G,i}^{\max} \qquad \forall i \in \mathcal{G} \tag{3.60e}$$

$$-q_{G,i} + z_{\epsilon_q} S_q\alpha_i \leqslant -q_{G,i}^{\min} \qquad \forall i \in \mathcal{G} \tag{3.60f}$$

$$u_i + 2z_{\epsilon_v} t_i^v \leqslant u_i^{\max} \qquad \forall i \in \mathcal{N}^+ \tag{3.60g}$$

$$-u_i + 2z_{\epsilon_v} t_i^v \leqslant -u_i^{\min} \qquad \forall i \in \mathcal{N}^+ \tag{3.60h}$$

$$\left\| T_i(\alpha)\Sigma_{p,q}^{1/2} \right\|_2 \leqslant t_i^v \qquad \forall i \in \mathcal{N}^+ \tag{3.60i}$$

$$a_{1,c}(f_i^p + z_{\epsilon_f}t_i^{f^p}) + a_{2,c}(f_i^q + z_{\epsilon_f}t_i^{f^q}) + a_{3,c}s_i^{\max} \leqslant 0 \quad \forall i \in \mathcal{N}^+,\ \forall c \in \{1,\ldots,12\}, \tag{3.60j}$$

---

1 $a_1 = [1, 1, 0.2679, -0.2679, -1, -1, -1, -1, -0.2679, 0.2679, 1, 1]$ indexed as $a_{1,c}$, $c = 1\ldots12$, $a_2 = [0.2679, 1, 1, 1, 1, 0.2679, -0.2679, -1, -1, -1, -1, -0.2679]$ indexed as $a_{2,c}$, $c = 1\ldots12$, $a_3 = [1, 1.366, 1, 1, 1.366, 1, 1, 1.366, 1, 1, 1.366, 1]$ indexed as $a_{3,c}$, $c = 1\ldots12$.

where we used $S_q = \sqrt{e^\top \Sigma_q e}$ and the reformulated expected cost from (3.23) in objective (3.60a).

3.5 CONCLUSION

In this chapter we derived tractable risk-aware modifications of OPF problem for transmission and distribution systems. We first showed how uncertainty can be incorporated into the linear DCOPF problem using chance constraints and presented the necessary assumptions and derivations to obtain an exact deterministic reformulation. We then modified the results of the CC-DCOPF formulation to derive two CC-ACOPF formulations. The first CC-ACOPF solves a risk-aware AC-complete OPF model tailored towards meshed transmission systems. The second CC-ACOPF relies the LinDistFlow approximation of the AC power flow equations for radial distribution systems. The CC-OPF formulations presented in this chapter will be the basis for the analyses presented in the following chapters.

4 DATA-DRIVEN ACTIVE DISTRIBUTION SYSTEM OPERATION

The CC-OPF models presented in previous Chapter 3 exploit the common assumption of modeling uncertain nodal power injections using standard probability distributions with *known parameters* such as mean and variance. However, this assumption does not hold in practice. Thus, this chapter shows a CC-OPF modification that inverse the necessary statistical information from historical data and leverages *distributionally robust optimization* to immunize the CC-OPF against uncertainty in the probabilistic models of forecast errors obtained from the available observations. This modification is applied to the radial CC-ACOPF for distribution systems and its effectiveness is presented in an illustrative case study.

The contents of this chapter have been published in 2018 as the article entitled "Data-driven distributionally robust optimal power flow for distribution systems" in the *IEEE Control Systems Letters*, [P1]. For this dissertation, the original article has been moderately adapted to ensure unified notations and connections to other chapters.

4.1 INTRODUCTION

Established operational paradigms of distribution system operations are under pressure handling the constantly increasing volatility of power generation due to rising numbers of DERs and aging infrastructure [114]. While the integration of DERs is a policy priority in many jurisdictions, reliability and safety concerns may limit the techno-economic benefits of these resources. Realizing the importance of the new and future role of active distribution grids, this chapter takes the perspective of DSOs and aims to facilitate further integration of DERs by leveraging a data-driven distributionally robust decision-making framework to overcome the impacts of uncertain power injections on distribution systems.

Decision-making tools based in OPF are routinely used to schedule and continuously dispatch controllable generators and loads to balance the system with minimal costs and losses with respect to the systems technical constraints (e.g. limits on generation outputs, voltage magnitudes and line flows). The inability to meet these limits may cause system instability and, eventually, lead to cascading failures [7].

To avoid violating these limits in the presence of uncertain power injections, stochastic programming and especially chance constrained-optimization has been leveraged for uncertainty-aware OPF models. The majority of such models have been designed for transmission systems, e.g. [7], [68], [102], and thus are tailored towards their operating needs. The studies in [7], [68], [102] present a risk-controlled CC-OPF leveraging the direct current (DC) power flow linearization. These CC-DCOPF models are proven to effectively tradeoff the likelihood of constraint violationsand the security cost to avoid these violations. On the other hand, DERs are primarily located in distribution systems, where they mainly complicate voltage regulation, [151], and therefore the DC approximation is not technically suitable since it parametrizes voltage magnitudes at rated values.

The models in [7], [68], [102], [151], and those presented in Chapter 3, exploit the common assumption of modeling uncertain nodal power injections using standard probability distributions with *known parameters* such as mean and variance. This assumption does not hold in practice (see, e.g., a data-driven wind power study in [145]). The underlying distribution is never observable, but must be inferred from data. However, a stochastic program tuned towards a given data set often performs poorly when confronted with a different data set, even if it is drawn from the same distribution [152]. Instead of immunizing optimal solutions against worst-case observations that are available (data-robust methods) *distributionally robust optimization* takes the worst-case over a family of distributions that are supported by the sample data [152]–[154]. In the OPF context, distributionally robust optimization has been extensively studied in the for transmission OPF models, e.g. [105], [155]. These studies use the DC power flow approximation to represent power flows in a form suitable for introducing chance constraints and assume knowledge of first and second order distribution moments [106].

This chapter presents a data-driven distributionally robust CC-ACOPF for distribution systems, building on the CC-ACOPF for distribution systems derived in previous Chapter 3. We robustify the formulation by introducing an ambiguous probability distribution of the uncertain input via a distributional uncertainty set (see e.g. [152]). Our case study corroborates the usefulness and scalability of the proposed distributionally robust CC-ACOPF.

4.2 PRELIMINARIES

We use the tractable formulation of the CC-ACOPF for radial distribution systems as presented in (3.60). For the sake of exposition we omit the constraints on apparent power flows and remark that real-life distribution systems are typically voltage-constrained and power flow limits can often be disregarded, e.g. future distribution operations are expected to have "*bounds on system frequency, voltage levels, and DER capacities*", [156]. If an explicit treatment of power flow constraints is required, the method proposed below can be extended accordingly. Further, we assume that the nodal forecast errors are uncorrelated, i.e. $\mathrm{Cov}(\omega_i, \omega_j) = 0 \ \forall i, j \in \mathcal{N} : i \neq j$, a common assumption in the relevant literature, e.g. [7], [69]. As a result we can rewrite some of the expressions in (3.60) as follows, [P1]:

$$S^2 = e^\top \Sigma e = \sum_{i \in \mathcal{N}^+} \mathrm{Var}(\omega_i) \tag{4.1}$$

$$S_q^2 = e^\top \Sigma_q e = \sum_{i \in \mathcal{N}^+} \mathrm{Var}(\omega_i^q) \tag{4.2}$$

$$\begin{aligned} \left\| (T_i(\alpha)\Sigma_{p,q}^{1/2} \right\|_2^2 = & \sum_{j \in \mathcal{N}^+} \mathrm{Var}(\omega_j)\Big(R_{ij} + \sum_{k \in \mathcal{N}^+} R_{ik}\alpha_k\Big)^2 \\ & + \sum_{j \in \mathcal{N}^+} \mathrm{Var}(\omega_j^q)\Big(X_{ij} + \sum_{k \in \mathcal{N}^+} X_{ik}\alpha_k\Big)^2 \end{aligned} \tag{4.3}$$

This leads to the following modification of (3.60), which has been proposed in [P1] and will be used for the remainder of this chapter:

$$\min \quad \sum_{i \in \mathcal{G}} \Big[c_i(p_{G,i}) + c_{2i}\alpha_i^2 \sum_{j \in \mathcal{N}^+} \mathrm{Var}(\omega_j)\Big] \tag{4.4a}$$

s.t. (3.48a)–(3.48e)

(3.58), (3.59), (3.60b), (3.60g) and (3.60h)

$$p_{G,i} + z_{\epsilon_p}\alpha_i \sqrt{\sum_{j \in \mathcal{N}^+} \mathrm{Var}(\omega_j)} \leqslant p_{G,i}^{\max} \qquad \forall i \in \mathcal{G} \tag{4.4b}$$

$$-p_{G,i} + z_{\epsilon_p}\alpha_i \sqrt{\sum_{j \in \mathcal{N}^+} \mathrm{Var}(\omega_j)} \leqslant -p_{G,i}^{\min} \qquad \forall i \in \mathcal{G} \tag{4.4c}$$

$$q_{G,i} + z_{\epsilon_p}\alpha_i \sqrt{\sum_{j \in \mathcal{N}^+} \mathrm{Var}(\omega_j^q)} \leqslant q_{G,i}^{\max} \qquad \forall i \in \mathcal{G} \tag{4.4d}$$

$$-q_{G,i} + z_{\epsilon_p}\alpha_i \sqrt{\sum_{j \in \mathcal{N}^+} \mathrm{Var}(\omega_j^q)} \leqslant -q_{G,i}^{\min} \qquad \forall i \in \mathcal{G} \tag{4.4e}$$

$$\begin{aligned} & \Big(\sum_{j \in \mathcal{N}^+} \mathrm{Var}(\omega_j)(R_{ij} + \sum_{k \in \mathcal{N}^+} R_{ik}\alpha_k)^2 \\ & + \sum_{j \in \mathcal{N}^+} \mathrm{Var}(\omega_j^q)(X_{ij} + \sum_{k \in \mathcal{N}^+} X_{ik}\alpha_k)^2\Big)^{1/2} \leqslant t_i^v \\ & \qquad\qquad \forall i \in \mathcal{N}^+. \end{aligned} \tag{4.4f}$$

4.3 DISTRIBUTIONALLY ROBUST FORMULATION

So far, the presented formulations solve the stochastic problem with the assumption of perfect knowledge of the underlying distribution of the random variable. However, this true distribution can not be known exactly, but is only informed by finite observations of previous realizations. The distribution that we use to define both the expected costs and the chance constraints therefore is ambiguous over the available data. To robustify the formulation robust against uncertain distributions, we redefine the CC-ACOPF objective as follows:

$$\min_{x} \sup_{\mathbb{P} \in \mathcal{P}} \mathbb{E}_{\mathbb{P}}[c(p_G(\boldsymbol{\omega}))], \tag{4.5}$$

where the set $\mathcal{P}$ is the set of all distributions that are supported by the available data within a predefined level of confidence and $\mathbb{E}_{\mathbb{P}}$ is the expectation taken with respect to the distribution $\mathbb{P}$. The task is to minimize the *worst-case expectation* based on the distributional uncertainty set that has been inferred by the data. The quality of the available historic data does not affect our proposed model inherently. However, the accuracy of forecasts and volatility of net loads depend on meteorological and circumstantial externalities. Since stochastic optimization is especially powerful for short-term (e.g. intra-day) system dispatch, it is reasonable to assume the availability of detrended data based on similar conditions (e.g. type of day, season, etc).

4.3.1 *Box-Constrained Ambiguity Set*

Let $\mathcal{H}(\boldsymbol{\omega}_i) := \{\hat{\omega}_{i,t}\}_{t \leqslant N}, i \in \mathcal{N}$ be the set of N observed realizations of the forecast error at bus i for either active or reactive power forecast, where $\hat{\omega}_i = \hat{p}_{D,i} - p_{D,i}$. We introduce the circumflex (^) to mark all values that are based on empirical data. As the forecast error is zero-mean and normally distributed, the distribution can be defined via the *sample variance* of the empirical data at each bus as:

$$\hat{\sigma}_i^2 = \frac{1}{N} \sum_{t \leqslant N} \hat{\omega}_{i,t}^2, \qquad i \in \mathcal{N}. \tag{4.6}$$

Note that the zero mean assumption allows the calculation of $\hat{\sigma}_i^2$ with the full degree of freedom N (as opposed to $N-1$ in the case of estimated mean).

Although the sample variance is the *minimum-variance unbiased estimator* of the unknown distribution, it will never resemble the true variance perfectly while $N < \infty$. It has been shown that the sample variance itself is a random variable following a Chi-Square (χ^2) distribution parameterized by the number of available samples N, [157]. We can use this property to define for each node i an interval $\mathcal{P}_i(\mathcal{H}(\boldsymbol{\omega}_i), \xi)$ that contains the true variance with probability $1-\xi$:

$$\mathcal{P}_i(\mathcal{H}(\boldsymbol{\omega}_i), \xi) = \left[\hat{\zeta}_i^{\text{low}}, \hat{\zeta}_i^{\text{up}}\right], \tag{4.7a}$$

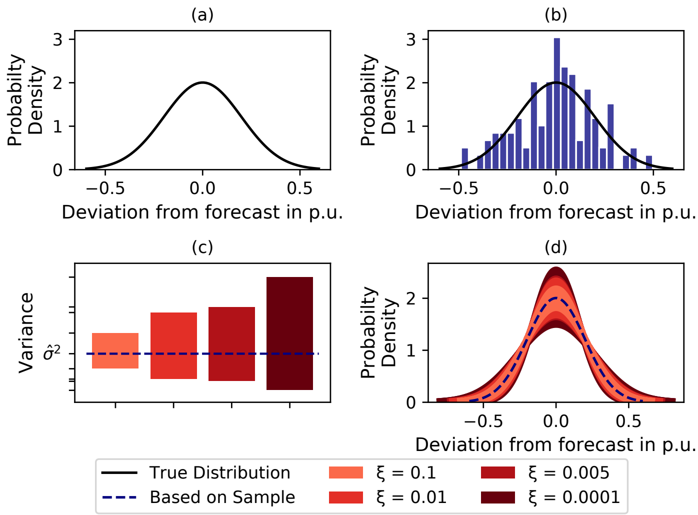

Figure 4.1: Exemplary true distribution, historic observations and uncertainty sets for a bus with a load of 1 p.u.: **(a)** True (unknown) error-distribution with a standard deviation of 20 % of the load. **(b)** $N = 100$ samples drawn from the true error-distribution (blue bar-histogram). **(c)** Uncertainty intervals around sample variance $\hat{\sigma}_N$ for different $(1-\xi)$. **(d)** Set of possible distributions based on $\hat{\sigma}_i$ and the uncertainty intervals, respectively.

where

$$\hat{\zeta}_i^{\text{low}} := \frac{N\hat{\sigma}_i^2}{\chi^2_{N,(1-\xi)/2}}, \quad \hat{\zeta}_i^{\text{up}} := \frac{N\hat{\sigma}_i^2}{\chi^2_{N,\xi/2}}. \tag{4.7b}$$

It is $\chi^2_{N,\xi}$ the ξ-quantile of the χ^2-distribution with N degrees of freedom. Note that the width of the interval will decrease with the amount of available samples and that the χ^2-distribution is not symmetric; The interval will therefore not be centered around $\hat{\sigma}^2$ (cf. Fig. 4.1 (c)). With (4.7a) and (4.7b) we define $\mathcal{P}$ as the set of centred multivariate normal distributions with zero correlation and variances given by sets $\mathcal{P}_i(\mathcal{H}(\boldsymbol{\omega}_i), \xi)$, $\forall i \in \mathcal{N}^+$:

4.3.2 *Worst-Case Expectation*

With the ambiguity set as defined above we can now find the solution to the inner maximization of the expected cost. Based on the generation cost model in (3.4), the expected system cost in (4.4a) is the sum of convex quadratic cost functions of individual generators, which includes the sum of the variances of the forecast errors. With respect to (4.7) the worst-case expectation is given as:

$$\begin{aligned}
&\sup_{\mathbb{P}\mathcal{P}} \mathbb{E}_{\mathbb{P}}[c(p_G(\boldsymbol{\omega}))] \\
&= \sup_{\sigma_i^2 \in \mathcal{P}_i,\ \forall i \in \mathcal{N}^+} \sum_{i \in \mathcal{G}} \Big[c_i(p_{G,i}) + c_{2i}\alpha_i^2 \sum_{j \in \mathcal{N}^+} \sigma_j^2 \Big] \\
&= \sum_{i \in \mathcal{G}} \Big[c_i(p_{G,i}) + c_{2i}\alpha_i^2 \sup_{\sigma_i^2 \in \mathcal{P}_i,\ \forall i \in \mathcal{N}^+} \sum_{j \in \mathcal{N}^+} \sigma_j^2 \Big] \\
&= \sum_{i \in \mathcal{G}} \Big[c_i(p_{G,i}) + c_{2i}\alpha_i^2 \sum_{j \in \mathcal{N}^+} \hat{\zeta}_{j,h} \Big].
\end{aligned} \tag{4.8}$$

The linear relation between the sum of the individual error variances at the nodes and the expected cost leads to the upper bound of the uncertainty region $\hat{\zeta}_i^{up}$ as the worst case expectation of the objective function (cf. [158]).

4.3.3 *Distributionally Robust Formulation*

We can now reformulate the CC-ACOPF problem such that the risk of constraint violations in the presence of uncertain load is minimized and also to account for our data-driven, incomplete knowledge of the underlying error distribution:

$$\min \quad \sum_{i \in \mathcal{G}} \Big[c_i(p_{G,i}) + c_{2i}\alpha_i^2 \sum_{j \in \mathcal{N}^+} \hat{\zeta}_{j,h} \Big] \tag{4.9a}$$

s.t. (3.48a)–(3.48e)

(3.58), (3.59), (3.60b), (3.60g) and (3.60h)

$$p_{G,i} + z_{\epsilon_p}\alpha_i \sqrt{\sum_{j \in \mathcal{N}^+} \hat{\zeta}_{j,h}} \leqslant p_{G,i}^{max} \qquad \forall i \in \mathcal{G} \tag{4.9b}$$

$$-p_{G,i} + z_{\epsilon_p}\alpha_i \sqrt{\sum_{j \in \mathcal{N}^+} \hat{\zeta}_i^{up}} \leqslant -p_{G,i}^{min} \qquad \forall i \in \mathcal{G} \tag{4.9c}$$

$$q_{G,i} + z_{\epsilon_p}\alpha_i \sqrt{\sum_{j \in \mathcal{N}^+} \hat{\zeta}_i^{up}} \leqslant q_{G,i}^{max} \qquad \forall i \in \mathcal{G} \tag{4.9d}$$

$$-q_{G,i} + z_{\epsilon_p}\alpha_i \sqrt{\sum_{j \in \mathcal{N}^+} \hat{\zeta}_i^{up}} \leqslant -q_{G,i}^{min} \qquad \forall i \in \mathcal{G} \tag{4.9e}$$

$$\begin{aligned}
&\Big(\sum_{j \in \mathcal{N}^+} \hat{\zeta}_i^{up} \big(R_{ij} + \sum_{k \in \mathcal{N}^+} R_{ik}\alpha_k\big)^2 \\
&+ \sum_{j \in \mathcal{N}^+} \hat{\zeta}_i^{up} \big(X_{ij} + \sum_{k \in \mathcal{N}^+} X_{ik}\alpha_k\big)^2 \Big)^{1/2} \leqslant t_i^v \\
&\qquad\qquad\qquad\qquad \forall i \in \mathcal{N}^+
\end{aligned} \tag{4.9f}$$

Thus, problem (4.9) is a distributionally robust CC-ACOPF. We use "dr-CC-ACOPF" as a shorthand to reference it. Note that the original problem structure, i.e. quadratic with second-order conic constraints, is retained and thus allows an efficient solution with off-the-shelf solvers.

4.4 ILLUSTRATIVE CASE STUDY

We use the 15-bus radial distribution system from [139] and add two fully controllable generators at nodes 6 and 11 with the production cost of \$10/MWh each in addition to the substation at the root node, which supplies at \$50/MWh. These costs are selected to incentivize the use of distributed generators. We assume that the net load forecasts are given for each node with the zero-mean forecast error and the standard deviation of $\sigma(\boldsymbol{\omega}_i) = 0.2p_{i,D}$. This relation has been shown as a feasible assumption based on empirical data in [106] and [145]. The latter reference also shows how to overcome data misfits inflicted by assuming a normal distribution. as in Fig. 4.1(a).We use this true distribution to obtain $N = 100$ error samples that maintain the node's power factor shown in the histogram of Fig. 4.1(b). In turn, we use these samples and (4.6) – (4.7) to derive uncertainty intervals for different ξ as shown in Fig. 4.1(c). Fig. 4.1(d) displays the resulting distribution used to solve the CC-ACOPF (dashed line) and the uncertainty sets used to solve the distributionally robust CC-ACOPF (colored areas). The CC-ACOPF and dr-CC-ACOPF formulations are then compared in terms of their constraint feasibility and operating cost. To this end, we solve each model and then test their solutions against 750 random samples generated from the true distribution in Fig. 4.1(a), which is sufficient to obtain stable empirical distributions in both cases. We implement the case study using the *Julia JuMP* package [159] and our code and input data can be downloaded from [160].

4.4.1 *In-Sample Evaluation*

Fig. 4.2 presents empirical probabilities of voltage constraint violations (either upper or lower limit) for different η_v. As η_v increases so does the frequency of observed violations. If $\eta_v > 1\%$, the CC-ACOPF and dr-CC-ACOPF have lower empirical violations than the postulated value of η_v. Note that the dr-CC-ACOPF systematically outpeforms the CC-ACOPF. On the other hand, the deterministic ACOPF systematically underperforms relative to both chance-constrained formulations. As ξ reduces, i.e. the uncertainty set in Fig. 4.1(c) spreads, the dr-CC-ACOPF solution becomes more conservative and returns less violations.

Fig. 4.3 compares the expected costs for each OPF formulation normalized by the expected cost of the CC-ACOPF formulation. The nat-

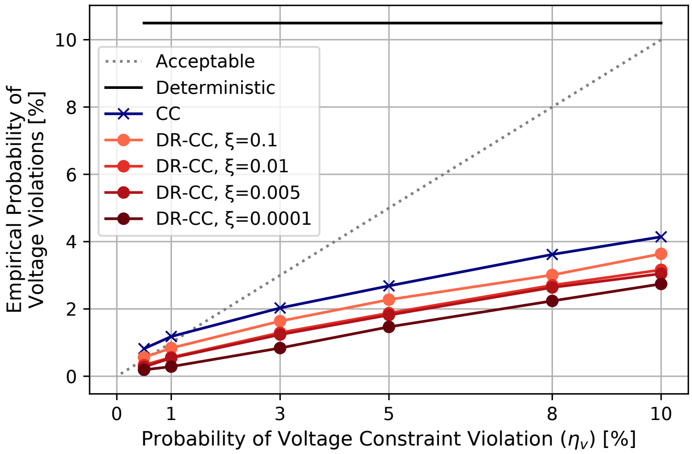

Figure 4.2: Empirical probability of voltage violation in 750 sample cases for different η_ν and ξ.

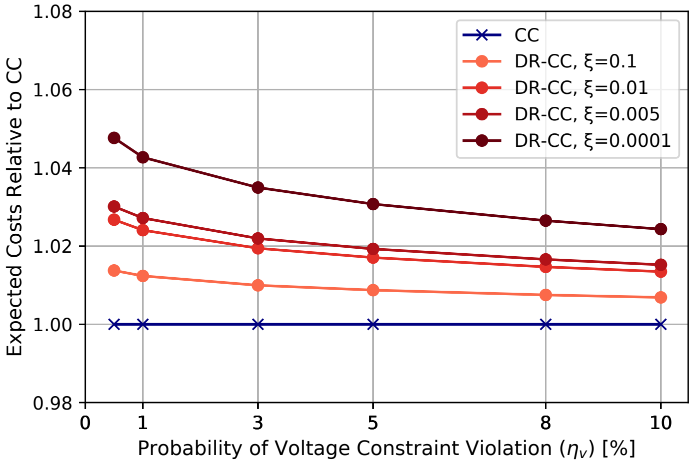

Figure 4.3: Relative expected cost for different η_ν and ξ.

ural conservatism of the dr-CC-ACOPF solution, as follows from better compliance with voltage limits in Fig. 4.2, results in a moderate increase in the expected cost relative to the CC-ACOPF solution. However, the gap between these two formulations narrows as η_ν increases. Similarly, as the width of the uncertainty set in Fig. 4.1(c) increases, so does the worst-case variance and thus the expected cost as per (4.8). Our numerical results suggest that the expected cost is more sensitive to changes in η_ν than to the width of the uncertainty set. The trade-off between the solution feasibility and expected cost is not trivial and DSOs tend to opt a costly, yet more reliable solution, which motivates our out-of-sample performance analysis below.

4.4.2 *Out-of-Sample Performance*

For the following analyses, we generate 750 samples drawn from newly parameterized distributions which are supported by the initial sample data in Fig. 4.1(b), but have a new value of σ^2 shifted towards the upper limit of the uncertainty set by parameter δ. Fig. 4.4 shows the three out-of-sample (OOS) cases and the resulting distributions from which the test samples have been drawn. We use these samples to compare the CC-ACOPF and dr-CC-ACOPF for $\eta_\nu = 3\,\%$ and $\eta_\nu = 5\,\%$ as shown in Fig. 4.5. The CC-ACOPF, which is not immunized against distribution ambiguity, does not satisfy the theoretical violation probability limit in all instances, except for the OOS distribution with $\hat{\sigma}^2 \rightarrow \sigma^2$. On the other hand, the dr-CC-ACOPF holds the theoretical violation probability limit in nearly all cases, except for the two cases related to the smallest distributional uncertainty set. As we can see in Fig. 4.4(a), two of the three OOS cases are outside this set, which explains the empirical violation of the defined η_ν. For other OOS cases, dr-CC-ACOPF meets the requirements posed by the theoretical violation probability limit.

4.4.3 *Computational Effort and Scalability*

The calculations for the case study have been performed on a PC with an Intel Core i5 processor at 2.1 GHz with 4 GB in less than one second each. In order to show the scalability of the proposed model, Table 4.1 summarizes computational performance for larger networks based on the IEEE distribution systems data sets. The results shown in Table 4.1 use the same values of $\epsilon_\nu = 0.05$ and $\xi = 0.005$ for all networks.

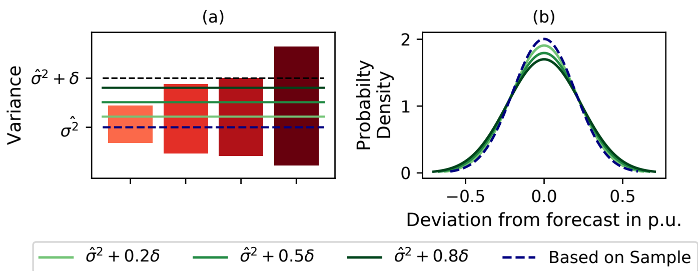

Figure 4.4: Distributions for out-of-sample testing. **(a)** Position of out-of-sample variances in the uncertainty intervals. **(b)**: Resulting error distributions in comparison to the distribution based on sample variance.

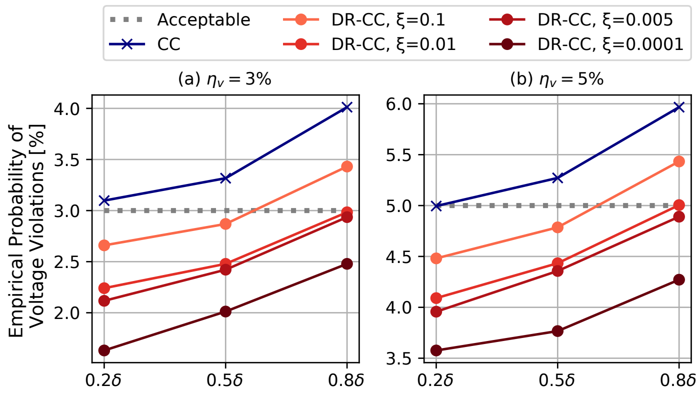

Figure 4.5: Out-of-sample performance: Empirical probability of voltage violations in 750 samples with increasing distance of the true error distribution from the estimated distribution for $\eta_v = 3\%$ (a) and $\eta_v = 5\%$ (b).

Table 4.1: Computation time for larger systems.

Case Name	Computing Time (s)
15-bus system, [139]	< 1
IEEE 37-bus system, [161]	< 1
IEEE 123-bus system, [161]	1.1
IEEE 8500-bus system, [161]	24.2

4.5 CONCLUSION

To overcome the untenable assumption of perfect knowledge of the underlying probability distributions, the risk-aware CC-ACOPF for radial distribution systems is extended to only rely on historical data. By introducing a distributional uncertainty set and leveraging methods of distributionally robust optimization, the formulation is immunized against uncertainty in the probabilistic models of forecast errors obtained from the available observations. The case study reveals that the distributionally robust formulation systemically reduces the empirical probability of voltage violations at a moderate increase in the expected costs. In the conducted out-of-sample performance evaluation, the proposed CC-ACOPF systematically outperforms CC-ACOPF, which is not able to guarantee the theoretical violation probability limit.

5 ONLINE LEARNING FOR NETWORK CONSTRAINED DEMAND RESPONSE

The previous chapter showed a CC-OPF modification that relied on data-informed uncertainty models and additionally robustified the decision making process against uncertainty in the estimated moments (variance). This chapter introduces an extension towards a multi-period decision making process. Here, the system operator tries to learn the statistical properties of demand-side uncertainty in an online fashion, while co-optimizing DER dispatch decisions, reserve allocations and DR pricing signals. Due to the regression-based learning approach, the resulting error distribution can not be modeled exactly and requires a distributionally-robust treatment that goes beyond the moment uncertainty introduced in previous Chapter 4. Further, this chapter discusses guarantees of the learning performance via analysis of regret.

The contents of this chapter have been published in 2019 as the article entitled "Online learning for network constrained demand response pricing in distribution systems" in the *IEEE Transactions on Smart Grid*, [P2]. For this dissertation, the original article has been moderately adapted to ensure unified notations and connections to other chapters.

5.1 INTRODUCTION

Leveraging flexible distributed loads via DR programs allows electric power distribution utilities to mitigate the volatility of intermittent RES and DERs, reducing peak loads, and avoiding electricity surcharges for customers, [24]. Such programs mainly target commercial and industrial loads that are relatively homogeneous in size and technical capabilities and, thus, are fairly easy to price and interface with energy managements systems used by utilities, [25]. On the other hand, enrolling residential-scale DR resources is challenging due to their heterogeneous characteristics and electricity usage patterns and preferences, even if cutting-edge metering and communication technologies are available, [28]. For example, Consolidated Edison of New York has recently introduced its voluntary "Smart Air Conditioner" program, [27]. During peak demand hours, the app-based system requests permission to adjust temperature setting of residential air conditioning units via a WiFi-connected module. In return, residents receive a certain amount of "points", which can be redeemed as retail gift cards. However, this program does not differentiate the

DR participants and, therefore, cannot provide customized incentives to accurately match participant preferences and utility needs. This chapter develops an online learning approach that estimates price sensitivities of residential DR participants and produces price signals that ensures a desired DR capacity.

Existing incentive-based DR programs, e.g. [162]–[164], optimize the amount of demand reduction needed by the system and price signals in a look-ahead manner. However, these approaches do not guarantee that the observed response of DR participants meets the expectation because there is no feedback communication channel from the DR participants to the utility. However, explicitly surveying price sensitivities or two-way *a priori* negotiation incurs a large communication overhead and may expose sensitive data such as consumption habits. Alternatively, utilities may prefer one-way (passive) approaches to learn consumption patterns and preferences of individual DR participants indirectly, [165]. Such indirectly collected data can suffer from various inaccuracies, thus also introducing uncertainty on the deliverable DR capacity.

To realistically estimate the response of each DR participant and reduce its uncertainty, [31], [32], [165], [166] develop online learning methods based on continuous regression. These methods learn the price sensitivity of each DR participants by inferring it from the historical price signals and observed DR responses, and use the inferred value to generate a more accurate price signal. The authors of [31] use an iterative regression algorithm to learn price sensitivities of individual DR participants that can be used by profit-seeking DR aggregators to optimize the total DR capacity offered to the utility. This algorithm is shown to achieve logarithmically progressing regret, i.e. the deviation from the perfect foresight case as a function of the learning horizon. Similarly to [31], the work in [32] develops a risk-averse learning approach for utilities operating residential DR programs, which can provide an explicit probabilistic guarantee on the anticipated payoff of utilities. In a more general approach, [166] develops a learning algorithm that allows for a utility or an DR aggregator to participate in a two-stage (day-ahead and real-time) whole-sale market. The proposed learning algorithm also has logarithmic regret over the learning horizon and is used to obtain the aggregated demand function of the DR participants to optimize the wholesale bidding strategy and arbitrage between the day-ahead and real-time stages. The common limitation of [31], [32], [165], [166] is that distribution network constraints, e.g. nodal voltage and line flow limits, are ignored, which can reduce deliverability of DR capacity in practice.

Modeling network constraints for distribution systems requires considering AC power flows to accurately account for both voltage magnitudes and line flows. Since AC power flow equations are NP-hard, [108], one can use relaxation [167] or linearization [168] tech-

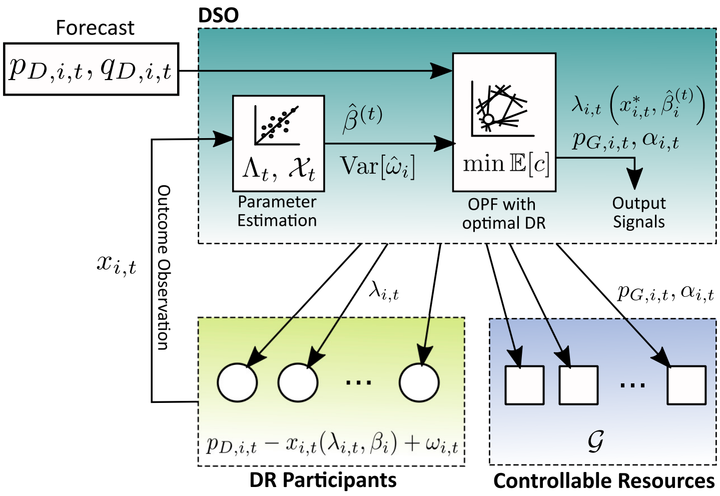

Figure 5.1: The proposed online learning approach in a distribution system with DR participants and controllable resources.

niques for the sake of computational tractability. Additionally, the effect of uncertain nodal injections on voltage magnitudes and line flows must be accounted for. To avoid dealing with computationally demanding scenario-based stochastic programming, we use the chance constrained framework, as introduced in Chapter 3.

This chapter aims to bridge the gap between online learning methods for estimating the price sensitivities of DR participants and the CC-OPF framework. The developed online learning method is a dynamic pricing scheme [169], [170] that optimizes price signals for DR participants with unknown prices and and co-dispatches the DR and system resources as shown in Fig. 5.1.

Given the price signals, the utility observes the response of DR participants and updates its knowledge of price sensitivities. Relative to [31], [32], [165], [166], this chapter internalizes the effects of network constraints and distributionally robust optimization on learning. Distributional robust optimization mitigates risk imposed by incomplete information on DR parameters and underlying uncertain disturbances. By explicitly treating risk as part of the optimization, the model will learn both the DR price sensitivities and the distribution of the load disturbances. Furthermore, by relying on the empirical distribution this work generalizes the approach of [P1] towards uncertain load errors that are potentially non-Gaussian and correlated.

5.2 DR MODEL FOR LEARNING PRICE SENSITIVITIES

This section describes the proposed DR model from the perspective of the utility. We adopt the common practice, where a single DSO controls the entire distribution system and possesses all measurements. Specifically, it is assumed that the DSO can characterize every time interval $t \in \mathcal{T}$ with set $\Lambda_t = \{\lambda_\tau \in \mathbb{R}^m, \forall \tau \leqslant t-1\}$, where λ_τ is the vector of price signals sent to the DR participants at preceding time intervals, and with set $\mathcal{X}_t = \{x_\tau \in \mathbb{R}^m, \forall \tau \leqslant t-1\}$, where x_τ is the vector of observed DR responses. For simplicity, it is assumed that every node of the distribution system hosts one participant that represents the aggregated behavior of all participants connected to that node and, therefore, vectors λ_τ and x_τ can further be itemized for every node such that $\lambda_t = \{\lambda_{i,t} \in \mathbb{R}, \forall i \in \mathcal{N}^+\}$ and $x_t = \{x_{i,t} \in \mathbb{R}, \forall i \in \mathcal{N}^+\}$, respectively. Additionally, the utility possess nodal active and reactive net demand forecasts $p_{D,t} = \{p_{i,D,t} \in \mathbb{R}, \forall i \in \mathcal{N}\}$ and $q_{D,t} = \{q_{i,D,t} \in \mathbb{R}, \forall i \in \mathcal{N}\}$.

Using this information, the DSO acts as follows:

1. It aims to maximize the expected operating cost considering the cost of electricity provision, remuneration for DR participants and revenues from selling energy to consumers.

2. It determines the dispatch of all dispatchable DERs (i.e. power outputs of controllable resources and the amount of reserve they provide) and ensures that all distribution system constraints are met.

3. It generates the DR price signal to achieve a desirable response from the DR participants.

5.2.1 *Price Sensitivity Model*

At time t the DR participant at node i receives the price signal $\lambda_{i,t}$ and has to decide on the amount of demand reduction $x_{i,t}$ that satisfies the trade-off between receiving the remuneration $\lambda_{i,t} x_{i,t}$ and the lost utility of not consuming $x_{i,t}$. Assume that the cost (or lost utility) $w_i(x_{i,t})$ of providing demand response $x_{i,t}$ follows a quadratic function [162] so that

$$w_i(x_{i,t}) = \frac{1}{2}\nu_{1,i} x_{i,t}^2 + \nu_{0,i} x_{i,t}, \tag{5.1}$$

where $\nu_{1,i}$, $\nu_{0,i}$ are participant-specific parameters. The profit maximization problem at each node is therefore given by:

$$\max_{x_{i,t}} \Pi_i(x_{i,t}) \coloneqq \lambda_{i,t} x_{i,t} - w_i(x_{i,t}). \tag{5.2}$$

Under first order optimality conditions, Π_i is maximized if

$$x_{i,t}^* = \frac{1}{\nu_{1,i}}\lambda_{i,t} - \frac{\nu_{0,i}}{\nu_{1,i}}, \tag{5.3}$$

which motivates the choice of the following linear DR model:

$$x_{i,t}(\lambda_{i,t}) = 2\beta_{1,i}\lambda_{i,t} + \beta_{0,i}, \tag{5.4}$$

where $\beta_{1,i} = \frac{1}{2\nu_{1,i}}$ and $\beta_{0,i} = -\frac{\nu_{0,i}}{\nu_{1,i}}$. Similarly to our result in (5.4), [171] shows that linear models fit the majority of price-sensitive demand models, because their dispatchable range is typically small and can be approximated linearly, [32], [172]. One can additionally limit the available DR amount by enforcing an upper bound to restrict the dispatchable DR range to its linear segment, e.g. similarly to (5.23) below.

Due to various externalities (e.g. some short-term adaptations of comfort-level constraints, [173]), the reaction of DR participants to price signal $\lambda_{i,t}$ will be subject to random deviations (noise). As a result, the demand reduction observed by the utility can be represented by random variable $\mathbf{x}_i(\lambda)$, which relates the price signal and uncertain DR capacity, with the following expectation and variance:

$$\mathbb{E}[\mathbf{x}_i(\lambda)] = h(\beta_i, \lambda) = 2\beta_{1,i}\lambda + \beta_{0,i} \tag{5.5}$$

$$\mathrm{Var}[\mathbf{x}_i(\lambda)] = \sigma_i^2 \tag{5.6}$$

where $\beta_i = \{\beta_{0,i}, \beta_{1,i}\}, \forall i \in \mathcal{N}$, are unknown parameters that the DSO needs to learn. In terms of the physical interpretation of this model, parameter $\beta_{0,i} = 0, \forall i \in \mathcal{N}$, ensures that there is no DR for $\lambda_{i,t} = 0$ and parameter $\beta_{1,i} \geqslant 0, \forall i \in \mathcal{N}$, so that the amount of demand reduction is (weakly) increasing as $\lambda_{i,t}$ increases. The variance of the observed DR capacity in (5.6) is constant within a given price range, since it depends on characteristics of the DR participant and does not typically exhibit any noticeable sensitivity to the price signal, [171].

Given (5.5), the error of the observed demand reduction is:

$$\boldsymbol{\omega}_i \coloneqq \mathbf{x}_i(\lambda) - \mathbb{E}[\mathbf{x}_i(\lambda)]. \tag{5.7}$$

As $\mathbb{E}[\mathbf{x}_i(\lambda)]$ is the expected value of $\mathbf{x}_i(\lambda)$, $\mathbb{E}[\boldsymbol{\omega}_i] = 0$ and $\mathrm{Var}[\boldsymbol{\omega}_i] = \mathrm{Var}[\mathbf{x}_i(\lambda)] = \sigma_i^2$ by definition.

Remark 5.1. While parameter $\beta_{0,i}$ in (5.4) is set to zero due to the physical interpretation of the price signal, i.e. $\lambda_{i,t} = 0$ when $x_{i,t} = 0$, we model $\beta_{0,i} \neq 0$ to provide an additional degree of freedom for the parameter estimation process. If $\beta_{0,i} \neq 0$, it captures systematic errors due to the imperfection of demand forecasting and learning.

5.2.2 *Observable Demand Response Error*

As per the model in (5.5), the total demand observed by the DSO at time t is given as:

$$\hat{p}_{D,i,t} = p_{D,i,t} - h(\lambda_{i,t}, \beta_i) - \omega_{i,t} \tag{5.8}$$

where $p_{D,i,t}$ is the forecast demand at node i at time t, $h(\lambda_{i,t}, \beta_i)$ is the true DR expectation based on unknown parameter β_i and price signal $\lambda_{i,t}$, and error $\omega_{i,t}$ is a given realization drawn from random vector $\boldsymbol{\omega}_i$. Since the DSO can only observe the total difference between the forecast and actual demand, $\omega_{i,t}$ includes both the forecast error of $p_{D,i,t}$ and the DR noise of $h(\lambda_{i,t}, \beta_i)$. Using this aggregated error, we recover the observed DR capacity as:

$$x_{i,t} = p_{D,i,t} - \hat{d}_{D,i,t}, \tag{5.9}$$

where $x_{i,t}$ internalizes aggregated demand variance regardless of its cause, which can be included in the CC-OPF below. In practice, net demand observations $\hat{p}_{D,i,t}$ for each time step t will be obtained from SCADA or user-end smart meter measurements. Since a typical temporal resolution of these measurements (subseconds to minutes) is smaller than the resolution of DR programs (minutes to hours), [28], random measurement errors can be mitigated by simple filtering, e.g. averaging, [174]. Since such a filtering procedure can be executed as a pre-processing step for the proposed learning scheme, $\hat{p}_{D,i,t}$ represents refined measurements.

Observing true disturbance $\omega_{i,t}$, however, is impossible without knowing the true expectation of $\mathbf{x}_i$, i.e. knowledge of true parameters β_i. Therefore, the DSO only observes the *residual* error that can be computed as follows:

$$\hat{\omega}_{i,\tau}^{(t)} = x_{i,\tau} - h(\lambda, \hat{\beta}_i^{(t)}) \qquad \forall \tau \leqslant t-1, \tag{5.10}$$

where $\hat{\beta}_i^{(t)}$ is the estimate of the price sensitivity parameters of node i available to the DSO at time t. If the estimate was perfect, i.e. $\hat{\beta}_i^{(t)} = \beta_i$, the residual error $\hat{\omega}_{\tau,i}^{(t)}$ would be equal to true disturbance $\omega_{\tau,i}$ for all previous timesteps $\tau \in \{1, \dots, t-1\}$.

5.2.3 *Learning Price Sensitivities*

At each time step the DSO computes estimates $\hat{\beta}_{0,i}^{(t)}$ and $\hat{\beta}_{1,i}^{(t)}$ of unknown parameters $\beta_{0,i}$, $\beta_{1,i}$ to update price sensitivity model $h(\lambda, \hat{\beta}_i^t)$ and to evaluate the residual error in (5.10). These estimates can be obtained from historical observations Λ_t and $\mathcal{X}_t$ using the least-square estimator (LSE) as follows:

$$\hat{\beta}_{1,i}^{(t)} = \frac{\sum_{\tau=1}^{t-1}(\lambda_{i,\tau} - \overline{\lambda}_{i,t})(x_{i,\tau} - \overline{x}_{i,t})}{2\sum_{\tau=1}^{t-1}(\lambda_{i,\tau} - \overline{\lambda}_{i,t})^2} \tag{5.11}$$

$$\hat{\beta}_{0,i}^{(t)} = \overline{x}_{i,t} - \hat{\beta}_{1,i}\overline{\lambda}_{i,t}, \tag{5.12}$$

with

$$\overline{\lambda}_{i,t} = \frac{1}{t-1}\sum_{\tau=1}^{t-1}\lambda_{i,\tau}, \quad \overline{x}_{i,t} = \frac{1}{t-1}\sum_{\tau=1}^{t-1}x_{i,\tau}. \tag{5.13}$$

These estimators are derived by minimizing the sum of the squared errors:

$$\min_{\hat{\beta}_{1,i}^{(t)},\hat{\beta}_{0,i}^{(t)}} \sum_{\tau=1}^{t-1} \left(2\hat{\beta}_{1,i}^{(t)}\lambda_{i,\tau} + \hat{\beta}_{0,i}^{(t)} - x_{i,\tau}\right)^2. \tag{5.14}$$

The resulting first-order optimality conditions are given by:

$$\left(\hat{\beta}_{1,i}^{(t)}\right): \quad \sum_{\tau=1}^{t-1} \left(2\hat{\beta}_{1,i}^{(t)}\lambda_{i,\tau}^2 + \hat{\beta}_{0,i}^{(t)}\lambda_{i,\tau} - \lambda_{i,\tau}x_{i,\tau}\right) = 0, \tag{5.15}$$

$$\left(\hat{\beta}_{0,i}^{(t)}\right): \quad \sum_{\tau=1}^{t-1} \left(\hat{\beta}_{0,i}^{(t)} + 2\hat{\beta}_{1,i}^{(t)}\lambda_{i,\tau} - x_{i,\tau}\right) = 0. \tag{5.16}$$

By using $\sum_{\tau=1}^{t-1} x_{i,\tau} = (t-1)\overline{x}_{i,t}$ and $\sum_{\tau=1}^{t-1} \lambda_{i,\tau} = (t-1)\overline{\lambda}_{i,t}$, we can insert (5.16) into (5.15) to obtain:

$$\hat{\beta}_{1,i}^{(t)} = \frac{\sum_{\tau=1}^{t-1} \lambda_{i,\tau}x_{i,\tau} - (t-1)\overline{\lambda}_{i,t}\overline{x}_{i,t}}{2\sum_{\tau=1}^{t-1} \lambda_{i,\tau}^2 - (t-1)\overline{\lambda}_{i,t}^2} \tag{5.17}$$

$$\hat{\beta}_{0,i}^{(t)} = \overline{x}_{i,t} - \hat{\beta}_{1,i}^{(t)}\overline{\lambda}_{i,t}. \tag{5.18}$$

By recasting $\sum_{\tau=1}^{t-1} \lambda_{i,\tau}x_{i,\tau} - (t-1)\overline{\lambda}_{i,t}\overline{x}_{i,t}$ into $\sum_{\tau=1}^{t-1}(\lambda_{i,\tau} - \overline{\lambda}_{i,t})(x_{i,\tau} - \overline{x}_{i,t})$ and $\sum_{\tau=1}^{t-1} \lambda_{i,\tau}^2 - (t-1)\overline{\lambda}_{i,t}^2$ into $\sum_{\tau=1}^{t-1}(\lambda_{i,\tau} - \overline{\lambda}_{i,t})^2$ we obtain the expressions (5.11) and (5.12). Note that for efficient practical implementation, instead of performing calculations (5.17) and (5.18), estimates $\hat{\beta}_i^(t)$ can be updated using $\hat{\beta}_i^(t-2)$ and new data points λ_{t-1}, x_{t_1}.

The estimation approach via LSE fundamentally matches the price sensitivity model (5.4) and using $\hat{\beta}_{1,i}^{(t)}$ and $\hat{\beta}_{0,i}^{(t)}$, we obtain the expected DR participation $h(\lambda, \hat{\beta}_i^{(t)})$ as a function of λ based on the available historical data. After estimating $h(\lambda, \hat{\beta}_i^{(t)})$, we obtain set of residual vectors $\hat{\mathcal{E}}_t = \{\hat{\omega}_1^{(t)}, \hat{\omega}_2^{(t)}, \dots, \hat{\omega}_{t-1}^{(t)}\}$, where each element $\hat{\omega}_\tau^{(t)}$ is a vector of nodal residual errors from (5.10) for each time t, i.e. $\hat{\omega}_\tau^{(t)} = \{\hat{\omega}_{i,\tau}^{(t)}, \forall i \in \mathcal{N}\}$. As the learning procedure progresses, set $\hat{\mathcal{E}}_t$ is updated at every time t because its elements depend on the value of parameters $\hat{\beta}_{0,i}^{(t)}$ and $\hat{\beta}_{1,i}^{(t)}$ obtained at time t.

The residual errors, estimated as described above, are then used to characterize random vector $\boldsymbol{\omega}$ in an empirical manner, i.e. based on the observations collected by the DSO. This residual-error-centric approach has multiple advantageous properties. First, since the random error is independent from the price signal, the LSE method yields that the expected value of the residual error observed by the DSO is zero, i.e. $\mathbb{E}[\hat{\omega}_t|\Lambda_t, \mathcal{X}_t] = 0$. Note that this property is obtained by not restricting $\hat{\beta}_{0,i}$ to zero but allowing the estimator to find the minimal error with all possible degrees of freedom. Second, at every time interval t the empirical mean vector $\hat{\mu}^{(t)}$ and empirical covariance matrix $\hat{\Sigma}^{(t)}$ can be computed as:

$$\hat{\mu}^{(t)} = \frac{1}{t-1} \sum_{\tau=1}^{t-1} \omega_\tau \tag{5.19}$$

$$\hat{\Sigma}^{(t)} = \frac{1}{t-2} \sum_{\tau=1}^{t-1} (\hat{\omega}_\tau - \hat{\mu}^{(t)})(\hat{\omega}_\tau - \hat{\mu}^{(t)}) \quad \forall i, j \in \mathcal{N}. \tag{5.20}$$

These parameters $\hat{\mu}^{(t)}$ and $\hat{\Sigma}^{(t)}$ can be leveraged toward the CC-OPF described below. Using these characteristics of the empirical distribution allows to overcome the limitation of making specific assumptions on the true underlying distribution (e.g. Gaussian as in [P1], [S1], [7], [69]). Rather, learning can be performed over empirical data sets, while fully accounting for spatio-temporal sensitivities captured in the covariance matrix. In the context of DR participant scattered across a given distribution system, such sensitivities are particularly self-manifesting due to similar external conditions. The LSE above can be adapted to deal with time-variable behavior of DR participants. For instance, if the price sensitivity varies across a given day (e.g. morning, afternoon, night), different sets of sensitivities can be learned for different time periods. This way, imperfections of linear response functions (e.g. minimum and maximum cut-off DR regions) can be mitigated. Furthermore, allowing for $\hat{\beta}_{0,i} \neq 0$ also contributes to improving the estimation of potential nonlinearites close to the bounds of the response domain (e.g. close to saturation), [175]. Further, the LSE can be adapted to either discard older data points or to weight relatively recent data points higher than older ones to capture systematic sensitivity changes. In this chapter, we only consider time-invariant price sensitivities.

5.3 DISTRIBUTIONALLY ROBUST SYSTEM MODEL

The DSO determines the optimal amount of *desired* DR participation $x^*_{i,t}$ at each node i and time t that leads to minimal cost to meet electricity demand while maintaining physical system limits with high probability. Its decision on optimal $x^*_{i,t}$ can only be based on previous estimates $\hat{\beta}_i^{(t)}$ of the unknown parameters.

5.3.1 *Radial CC-ACOPF with Demand Response*

The uncertain nature of DR responses are accounted for in the optimal DSO decision via a suitable CC-ACOPF formulation. Here, we use the formulation from Section 3.4 but modify the expression of uncertain net-demand from (3.43) to include the desired demand response x^* as:

$$p_{D,i}(\omega, x^*) = p_{D,i,t} - (x^*_{i,t} + \omega_i) \tag{5.21}$$
$$q_{D,i}(\omega, x^*) = q_{D,i,t} - \gamma_{i,t}(x^*_{i,t} + \omega_i). \tag{5.22}$$

Note, that in this chapter we opt for treating changes in reactive power consumption to be connected to changes in active power consumption via factor $\gamma_{i,t}$, see also (3.44) and discussion in Section 3.4. The available amount of demand reduction is limited by the nodal demand:

$$\overline{p}_{D,i,t} - x^*_{i,t} \geqslant 0. \tag{5.23}$$

With (5.21) and (5.22) the *LinDistFlow* power balance equations (3.48c) and (3.48d) become:

$$(p_{D,i,t} - x^*_{i,t} - p_{G,i,t}) + \sum_{j \in \mathcal{C}_i} f^p_{j,t} = f^p_{\mathcal{A}_i,t} \quad \forall t, \forall i \in \mathcal{N}^+ \tag{5.24}$$
$$(q_{D,i,t} - \gamma_{i,t} x^*_{i,t} - q_{G,i,t}) + \sum_{j \in \mathcal{C}_i} f^q_{j,t} = f^q_{\mathcal{A}_i,t} \quad \forall t, \forall i \in \mathcal{N}^+. \tag{5.25}$$

For the expressions for uncertain flows and voltages we get:

$$f^p_{i,t}(\omega) = f^p_{i,t} A_i (e - \alpha_t e^\top)\omega \tag{5.26}$$
$$f^q_{i,t}(\omega) = f^q_{i,t} A_i (e - \alpha_t e^\top)\operatorname{diag}(\gamma_t)\omega, \tag{5.27}$$
$$\begin{aligned} u_{i,t}(\omega) &= u_{i,t} - 2X_i(I - \alpha_t e^\top) - 2R_i(I - \alpha_t e^\top)\operatorname{diag}(\gamma_t) \\ &= u_{i,t} - T^v_i(\alpha_t, \gamma_t), \end{aligned} \tag{5.28}$$

with matrices A, R, X as defined in (3.49)–(3.51).

Further, expected system cost need to be extended to capture the lost revenue from not selling $\sum_{i \in \mathcal{N}^+} x_i$ at retail tariff κ_t and remunerating the DR participants:

$$\mathbb{E}[\mathbf{C}^{\text{total}}] = \mathbb{E}[c(p_G(\omega))] + \mathbb{E}[\mathbf{C}^{(\text{sale})}_t] + \mathbb{E}[\mathbf{C}^{(\text{DR})}_t]. \tag{5.29}$$

Lost revenue $\mathbb{E}[\mathbf{C}^{(\text{sale})}_t]$ can be written as

$$\mathbb{E}[\mathbf{C}^{(\text{sale})}_t] = \kappa_t \sum_{i \in \mathcal{N}} x^*_{i,t}, \tag{5.30}$$

where we used the fact that the expected DR $h(\lambda, \hat{\beta}^{(t)}_i)$ based on estimators $\hat{\beta}^{(t)}_i$ is unbiased. Further, the DR remuneration $\mathbb{E}[\mathbf{C}^{(\text{DR})}_t]$ depends on the desired amount of demand response $x^*_{i,t}$ and price signal λ. Using (5.5) and the desired DR capacity $x^*_{i,t}$, price signal $\lambda_{i,t}$ can be computed as follows:

$$\lambda_{i,t} = \frac{x^*_{i,t} - \hat{\beta}^{(t)}_{0,i}}{2\hat{\beta}^{(t)}_{1,i}}, \tag{5.31}$$

where we have to make the technical assumption $\hat{\beta}_{1i}^{(t)} \neq 0$. This assumption is not restrictive because estimations close to zero will lead to prohibitively high price signals, which will lead to the same result as if true parameter $\beta_{1,i}$ were actually equal to zero (i.e. a node that is insensitive to DR incentive signals). Accordingly, the last term in (5.29) can be recast as:

$$\mathbb{E}[\mathbf{C}_t^{(DR)}] = \sum_{i \in \mathcal{N}} x_{i,t}^* \frac{x_{i,t}^* - \hat{\beta}_{0,i}^{(t)}}{2\hat{\beta}_{1,i}^{(t)}}. \tag{5.32}$$

The resulting radial CC-ACOPF with demand response used in this chapter is thus given as:

$$\begin{aligned}
&\min \quad \mathbb{E}[\mathbf{C}^{\text{total}}] && && \text{(5.33a)}\\
&\text{s.t. } \forall t \in \mathcal{T},\ \forall \boldsymbol{\omega}: && && \\
&\quad (5.24) \text{ and } (5.25) && && \\
&\quad p_{G,0} - \sum_{j \in \mathcal{C}_0} f_j^p = 0 && && \text{(5.33b)}\\
&\quad q_{G,0} - \sum_{j \in \mathcal{C}_0} f_j^q = 0 && && \text{(5.33c)}\\
&\quad u_{i,t} + 2(r_i f_{i,t}^p + x_i f_{i,t}^q) = u_{\mathcal{A}_i} && \forall i \in \mathcal{N}^+ && \text{(5.33d)}\\
&\quad \sum_{i \in \mathcal{G}} \alpha_i = 1 && && \text{(5.33e)}\\
&\quad \mathbb{P}[p_{D,i,t}(\boldsymbol{\omega}) \leqslant p_i^{\max}] \geqslant 1 - \epsilon_p, && \forall i \in \mathcal{N}^+ && \text{(5.33f)}\\
&\quad \mathbb{P}[p_{D,i,t}(\boldsymbol{\omega}) \geqslant p_i^{\min}] \geqslant 1 - \epsilon_p, && \forall i \in \mathcal{N}^+ && \text{(5.33g)}\\
&\quad \mathbb{P}[p_{D,i,t}(\boldsymbol{\omega}) \leqslant p_i^{\max}] \geqslant 1 - \epsilon_p, && \forall i \in \mathcal{N}^+ && \text{(5.33h)}\\
&\quad \mathbb{P}[p_{D,i,t}(\boldsymbol{\omega}) \geqslant p_i^{\min}] \geqslant 1 - \epsilon_p, && \forall i \in \mathcal{N}^+ && \text{(5.33i)}\\
&\quad \mathbb{P}[u_{i,t}(\boldsymbol{\omega}) \leqslant u_i^{\max}] \geqslant 1 - \epsilon_v, && \forall i \in \mathcal{N}^+ && \text{(5.33j)}\\
&\quad \mathbb{P}[u_{i,t}(\boldsymbol{\omega}) \geqslant u_i^{\min}] \geqslant 1 - \epsilon_v, && \forall i \in \mathcal{N}^+ && \text{(5.33k)}\\
&\quad (f_{i,t}^p(\boldsymbol{\omega}))^2 + (f_{i,t}^q(\boldsymbol{\omega}))^2 \geqslant (s_i^{\max})^2 i && \in \mathcal{N}^+ && \text{(5.33l)}
\end{aligned}$$

Note that constraints on thermal transmission capacity are treated deterministically for simplicity as discussed in Section 4.2.

5.3.2 *Distributionally Robust Solution*

As the uncertainty distribution underlying $\boldsymbol{\omega}$ is unknown *a priori*, the chance constraints cannot be reformulated into SOC constraints as common for various parametric distributions, see Chapter 3. Additionally, the regression-based learning approach obstructs the derivation of an exact underlying distribution. Consistently with distribution-free assumptions in price sensitivity learning in Section 5.2.3, we extend the CC-ACOPF formulation to a distributionally robust form that eliminates the need of invoking potentially erroneous distribution assumptions. In contrast to the distributionally robust formulations in previous Chapter 4, the approach in this Chapter relies on empirical moments without modeling a specific distribution function.

Empirical mean and variance values of the residual errors given in (5.19)-(5.20) can be associated with multiple distributions that are collected in set $\mathcal{P}$. In the following we show the exemplary derivation of the distributionally robust chance-constraint for upper voltage chance constraint (5.33j). Using set $\mathcal{P}$, this constraint yields the following general distributionally robust formulation:

$$\inf_{\mathbb{P}\in\mathcal{P}} \mathbb{P}[u_{i,t}(\boldsymbol{\omega}_t) \leqslant u_i^{\max}] \geqslant 1-\epsilon_v \qquad \forall t \in \mathcal{T}, \forall i \in \mathcal{N}. \tag{5.34}$$

To reformulate distributionally robust constraint (5.34) in a tractable form, we use $T_i^v(\alpha_t, \gamma_t)$ from (5.28), which captures the effect of fluctuations imposed by random vector $\boldsymbol{\omega}_t$ on the voltage magnitude at node i, depending on the chosen α_t and current γ_t. These fluctuations must be contained within given voltage limits u_i^{max}:

$$u_i^{\max} - s_{i,t}^{v,\max} \geqslant u_{i,t}, \tag{5.35}$$

where $s_{i,t}^{v,max}$ is a slack variable that represents the distance between baseline value $u_{i,t}$ and its limit u_i^{max}. Naturally, if $T_i(\alpha_t, \gamma_t)\omega_t \leqslant s_{i,t}^{v,max}$ holds for a given realization ω_t of $\boldsymbol{\omega}$ then the fluctuations are within the limit. Therefore, in combination with (5.35), distributionally robust constraint (5.34) can be equivalently reformulated as:

$$u_i^{\max} - s_{i,t}^{v,\max} \geqslant u_{i,t} \tag{5.36a}$$

$$\inf_{s_{i,t}^{v,\max}, \mathbb{P}\in\mathcal{P}} \mathbb{P}[s_{i,t}^{v,\max} \geqslant T_i(\alpha_t, \gamma_t)\boldsymbol{\omega}] \geqslant 1-\epsilon_v. \tag{5.36b}$$

The optimal solution of (5.36) is the smallest value of slack variable $s_{i,t}^{v,\max}$ that ensures that the distributionally robust chance constraints holds with confidence level $1-\epsilon_v$. This interpretation relates the solution of (5.36) to the concept of conditional-value-at-risk (CVaR). Accordingly, the optimal value of $s_{i,t}^{v,\max}$ is attained, if (5.36) is replaced by the following set of matrix inequalities using [176, Theorem 2.1]:

$$\forall t \in \mathcal{T}, \forall i \in \mathcal{N}:$$

$$M_{i,t}^{v,\max} \succeq 0 \tag{5.37a}$$

$$s_{i,t}^{v,\max} + \frac{1}{\epsilon_v}\langle \hat{\Omega}^{(t)}, M_{i,t}^{v,\max}\rangle \leqslant 0, \tag{5.37b}$$

$$M_{i,t}^{v,\max} - \begin{bmatrix} 0 & \frac{1}{2}T_i^v(\alpha_t,\gamma_t)^\top \\ \frac{1}{2}T_i^v(\alpha_t,\gamma_t) & u_{i,t} - u_i^{\max} - s_{i,t}^{v,\max} \end{bmatrix} \succeq 0, \tag{5.37c}$$

where $s^{v,\max}_{i,t}$ and auxiliary matrix $M^{v,\max}_{i,t}$ are decision variables and $\hat{\Omega}^{(t)}$ is the second-order moment matrix:

$$\hat{\Omega}^{(t)} := \begin{bmatrix} \hat{\Sigma}^{(t)} + \hat{\mu}^{(t)}(\hat{\mu}^{(t)})^\top & \hat{\mu}^{(t)} \\ (\hat{\mu}^{(t)})^\top & 1 \end{bmatrix}, \tag{5.38}$$

where parameters $\hat{\mu}^{(t)}$ and $\hat{\Sigma}^{(t)}$ are learned from the LSE as explained in (5.19) and (5.20), respectively. Eq. (5.37a)-(5.37c) contain semidefinite constraints that can be solved efficiently by off-the-shelf solvers, e.g. MOSEK [177]. By inferring the security margin of the chance-constraints from the empirical error distribution, the model can learn the price sensitivity and optimize price signals that solve the trade-off between larger security margins and higher costs.

The same procedure can be applied to obtain semidefinite reformulation of other chance constraints by defining the respective system responses in analogy to (5.34) and defining additional auxiliary variables $s^{v,\min}_{i,t}$, $s^{p_G,\max}_{i,t}$, $s^{,\min p_G}_{i,t}$, $s^{q_G,\max}_{i,t}$, and $s^{,\min q_G}_{i,t}$, as well as matrices $M^{v,\min}_{i,t}$, $M^{p_G,\max}_{i,t}$, $M^{p_G,\min}_{i,t}$, $M^{q_G,\max}_{i,t}$, and $M^{q_G,\min}_{i,t}$. The resulting sets of equations are shown in Section 5.7 on page 84.

Remark 5.2. The proposed approach requires a distributionally robust optimization method to accommodate the mixture of errors in the observable residuals and, thus, the unknown error distribution. The proposed distributionally robust formulation is independent from the parameter learning process and its conservatism can be tuned via risk parameter ϵ.

5.4 REGRET ANALYSES

The learning performance can be evaluated *ex post* in terms of *regret*, i.e. comparing the decision that has been made based on the available observations with the decision that would have been optimal in hindsight, after the outcome is known. The anticipated regret associated with the proposed learning approach can be defined as the expected difference between the cost attained with estimated parameters and the cost postulated for true (unknown) parameters.

Proposition 5.1. *The total regret can be computed in the form of* $\zeta(t) = \zeta^{(en)}(t) + \zeta^{(bal)}(t)$, *where the expected regret due to the cost of energy procurement is:*

$$\zeta^{(en)}(t) = \sum_{i\in\mathcal{N}} \underbrace{\left((\frac{1}{2\hat{\beta}^{(t)}_{1,i}} - \frac{1}{2\beta_{1,i}})(x^*_{i,t})^2 - (\frac{\hat{\beta}^{(t)}_{0,i}}{2\hat{\beta}^{(t)}_{1,i}} - \frac{\beta_{0,i}}{2\beta_{1,i}})x^*_{i,t} \right)}_{:=\zeta^{(en)}_i(t)} \tag{5.39}$$

and the expected regret due to the balancing cost is:

$$\zeta^{(bal)}(t) = \sum_{i\in\mathcal{N}} \underbrace{\left(\alpha_i^2 c_{2i} e^\top (\hat{\Sigma}^{(t)} - \Sigma) e \right)}_{:=\zeta^{(bal)}_i(t)}. \tag{5.40}$$

Proof. The expected cost as given by (5.29) are reformulated as:

$$\begin{aligned}\mathbb{E}[\mathbf{C}_t] = &\overbrace{\sum_{i\in\mathcal{G}}(c_i(p^p_{G,i,t})}^{\text{Exp. Generation Cost}} + \overbrace{c_{i2}\alpha_i^2 e^\top \hat{\Sigma}^{(t)} e)}^{\text{Exp. Balancing Cost}} \\ &+ \underbrace{\sum_{i\in\mathcal{N}} \frac{1}{2\hat{\beta}_{1,i}}(x^*_{i,t})^2 - \frac{\hat{\beta}_{1,i}}{2\hat{\beta}_{1,i}}x^*_{i,t} + \kappa_t \sum_{i\in\mathcal{N}} x^*_{i,t}}_{\text{Exp. total Cost of DR}}\end{aligned} \tag{5.41}$$

Since there is no parameter uncertainty in the cost of generation, expected regret due to the expected energy provision is computed as:

$$\begin{aligned}\zeta^{(en)}(t) \coloneqq &\sum_{i\in\mathcal{N}}\left(\frac{1}{2\hat{\beta}^{(t)}_{1i}}(x^*_{i,t})^2 - (\frac{\hat{\beta}^{(t)}_{0,i}}{2\hat{\beta}^{(t)}_{1,i}} - \kappa_t)x^*_{i,t}\right) \\ &- \sum_{i\in\mathcal{N}}\left(\frac{1}{2\beta_{1i}}(x^*_{i,t})^2 - (\frac{\beta_{0,i}}{2\beta_{1,i}} - \kappa_t)x^*_{i,t}\right) \\ = &\sum_{i\in\mathcal{N}}\left((\frac{1}{2\hat{\beta}^{(t)}_{1,i}} - \frac{1}{2\beta_{1,i}})(x^*_{i,t})^2 - (\frac{\hat{\beta}^{(t)}_{0,i}}{2\hat{\beta}^{(t)}_{1,i}} - \frac{\beta_{0,i}}{2\beta_{1,i}})x^*_{i,t}\right).\end{aligned} \tag{5.42}$$

Similarly, the expected regret due to the expected cost of balancing is computed as:

$$\begin{aligned}\zeta^{(bal)}(t) \coloneqq &\sum_{i\in\mathcal{N}}\left(\alpha_i^2 c_{2i}(e^\top\hat{\Sigma}^{(t)}e\right) - \sum_{i\in\mathcal{N}}\left(\alpha_i^2 c_{2i}e^\top\Sigma e\right) \\ = &\sum_{i\in\mathcal{N}}\left(\alpha_i^2 c_{2i}e^\top(\hat{\Sigma}^{(t)} - \Sigma)e\right).\end{aligned} \tag{5.43}$$

Thus, the total regret at every time step is computed as:

$$\zeta(t) = \zeta^{(en)}(t) + \zeta^{(bal)}(t). \tag{5.44}$$

$\square$

Regret component $\zeta^{(en)}$ in (5.39) depends on the parameter estimation error, i.e. the discrepancy between $\hat{\beta}^{(t)}_i$ and β_i, and the amount of desired demand response $x^*_{i,t}$ at each node. On the other hand, regret component $\zeta^{(bal)}$ is driven by the empirical variance of the desired demand response ($\hat{\Sigma}^{(t)}$), see (5.20). To further analyze $\zeta^{(en)}$ and $\zeta^{(bal)}$, we first consider the optimality condition for $x^*_{i,t}$:

Proposition 5.2. *Consider the CC-ACOPF problem and let $\pi^p_{i,t}$ and $\pi^q_{i,t}$ be the Lagrangian dual multipliers of the active and reactive nodal power balances (5.24) and (5.25) at node i and time t in (5.24) and (5.25). Then the optimal desired DR at each node i is given as*

$$x^*_{i,t} = \hat{\beta}^{(t)}_{1,i}(\pi^p_{i,t} + \gamma_i\pi^q_{i,t} - \kappa_t) + \hat{\beta}^{(t)}_{0,i}. \tag{5.45}$$

Proof. The first-order optimality condition of $x^*_{i,t}$ in (5.33) is:

$$\pi^p_{i,t} + \gamma_i \pi^q_{i,t} = \frac{1}{\hat{\beta}^{(t)}_{1,i}} x^*_{i,t} - \frac{\hat{\beta}^{(t)}_{i,t}}{\hat{\beta}^{(t)}_{1,i}} + \kappa_t. \tag{5.46}$$

Re-arranging (5.46) immediately leads to (5.45). □

It follows from Proposition 5.2 and (5.31) that the optimal price signal to achieve optimal $x^*_{i,t}$ is given as:

$$\lambda^*_{i,t} = \pi^p_{i,t} + \gamma_i \pi^q_{i,t} - \kappa_t. \tag{5.47}$$

Since $\lambda^*_{i,t} \geqslant 0$ by definition, any node i receives a non-zero price signal in t only if $\pi^p_{i,t} + \gamma_i \pi^q_{i,t} > \kappa_t$. Next, we analyze the convergence of the parameter estimation error using the results of Proposition 5.2.

Proposition 5.3. *Let $\lambda^*_{i,t}$ be the broadcast price signal at node i and time t, and $\pi^p_{i,t}$, $\pi^q_{i,t}$ the Lagrangian dual multipliers of the active and reactive nodal power balances at node i and time t of the CC-ACOPF, and let $B_t \coloneqq \hat{\beta}^{(t)}_i - \beta_i$ be the parameter estimation error. If the broadcast price is given by*

$$\lambda^*_{i,t} = \max(\pi^p_{i,t} + \gamma_i \pi^q_{i,t} - \kappa_t, 0), \tag{5.48}$$

then parameter estimation error B_t converges to zero for all t, where $\lambda_{i,t} > 0$.

Proof. Consider the parameter estimation error as:

$$B_t = \begin{bmatrix} \hat{\beta}^{(t)}_{1,i} - \beta_{1,i} \\ \hat{\beta}^{(t)}_{0,i} - \beta_{0,i} \end{bmatrix} = \mathcal{F}^{-1}_{i,t} \left(\sum_{\tau=1}^{t-1} \begin{bmatrix} \lambda_{i,\tau} \\ 1 \end{bmatrix} \hat{\omega}^{(t)}_{\tau} \right), \tag{5.49}$$

where:

$$\mathcal{F}_{i,t} = \begin{bmatrix} \sum_{\tau=1}^{t-i} \lambda^2_{i,\tau} & \sum_{\tau=1}^{t-i} \lambda_{i,\tau} \\ \sum_{\tau=1}^{t-i} \lambda_{i,\tau} & (t-1) \end{bmatrix}, \tag{5.50}$$

is the Fisher information of node i at time t, [169], [170]. It follows from (5.49) that the parameter estimation error converges to zero, if the minimum eigenvalue of $F_{i,t}$ increases unbounded over time, [169], [170] Recalling [170, Lemma 2], the minimum eigenvalue of $F_{i,t}$ is bounded from below as:

$$\begin{aligned} L_{i,t} &= \sum_{\tau=1}^{t-i} (\lambda_{i,\tau} - \bar{\lambda}_{i,t})^2 \\ &= (t-2)\,\mathrm{Var}([\lambda_{i,\tau}, \tau = \{1, ..., t-1\}]). \end{aligned} \tag{5.51}$$

Eq. (5.51) shows that $L_{i,t}$ increases over time if the variance of the broadcast price signals $\mathrm{Var}([\lambda_{i,\tau}, \tau = \{1, ..., t-1\}])$ does not converge to zero. Under the non-restrictive assumption that the root node electricity price ω_t changes over time, i.e. is different for different t, $\pi^p_{i,t}$

and $\pi^q_{i,t}$ are similarly changing over time due to their dependency on the cost of energy provision and the active network constraints, [139]. It follows from the relation between $\lambda^*_{i,t}$ and $\pi^p_{i,t}$, $\pi^q_{i,t}$ given by (5.48) that $\lambda^*_{i,t} \neq 0$ will not be uniform across different t. Thus, if $\mathcal{T}^+_i \subseteq \{1, ..., t-1\}$ is the set of timesteps with $\lambda_{i,t} > 0$, then

$$\mathrm{Var}([\lambda^*_{i,\tau}, \tau \in \mathcal{T}^+_i]) > 0. \tag{5.52}$$

It follows from (5.52) and [170, Lemma 2] that parameter estimation error B_t given in (5.49) converges to zero over time. □

The results of Propositions 5.2 and 5.3 lead to the following result on the convergence of regret:

Proposition 5.4. *Let the regret be $\zeta(t) = \zeta^{(en)}(t) + \zeta^{(bal)}(t)$, where $\zeta^{(en)}(t)$ and $\zeta^{(bal)}(t)$ are given by (5.39) and (5.40). If at every time step t the price signal is chosen as (5.48), then aggregated regret $\frac{1}{t}\sum_{\tau=1}^{t-i} \zeta(t)$ is sublinear over t.*

Proof. First, consider:

$$\sum_{\tau}^{t-1} \zeta^{(en)}(\tau) = \sum_{i \in \mathcal{N}} \left(\sum_{\tau \in \mathcal{T}^+_i} \zeta^{(en)}_i(\tau) + \sum_{\mathcal{T}^0_i} \zeta^{\tau \in (en)}_i(\tau) \right). \tag{5.53}$$

where $\mathcal{T}^0 = \{1, ..., t-1\} \setminus \mathcal{T}^+_i$ so that $\mathcal{T}^+_i \cup \mathcal{T}^0 = \{1, ..., t-1\}$ and $\mathcal{T}^+_i \cap \mathcal{T}^0 = \emptyset$. As shown in Proposition 5.3, at every time step t with $\lambda^*_{i,t} \neq 0$ the parameter estimation error at this node decreases on average. Therefore, as follows from (5.39), the regret contribution of this node decreases on average as well. On the other hand, any node i where $\pi^p_{i,t} + \gamma_i \pi^q_{i,t} < \kappa_t$ and thus $\lambda^*_{i,t} = x^*_{i,t} = 0$, has a zero contribution to $\zeta^{(en)}$ as per (5.39) so that $\sum_{\tau \in \mathcal{T}^0_i} \zeta^{(en)}_i(\tau) = 0$.

Next, we consider $\zeta^{(bal)}$ in (5.40). Unlike for $\zeta^{(en)}$, information on the random error is acquired at every time step, even if desired DR participation $x^*_{i,t} = 0$, which leads to the convergence of $\zeta^{(bal)}$. The convergence of the individual regret components $\lim_{t\to\infty} \zeta^{(en)}(t) = \lim_{t\to\infty} \zeta^{(bal)}(t) = 0$ leads to

$$\frac{1}{t}\sum_{\tau=1}^{t-i} \left(\zeta^{(en)}(\tau) + \zeta^{(bal)}(\tau) \right) = \Theta(\log(t)), \tag{5.54}$$

where $\Theta(\cdot)$ is the Big-O complexity notation. Hence, regret has a sublinear trajectory over time. □

Note that if the network is unconstrained (i.e. no line or voltage constraint is binding), then $\pi^p_{i,t} = \pi^p_t, \forall i \in \mathcal{N}$, and $\pi^q_{i,t} = \pi^q_t, \forall i \in \mathcal{N}$, resulting in $\lambda^*_{i,t} = \lambda^*_t, \forall i \in \mathcal{N}$, which leads to the similar regret guarantees as in [31], where no physical network constraints are modeled.

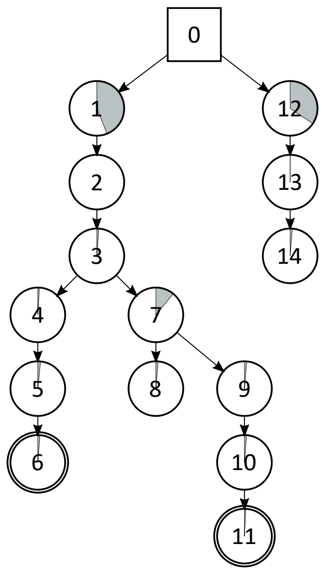

Figure 5.2: The 15-node test system from [139], where the square root node (substation) and the double contour nodes denotes controllable resources. At each node, the filled ratio of the circle indicates the share of the node in the total forecast demand.

5.5 ILLUSTRATIVE CASE STUDY

Fig. 5.2 illustrates the 15-node test system from [139], that we also used in Chapter 4, with two controllable generators added to nodes 6 and 11. Each generator has a linear cost curve with $c_{i,1} = \$10\,/\text{MWh}$ and $p_{G,i}^{\max} = 0.8\,\text{MW}$. The time horizon is given by 500 hourly intervals, i.e. $\mathcal{T} = \{1, 2, ..., 500\}$. At each interval, the cost of electricity at the root node is sampled from the range between $\$30\,/\text{MWh}$ and $\$200\,/\text{MWh}$ using a uniform distribution. The retail tariff is set to $\kappa_t = \$25/MWh, \forall t$. The desired likelihood of chance constraint violations is $\epsilon_v = \epsilon_p = 0.1$. We use the active and reactive demand from [139] as the forecasted baseline and the simulated reaction of the DR participants is generated from the DR model set to the following parameters: $\beta_{1,i} = {}^{1}/_{150}\,\text{MWh}\$^{-1}, \forall i \in \mathcal{N}^+$, $\beta_{0,i} = 0, \forall i \in \mathcal{N}^+$, and $\sigma_i = 0.1 p_{D,i,t}, \forall i \in \mathcal{N}^+$, with no correlation among the nodes. Those are the parameters that the model needs to learn over time.

To evaluate the effectiveness of the proposed learning procedure, the following four cases representing different levels of information available to the DSO are compared:

- *Fully oracle*: The DSO uses the true values of β_i and Ω.
- β_i-*oracle*: The DSO uses the true values of β_i, but Ω is unavailable and, therefore, $\hat{\Omega}$ needs to be learned.
- Ω-*oracle*: The DSO uses the true values of Ω, but β_i is unavailable and, therefore, $\hat{\beta}_i$ needs to be learned.

- *Fully oblivious*: The DSO must learn both $\hat{\Omega}$ and $\hat{\beta}_i$.

Additionally, each of the cases above is analyzed for different sets of network constraints in the distribution system:

- *No network*: The network (voltage, apparent power flow) constraints are ignored.
- *Flow-constrained*: Only the the apparent power flow constraints are enforced.
- *Voltage-constrained*: Only the voltage constraints are enforced.
- *Fully constrained*: All network constraints are enforced.

All models in the case study are implemented using the *Julia JuMP* package [159]. The code and input data can be downloaded from [178].

5.5.1 *DR Learning*

OPTIMAL DR USAGE: Table 5.1 compares the optimal usage of DR resources for different learning cases and sets of network constraints in terms of the total DR amount exercised relative to the total demand in the system, i.e. $x^*_{i,t}/\sum_i p_{D,i,t}, \forall t \in \mathcal{T}$. The case with no network limits enforced leads to a significantly lower usage of DR resources since the DSO can take advantage of the two controllable DERs at node 6 and 11 with production costs lower than the supply from the root node.

However, when the network limits are imposed, the dispatch of DERs becomes more constrained and, therefore, the DSO elects to exercise more DR resources. The usage of DR resources is more affected by voltage limits than by power flow limits due to two factors. First, the distribution systems are typically voltage constrained rather than power flow constrained. Second, as it can also be seen in Table 5.1, power flow limits prevent the use of controllable DERs by roughly a factor of two relative to the voltage limits. Notably, the fully constrained case does not necessarily lead to the maximum DR utilization relative to other less constrained cases. This result defies the intuition that a more constrained case would require more flexibility. However, the cost of exercising DR flexibility appear suboptimal in our simulations as network limits affect DR deliverability and more cost-effective resources are available.

The effect of parameter learning on the optimal usage of DER resources observed in Table 5.1 is two-fold. First, as the DSO becomes more oblivious to characteristics of DR resources, DR utilization increases relative to the oracle case, while the use of controllable DERs remains nearly the same. Thus, due to a lack of oracular knowledge about DR resources, the DSO is forced to overuse its available DR

Table 5.1: Relative optimal DR usage ($x^{*}_{i,t}/\sum_i p_{D,i,t}$): (a): Maximum relative optimal DR, (b): Median relative optimal DR, (c): Minimum relative optimal DR, (d): Median of relative optimal DER utilization, all in percent.

		Oracle	β-oracle	Ω-oracle	Oblivious
No Network	(A)	11.40	11.40	11.40	11.40
	(B)	11.40	11.40	11.40	11.40
	(C)	9.312	9.312	9.318	9.439
	(D)	100.0	100.0	100.0	100.0
Only Flows	(A)	67.28	67.28	69.76	69.76
	(B)	40.32	40.31	40.31	40.32
	(C)	5.091	5.187	5.202	5.069
	(D)	34.16	34.16	34.17	34.15
Only Voltage	(A)	42.06	42.78	42.09	42.74
	(B)	42.02	41.91	41.85	41.19
	(C)	0.0	0.0	0.0	0.0
	(D)	65.4	64.86	65.4	64.86
Fully Constrained	(A)	52.8	67.37	52.86	60.50
	(B)	40.2	40.25	40.24	40.24
	(C)	5.04	5.042	0.0	0.0
	(D)	34.04	34.07	34.05	34.05

resources to meet the system-wide demand and avoid violating network limits. Second, as network operations become more restrictive, the difference in the amounts of DR resources used in the fully oracle and fully oblivious cases increases.

The aggregated DR usage in the fully oblivious case in Table 5.1 are itemized for each node and each time interval in Fig. 5.3. While the median aggregated utilization of DR resources reported in Table 5.1 is roughly the same for all network-constrained cases, the nodal distribution shown in Fig. 5.3 is differently affected by limits imposed. This empirical evidence suggests that tighter network limits forces the DSO to use the DR resources more uniformly across the system.

PARAMETER LEARNING: Consistently with the cases presented in Fig. 5.3, this section discusses the effect of learning on the DSO objective and presents the outcomes of price learning. Fig. 5.4 compares the DSO objective in the three non-fully-oracular cases, in which some information about DR resources is oblivious, and the fully oracular case under randomly sampled prices at the root node. As the learning progresses, the accuracy of parameters available to the DSO increases, which reduces the difference between the objective in the oracular and non-oracular cases. This improvement in accuracy is insensitive to the substation price, which indicates the robustness of the pro-

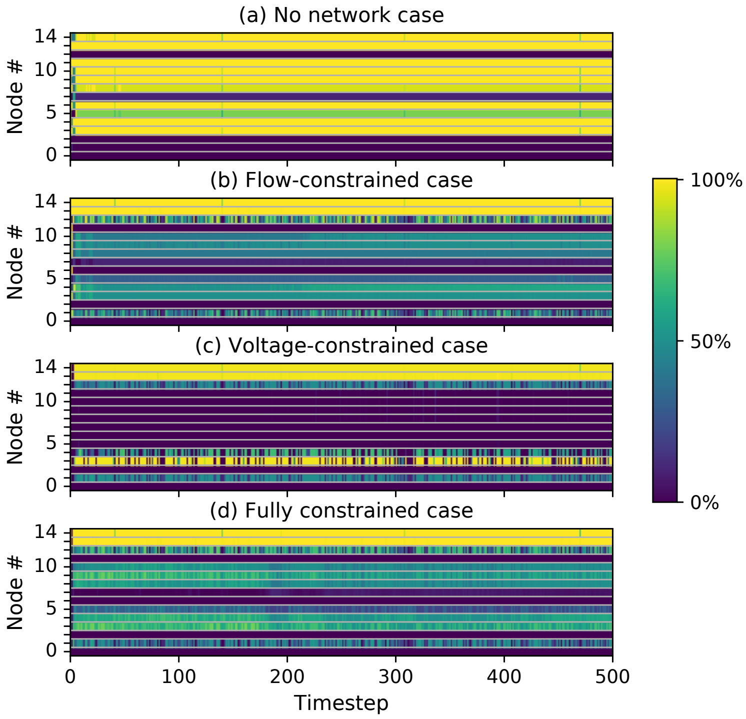

Figure 5.3: Optimal DR usage at nodes relative to the nodal forecast demand, i.e. $x^*_{i,t}/p_{D,i,t}$.

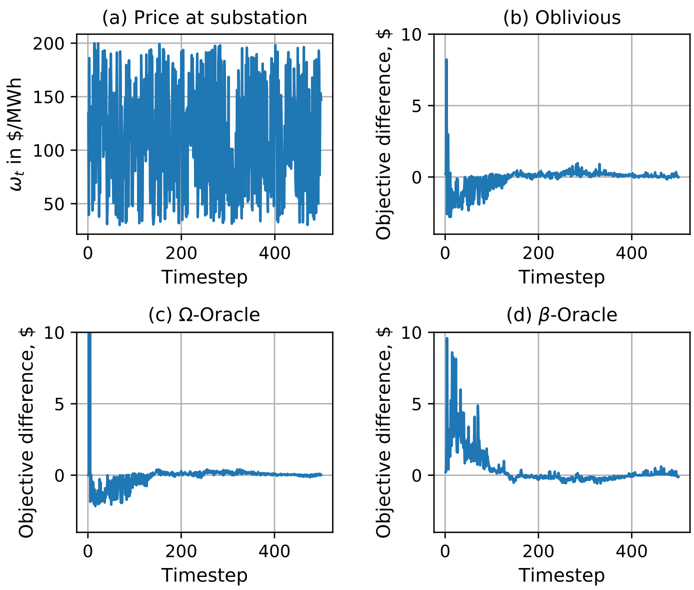

Figure 5.4: (a) Randomly sampled energy price at the root node (substation). (b)-(d) Difference in the DSO objective function between the oracular and non-oracular cases.

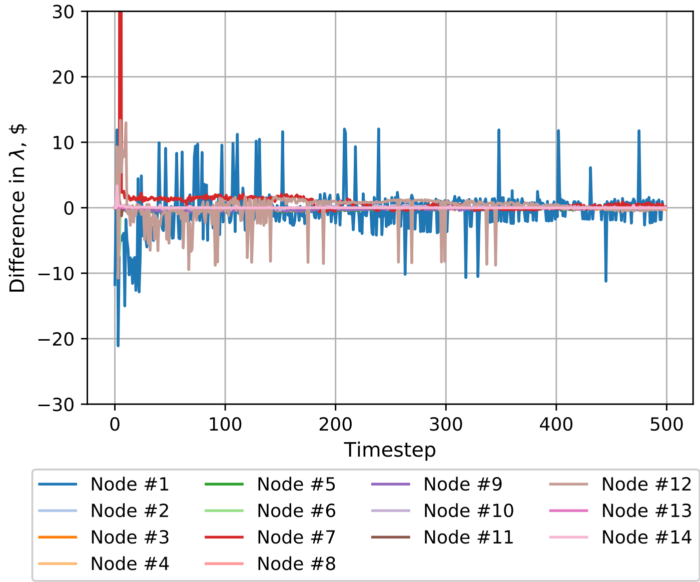

Figure 5.5: Difference between price signals (λ) obtained in the oracle case and the oblivious case with fully constrained network.

posed learning approach. Among the three cases with non-oracular information, there is no significant difference in convergence.

Similarly to the DSO objective, price signals produced by the proposed learning approach in all non-oracular cases with all network limits enforced converge to the oracular values, as shown in Fig. 5.5. Notably that price signals for all nodes but nodes 1 and 12 converge fairly quickly. The price spikes observed at these two nodes are explained by two factors. First, these nodes carry 75% of the total load, see Fig. 5.2, which exacerbates the absolute price difference in Fig. 5.5 even for small parameter estimation errors. Second, these two nodes are adjacent to the root node of the distribution system, which amplifies spikes in the price at the root node, see randomly generated samples in Fig. 5.4(a). However, the frequency of price spikes at nodes 1 and 12 gradually reduces as the learning procedure progresses.

5.5.2 *Empirical Analysis of Learning Errors*

In the non-oracular cases, the learning errors steams from the uncertainty ϵ and misestimation of $\hat{\beta}$ and $\hat{\Omega}$. To isolate the effect of misestimated parameters $\hat{\beta}$ and $\hat{\Omega}$ from ϵ, we compute the difference between the expected DSO objective and the observed DSO objective in each case, i.e. $\Delta_t^\diamond = C_t^\diamond - \mathbb{E}[C_t^\diamond]$, where $\diamond$ denotes the oracular, β-oracular, Ω-oracular and oblivious cases, respectively. Since in the oracular case the error inflicted by parameter learning is null by definition, we obtain $\Delta_t^{[\text{oracle}]} = \Delta_t^{[\omega]}$, which is the error inflicted by the uncontrollable disturbance ϵ in Eq. (5.8). This error is the

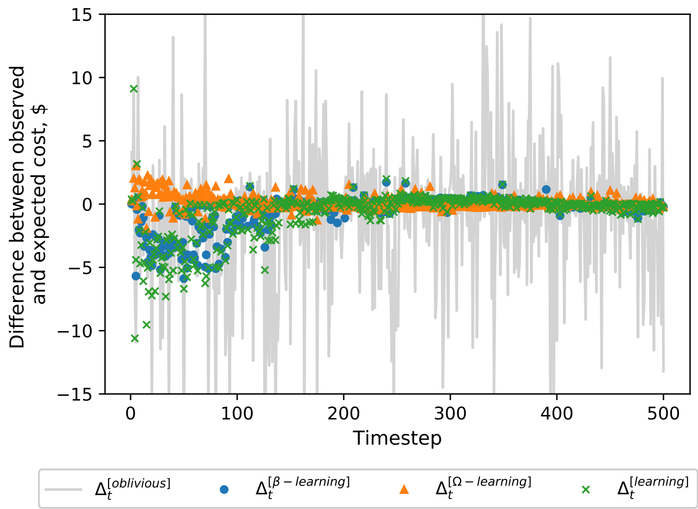

Figure 5.6: Empirical analysis of learning errors for the expected and observed DSO objectives.

same in the oracular and non-oracular cases and, therefore, the learning error in the three non-oracular cases can be recovered as $\Delta_t^{[\beta\text{-learning}]} = \Delta_t^{[\Omega\text{-oracle}]} - \Delta_t^{[\omega]}$, $\Delta_t^{[\Omega\text{-learning}]} = \Delta_t^{[\beta\text{-oracle}]} - \Delta_t^{([\omega])}$ and $\Delta_t^{[\text{learning}]} = \Delta_t^{[\text{oblivious}]} - \Delta_t^{[\omega]}$, respectively.

Fig. 5.6 itemizes the learning errors computed as explained above for the cases considered in Fig. 5.4. In all cases, the systematic errors $\Delta_t^{[\beta\text{-learning}]}$, $\Delta_t^{[\Omega\text{-learning}]}$ and $\Delta_t^{[\text{learning}]}$ converge to zero as the learning progresses. This result demonstrates that the misestimation errors induced by the learning approach can be overcome if sufficient data sets are available.

5.5.3 *Experimental Regret Analysis*

Analysis of regret, i.e. the difference between the decision of the oblivious model and the oracle (perfect foresight) model, allows assessment of the performance of the learning process. We define two regret metrics similar to [31]. First, the *expected regret* defines the difference between the objective values of the oblivious and oracle models:

$$\zeta^{[\text{exp}]}(t) \coloneqq \sum_{\tau=1}^{t} \left(\mathbb{E}[\mathbf{C}_\tau]^{[\text{oblivious}]} - \mathbb{E}[\mathbf{C}_\tau]^{[\text{oracle}]} \right)^2 . \tag{5.55}$$

Second, we compute the *observed regret* as the difference between the objective functions of the oblivious and oracle cases after observing the true outcome at each time step:

$$\zeta^{[\text{obs}]}(t) \coloneqq \sum_{\tau=1}^{t} \left(C_\tau^{[\text{oblivious}]} - C_\tau^{[\text{oracle}]} \right)^2 . \tag{5.56}$$

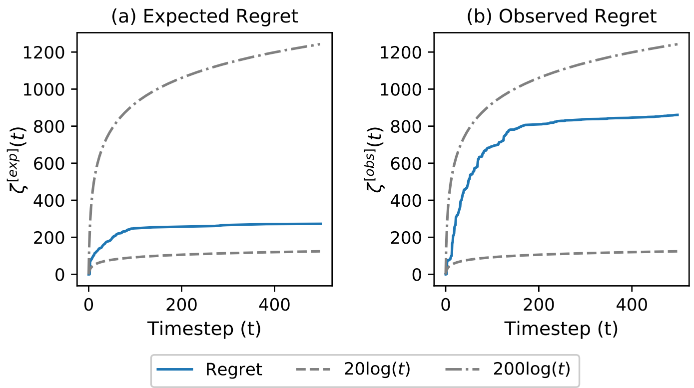

Figure 5.7: Analyses of the expected and observed regret shown within a logarithmic envelope.

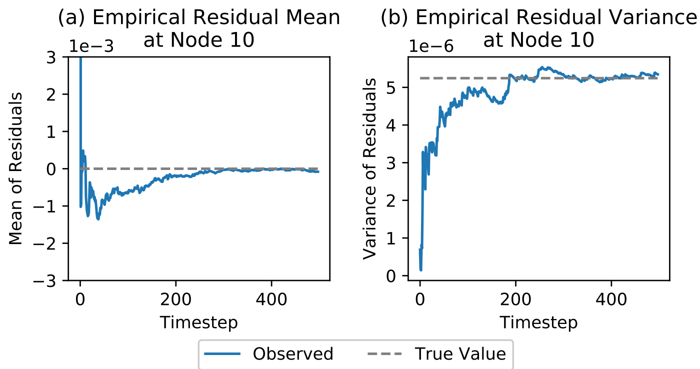

Figure 5.8: Development of empirical mean and variance at node 10.

Using (5.55) and (5.56), we seek a sublinear and asymptotically zero regret, i.e. $\lim_{t\to\infty} {}^{\zeta(t)}/t = 0$, [32], [169]. Fig. 5.7 illustrates the evolution of the expected and observed regret metrics. Although the absolute regret value increases as the learning progresses, both regret metrics exhibit a logarithmic trend with the required rate of saturation of $^1/t$, as shown by the logarithmic envelope in Fig. 5.7. Note that the scale of the envelope ($20\log(t)$, $200\log(t)$) has been chosen to fit the scale of the shown regret. This shows that the regret increment at each time step is on average smaller than at the previous time step, which indicates learning progress at each step. The same trend is observed for the evolution of the moments of the residual error, where the difference between the mean and variance in the oblivious and oracle cases reduces as the learning time increases. Fig. 5.8 illustrates this evolution for node 10, which was selected since our experiments show that the optimal DR participation at this node has the least sensitivity to the price volatility at the substation. Despite this low sensitivity, we observe that the parameter estimates at node 10 converge. We observe similar convergence trends at the other nodes of the system.

Table 5.2: Computing times in seconds.

	15-node system	141-node system
Average computing time per time step	0.019	2.427
Standard deviation of the computing time per time step	0.006	0.262

5.5.4 *Scalability and Computational Performance*

To evaluate scalability to larger distribution systems, we use the 141-node test system from [179] and additionally populate it with controllable generators at nodes 30, 40, 50, 60, 70, 80, 101 and 121 with the production cost in the range $\$10 - \$17$ per MWh. In the following, we use the fully constrained DRCC-OPF since it is the most computationally demanding case. All simulations were carried out on a PC with an Intel Core i7 processor with 2.50 GHz and 8 GB of memory. Table 5.2 compares the computing times for 15- and 141-node test systems. In our case study we did not observe any computational abnormalities.

Fig. 5.9 shows the difference between the objective functions in the oracle and oblivious cases. As the number of time steps increases, so does the difference between the objective functions. As compared to the results in Fig. 5.4(b) for the 15-node system, the convergence of the proposed learning scheme is similar in relative terms, but the residual differences are greater for the same time intervals due to a higher value of the objective function. The median DR utilization factor is 58.26 % of the available DR capacity in the system. We also observe that some fairly cheap DR flexibility and controllable generators are blocked by the voltage and flow limits. The regret performance is similar to the 15-node test system showing a logarithmic progression. For instance, the average observed regret per time step is $\zeta^{[\text{obs}]} = 22.14\,\$^2$ in the first 10 time steps and it reduces to $\zeta^{[\text{obs}]} = 1.03\,\$^2$ for subsequent time steps (11 to 500).

5.6 Conclusion

This chapter described a learning approach that is capable of learning price sensitivities of residential DR resources and improves the utilization of these resources in the distribution system. The approach connects the least-square estimator and distributionally robust chance-constrained optimal power flow model that co-optimizes DR resources on a par with other dispatchable resources, while re-

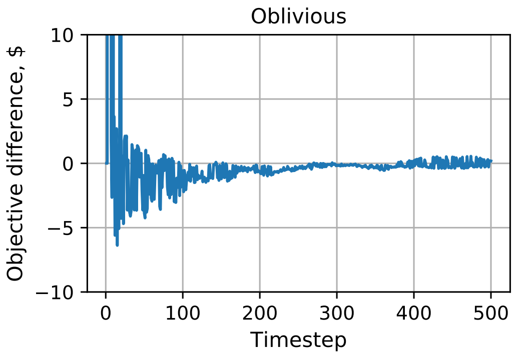

Figure 5.9: Difference in the DSO objective function between the oblivious and oracular cases for the 141-node test system.

specting operating limits on the distribution system. As the learning approach progresses, it reduces the systematic error inflicted by insufficient knowledge about price sensitivities of DR participants from the DSO perspective. The case study describes the usefulness of the proposed learning approach for different network instances.

5.7 REMAINING REFORMULATED CHANCE CONSTRAINTS

This section shows the remaining distributionally robust reformulations of the chance-constraints, which have been omitted in Section 5.3.2 to improve readability.

- For the lower voltage constraint:

$$\forall t \in \mathcal{T}, \forall i \in \mathcal{N}:$$

$$M^{v,\min}_{i,t} \succeq 0 \tag{5.57a}$$

$$s^{v,\min}_{i,t} + \frac{1}{\epsilon_v}\langle \hat{\Omega}^{(t)}, M^{v,\min}_{i,t}\rangle \leqslant 0, \tag{5.57b}$$

$$M^{v,\min}_{i,t} - \begin{bmatrix} 0 & \frac{1}{2}T^{v}_{i}(\alpha_t,\gamma_t)^\top \\ \frac{1}{2}T^{v}_{i}(\alpha_t,\gamma_t) & -u_{i,t} + u^{\min}_{i} - s^{v,\min}_{i,t} \end{bmatrix} \succeq 0. \tag{5.57c}$$

- For the upper and lower active generation constraints:

$$\forall t \in \mathcal{T}, \forall i \in \mathcal{N}:$$

$$M^{p_G,\max}_{i,t} \succeq 0 \tag{5.58a}$$

$$s^{p_G,\max}_{i,t} + \frac{1}{\epsilon_v}\langle \hat{\Omega}^{(t)}, M^{p_G,\max}_{i,t}\rangle \leqslant 0, \tag{5.58b}$$

$$M^{p_G,\max}_{i,t} - \begin{bmatrix} 0 & \frac{1}{2}T^{p_G}_{i}(\alpha_t,\gamma_t)^\top \\ \frac{1}{2}T^{p_G}_{i}(\alpha_t,\gamma_t) & p_{G,i,t} - p^{\max}_{G,i} - s^{p_G,\max}_{i,t} \end{bmatrix} \succeq 0, \tag{5.58c}$$

and

$$\forall t \in \mathcal{T}, \forall i \in \mathcal{N}:$$

$$M_{i,t}^{p_G,\min} \succeq 0 \tag{5.59a}$$

$$s_{i,t}^{p_G,\min} + \frac{1}{\epsilon_v}\langle \hat{\Omega}^{(t)}, M_{i,t}^{p_G,\min}\rangle \leqslant 0, \tag{5.59b}$$

$$M_{i,t}^{p_G,\min} - \begin{bmatrix} 0 & \frac{1}{2}T_i^{p_G}(\alpha_t,\gamma_t)^\top \\ \frac{1}{2}T_i^{p_G}(\alpha_t,\gamma_t) & -p_{G,i,t} + p_{G,i}^{\min} - s_{i,t}^{p_G,\min} \end{bmatrix} \succeq 0, \tag{5.59c}$$

using $T_i^{p_G}(\alpha_t,\gamma_t) \coloneqq \alpha_i e^\top$.

- For the upper and lower reactive generation constraints:

$$\forall t \in \mathcal{T}, \forall i \in \mathcal{N}:$$

$$M_{i,t}^{q_G,\max} \succeq 0 \tag{5.60a}$$

$$s_{i,t}^{q_G,\max} + \frac{1}{\epsilon_v}\langle \hat{\Omega}^{(t)}, M_{i,t}^{q_G,\max}\rangle \leqslant 0, \tag{5.60b}$$

$$M_{i,t}^{q_G,\max} - \begin{bmatrix} 0 & \frac{1}{2}T_i^{q_G}(\alpha_t,\gamma_t)^\top \\ \frac{1}{2}T_i^{q_G}(\alpha_t,\gamma_t) & q_{G,i,t} - q_{G,i}^{\max} - s_{i,t}^{q_G,\max} \end{bmatrix} \succeq 0, \tag{5.60c}$$

and

$$\forall t \in \mathcal{T}, \forall i \in \mathcal{N}:$$

$$M_{i,t}^{q_G,\min} \succeq 0 \tag{5.61a}$$

$$s_{i,t}^{q_G,\min} + \frac{1}{\epsilon_v}\langle \hat{\Omega}^{(t)}, M_{i,t}^{q_G,\min}\rangle \leqslant 0, \tag{5.61b}$$

$$M_{i,t}^{q_G,\min} - \begin{bmatrix} 0 & \frac{1}{2}T_i^{q_G}(\alpha_t,\gamma_t)^\top \\ \frac{1}{2}T_i^{q_G}(\alpha_t,\gamma_t) & -q_{G,i,t} + q_{G,i}^{\min} - s_{i,t}^{q_G,\min} \end{bmatrix} \succeq 0, \tag{5.61c}$$

using $T_i^{q_G}(\alpha_t,\gamma_t) \coloneqq \alpha_i e^\top \operatorname{diag}(\gamma)$.

Part III

RISK-AWARE COORDINATION

6 RISK-AWARE COORDINATION IN ACTIVE DISTRIBUTION SYSTEMS

The chapters in previous Part II explored the CC-OPF framework to internalize uncertainty into dispatch and balancing control decisions and introduced data-driven and distributionally robust extensions. This chapter leverages the convex properties of the CC-OPF to study risk-aware equilibrium prices that can be derived from duality theory. These prices can be used to coordinate DERs by incentivizing system-beneficial dispatch decisions and reserve provisions. Further, this chapter extends the previously lossless formulation of the radial CC-ACOPF to include a loss approximation and studies their effect on prices and their components.

The contents of this chapter have been published in 2019 as the article entitled "Distribution electricity pricing under uncertainty" in the *IEEE Transactions on Power Systems*, [P3]. For this dissertation, the original article has been moderately adapted to ensure unified notations and connections to other chapters.

6.1 INTRODUCTION

Nodal electricity pricing has been shown to support the efficient scheduling and dispatch of energy resources at the transmission (wholesale) level [120]. However, the proliferation of DERs in low-voltage distribution systems and the subsequent growth of independent, small-scale energy producers has weakened a correlation between wholesale electricity prices and distribution electricity rates (tariffs), thus distorting economic signals experienced by end-users, [133]. To overcome these distortions, DLMPs have been proposed to incentivize optimal operation and DER investments in low-voltage distribution systems, [23], [134]–[138], and to facilitate the coordination between the transmission and distribution systems, [12], [139]–[141]. However, implementing DLMPs in practice is obstructed by the inability to accurately capture stochasticity of renewable generation resources (e.g. solar or wind) in the price formation process, [7], [9], [43], [69], [72], [73], [124]. As a result, prospective distribution market designs lack completeness, i.e. do not offer customized financial instruments to deal with each source of uncertainty, which may result in market inefficiencies and welfare losses, [130], [131]. Motivated by the need to complete distribution market designs with uncertainty and risk information on renewable generation resources, this chapter proposes a new approach to obtain DLMPs that explicitly incorporate the stochasticity of renewable generation resources and analyzes the effect of risk and uncertainty parameters on the price formation process.

Previously, DLMPs have been considered for numerous applications. Similarly to wholesale markets, [23], [137] propose a distribution day-ahead market to alleviate congestion caused by electric vehicle charging using a welfare-maximizing DCOPF model for DLMP computations. Alternatively, the model in [134] introduces power losses in DLMP computations to properly reward DERs for reducing system-wide power losses. In [135], the authors compute energy, congestion, and power loss DLMP components in the presence of advanced smart grid devices, e.g. solid state transformers and variable impedance lines. Furthermore, DLMPs have been shown to support the system operation, e.g. by incentivizing voltage support from DERs, [136], or by mitigating voltage imbalance in a three-phase system, [138]. Papavasiliou [139] comprehensively analyzes DLMPs and their properties using the branch AC power flow model and its convex second-order conic (SOC) relaxation. The branch power flow model facilitates the use of spot electricity pricing to analyze the effect of the substation prices, power losses, voltage constraints and thermal line limits on DLMP computations, but yields significant computational complexity even for small networks. On the other hand, its SOC relaxation makes it possible to represent DLMPs in terms of local information, i.e. parameters of a given distribution node and its neighbors. However, all DLMP computations in [23], [134]–[139] disregard stochasticity of renewable DER technologies and, therefore, the resulting prices do not provide proper incentives to efficiently cope with balancing regulation needs. The need to consider stochasticity of renewable generation resources in the price formation process is recognized for transmission (wholesale) electricity pricing, e.g. [43], [72], [73], [124], [127], [180], but there is no framework for stochasticity-aware pricing in emerging distribution markets.

Chance-constrained programming can be leveraged to deal with stochasticity of DERs in the distribution system and to robustify operating decisions of the DSO, [P1], [P2], [S1], [69], [173], [181]. The models in [P1], [P2], [S1], [69], [181] improve compliance with distribution system limits at a moderate, if any, increase in operating costs. However, with the exception of the work in [P4], [9], [127], their application for electricity pricing has not been considered. This chapter fills this gap and derives DLMPs that internalize stochasticity using the chance-constrained framework.

This framework offers some significant advantages over other uncertainty-aware methods such as robust or scenario-based stochastic optimization. First, chance constraints internalize continuous probability distributions of uncertain parameters, which are readily available from historical data (e.g. weather data can be obtained from national weather services, [145], and load data can be retrieved from archived forecasts, [P2]). Further, they can accommodate a broad variety of parametric distributions, [106], [145], and attain distributional robustness, [P1], [9]. Hence, unlike scenario-based stochastic and robust optimization methods, chance constraints do not require discretizing a probability space for scenario sampling or for deriving a finite uncertainty set. In the electricity pricing and market design context, avoiding such somewhat arbitrary and non-transparent input data manipulations can improve acceptance of stochastic markets among market participants, [43]. Second, chance-constrained programs can be solved efficiently at scale, [143], and generally yield less conservative results, [7]. The residual conservatism can be tuned via a confidence interval, which can be related to established system reliability metrics, e.g. loss of load probability (LOLP) or expected energy not served (EENS), [182]. Third, the CC-OPF automatically fulfills all internalized market design considerations, e.g. revenue adequacy, cost recovery and incentive compatibility, for all potential outcomes and does not require scenario-specific adjustments, [9], which cause social welfare losses if scenario-based stochastic optimization methods are used, [43]. Additional discussion on chance constraints and chance-constrained markets can be found in Chapter 2.

To take advantage of chance constraints, we build on the CC-ACOPF model for a distribution system with renewable DERs as shown in Chapter 3. The convex SOC formulation enables the use of duality theory for the main propositions of this chapter:

(i) to compute DLMPs that internalize the stochasticity of renewable DERs and risk tolerance of the DSO and

(ii) to itemize DLMP components related to nodal active and reactive power production and demand, balancing regulation, network power losses and voltage support.

From a market perspective, this chapter describes an approach to price generic distribution-level energy and reserve products ahead of real-time operations (e.g. daily, hourly or sub-hourly). In that sense, the model and pricing approach presented below are similar to a centralized market clearing problem in [12], which minimizes social costs, schedules the available capacity of resources, and derives marginal-cost-based transmission and distribution prices for day-ahead, hour-ahead, or 5-min real-time markets. However, unlike in [12], chance constraints endogenously determine both the system reserve requirement and its network-constrained allocation given a desired risk level and uncertainty parameters. The resulting stochastic DLMPs capture these requirements and allocations and can be used to establish a co-optimized stochastic distribution market, which attains a market equilibrium under the assumption that all market participants share similar knowledge about uncertain parameters. With increasing participation of DERs in the provision of grid support services, such a distribution marketplace will allow for coordinating grid support services among transmission and distribution systems. For example, DER aggregators in Germany and Belgium seek to provide regulation services at both the transmission and distribution level, [183]. However, only the former provision is administrated on a market basis, which makes distribution services less attractive for DER aggregators. Hence, DLMPs that internalize desired risk levels and uncertainty parameters can support the DSO in rolling out efficient market platforms to incentivize DER participation in supporting distribution system operations.

6.2 MODEL FORMULATION

This chapter uses the CC-ACOPF for radial distribution systems as derived in Section 3.4 with few modified notations as summarized in Section 6.2.1 to simplify later derivations. Section 6.2.2 then extends the model to include system losses.

6.2.1 *Radial CC-ACOPF Modifications*

REFORMULATED COST FUNCTION We use the quadratic cost function

$$c_i(p_{G,i}) = c_{2,i}(p_{G,i})^2 + c_{1,i}p_{G,i} + c_{0,i}$$

as introduced in (3.4), but for compactness of the following formulations, we denote $c_{2,i} = 1/2b_i$, $c_{1,i} = a_i/b_i$, $c_{0,i} = a_i^2/2b_i$. Given these notations, the deterministic equivalent of the expected cost $\mathbb{E}[c_i(p_{G,i}(\omega))]$ (see (3.23) on page 38 for the detailed derivation), is:

$$\mathbb{E}[c_i(\mathbf{g}_i^p)] = \frac{(p_{G,i} + a_i)^2}{2b_i} + \frac{\alpha_i^2}{2b_i}S^2, \tag{6.1}$$

where $a_i \geqslant 0$ and $b_i > 0$ are given parameters and $S^2 \coloneqq e^\top \Sigma e$.

REACTIVE POWER UNCERTAINTY For ease of exposition, this chapter assumes no uncertainty in the reactive power component. This assumption may be valid if active power deviation ω is sufficiently small so that coupled reactive power fluctuations can directly be compensated by the power electronic interface between the DER and the grid with suitable control policies, [20]. However, if uncertainty in reactive power can not be neglected, the results in this Chapter can be extended as similarly shown in Chapter 7. With setting

$\omega_q = 0$ and using the previously established affine balancing policy, see (3.7), we have:

$$p_{G,i}(\omega) = p_{G,i} - \alpha_i e^\top \omega \tag{6.2}$$
$$q_{G,i}(\omega) = q_{G,i} \tag{6.3}$$
$$u_i(\omega) = u_i - R_i(I - \alpha e^\top)\omega \tag{6.4}$$
$$f_i^p(\omega) = f_i^p + A_i(I - \alpha e^\top)\omega \tag{6.5}$$
$$f_i^q(\omega) = f_i^q. \tag{6.6}$$

Noticeably (6.2) and (6.5) remain unchanged relative to (3.60).

SEPARATION OF PARTICIPATION FACTORS FROM CONES As derived in Section 3.4, the standard deviation of $u_i(\omega)$, as defined in (6.4), is given by the second order conic expression

$$\sigma(u_i(\omega)) = \left\| R_i(I - \alpha e^\top)\Sigma \right\|_2. \tag{6.7}$$

To simplify differentiation with respect to α we first define auxiliary vector

$$\rho^\nu = R\alpha, \tag{6.8}$$

and note that the i-th entry of ρ^ν is given as $\rho_i^\nu = R_i\alpha$. Next we define $\check{R} = R^{-1}$. Since $R := A^\top \operatorname{diag}(r) A$ as per (3.50) and all r_i in r are positive and non-zero line resistances, R is positive definite and R^{-1} exists. As a result we have that

$$\alpha = \check{R}\rho^\nu \tag{6.9}$$

and not that $\alpha_i = \check{R}_i\rho^\nu$. Finally, we can formulate (6.7) as the following two constraints:

$$t_i^\nu \geqslant \left\| (R_i - \rho_i^\nu e^\top)\Sigma_\omega \right\|_2 \qquad \forall i \in \mathcal{N}^+ \tag{6.10a}$$
$$\alpha_i = \check{R}_i \rho^\nu \qquad \forall i \in \mathcal{N}^+. \tag{6.10b}$$

The same can be achieved for flows with $\rho^f := A\alpha$ and $\check{A} = A^{-1}$.

COMPLETE MODEL FORMULATION We now introduce dual multipliers to all constraints of the resulting CC-ACOPF, which is restated below for this purpose:

$$\text{EQV-CC:} \quad \min_{\substack{\{p_{G,i}, q_{G,i}, \alpha_i\}_{i \in \mathcal{G}},\\ \{f_i^p, f_i^q, u_i\}_{i = \mathcal{N}^+}}} \sum_{i=0}^{n} \left(c_i(p_{G,i}) + \frac{\alpha_i^2}{2b_i} S^2 \right) \tag{6.11a}$$

s.t.

$$(\lambda_0^p): \qquad p_{G,0} - \sum_{j \in \mathcal{C}_0} f_j^p = 0 \tag{6.11b}$$

$$(\lambda_0^q): \quad q_{G,0} - \sum_{j \in \mathcal{C}_0} f_j^q = 0 \tag{6.11c}$$

$$(\lambda_i^p): \quad f_i^p + p_{G,i} - \sum_{j \in \mathcal{C}_i} f_j^p = p_{D,i} \qquad i \in \mathcal{N}^+ \tag{6.11d}$$

$$(\lambda_i^q): \quad f_i^q + q_{G,i} - \sum_{j \in \mathcal{C}_i} f_j^q = q_{D,i} \qquad i \in \mathcal{N}^+ \tag{6.11e}$$

$$(\beta_i): \quad u_i + 2(r_i f_i^p + x_i f_i^q) = u_{\mathcal{A}_i} \qquad i \in \mathcal{N}^+ \tag{6.11f}$$

$$(\chi): \quad \sum_{i=1}^{n} \alpha_i + \alpha_0 = 1 \tag{6.11g}$$

$$(\delta_i^+): \quad p_{G,i} + z_{\epsilon_p} S \alpha_i \leqslant p_{G,i}^{\max} \qquad i \in \mathcal{G} \tag{6.11h}$$

$$(\delta_i^-): \quad -p_{G,i} + z_{\epsilon_p} S \alpha_i \leqslant -p_{G,i}^{\min} \qquad i \in \mathcal{G} \tag{6.11i}$$

$$(\theta_i^+): \quad q_{G,i} \leqslant q_{G,i}^{\max} \qquad i \in \mathcal{G} \tag{6.11j}$$

$$(\theta_i^-): \quad -q_{G,i} \leqslant -q_{G,i}^{\min} \qquad i \in \mathcal{G} \tag{6.11k}$$

$$(\zeta_i): \quad t_i^v \geqslant \left\| (R_i + \rho_i^v e^\top) \Sigma^{1/2} \right\|_2 \qquad i \in \mathcal{N}^+ \tag{6.11l}$$

$$(\nu_i^v): \quad \sum_{j=1}^{n} \check{R}_{ij} \rho_j^v = \alpha_i \qquad i \in \mathcal{G} \tag{6.11m}$$

$$(\mu_i^+): \quad u_i + 2 z_{\epsilon_v} t_i^v \leqslant u_i^{\max} \qquad i \in \mathcal{N}^+ \tag{6.11n}$$

$$(\mu_i^-): \quad -u_i + 2 z_{\epsilon_v} t_i^v \leqslant -u_i^{\min} \qquad i \in \mathcal{N}^+ \tag{6.11o}$$

$$(\nu_i^f): \quad \sum_{i=1}^{n} \check{A}_{ij} \rho_j^f = \alpha_i \qquad i \in \mathcal{G} \tag{6.11p}$$

$$(\zeta_i^f): \quad t_i^f \geqslant \left\| (A_i - \rho_i^f e^\top) \Sigma^{1/2} \right\|_2 \qquad i \in \mathcal{N}^+ \tag{6.11q}$$

$$(\eta_{i,c}): \quad a_{1,c}(f_i^p + z_{\epsilon_f} t_i^f) + a_{2,c} f_i^q + a_{3,c} s_i^{\max} \leqslant 0 \qquad i \in \mathcal{N}^+, c \in \{1, \dots, 12\} \tag{6.11r}$$

Greek letters in parentheses are the dual multipliers assigned to each constraint. See Appendix A on page 153 for more information on dual multipliers. Also, note that balancing adequacy constraint (6.11g) has been reformulated to separate the balancing contribution α_0 of the root node (substation) from the balancing participation $\alpha_i,\ i \in \mathcal{N}^+$ of the DERs in the system.

6.2.2 *Extension with Loss Factors*

Model (6.11) can be extended to incorporate power losses to account for their effect on prices. For this purpose we derive an approximate linear mapping of nodal net injections into power losses, [68], [136], [184]. We use the SOC-relaxed branch flow model as derived in Section B.5. Here, the active and reactive power losses on edge i are given by $l_i r_i$ and $l_i x_i$, where l_i is the squared current on edge i. Using the available demand forecast, we solve:

$$\min_{\substack{\{p_{G,i},q_{G,i},\alpha_i\}_{i\in\mathcal{G}},\\ \{f_i^p,f_i^q,u_i\}_{i=\mathcal{N}^+}}} \sum_{i=0}^{n} \left(c_i(p_{G,i}) + \frac{\alpha_i^2}{2b_i} S^2 \right) \tag{6.12a}$$

s.t. (6.11g)–(6.11k)

$$f_i^p + p_{G,i} - \sum_{j\in\mathcal{C}_i} (f_j^p + l_j r_j) = d_i^p \qquad i\in\mathcal{N} \tag{6.12b}$$

$$f_i^q + q_{G,i} - \sum_{j\in\mathcal{C}_i} (f_j^q + l_j x_j) = d_i^q \qquad i\in\mathcal{N} \tag{6.12c}$$

$$u_i + 2(r_i f_i^p + x_i f_i^q) + l_i(r_i^2 + x_i^2) = u_{\mathcal{A}_i} \qquad i\in\mathcal{N}^+ \tag{6.12d}$$

$$\frac{(f_i^p)^2 + (f_i^q)^2}{u_i} \leqslant l_i \qquad i\in\mathcal{N}^+ \tag{6.12e}$$

$$u_i^{\min} \leqslant u_i \leqslant u_i^{\max} \qquad i\in\mathcal{N}^+ \tag{6.12f}$$

$$(f_i^p)^2 + (f_i^q)^2 \leqslant (s_i^{\max})^2 \qquad i\in\mathcal{N}^+ \tag{6.12g}$$

$$(f_i^p - l_i^p r_i)^2 + (f_i^q - l_i^q x_i)^2 \leqslant (s_i^{\max})^2 \qquad i\in\mathcal{N}^+. \tag{6.12h}$$

The branch flow model in (6.12), which accounts for the power losses in (6.12b) and (6.12c), is modified to include decision variables $\alpha_i, i \in \mathcal{G}$ and the (linear) deterministic equivalents of the generation chance constraints (6.11h) and (6.11i) to compute reserve $z_{\epsilon_p} s\alpha_i, i \in \mathcal{G}$. The solution of (6.12) is used below as a linearization point to compute loss factors. We denote this linearization point as $\{\overline{p}_i, i \in \mathcal{G}; \overline{q}_i, i \in \mathcal{G}; \overline{f}_i^p, i \in \mathcal{N}^+; \overline{f}_i^q, i \in \mathcal{N}^+; \overline{u}_i, i \in \mathcal{N}; \overline{l}_i, i \in \mathcal{N}^+\}$.

Since the power losses of each edge j in (6.12b) and (6.12c) are allocated to its upstream node $\mathcal{A}_j$, terms $\sum_{j\in\mathcal{C}_i} l_j r_j$, $\sum_{j\in\mathcal{C}_i} l_j x_j$ at each node i can be interpreted as a (additional) fictitious nodal demand (FND) at node i, [136]. To approximate the FND around the linearization point, we first obtain the sensitivity of current $\overline{l}_i(\overline{f}_i^p, \overline{f}_i^q, \overline{u}_i)$ at the linearization point with respect to changes in active and reactive nodal net demand and production. Assuming that (6.12e) is tight at the optimum of (6.12), [185], we compute:

$$L_{ik}^p \coloneqq \frac{\partial \overline{l}_i}{\partial p_{D,k}} = -\frac{\partial \overline{l}_i}{\partial p_{G,k}} = \left(2\overline{f}_i^p A_{ik} + 2\overline{f}_i^q A_{ik}\right) \frac{1}{\overline{u}_i} \tag{6.13}$$

$$L_{ik}^q \coloneqq \frac{\partial \overline{l}_i}{\partial q_{D,k}} = -\frac{\partial \overline{l}_i}{\partial q_{G,k}} = \left(2\overline{f}_i^p A_{ik} + 2\overline{f}_i^q A_{ik}\right) \frac{1}{\overline{u}_i}, \tag{6.14}$$

where L_{ik}^p and L_{ik}^q define the sensitivity of power losses of edge i to active and reactive power changes at node k. Next, using (6.13) and (6.14), we can find the sensitivity of the active FND at node i

to active and reactive net demand deviations from the linearization point at node j as:

$$LP^p_{ij} = \sum_{k\in\mathcal{C}_i} L^p_{kj} r_k, \quad LP^q_{ij} = \sum_{k\in\mathcal{C}_i} L^q_{kj} r_k \tag{6.15}$$

and the sensitivity of reactive FND at node i to active and reactive net demand deviations from the linearization point at node j as:

$$LQ^p_{ij} = \sum_{k\in\mathcal{C}_i} L^p_{kj} x_k, \quad LQ^q_{ij} = \sum_{k\in\mathcal{C}_i} L^q_{kj} x_k. \tag{6.16}$$

Since the forecast demand is fixed, the linearized FND only depends on the deviation of active and reactive production levels $(p_{G,i} - \overline{p}_{G,i}), i \in \mathcal{G}$, and $(q_{G,i} - \overline{q}_{G,i}), i \in \mathcal{G}$. Thus, the loss-aware nodal power balance constraints are given as:

$$(\lambda^p_i) : f^p_i + p_{G,i} - \sum_{j\in\mathcal{C}_i} (f^p_j + \bar{l}_j r_j) + \mathrm{Ploss}_i(p_G, p_G) = p_{D,i} \tag{6.17}$$

$$(\lambda^q_i) : f^q_i - q_{G,i} - \sum_{j\in\mathcal{C}_i} (f^q_j + \bar{l}_j x_j) + \mathrm{Qloss}_i(p_G, p_G) = q_{D,i}, \tag{6.18}$$

where:

$$\mathrm{Ploss}_i(p_G, q_G) \coloneqq \sum_{j\in\mathcal{G}} (LP^p_{ij}(p_{G,j} - \overline{p}_{G,j}) + LP^q_{ij}(q_{G,j} - \overline{q}_{G,j})) \tag{6.19}$$

$$\mathrm{Qloss}_i(p_G, q_G) \coloneqq \sum_{j\in\mathcal{G}} (LQ^p_{ij}(p_{G,j} - \overline{p}_{G,j}) + LQ^q_{ij}(q_{G,j} - \overline{q}_{G,j})). \tag{6.20}$$

To determine the impact of power losses with respect to uncertainty $\boldsymbol{\omega}$, we define matrices LP^p and LQ^p with elements LP^p_{ij} and LQ^p_{ij} given by (6.15) and (6.16). Using these matrices, we define the loss-aware extensions of matrices A and R denoted as A^L and R^L:

$$A^L \coloneqq A(I + LP^p) \tag{6.21}$$

$$R^L \coloneqq A^\top(\mathrm{diag}(r)A^L + \mathrm{diag}(x)A\, LQ^p). \tag{6.22}$$

Therefore, the loss-aware modification of the EQV-CC is obtained by substituting A with A^L and R with R^L and extending the nodal power balances as given in (6.17) and (6.18). The CC-ACOPF model with power losses is presented in detail in Section 6.3.3, see (6.46).

6.3 DLMPS WITH CHANCE-CONSTRAINED LIMITS

This section derives DLMPs from the EQV-CC in (6.11).

6.3.1 *DLMPs with Chance-Constrained Generation Limits*

In this subsection, we consider a modification of the EQV-CC in (6.11) that models chance constraints on the generation outputs in (6.11h)–(6.11i) and other constraints are considered deterministically. This modification is given below:

$$\text{GEN-CC:} \quad \min_{\substack{\{p_{G,i}, q_{G,i}, \alpha_i\}_{i \in N},\\ \{f_i^p, f_i^q, u_i\}_{i=N^+}}} \sum_{i=0}^{n} \left(c_i(p_{G,i}) + \frac{\alpha_i^2}{2b_i} S^2 \right) \tag{6.23a}$$

$$\begin{aligned}
&\text{s.t.} && (6.11b)\text{–}(6.11k) && \\
&(\mu_i^+): && u_i \leqslant u_i^{\max} && i \in \mathcal{N}^+ \quad (6.23b)\\
&(\mu_i^-): && -u_i \leqslant -u_i^{\min} && i \in \mathcal{N}^+ \quad (6.23c)\\
&(\eta_i): && (f_i^p)^2 + (f_i^q)^2 \leqslant (s_i^{\max})^2 && i \in \mathcal{N}^+. \quad (6.23d)
\end{aligned}$$

We use the GEN-CC to compute the power and balancing regulation prices, which are given by dual multiplier λ_i^p and λ_i^q of the power balance constraint (6.11d) and (6.11e), as well as dual multiplier χ of the system-wide balancing regulation condition in (6.11g). Thus, we formulate and prove:

Proposition 6.1. *Consider the GEN-CC in* (6.23)*. Let λ_i^p and λ_i^q be the active and reactive power prices defined as dual multipliers of constraints* (6.11d) *and* (6.11e)*. Then λ_i^p and λ_i^q are given by the following functions:*

$$\lambda_i^p = \lambda_{\mathcal{A}_i}^p + (\lambda_i^q - \lambda_{\mathcal{A}_i}^q)\frac{r_i}{x_i} - 2\eta_i \left(f_i^p + \frac{r_i}{x_i} f_i^q \right) \tag{6.24}$$

$$\lambda_i^q = \lambda_{\mathcal{A}_i}^q + (\lambda_i^p - \lambda_{\mathcal{A}_i}^p)\frac{x_i}{r_i} - 2\eta_i \left(f_i^q + \frac{x_i}{r_i} f_i^p \right), \tag{6.25}$$

where η_i is a dual multiplier of (6.23d)*.*

Proof. The Karush-Kuhn-Tucker (KKT) optimality conditions for the GEN-CC in (6.23) are:

$$\begin{aligned}
&(p_{G,i}): && \frac{(p_{G,i} + a_i)}{b_i} + \delta_i^+ - \delta_i^- - \lambda_i^p = 0 && i \in \mathcal{G} \quad (6.26a)\\
&(q_{G,i}): && \theta_i^+ - \theta_i^- - \lambda_i^q = 0 && i \in \mathcal{G} \quad (6.26b)\\
&(u_i): && \beta_i - \sum_{j \in \mathcal{C}_i} \beta_j + \mu_i^+ - \mu_i^- = 0 && i \in \mathcal{N}^+ \quad (6.26c)\\
&(f_i^p): && \lambda_i^p - \lambda_{\mathcal{A}_i}^p + 2r_i\beta_i + 2f_i^p\eta_i = 0 && i \in \mathcal{N}^+ \quad (6.26d)\\
&(f_i^q): && \lambda_i^q - \lambda_{\mathcal{A}_i}^q + 2x_i\beta_i + 2f_i^q\eta_i = 0 && i \in \mathcal{N}^+ \quad (6.26e)\\
&(\alpha_i): && \frac{\alpha_i}{b_i}S^2 + z_{\epsilon_p}s(\delta_i^+ + \delta_i^-) - \chi = 0 && i \in \mathcal{N}^+ \quad (6.26f)\\
&(\alpha_0): && \frac{\alpha_0}{b_0}S^2 - \chi = 0 && \quad (6.26g)
\end{aligned}$$

$$0 \leqslant \delta_i^+ \perp p_{G,i}^{max} - p_{G,i} - z_{\epsilon_p} \alpha_i s \geqslant 0 \qquad i \in \mathcal{G} \tag{6.26h}$$
$$0 \leqslant \delta_i^- \perp p_{G,i} - z_{\epsilon_p} \alpha_i s - p_{G,i}^{min} \geqslant 0 \qquad i \in \mathcal{G} \tag{6.26i}$$
$$0 \leqslant \theta_i^+ \perp q_{G,i}^{max} - q_{G,i} - \geqslant 0 \qquad i \in \mathcal{G} \tag{6.26j}$$
$$0 \leqslant \theta_i^- \perp q_{G,i} - q_{G,i}^{min} \geqslant 0 \qquad i \in \mathcal{G} \tag{6.26k}$$
$$0 \leqslant \mu_i^+ \perp u_i^{max} - u_i \geqslant 0 \qquad i \in \mathcal{N}^+ \tag{6.26l}$$
$$0 \leqslant \mu_i^- \perp u_i - u_i^{min} \geqslant 0 \qquad i \in \mathcal{N}^+ \tag{6.26m}$$
$$0 \leqslant \eta_i \perp (s_i^{max})^2 - (f_i^p)^2 - (f_i^q)^2 \geqslant 0 \qquad i \in \mathcal{N}^+. \tag{6.26n}$$

Expressing λ_i^p and λ_i^q from (6.26d) and (6.26e) instantly yields the expressions in (6.24) and (6.25). □

Remark 6.1. Eqs. (6.24) and (6.25) can also be used to couple DLMPs and transmission LMPs for active and, if available, reactive power obtained from wholesale market-clearing outcomes. Indeed, transmission LMPs can be parameterized in (6.24) and (6.25) as prices at the root node, i.e. λ_0^p and λ_0^q.

Proposition 6.1 allows for multiple insights on the price formation process. First, both λ_i^p and λ_i^q do not explicitly depend on uncertainty and risk parameters. Next, as the second terms in (6.24) and (6.25) reveal, λ_i^p and λ_i^q are mutually dependent. Furthermore, the third terms in (6.24) and (6.25) demonstrates that λ_i^p and λ_i^q are both equally dependent on active and reactive power flows f_i^p and f_i^q, as well as edge characteristics r_i and x_i. Finally, if the distribution system is not power-flow-constrained, i.e. $\eta_i = 0$ and (6.23d) is not binding, the third terms disappear in (6.24) and (6.25). However, even in this case the DLMPs at different nodes would not be the same due the need to provide both reactive and active power.

Since Proposition 6.1 relates prices λ_i^p and λ_i^q at neighboring nodes, it implies that changing a real power injection at any node i can be compensated by active and reactive power adjustments at either the ancestor node or that node without any other changes in the system. However, similarly to the discussion in [139], the physical dependencies between the nodes are more complex and net injection changes at one node will shift operating conditions at all other nodes. This becomes clear when we reinterpret the results of Proposition 6.1 in terms of the voltage limits given by (6.23b) and (6.23c). For this purpose we express β_i from (6.26c) and use it in (6.26d) and (6.26e). Expressing λ_i^p and λ_i^q from (6.26d) and (6.26e) leads to:

$$\lambda_i^p = \lambda_{\mathcal{A}_i}^p - 2r_i \sum_{j \in \mathcal{D}_i} (\mu_j^+ - \mu_j^-) + 2f_i^p \eta_i \tag{6.27}$$
$$\lambda_i^q = \lambda_{\mathcal{A}_i}^q - 2x_i \sum_{j \in \mathcal{D}_i} (\mu_j^+ - \mu_j^-) + 2f_i^q \eta_i. \tag{6.28}$$

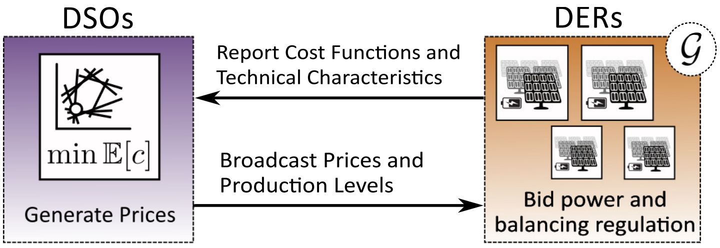

Figure 6.1: A schematic representation of the auction.

Thus, if voltage limits are binding at downstream nodes $j \in \mathcal{D}_i$ of node i, i.e. $\mu_j^+ \neq 0$ or $\mu_j^- \neq 0$, they will contribute to the resulting values of λ_i^p and λ_i^q. Furthermore, expressions in (6.27) and (6.28) show that if the distribution system is not voltage- or power-flow-congested, i.e. $\mu_i^+ = \mu_i^- = \eta_i = 0, i \in \mathcal{N}$, DLMPs reduce to system-wide prices equal to the prices at the root node, i.e. $\lambda_i^p = \lambda_0^p$ and $\lambda_i^q = \lambda_0^q$.

Unlike λ_i^p and λ_i^q, we find that the price for balancing regulation explicitly depends on uncertainty and risk parameters:

Proposition 6.2. *Consider the GEN-CC in (6.23). Let χ be the balancing regulation price defined as a dual multiplier of constraint (6.11g). Then the following function defines χ:*

$$\chi = \frac{s}{\sum_{i=0}^{n} b_i}\left(s + z_\epsilon \sum_{i=1}^{n}(\delta_i^+ + \delta_i^-)b_i\right). \tag{6.29}$$

Proof. Expressing α_i and α_0 from (6.26f) and (6.26g) in terms of χ and using it (6.11g) yields:

$$1 + \frac{\chi b_0}{S^2} = -\sum_{i=1}^{n}\left[\chi + z_{\epsilon_p} s(\delta_i^+ + \delta_i^-)\right]\frac{b_i}{S^2}, \tag{6.30}$$

which immediately leads to (6.29). □

As per (6.29), χ depends on uncertainty, since $S^2 := e^\top \Sigma e$, as well as risk tolerance of the DSO, since $z_{\epsilon_p} = \Phi^{-1}(1-\epsilon_p)$. Notably, the balancing regulation price is always non-zero if there is uncertainty in the system (i.e. $S \neq 0$). This is true even if none of the chance constraints on output limits of DERs in (6.11h)-(6.11i) are binding, i.e. $\delta_i^+ = \delta_i^- = 0, i \in \mathcal{N}$. In other words, as long as the forecast is not perfect, there is a value on procuring a non-zero amount of balancing regulation.

The prices resulting from Propositions 6.1 and 6.2 can be leveraged by the DSO to organize a stochastic distribution electricity market, e.g. via a centralized auction. Fig. 6.1 illustrates such an auction, where, first, producers truthfully report their cost functions and technical characteristics to the DSO. Next, the DSO determines the optimal dispatch decisions and resulting prices for each market product using the best available forecast information. Finally, these decisions and prices are communicated by the DSO to all producers. For this stochastic electricity market, we define a *competitive equilibrium* as a set of production levels and prices $\{p_{G,i}, i \in \mathcal{G}; \alpha_i, i \in \mathcal{G}; \pi_i^p, i \in \mathcal{G}; \pi^\alpha\}$ that (i) clears the market so that the production and demand quantities are balanced and $\sum_{i\in\mathcal{G}} \alpha_i = 1$ and (ii) maximizes the profit of all producers, under the market payment structured as $\pi^p p^{G,i} + \pi^\alpha \alpha_i$, so that there is no incentive to deviate from the market outcomes. See Appendix C for a more detailed discussion on competitive equilibrium.

To show that the prices from Propositions 6.1 and 6.2 support the competitive equilibrium, we consider the GEN-CC in (6.23) and the behavior of each producer (controllable DER) is modeled as a risk-neutral, profit-maximization:

$$\left\{ \begin{aligned} &\max_{p_{G,i},\alpha_i} \Pi_i = \overbrace{\pi_i^p p_{G,i} + \pi^\alpha \alpha_i}^{\text{Payment}} \overbrace{- c_i(p_{G,i}) - \alpha_i^2 \frac{S^2}{2b_i}}^{\text{Cost}} \\ &\text{s.t } (\delta_i^-, \delta_i^+): \; p_{G,i}^{\min} + z_{\epsilon_p} \alpha_i s \leqslant p_{G,i} \leqslant p_{G,i}^{\max} - z_{\epsilon_p} \alpha_i s \end{aligned} \right\} \quad i \in \mathcal{G}, \tag{6.31}$$

where Π_i denotes the profit function of each controllable DER at node i and $\{\pi_i^p, \pi^\alpha\}$ are active power and balancing regulation prices.

Remark 6.2. Since uncertainty and risk parameters, i.e. $S^2 = e^\top \Sigma e$ and z_{ϵ_p}, are shared by the DSO and producers, we assume that this knowledge is common and consensual. Although these parameters can be exploited by the DSO to advance their self-interest and increase security margins above reasonable levels at the expense of customers, this behavior can be mitigated using benchmarking and performance-based rate design practices, [186]–[188].

Considering this stochastic market, as in Fig. 6.1, we prove:

Theorem 6.1. *Let* $\{p_{G,i}^*, \alpha_i^*, i \in \mathcal{G}\}$ *be an optimal solution of the GEN-CC in* (6.23) *and let* $\{\lambda_i^{P,*}, i \in \mathcal{N}; \chi^*\}$ *be the dual variables of* (6.11d) *and* (6.11e)*, then the set of production levels and prices* $\{p_{G,i}^*, i \in \mathcal{G}; \alpha_i^*, i \in \mathcal{G}; \pi_i^p, i \in \mathcal{G}; \pi^\alpha\}$ *is a competitive equilibrium if* $\pi_i^p = \lambda_i^{P,*}, i \in \mathcal{G}$, *and* $\pi^\alpha = \chi^*$.

Proof. The KKT optimality conditions for (6.31) are:

$$(p_{G,i}): \qquad \frac{(p_{G,i} + a_i)}{b_i} + \delta_i^+ - \delta_i^- - \pi_i^p = 0 \tag{6.32a}$$

$$(\alpha_i): \qquad \frac{\alpha_i}{b_i} S^2 + z_{\epsilon_p} s(\delta_i^+ + \delta_i^-) - \pi^\alpha = 0 \tag{6.32b}$$

$$0 \leqslant \delta_i^+ \perp p_{G,i}^{\max} - p_{G,i} + z_{\epsilon_p} \alpha_i \geqslant 0 \tag{6.32c}$$

$$0 \leqslant \delta_i^- \perp p_{G,i} - z_{\epsilon_p} \alpha_i s - p_{G,i}^{\min} \geqslant 0. \tag{6.32d}$$

Using (6.32a) and (6.32b), we express $\pi_i^p = -\frac{(p_{G,i}-a_i)}{b_i} - \delta_i^+ + \delta_i^-$ and $\pi^\alpha = -\frac{\alpha_i}{b_i}S^2 - z_{\epsilon_p}S(\delta_i^+ + \delta_i^-)$. Similarly, we express λ_i^p and χ from (6.26a) and (6.26f). Therefore, $\lambda_i^p = -\frac{(p_{G,i}-a_i)}{b_i} - \delta_i^+ + \delta_i^- = \pi_i^p$ and $\chi = -\frac{\alpha_i}{b_i}S^2 - z_{\epsilon_p}s(\delta_i^+ + \delta_i^-) = \pi^\alpha$. If $\{p_{G,i}^*, \alpha_i^*, i \in \mathcal{G}\}$, it follows that $\lambda_i^{P,*} = \pi_i^g$ and $\chi^* = \pi_i^\alpha$, i.e. $\{p_{G,i}^*, i \in \mathcal{G}; \alpha_i^*, i \in \mathcal{G}; \pi_i^p, i \in \mathcal{G}; \pi^\alpha\}$ solves (6.31) and maximizes Π_i. Therefore, $\{p_{G,i}^*, i \in \mathcal{G}; \alpha_i^*, i \in \mathcal{G}; \pi_i^p, i \in \mathcal{G}; \pi^\alpha\}$ is a competitive equilibrium. $\square$

Since both the DSO and producers are modeled as risk-neutral, see (6.11) and (6.31), and share common knowledge about underlying uncertainty parameters, the competitive equilibrium established by Theorem 6.1 also corresponds to the welfare-maximization (cost-minimization) solution, [130]. Notably, this property will hold as long as the DSO and producers continue sharing common knowledge about underlying uncertainty parameters, even if their attitudes toward risk vary based on a given coherent risk measure, [130]. The impact of risk-averse behavior is studied in Chapter 8. Although, from the viewpoint of customers, internalizing the uncertainty and risk parameter in the equilibrium prices from Theorem 6.1 may increase electricity prices relative to the deterministic case, stochasticity-aware prices will provide incentives to reduce their uncertainty, thus reducing balancing regulation needs in the system, or to exercise more flexibility (e.g. to shift their demand to time periods with lower DLMPs).

Hence, using the competitive equilibrium of Theorem 6.1, we can analyze the effect of the prices on the capacity allocation between the power production and balancing regulation from the perspective of each producer modeled as in (6.31). Let $\{\pi_i^p, \pi^\alpha\}$ be given prices and let $\{p_{G,i}^*, \alpha_i^*\}$ be the optimal solution of (6.31) for these prices. The KKT optimality conditions in (6.32a)–(6.32d) can be used to find parametric functions that determine the optimal dispatch of each controllable DER. These functions depend on whether constraints in (6.31) are binding or not. Since (6.31) has two inequality constraints, we consider the following four cases:

1. $\delta_i^{+,*} = \delta_i^{-,*} = 0$: When (6.31) has no binding constraints, it follows from (6.32a) and (6.32b) that:

$$p_{G,i}^* = \pi_i^g b_i - a_i, \quad \alpha_i^* = \frac{\pi^\alpha b_i}{S^2} \tag{6.33}$$

Inserting the optimal dispatch given by (6.33) into (6.32c) and (6.32d) leads to the following relationship between prices π_i^g and π^α:

$$\frac{p_{G,i}^{\min} + a_i}{b_i} + z_{\epsilon_p}\frac{\pi^\alpha}{S} \leqslant \pi_i^p \leqslant \frac{p_{G,i}^{\max} + a_i}{b_i} - z_{\epsilon_p}\frac{\pi^\alpha}{S}. \tag{6.34}$$

2. $\delta_i^{+,*} \neq 0, \delta_i^{-,*} = 0$: Since $\delta_i^{+,*} \neq 0$, only the upper limit is binding. Thus, (6.32c) yields $p_{G,i}^* + z_{\epsilon_p}\alpha_i^* S - p_{G,i}^{\max} = 0$, which in combination with (6.32a) and (6.32b) leads to:

$$p_{G,i}^* = p_{G,i}^{\max} - z_{\epsilon_p} S \alpha_i^* \tag{6.35a}$$

$$\alpha_i^* = \frac{z_{\epsilon_p} S(p_{G,i}^{\max} + a_i - b_i \pi_i^g) + \pi^\alpha b_i}{S^2(1 + z_{\epsilon_p}^2)}. \tag{6.35b}$$

With the upper constraint binding, it follows from (6.34) that (6.35) holds if:

$$\pi_i^p \geqslant \frac{p_{G,i}^{\max} + a_i}{b_i} - z_{\epsilon_p}\frac{\pi^\alpha}{S}. \tag{6.36}$$

3. $\delta_i^{+,*} = 0, \delta_i^{-,*} \neq 0$: This case is the opposite of the previous one since only the lower limit is binding. Therefore, (6.32d) yields $-p_{G,i}^* + z_{\epsilon_p}\alpha_i^* S + p_{G,i}^{P,\min} = 0$, which in combination with (6.32a) and (6.32b) leads to:

$$p_{G,i}^* = p_{G,i}^{\min} + z_{\epsilon_p} S \alpha_i^* \tag{6.37a}$$

$$\alpha_i^* = \frac{z_{\epsilon_p} S(g^{\min} + a_i - b_i \pi_i^g) - \pi^\alpha b_i}{S^2(1 + z_{\epsilon_p}^2)}. \tag{6.37b}$$

With the lower constraint binding it follows from (6.34) that (6.37) holds if:

$$\pi_i^p \leqslant \frac{p_{G,i}^{\min} + a_i}{b_i} + z_{\epsilon_p}\frac{\pi^\alpha}{S}. \tag{6.38}$$

4. $\delta_i^{+,*} \neq 0, \delta_i^{-,*} \neq 0$: When both constraints of (6.31) are binding it follows from (6.32c) and (6.32d) that:

$$p_{G,i}^* = \frac{p_{G,i}^{\max} + p_{G,i}^{\min}}{2}, \quad \alpha_i^* = \frac{p_{G,i}^{\max} - p_{G,i}^{\min}}{2 z_{\epsilon_p} S}, \tag{6.39}$$

where $p_{G,i}^*$ is the midpoint of the dispatch range and the upward $(p_{G,i}^{\max} - p_{G,i}^*)$ and downward $(p_{G,i}^* - p_{G,i}^{\min})$ margins are fully used for providing balancing regulation. In this case, it follows from (6.34) that π^α is independent of π_i^p and must be as follows:

$$\pi^\alpha \geqslant \frac{S(p_{G,i}^{\max} - p_{G,i}^{\min})}{2 z_{\epsilon_p} b_i}. \tag{6.40}$$

The dispatch policies in (6.33), (6.35), (6.37) and (6.39) support the competitive equilibrium established by Theorem 6.1 and can be implemented locally at each DER, if there is communication to broadcast prices π_i^p and π^α.

Remark 6.3. Eqs. (6.33)–(6.40) provide a parametric model of the reaction of each producer to given price signals. By observing the provided production levels and balancing participation factors for given prices over time, the DSO can use machine learning methods to estimate these parameters. This enables the DSO to either verify reported cost functions and technical characteristics or to establish a one-way communication market framework as implemented in Chapeter 5 and [P2] for demand-side management.

6.3.2 *DLMPs with Chance-Constrained Voltage Limits*

The the GEN-CC in (6.23) has deterministic voltage limits as given by (6.23b) and (6.23c). We recast these limits as chance constraints, which leads to the following optimization:

$$\text{VOLT-CC:} \min_{\substack{\{p_{G,i},q_{G,i},\alpha_i\}_{i\in N},\\ \{f_i^p,f_i^q,u_i\}_{i=N^+}}} \sum_{i=0}^{n}\left(c_i(p_{G,i})+\frac{\alpha_i^2}{2b_i}S^2\right) \tag{6.41a}$$

$$\text{s.t.} \qquad (6.11b)\text{–}(6.11o) \text{ and } (6.23d).$$

Similarly to the GEN-CC in (6.23) we formulate and prove for the VOLT-CC in (6.41) the following proposition:

Proposition 6.3. *Consider the VOLT-CC in (6.41). Let λ_i^p, λ_i^q and χ be the active power, reactive power and balancing regulation prices at node i. Then λ_i^p, λ_i^q are given by (6.27), (6.28) and χ is given by*

$$\chi=\frac{S}{\sum_{i=0}^{n}b_i}\left(S+z_\epsilon\sum_{i=1}^{n}(\delta_i^++\delta_i^-)b_i+\sum_{i=1}^{n}b_i\nu_i^v\right), \tag{6.42}$$

where ν_i^v is the dual multiplier of (6.11m) given as:

$$\nu_i^v=2z_{\epsilon_v}\sum_{j=1}^{n}R_{ji}(\mu_j^++\mu_j^-)\frac{R_j(\Sigma e+S^2\alpha)}{\sigma[u_j(\omega,\alpha)]}. \tag{6.43}$$

Proof. The KKT optimality conditions for (6.41) are:

$$(6.26a)\text{–}(6.26e),\ (6.26g)\text{–}(6.26k) \text{ and } (6.26n)$$

$$(\alpha_i): \quad \frac{\alpha_i}{b_i}S^2+z_\epsilon s(\delta_i^++\delta_i^-)-\chi+\nu_i^v=0 \qquad i\in\mathcal{N}^+ \tag{6.44a}$$

$$(t_i^v): \quad 2z_\epsilon(\mu_i^++\mu_i^-)-\zeta_i=0 \qquad i\in\mathcal{N}^+ \tag{6.44b}$$

$$(\rho_i^v): \quad \sum_{j=1}^{n}\nu_j^v\check{R}_{ji}+\zeta_i\frac{(R_i+\rho_i^v e^\top)\Sigma e}{t_i^v}=0 \qquad i\in\mathcal{N}^+ \tag{6.44c}$$

$$0 \leqslant \mu_i^+ \perp u_i^{max} - u_i - 2z_{\epsilon_v} t_i^v \geqslant 0 \qquad i \in \mathcal{N}^+ \tag{6.44d}$$

$$0 \leqslant \mu_i^- \perp u_i - 2z_{\epsilon_v} t_i^v - u_i^{min} \geqslant 0. \qquad i \in \mathcal{N}^+. \tag{6.44e}$$

Note that the KKT conditions hold due to the convex properties of the SOC program, see Appendix A.3. It follows that the expressions for λ_i^p, λ_i^q are equal to the results of Proposition 6.1. Expression (6.42) is obtained analogously to the proof of Proposition 6.2. To find (6.43) we first express ρ_i from (6.11m) and ζ_i from (6.44b) and insert these expressions into (6.44c). Second, if $\zeta_i \neq 0$, then (6.11l) is tight which means $t_i^v = \sigma(u_j(\boldsymbol{\omega}, \alpha))$ as per (6.7). Finally, given that $\check{R} = R^{-1}$ as shown in Section 6.2.1, (6.44c) can be recast as (6.43). □

Proposition 6.3 highlights the difficulty of enforcing probabilistic guarantees on system constraints (e.g. voltage limits) through such individual price signals. While the structure of prices λ_i^p, λ_i^q does not change relative to Proposition 6.1, price χ in (6.42) includes $\sum_{i=1}^n b_i \nu_i^v$ in addition to the terms in (6.29). This additional term leads to a discrepancy between the amounts of balancing participation deemed optimal by the DSO, which seeks to minimize the system-wide operating cost, and by individual producers, which seek to maximize their individual profit. Notably, the expression for ν_i^v in (6.43) depends on vector α, which includes participation factors at all nodes. Hence, introducing voltage chance constraints makes balancing regulation price χ dependent on the choice of participation factors at all nodes and cannot be explained by purely local or neighboring voltage conditions, even in radial networks. Thus, if node i is such that it has a high influence on the voltage magnitudes at other nodes (i.e. as captured by matrix R, see (3.50)), the controllable DER at this node is implicitly discouraged from providing balancing regulation and, therefore, ν_i^v drives the optimal choice of α_i from the system perspective. However, since ν_i^v is not part of (6.31) and thus uncontrolled by DERs, it will not affect (6.32). This result shows that internalizing the effect of stochasticity on voltage limits, which are enforced by the DSO and by producers, will prevent the existence of a competitive equilibrium enforced by Theorem 6.1 and, in this case, balancing participation price χ must be adjusted to reflect this difference between the decision-making process of the DSO and controllable DERs. Assume $\alpha_i^{*,DSO}$ is the optimal amount of balancing regulation determined by the DSO by solving VOLT-CC. If the DSO broadcasts $\pi^\alpha = \chi^*$ then DER i will decide on its optimal participation $\alpha_i^{*,DER}$ by solving (6.31). The resulting difference between those balancing participation factors can then be quantified as:

$$\alpha_i^{*,DER} - \alpha_i^{*,DSO} = \frac{b_i}{s} \nu_i^v \tag{6.45}$$

Note that (6.45) is inversely proportional to the total uncertainty in the distribution system (recall that $S = \sqrt{e \Sigma e^\top}$), i.e. the discrepancy between the DER and DSO perspectives decreases as more uncertainty is observed.

6.3.3 *DLMPs with Losses*

To asses the effect of power losses on DLMPs, we consider the following optimization problem:

$$\text{LVOLT-CC:} \min_{\substack{\{p_{G,i},q_{G,i},\alpha_i\}_{i\in N},\\ \{f_i^p,f_i^q,u_i\}_{i=N^+}}} \sum_{i=0}^{n}\left(c_i(p_{G,i}) + \frac{\alpha_i^2}{2b_i}S^2\right) \tag{6.46a}$$

$$\begin{aligned}
&\text{s.t.} && (6.17) \text{ and } (6.18) && \\
& && (6.11f)\text{–}(6.11k),\ (6.11n),\ (6.11o) \text{ and } (6.23d) && \\
&(\zeta_i): && t_i^v \geqslant \left\|(R_i^L + \rho_i^v e^\top)\Sigma^{1/2}\right\|_2 && i\in\mathcal{N}^+ \quad (6.46b)\\
&(\nu_i^v): && \sum_{j=1}^{n} \check{R}_{ij}^L \rho_j^v = \alpha_i, && i\in\mathcal{G} \quad (6.46c)
\end{aligned}$$

where $\check{R}^L := (R^L)^{-1}$ and claim:

Proposition 6.4. *Consider the LVOLT-CC in (6.46). Let λ_i^p, λ_i^q and χ be the active power, reactive power and balancing regulation prices at node i. Then:*

a) Prices λ_i^p, λ_i^q are given by (6.27), (6.28) and χ is given by:

$$\chi = \frac{1}{\sum_{i=0}^{n} b_i}\left(S^2 + z_\epsilon S\sum_{i=1}^{n}(\delta_i^+ + \delta_i^-)b_i + \sum_{i=1}^{n} b_i\nu_i^v\right), \tag{6.47}$$

where:

$$\nu_i^v = 2z_{\epsilon_v}\sum_{j=1}^{n} R_{ji}^L(\mu_j^+ + \mu_j^-)\frac{R_j^L(\Sigma e + S^2\alpha)}{\sigma[u_j(\omega,\alpha)]}. \tag{6.48}$$

b) The optimal active production level $p_{G,i}^*$ is:

$$p_{G,i}^* = b_i(\lambda_i^p - (\delta_i^+ - \delta_i^-) + \xi_i^p(\lambda^p,\lambda^q)) - a_i, \tag{6.49}$$

where

$$\xi_i^p(\lambda^p,\lambda^q) := \sum_{j=1}^{N} LP_{ji}^p\lambda_j^p + \sum_{j=1}^{N} LQ_{ji}^p\lambda_j^q \tag{6.50}$$

Proof. Consider the KKT optimality conditions for (6.46):

$$
\begin{aligned}
& && (6.26c)\text{–}(6.26e) \text{ and } (6.26g)\text{–}(6.26k) \\
& && (6.26n),\ (6.44d) \text{ and } (6.44e) \\
&(p_{G,i}): && \frac{(p_{G,i}+a_i)}{b_i} + \delta_i^+ - \delta_i^- - \lambda_i^p && (6.51a)\\
& && \qquad \underbrace{-\sum_{j=1}^{N} LP_{ji}^p \lambda_j^p + \sum_{j=1}^{N} LQ_{ji}^p \lambda_j^q}_{\xi_i^p(\lambda^p,\lambda^q)} = 0 \qquad i \in \mathcal{G} \\
&(q_{G,i}): && \theta_i^+ - \theta_i^- - \lambda_i^q && (6.51b)\\
& && -\sum_{j=1}^{N} LP_{ji}^p \lambda_j^p + \sum_{j=1}^{N} LQ_{ji}^p \lambda_j^q = 0 \qquad i \in \mathcal{G} \\
&(\rho_i^v): && \sum_{j=1}^{n} \eta_j^v \check{R}_{ji}^L + \zeta_i \frac{(R_i^L + \rho_i^v e^\top)\Sigma e}{t_i} = 0. && (6.51c)\\
& && \qquad i \in \mathcal{N}^+
\end{aligned}
$$

Our result in Proposition 6.4a) follows directly from the proofs of Propositions 6.1 and 6.3 with R replaced by R^L (see (6.51c)). Then, our result in Proposition 6.4b) follows directly from (6.51a) and (6.51b). □

The term in (6.50) relates the DLMP and optimal production level at node i to the DLMPs at all other nodes via the loss factors. For example, if production at i has a high impact on active power losses at node j (given by LP_{ji}^p) and DLMP λ_j^p is high, then active power production at node i is discouraged by a lower DLMP λ_i^p. Similarly to Proposition 6.3, Proposition 6.4 reveals that power losses distort a competitive equilibrium because they are not part of the individual producers decisions.

6.4 ILLUSTRATIVE CASE STUDY

The case study is performed on the 15-node radial feeder from [139] with two minor modifications: one controllable DER is added at node 11 (see Fig. 6.2) and the power flow limit of edges 2 and 3 is doubled to avoid congestion in the deterministic case. Cost parameters of DERs at nodes 6 and 11 are set to $c_{1,i} = 10$ \$/MWh, $c_{2,i} = 5$ \$/MWh², $c_{0,i} = 0$. The substation cost is set to $c_{1,0} = 50$ \$/MWh, $c_{2,0} = 400$ \$/MWh², $c_{0,0} = 0$. Note that this selection incentivizes the use of DERs. The data of [139] is used as scheduled net demand with a normally distributed zero-mean error, standard deviation of $\sigma_i^p = 0.2 p_{D,i}$ and no covariance among the nodes. The security parameter of the chance constraints is set to $\epsilon_p = 5\,\%$ and $\epsilon_v = 1\,\%$. All models in the case

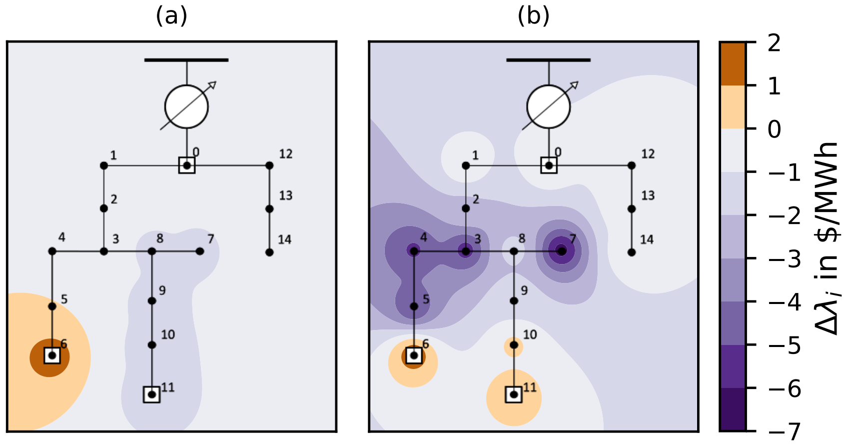

Figure 6.2: DLMP difference $\Delta\lambda_i^p$ of (a) GEN-CC and (b) VOLT-CC relative to the deterministic case.

study are implemented using the Julia JuMP package and our code can be downloaded from [178].

6.4.1 *Effect of uncertainty on DLMPs*

Tables 6.1–6.3 summarize the optimal solution and prices in the deterministic, GEN-CC and VOLT-CC cases. Note that the deterministic case is solved for the expected net demand and $\alpha_i = 0, \forall i$. In the deterministic and GEN-CC cases, none of the generator limits are active and, therefore, their power production does not differ. Similarly the resulting voltage magnitudes do not change as the GEN-CC considers deterministic voltage constraints and only the flow limit of edges 8 and 6 are binding. In the VOLT-CC, however, the resulting voltage magnitudes are closer to unity in order to accommodate real-time power imbalances. As a result, the voltage constraints (6.11l)–(6.11o) in the VOLT-CC yield non-zero dual multipliers. Fig. 6.2 itemizes the effect of uncertainty on λ_i^p relative to the deterministic case, where $\Delta\lambda_i^p = \lambda_i^{p,(\text{GEN-CC/VOLT-CC})} - \lambda_i^{p,(\text{DET})}$. While the passive branch of the system (nodes 12 to 14 without any controllable DERs) shows no changes in DLMPs as it is fully supplied by the substation, DLMPs vary in the branches with DERs.

6.4.2 *Price Decomposition*

Tables 6.4 and 6.5 itemize the components of the energy price following Proposition 6.1. Additionally, Fig. 6.3 illustrates the nodes and edges with binding limits and, thus, non-zero Lagrangian multipliers. Since the GEN-CC has no active voltage constraints the energy price at each node is determined by $\lambda_{\mathcal{A}_i}^p$, i.e. the energy price at the ancestor node, and the congestion as per (6.24). There is no reactive

Table 6.1: Optimal Deterministic Solution

i	$p_{G,i}$	$q_{G,i}$	α_i	$\sqrt{(f_i^p)^2 + (f_i^q)^2}$	ν_i	λ_i^p
0	0.994	0.344	–	0.000	1.000	50.000
1	–	–	–	0.404	0.975	50.000
2	–	–	–	0.446	1.012	50.000
3	–	–	–	0.446	1.067	50.000
4	–	–	–	0.210	1.071	50.000
5	–	–	–	0.227	1.074	50.000
6	0.278	0.006	–	0.256*	1.086	10.411
7	–	–	–	0.197	1.086	10.208
8	–	–	–	0.256*	1.077	10.208
9	–	–	–	0.083	1.078	10.208
10	–	–	–	0.108	1.081	10.208
11	0.140	0.032	–	0.130	1.082	10.208
12	–	–	–	0.660	0.983	50.000
13	–	–	–	0.025	0.978	50.000
14	–	–	–	0.024	0.975	50.000

* Constraint is binding

Table 6.2: Optimal GEN-CC Solution

i	$p_{G,i}$	$q_{G,i}$	α_i	$\sqrt{(f_i^p)^2 + (f_i^q)^2}$	ν_i	λ_i^p	χ
0	0.994	0.344	0.003	0.000	1.000	50.00	0.273
1	–	–	–	0.404	0.975	50.00	–
2	–	–	–	0.446	1.012	50.00	–
3	–	–	–	0.446	1.067	50.00	–
4	–	–	–	0.210	1.071	50.00	–
5	–	–	–	0.227	1.074	50.00	–
6	0.278	0.006	0.646	0.256*	1.086	11.99	–
7	–	–	–	0.197	1.086	8.769	–
8	–	–	–	0.256*	1.077	8.769	–
9	–	–	–	0.083	1.078	8.769	–
10	–	–	–	0.108	1.081	8.769	–
11	0.140*	0.032	0.351	0.130	1.082	8.769	–
12	–	–	–	0.660	0.983	50.00	–
13	–	–	–	0.025	0.978	50.00	–
14	–	–	–	0.024	0.975	50.00	–

* Constraint is binding

Table 6.3: Optimal VOLT-CC Solution

i	$p_{G,i}$	$q_{G,i}$	α_i	$\sqrt{(f_i^p)^2+(f_i^q)^2}$	v_i	λ_i^p	χ
0	1.033	0.490	0.377	0.000	1.000	50.00	31.51
1	–	–	–	0.523	0.956	49.97	–
2	–	–	–	0.439	0.972	47.88	–
3	–	–	–	0.439	0.996	44.59	–
4	–	–	–	0.208	0.997	44.83	–
5	–	–	–	0.222	0.999*	45.056	–
6	0.258	-0.068	0.370	0.256*	1.005*	12.03	–
7	–	–	–	0.197	1.011*	3.884	–
8	–	–	–	0.256*	1.001	8.577	–
9	–	–	–	0.090	1.001	9.111	–
10	–	–	–	0.100	1.001*	10.39	–
11	0.121	-0.040	0.253	0.116	1.002*	10.95	–
12	–	–	–	0.660	0.983	50.00	–
13	–	–	–	0.025	0.978	50.00	–
14	–	–	–	0.024	0.975	50.00	–

* Constraint is binding

power price component due to inactive voltage limits. In the VOLT-CC case, on the other hand, the voltage limits become active and therefore reactive power price is non-zero.

In Fig. 6.2 we observe higher prices at and close to the nodes with DERs. As follows from Eq. (6.27) and summarized in Table 6.6, prices at those nodes are dominated by the lower voltage limits, thus quantifying the value of downward regulation. A negative net demand value at node 7 indicates a high uncontrolled behind-the-meter generation, which leads to low prices dominated by the upper voltage limit. This incentivizes a higher demand and lower generation. At node 6 both the upper and lower voltage limits are binding (see Fig. 6.3 and non-zero μ_6^+, μ_6^- in the bottom row of Table 6.6), thus indicating that no more balancing regulation at this node is possible without increasing the likelihood of voltage limit violations. Hence, the trade-off between the power output and balancing regulation of the DER at node 6 is no longer driven by its profit-maximizing objective, but rather by the the physical limits of the system.

The regulation price in the GEN-CC case ($\chi^{\text{GEN-CC}} = 0.273$) is notably lower relative to the VOLT-CC case ($\chi^{\text{VOLT-CC}} = 31.511$). As per Proposition 6.2, $\chi^{\text{GEN-CC}}$ is only driven by the power output limits (Table 6.7), where only the lower output limit at node 11 is binding. Due to a low power price at node 11 as compared to node 6, the scheduled power production is also low, which limits the downward regulation capacity provided. By introducing voltage chance constraints in the VOLT-CC case, the DLMP composition changes as

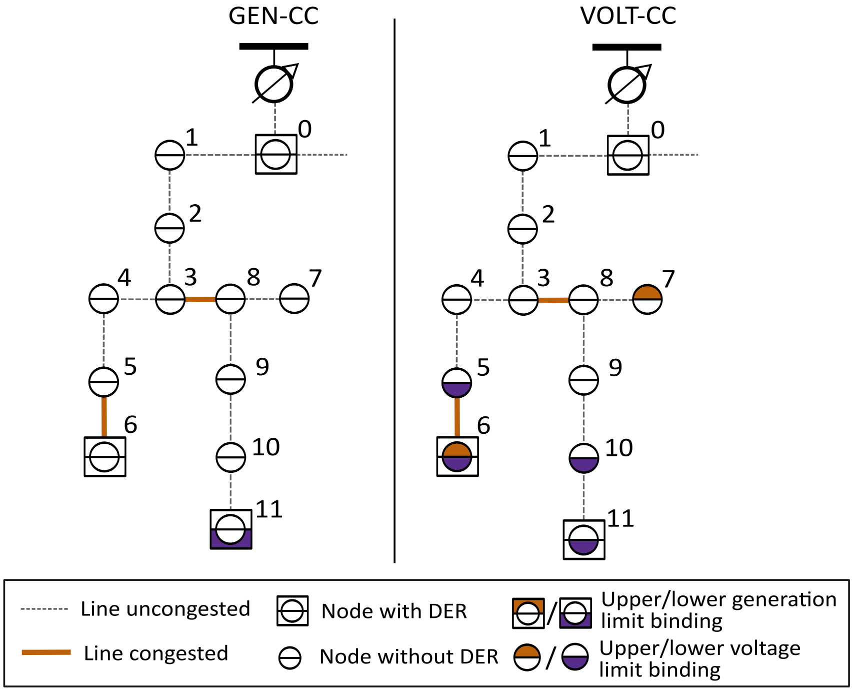

Figure 6.3: Illustration of binding edge, voltage and generation limits in the GEN-CC and the VOLT-CC.

per Proposition 6.3 (Table 6.7). Each node with binding voltage constraints $(5, 6, 7, 10, 11)$ contributes to the formation of χ by weighting the impact of the system-wide regulation participation on the voltage standard deviation against the marginal value of relaxed voltage limits for each node (Eq. 6.43).

6.4.3 *Impact of Losses*

Table 6.8 summarizes the optimal LVOLT-CC solution obtained by using loss factor matrices LP^p, LP^q, LQ^p, LQ^q as defined in (6.15) and (6.16) and shown in Fig. 6.4. Negative elements of the matrices shown in Fig. 6.4 indicate that additional DER production at node j will increase power losses allocated to node i based on FND. For example, LP^p shows that additional active production at nodes 0 to 11 will increase active power losses. On the other hand, additional active production on the passive branch (nodes 12 to 14), where no DERs are installed, will reduce active power losses.

Since increasing DER production at nodes 6 and 11 increases system losses, see Fig. 6.4, we observe that the power output of controllable DERs changes slightly, as compared to the results of the VOLT-CC, and the additional power needed to compensate for system losses is provided by the substation (node 0). By internalizing the loss factors into the voltage chance constraints via matrix R^L as in (6.22), the impact of balancing participation on the voltage limits is no longer symmetric

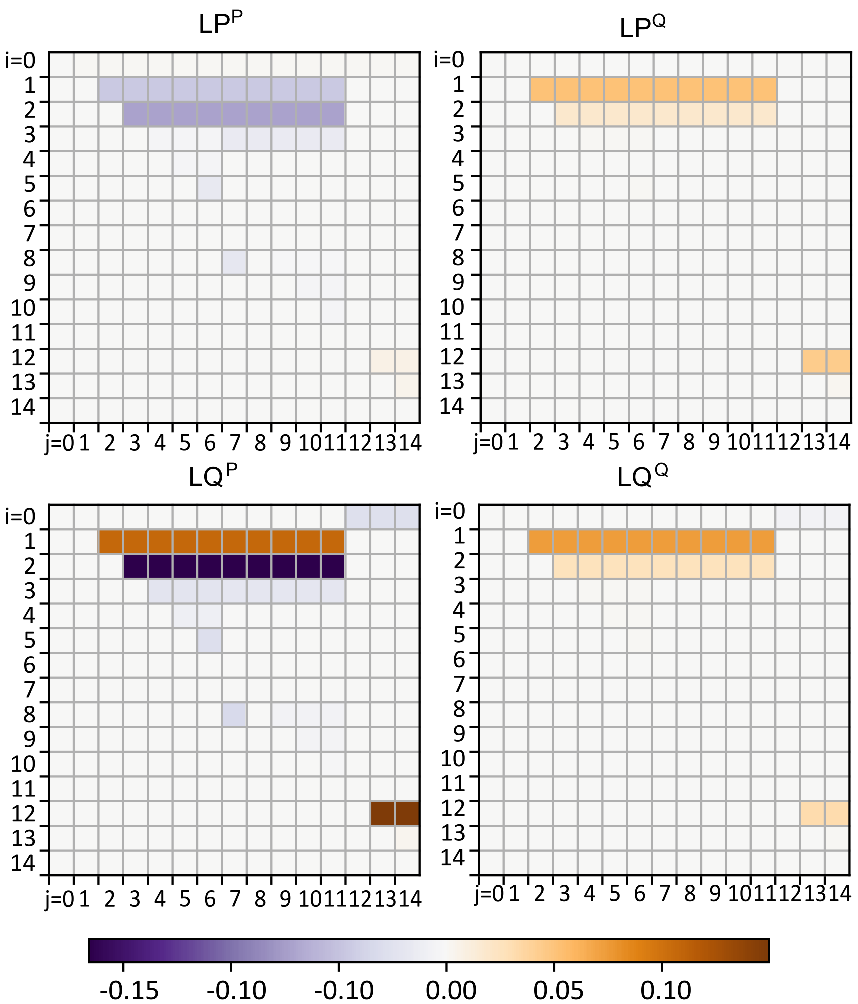

Figure 6.4: Illustration of loss factor matrices LP^p, LP^q, LQ^p, LQ^q itemizing the sensitivity of active and reactive nodal net injections at node j ('x-axis') on the active and reactive FND of node i ('y-axis').

Table 6.4: DLMP Decomposition of the GEN-CC, cf. Eq. (6.24)

i	λ_i^p	$\lambda_{\mathcal{A}_i}^p$	$\lambda_i^q \frac{r_i}{x_i}$	$\lambda_{\mathcal{A}_i}^q \frac{r_i}{x_i}$	$2\eta_i(f_i^p + \frac{r_i}{x_i} f_i^q)$
0	50.000	-0.000	-0.000	-0.000	0.000
1	50.000	50.000	0.000	0.000	-0.000
2	50.000	50.000	0.000	0.000	0.000
3	50.000	50.000	0.000	0.000	0.000
4	50.000	50.000	0.000	0.000	-0.000
5	50.000	50.000	0.000	0.000	0.000
6	11.996	50.000	0.000	0.000	38.004
7	8.769	8.769	0.000	0.000	0.000
8	8.769	50.000	0.000	0.000	41.231
9	8.769	8.769	0.000	0.000	-0.000
10	8.769	8.769	0.000	0.000	0.000
11	8.769	8.769	0.000	0.000	-0.000
12	50.000	50.000	0.000	0.000	0.000
13	50.000	50.000	0.000	0.000	0.000
14	50.000	50.000	0.000	0.000	0.000

as in (3.50). Thus, we observe higher balancing participation factors of the DERs at nodes 6 and 11 relative to the VOLT-CC. Additionally, a greater power supply from the substation and the DER at node 11 leads to non-binding voltage constraints and, thus, uniform DLMPs at nodes 8 to 11. In line with the theoretical results of Proposition 6.4a), the additional power losses have almost no impact on the price for balancing regulation. The small difference relative to the VOLT-CC is mainly caused by non-binding voltage constraints at nodes 10 and 11.

6.5 CONCLUSION

This chapter described an approach to derive stochasticity-aware DLMPs for electricity pricing in low-voltage electric power distribution systems that explicitly internalize uncertainty and risk parameters. These DLMPs are also shown to constitute a robust competitive equilibrium, which can be leveraged towards emerging distribution electricity market designs. In the future, our work will focus on the application of the proposed pricing theory to decentralized and communication-constrained control of DERs and for enabling electricity pricing in distribution systems with a high penetration rate ofDERs and near-zero marginal production costs. Methodological extensions can encompass uncertainty internalization via semidefinite programming to allow for non-linear power flow representations, [189], and the impact of asymmetric information and strategic behavior.

Table 6.5: DLMP Decomposition of the VOLT-CC, cf. Eq. (6.24)

i	λ_i^p	$\lambda_{\mathcal{A}_i}^p$	$\lambda_i^q \frac{r_i}{x_i}$	$\lambda_{\mathcal{A}_i}^q \frac{r_i}{x_i}$	$2\eta_i(f_i^p + \frac{r_i}{x_i} f_i^q)$
0	50.000	-0.000	-0.000	-0.000	0.000
1	49.976	50.000	0.024	0.000	-0.000
2	47.881	49.976	4.088	1.993	0.000
3	44.596	47.881	7.373	4.088	0.000
4	44.836	44.596	7.132	7.373	-0.000
5	45.056	44.836	6.887	7.108	0.000
6	12.025	45.056	0.000	6.911	39.942
7	3.884	8.577	7.072	2.379	0.000
8	8.577	44.596	2.376	7.369	41.012
9	9.111	8.577	1.842	2.376	-0.000
10	10.399	9.111	0.552	1.840	0.000
11	10.949	10.399	0.000	0.550	-0.000
12	50.000	50.000	0.000	0.000	0.000
13	50.000	50.000	0.000	0.000	0.000
14	50.000	50.000	0.000	0.000	0.000

Table 6.6: DLMP Decomposition of the VOLT-CC based on voltage constraints, cf. Eq. (6.27)

i	λ_i^p	$(\mu_i^+ - \mu_i^-)$	$\lambda_{\mathcal{A}_i}^p$	$2r_i \sum_{j \in \mathcal{D}_i} (\mu_j^+ - \mu_j^-)$	$2f_i^p \eta_i$
0	50.000	0.000	-0.000	-0.000	0.000
1	49.976	-0.000	50.000	0.024	-0.000
2	47.881	-0.000	49.976	2.096	0.000
3	44.596	-0.000	47.881	3.285	0.000
4	44.836	-0.000	44.596	-0.240	-0.000
5	45.056	-0.001	44.836	-0.220	0.000
6	12.025	-6.290†	45.056	-0.606	33.638
7	3.884	44.871	8.577	4.694	0.000
8	8.577	-0.000	44.596	1.478	34.541
9	9.111	-0.000	8.577	-0.534	-0.000
10	10.399	-0.004	9.111	-1.288	0.000
11	10.949	-26.709	10.399	-0.550	-0.000
12	50.000	-0.000	50.000	-0.000	0.000
13	50.000	-0.000	50.000	-0.000	0.000
14	50.000	-0.000	50.000	-0.000	0.000

† $\mu_6^+ = 20.186$, $\mu_6^- = 26.476$

Table 6.7: Regulation Price Decomposition of the VOLT-CC

		GEN-CC		VOLT-CC		
i	b_i	δ_i^+	δ_i^-	δ_i^+	δ_i^-	ν_i
0	0.0005	–	–	–	–	–
1	–	–	–	–	–	0.120
2	–	–	–	–	–	10.699
3	–	–	–	–	–	27.281
4	–	–	–	–	–	28.199
5	–	–	–	–	–	29.040
6	0.1	-0.000	-0.000	-0.000	-0.000	31.357
7	–	–	–	–	–	32.533
8	–	–	–	–	–	30.201
9	–	–	–	–	–	30.472
10	–	–	–	–	–	31.126
11	0.1	-0.000	0.310	-0.000	-0.000	31.406
12	–	–	–	–	–	0.000
13	–	–	–	–	–	0.000
14	–	–	–	–	–	0.000

Table 6.8: Optimal LVOLT-CC Solution

i	$p_{G,i}$	$q_{G,i}$	α_i	$\sqrt{(f_i^p)^2 + (f_i^q)^2}$	ν_i	λ_i^p	χ
0	1.075	0.607	0.144	0.000	1.000	50.000	30.254
1	–	–	–	0.576	0.952	49.971	–
2	–	–	–	0.422	0.966	47.417	–
3	–	–	–	0.433	0.997	43.414	–
4	–	–	–	0.209	0.998	43.666	–
5	–	–	–	0.223	0.999	43.897	–
6	0.256	-0.077	0.515	0.256*	1.005*	14.005	–
7	–	–	–	0.197	1.016*	6.372	–
8	–	–	–	0.256*	1.006	4.169	–
9	–	–	–	0.079	1.007	4.169	–
10	–	–	–	0.102	1.009	4.169	–
11	0.137	0.012	0.341	0.124	1.011	4.169	–
12	–	–	–	0.661	0.983	50.000	–
13	–	–	–	0.026	0.978	50.000	–
14	–	–	–	0.024	0.975	50.000	–

* Constraint is binding

7 RISK- AND VARIANCE-AWARE COORDINATION IN TRANSMISSION SYSTEMS

This chapter departs from studying (radial) distribution systems and generalizes the results of previous Chapter 6 towards a (meshed) AC system formulation. Assuming a complete electricity market, this chapter corroborates the existence of a competitive equilibrium from these risk-aware prices. Additionally, this chapter shows how the previously passively limited volatility of system state-variables can be reduced to improve system stability and equipment durability.

The contents of this chapter have been published in 2020 as the article entitled "Risk- and variance-aware electricity pricing" in the *Electric Power Systems Research* journal, [P4]. For this dissertation, the original article has been moderately adapted to ensure unified notations and connections to other chapters.

7.1 INTRODUCTION

Power systems and electricity markets struggle to accommodate the massive roll-out of RES, which are stochastic in nature and impose additional risks on the system operations and market-clearing decisions. The current industry practice to mitigate these risks is based on procuring additional reserves, which are selected based on exogenous and often ad-hoc policies (e.g., 95-percentile rule in ERCOT, [63], or (5+7) rule in CAISO, [64]).

Alternatively, such risk assessments can be carried out endogenously, i.e. while optimizing operational and market-clearing decisions, using high-fidelity prediction and historical data parameters the RES stochasticity. As discussed in previous Chapters, the CC-OPF has been shown to scale efficiently for large networks [143], accommodate various assumptions on the RES stochasticity (e.g. parametric distributions and distributional robustness) [P1], [P2], [143], [190], [191], as well as to accurately account for AC power flow physics, [68], [102]. However, this framework has primarily been applied to risk-aware operational planning in a vertically integrated environment, neglecting market considerations. From a market design perspective, RES stochasticity has been primarily dealt with using scenario-based stochastic programming, e.g. [43], [72], [73], which is more computationally demanding than chance constraints, [7].

With the exception of [P3], [9], [127], chance constraints have so far been overlooked in electricity pricing applications. The chance-constrained market design proposed in [9] leads to a stable robust equilibrium that, unlike scenario-based approaches in [43], [72], [73], guarantees desirable market properties, i.e. welfare maximization, revenue adequacy and cost recovery, under various assumptions on the RES stochasticity. Therefore, the resulting energy and reserve prices make it possible to better approximate real-time operating conditions for look-ahead dispatch applications, thus improving consistency between look-ahead and real-time stages. However, [9] neglects network constraints, an important modeling feature for real-life market applications.

In this Chapter we use the CC-ACOPF from Chapter 3 to derive network-aware electricity prices that internalize the RES stochasticity with the intention to produce more accurate signals to market participants. This convex formulation allows the use of duality theory to derive risk-aware marginal-cost-based prices, which are similar to traditional deterministic locational marginal prices (LMPs) based on linear duality, [120]. Furthermore, the CC-ACOPF can explicitly consider reactive power and voltage support services and analyze their role in the deliverabilty of active power, thus supporting the design of a more "complete" electricity market, [192], [193]. Completing the market by allowing all assets and services (active and reactive power, reserve capacity, transmission and voltage support) to be transacted, [193], makes it possible to co-align technical needs and requirement imposed by the physical aspects of power system operations and price signals received by market participants. Notably, the proposed CC-ACOPF market clearing enables the completion of the wholesale electricity market, but also accommodates the operational requirements of sub-transmission and distribution networks, e.g. for the design of distribution or local electricity markets, [P3]. We also extend the CC-ACOPF to follow a *variance-aware* dispatch paradigm, introduced in [142], to compute variance-aware prices and analyze the relationship between the system cost, risk and variance.

7.2 MODEL FORMULATION

We use the CC-ACOPF from Section 3.3 with the modified objective from Section 6.2.1 and assign dual variables (Greek letters in parentheses) to all constraints:

$$\text{EQV-CC}: \qquad \min_{\substack{p_G, q_G \\ v, \alpha, \theta}} \sum_{i \in \mathcal{G}} c_i(p_{G,i}) + \sum_{i \in \mathcal{G}} \frac{\alpha_i^2}{2b_i} S^2 \tag{7.1a}$$

s.t.

$$(\lambda_i^p, \lambda_i^q): \qquad (3.27), (3.28) \tag{7.1b}$$

$$(\beta_{ij}^p, \beta_{ij}^q): \qquad (3.29), (3.30) \tag{7.1c}$$

$$(\chi): \qquad \sum_{i \in \mathcal{G}} \alpha_i = 1 \tag{7.1d}$$

$$
\begin{aligned}
&(\delta_i^{p,+}): && p_{G,i} + \alpha_i z_{\epsilon_p} S \leqslant p_{G,i}^{max} && i \in \mathcal{G} && (7.1e)\\
&(\delta_i^{p,-}): && -p_{G,i} + \alpha_i z_{\epsilon_p} S \leqslant -p_{G,i}^{min} && i \in \mathcal{G} && (7.1f)\\
&(\delta_i^{q,+}): && q_{G,i} + z_{\epsilon_q} t_i^q \leqslant q_{G,i}^{max} && i \in \mathcal{G} && (7.1g)\\
&(\delta_i^{q,-}): && -q_{G,i} + z_{\epsilon_q} t_i^q \leqslant -q_{G,i}^{min} && i \in \mathcal{G} && (7.1h)\\
&(\zeta_i^q): && \left\|(R_i^q - \rho_i^q e^\top + X_i^q \operatorname{diag}(\gamma))\Sigma^{1/2}\right\|_2 \leqslant t_i^q && i \in \mathcal{G} && (7.1i)\\
&(\nu_i^q): && R_i^q \alpha = \rho_i^q && i \in \mathcal{G} && (7.1j)\\
&(\mu_i^+): && v_i + z_{\epsilon_v} t_i^v \leqslant v_i^{max} && i \in \mathcal{N} && (7.1k)\\
&(\mu_i^-): && -v_i + z_{\epsilon_v} t_i^v \leqslant -v_i^{min} && i \in \mathcal{N} && (7.1l)\\
&(\zeta_i^v): && \left\|(R_i^v - \rho_i^v e^\top + X_i^v \operatorname{diag}(\gamma))\Sigma^{1/2}\right\|_2 \leqslant t_i^v && i \in \mathcal{G} && (7.1m)\\
&(\nu_i^v): && R_i^v \alpha = \rho_i^v && i \in \mathcal{N} && (7.1n)\\
&(\eta_{ij}): && (a_{ij}^{f^p})^2 + (a_{ij}^{f^q})^2 \leqslant (s_{ij}^{max})^2, && ij \in \mathcal{L} && (7.1o)\\
&(\xi_{ij}^{f^p,+}): && -a_{ij}^{f^p} + z_{\epsilon_f/2.5} t_{ij}^{f^p} \leqslant f_{ij}^p && ij \in \mathcal{L} && (7.1p)\\
&(\xi_{ij}^{f^p,-}): && -a_{ij}^{f^p} + z_{\epsilon_f/2.5} t_{ij}^{f^p} \leqslant -f_{ij}^p && ij \in \mathcal{L} && (7.1q)\\
&(\xi_{ij}^{f^p,0}): && z_{\epsilon/5} t_{ij}^{f^p} \leqslant a_{ij}^{f^p} && ij \in \mathcal{L} && (7.1r)\\
&(\xi_{ij}^{f^q,+}): && -a_{ij}^{f^q} + z_{\epsilon_f/2.5} t_{ij}^{f^q} \leqslant f_{ij}^q, && ij \in \mathcal{L} && (7.1s)\\
&(\xi_{ij}^{f^q,-}): && -a_{ij}^{f^q} + z_{\epsilon_f/2.5} t_{ij}^{f^q} \leqslant -f_{ij}^q, && ij \in \mathcal{L} && (7.1t)\\
&(\xi_{ij}^{f^q,0}): && z_{\epsilon_f/5} t_{ij}^{f^q} \leqslant a_{ij}^{f^q} && ij \in \mathcal{L} && (7.1u)\\
&(\zeta_{ij}^{\diamond}): && \left\|(R_i^{\diamond} - \rho_i^{\diamond} e^\top + X_i^{\diamond} \operatorname{diag}(\gamma))\Sigma^{1/2}\right\|_2 \leqslant t_i^{\diamond} && &&\\
& && && ij \in \mathcal{L}, \diamond = f^p, f^q && (7.1v)\\
&(\nu_{ij}^{\diamond}): && R_{ij}^{\diamond} \alpha = \rho_{ij}^{\diamond} && ij \in \mathcal{L}, \diamond = f^p, f^q, && (7.1w)
\end{aligned}
$$

Objective (7.1a) minimizes the expected cost as in (6.1). Eqs. (7.1b) and (7.1c) are the active and reactive power balances and flows based on the linearized AC power flow equations. Eq. (7.1d) is the balancing reserve adequacy constraint and (7.1e)–(7.1w) are the deterministic chance constraints reformulation, see Section 3.3 on page 39. Constraints (7.1e) and (7.1f) limit the active power production $p_{G,i}$ and the amount of reserve $\alpha_i z_{\epsilon_p} S$ provided by each generator, [P3], [9]. As before, risk parameters are given by $z_\epsilon = \Phi^{-1}(1-\epsilon)$. Although less restrictive assumptions on the distribution of $\boldsymbol{\omega}$ can be invoked in (7.1), e.g. by means of non-Gaussian parametric distributions [190] or distributionally robust formulations [P1], [9], this chapter assumes normally distributed forecast errors for the sake of presentation clarity. See also discussion in Box 1 on page 32. The standard deviation of reactive power outputs, voltage levels and flows resulting from the uncertainty and the system response is given by the SOC constraints (7.1i), (7.1m) and (7.1v). Given the convexity of the SOC constraints, auxiliary variables t_i^q, t_i^v, $t_{ij}^{f^p}$, $t_{ij}^{f^q}$ relate these standard deviations to the reactive output limits (7.1g) and (7.1h), voltage bounds (7.1k) and (7.1l) and flow limits (7.1p)–(7.1u). Due to its quadratic dependency on the uncertain variable, the transmission limit chance constraints require a more complex reformulation, see Section 3.3.3. To accommodate this reformulation, we introduce auxiliary variables a_{ij}^{fp}, a_{ij}^{fq} and risk parameters $\epsilon_f/2.5$ and $\epsilon_f/5$ (i.e. ϵ_f divided by 2.5 and 5), respectively. Auxiliary variables ρ_i^v, ρ_{ij}^{fp}, ρ_{ij}^{fq} and constraints (7.1j), (7.1n) and (7.1w) have been introduced to simplify subsequent derivations, see Section 6.2.1. Noticeably, (7.1) includes convex quadratic objective and second-order conic constraints. Although it can be reformulated into a purely conic program to gain computational tractability, see Appendix A.3 or [177], [194], the form in (7.1) allows for a clear presentation below.

7.3 RISK-AWARE PRICING

The EQV-CC in (3.42) endogenously trades off the expected operating point $(p_G, q_G, v, \theta, \gamma, \alpha)$ and the risk of system limit violations defined by the choice of parameters $z_{\epsilon_p}, z_{\epsilon_q}, z_{\epsilon_v}, z_{\epsilon_f/2.5}, z_{\epsilon_f/5}$. Since the EQV-CC is a convex program, we can use its dual form to compute the marginal prices for active and reactive power, and balancing reserve that internalize this trade-off.

7.3.1 *Prices with Chance Constraints on Generation*

First, we consider a modification of the EQV-CC given as:

$$
\begin{aligned}
&\text{GEN-CC}: && \min_{\substack{p_G, q_G \\ v, \alpha, \theta}} \sum_{i \in \mathcal{N}} c_i(p_{G,i}) + \sum_{i \in \mathcal{N}} \frac{\alpha_i^2}{2b_i} S^2 && (7.2a)\\
&\text{s.t.} && (7.1b)\text{–}(7.1f) &&\\
&(\delta_i^{q,+}, \delta_i^{q,-}): && q_{G,i}^{min} \leqslant q_{G,i} \leqslant q_{G,i}^{max} && (7.2b)\\
&(\mu_i^-, \mu_i^+): && v_i^{min} \leqslant v_i \leqslant v_i^{max} && (7.2c)\\
&(\eta_{ij}): && (f_{ij}^p)^2 + (f_{ij}^q)^2 \leqslant (s_{ij}^{max})^2, && (7.2d)
\end{aligned}
$$

where, relative to the EQV-CC in (7.1), chance constraints are only enforced on active power generation limits and reactive power, voltage and power flow constraints are enforced deterministically by (7.2b)–(7.2d). In other words, the GEN-CC determines the optimal balancing participation of each generator and, thus, the optimal amount and allocation of committed reserve given by $\alpha_i z_{\epsilon_p} S$. Therefore, the GEN-CC replicates a traditional deterministic OPF that allocates the reserve requirement ($\sum_{i \in \mathcal{G}} \alpha_i z_{\epsilon_p} S = z_{\epsilon_p} S$) among individual generators, see [9].

Using the GEN-CC, we compute the following prices:

Proposition 7.1. *Consider the GEN-CC in (7.2). Let λ_i^p, λ_i^q be dual multipliers of the nodal active and reactive power balance at node i in (7.1b). Then λ_i^p and λ_i^q are given as:*

$$\lambda_i^p = \frac{p_{G,i} + a_i}{b_i} + \delta_i^{p,-} - \delta_i^{p,+} \tag{7.3}$$

$$\lambda_i^q = \delta_i^{q,-} - \delta_i^{q,+}. \tag{7.4}$$

Proof. The first order optimality conditions of (7.2) for $p_{G,i}$, $q_{G,i}$, α_i, f_{ij}^p, f_{ij}^q are:

$$(p_{G,i}): \quad \lambda_i^p + (\delta_i^{p,+} - \delta_i^{p,-}) = \frac{p_{G,i} + a_i}{b_i} \quad i \in \mathcal{G} \tag{7.5a}$$

$$(q_{G,i}): \quad \lambda_i^q + (\delta_i^{q,+} - \delta_i^{q,-}) = 0 \quad i \in \mathcal{G} \tag{7.5b}$$

$$(\alpha_i): \quad z_{\epsilon_p} S(\delta_i^{p,+} + \delta_i^{p,-}) + \chi = \frac{\alpha_i}{b_i} S^2 \quad i \in \mathcal{G} \tag{7.5c}$$

$$(f_{ij}^p): \quad 2f_{ij}^p \eta_{ij} + \beta_{ij}^{fp} = 0 \quad ij \in \mathcal{L} \tag{7.5d}$$

$$(f_{ij}^q): \quad 2f_{ij}^q \eta_{ij} + \beta_{ij}^{fq} = 0 \quad ij \in \mathcal{L}. \tag{7.5e}$$

Eqs. (7.3) and (7.4) follow directly from (7.5a) and (7.5b). □

Dual multiplier λ_i^p of the active power balance, itemized in (7.3), is interpreted as the real power LMP at node i and a function of production cost coefficients a_i, b_i and scarcity rent $\delta_i^{p,+}$, $\delta_i^{p,-}$ related to active generation limits. Dual multiplier λ_i^q of the reactive power balance, itemized in (7.4), is interpreted as the reactive power LMP given by scarcity rent $\delta_i^{q,+}$, $\delta_i^{q,-}$ related to reactive generation limits. Although there is no explicit production cost for reactive power in (7.1a), providing reactive power can have a non-zero value, if at least one reactive power limit is binding. Further, Proposition 7.1 shows that both λ_i^p and λ_i^q in (7.3) and (7.4) do not explicitly depend on uncertainty and risk parameters.

In contrast, the price for balancing reserve explicitly depends on the uncertainty and set risk levels:

Proposition 7.2. *Consider the GEN-CC in (7.2). Let χ be the dual multiplier of the balancing adequacy constraint in (7.1d). Then χ is given as:*

$$\chi = \frac{1}{\sum_{i \in \mathcal{G}} b_i} \Big(S^2 + z_{\epsilon_p} S \sum_{i \in \mathcal{G}} b_i (\delta_i^{p,+} + \delta_i^{p,-}) \Big). \tag{7.6}$$

Proof. Using (7.1d) to eliminate α_i in (7.5c) yields (7.6). □

Dual multiplier χ of (7.1d) is interpreted as the price for balancing reserve, because it enforces sufficiency of the system-wide reserve. As per (7.6), χ is an explicit function of the uncertainty $S^2 = e^\top \Sigma e$ and risk parameter z_{ϵ_p}. Notably, the balancing reserve price is always non-zero, if there is uncertainty in the system (i.e. $S > 0$), even if all constraints (7.1e) and (7.1f) are inactive, i.e. $\delta_i^{p,+} = \delta_i^{p,-} 0, \forall i \in \mathcal{G}$. In this case, χ is independent of the risk parameters and is determined by the total uncertainty S^2 weighted by the total marginal generator cost $\sum_{i\in\mathcal{G}} b_i$ of all generators, $i \in \mathcal{G}$, including those generators that do not provide any balancing reserve, i.e. $\alpha_i = 0$.

7.3.2 *Prices with Complete Chance Constraints*

We now consider the complete EQV-CC in (7.1), i.e. including chance constraints on reactive power generation, voltages and flows, and prove the following proposition:

Proposition 7.3. *Consider the EQV-CC in (7.1). Let λ_i^p, λ_i^q be dual multipliers of the nodal active and reactive power balances at node i as in (7.1b). Further, let χ be the dual multiplier of the balancing adequacy constraint in (7.1d). Then (i) λ_i^p and λ_i^q are given as (7.3) and (7.4) and (ii) χ is given as:*

$$\chi = \frac{1}{\sum_{i\in\mathcal{G}} b_i}\Big(\overbrace{S^2 + z_\epsilon S \sum_{i\in\mathcal{G}} b_i(\delta_i^+ + \delta_i^-)}^{\text{Influenced by generator decisions}} + \overbrace{\sum_{i\in\mathcal{G}} b_i(y_i^q + y_i^v + y^{f^p} + y^{f^q})}^{\text{Influenced by system decisions}}\Big), \quad (7.7)$$

where:

$$y_i^q = z_{\epsilon_q} \sum_{j\in\mathcal{G}} [R_j^q]_i \delta_j^q \frac{(R_j^q + X_j^q \operatorname{diag}(\gamma))\Sigma e - R_j^q \alpha S^2}{\sigma_{q_{G,j}}(\alpha,\gamma)} \quad (7.8)$$

$$y_i^v = z_{\epsilon_v} \sum_{j\in\mathcal{N}} [R_j^v]_i \mu_j \frac{(R_j^v + X_j^v \operatorname{diag}(\gamma))\Sigma e - R_j^v \alpha S^2}{\sigma_{v_j}(\alpha,\gamma)} \quad (7.9)$$

$$y_i^\diamond = 2 \sum_{jk\in\mathcal{L}} [R_{jk}^\diamond]_i \zeta_{ij}^\diamond \frac{(R_{jk}^\diamond + X_{jk}^\diamond \operatorname{diag}(\gamma))\Sigma e - R_{jk}^\diamond \alpha S^2}{\sigma_{\diamond_{jk}}(\alpha,\gamma)}, \quad (7.10)$$

where $\diamond = f^p, f^q$ and $\delta_j^q = \delta_j^{q,+} + \delta_j^{q,-}$, $\mu_j = \mu_j^+ + \mu_j^-$, and $\zeta_{ij}^\diamond = z_{\epsilon_f/2.5}(\xi_{ij}^{\diamond,+} + \xi_{ij}^{\diamond,-}) + z_{\epsilon_f/5}\xi_{ij}^{\diamond,0}$. Terms $\sigma_{q_{G,j}}(\alpha,\gamma), \sigma_{v_j}(\alpha,\gamma)$, $\sigma_{f^p_{jk}}(\alpha,\gamma)$, $\sigma_{f^q_{jk}}(\alpha,\gamma)$ denote the standard deviations of reactive power at node j, voltage at node j, active power flow on line jk and reactive power flow on line jk, respectively, and $[\cdot]_i$ denotes the i-th element of a vector.

Proof. The first order optimality conditions of (7.1) for $p_{G,i}$, $q_{G,i}$, α_i, f_{ij}^p, f_{ij}^q and auxiliary variables are:

(7.5a), (7.5b), (7.11b) and (7.11c)

$$(\alpha_i): \quad \chi + z_{\epsilon_p} S(\delta_i^{p,+} + \delta_i^{p,-}) + \sum_{j\in\mathcal{G}} \nu_j^q [R_j^q]_i + \sum_{j\in\mathcal{N}} \nu_j^v [R_j^v]_i$$
$$+ \sum_{jk\in\mathcal{L}} \nu_{jk}^{f^p} [R_{jk}^{f^p}]_i + \sum_{jk\in\mathcal{L}} \nu_{jk}^{f^q} [R_{jk}^{f^q}]_i = \frac{\alpha_i}{b_i} S^2$$
$$i \in \mathcal{G} \quad (7.11a)$$

$$(t_i^q): \quad z_{\epsilon_p}(\delta_i^{q,+}+\delta_i^{q,-})-\zeta_i^q=0 \qquad i\in\mathcal{G} \qquad (7.11b)$$

$$(\rho_i^q): \quad \zeta_i^q \frac{(R_i^q-\rho_i^q e^\top + X_i^q \operatorname{diag}(\gamma))\Sigma e}{\left\|(R_i^q-\rho_i^q e^\top + X_i^q \operatorname{diag}(\gamma))\Sigma^{1/2}\right\|_2} - \nu_i^q = 0 \qquad i\in\mathcal{G} \qquad (7.11c)$$

$$(\rho_i^v): \quad \zeta_i^v \frac{(R_i^v-\rho_i^v e^\top + X_i^v \operatorname{diag}(\gamma))\Sigma e}{\left\|(R_i^v-\rho_i^v e^\top + X_i^v \operatorname{diag}(\gamma))\Sigma^{1/2}\right\|_2} - \nu_i^v = 0 \qquad i\in\mathcal{N} \qquad (7.11d)$$

$$(t_i^v): \quad z_{\epsilon_v}(\mu_i^+ + \mu_i^-)-\zeta_i^v=0 \qquad i\in\mathcal{N} \qquad (7.11e)$$

$$(f_{ij}^p): \quad \beta_{ij}^{f^p} - \xi_{ij}^{f^p,+} + \xi_{ij}^{p,-} = 0 \qquad ij\in\mathcal{L} \qquad (7.11f)$$

$$(f_{ij}^q): \quad \beta_{ij}^{q} - \xi_{ij}^{f^q,+} + \xi_{ij}^{f^q,-} = 0 \qquad ij\in\mathcal{L} \qquad (7.11g)$$

$$(\rho_{ij}^\diamond): \quad \zeta_i^v \frac{(R_{ij}^\diamond-\rho_{ij}^\diamond e^\top + X_{ij}^\diamond \operatorname{diag}(\gamma))\Sigma e}{\left\|(R_{ij}^\diamond-\rho_i^v e^\top + X_{ij}^\diamond \operatorname{diag}(\gamma))\Sigma^{1/2}\right\|_2} - \nu_{ij}^\diamond = 0 \qquad ij\in\mathcal{L}, \diamond = f^p, f^q \qquad (7.11h)$$

$$(a_{ij}^\diamond): \quad 2\eta_{ij} a_{ij}^\diamond - (\xi_{ij}^{\diamond,+}+\xi_{ij}^{\diamond,-}) - \xi_{ij}^{\diamond,0} = 0 \qquad ij\in\mathcal{L}, \diamond = f^p, f^q \qquad (7.11i)$$

$$(t_{ij}^\diamond): \quad z_{\epsilon_f/2.5}(\xi_{ij}^{\diamond,+}+\xi_{ij}^{\diamond,-}) + z_{\epsilon_f/5}\xi_{ij}^{\diamond,0} - \zeta_{ij}^\diamond = 0 \qquad ij\in\mathcal{L}, \diamond = f^p, f^q \qquad (7.11j)$$

The result (i) follows directly from the proof of Proposition 7.1. The result (ii) follows from (7.11a) by eliminating α_i using (7.1d). Note that terms ν_i^q, ν_i^v, $\nu_{ij}^{f^p}$, $\nu_{ij}^{f^q}$ are given by (7.11c), (7.11d) and (7.11h). Further, $t_i^q = \sigma_{q_{G,i}}(\alpha,\gamma)$, if $\zeta_i^q > 0$ as per (7.1i), $t_i^v = \sigma_{v_j}(\alpha,\gamma)$, if $\zeta_i^v > 0$ as per (7.1m) and $t_{ij}^\diamond = \sigma_{\diamond_{jk}}(\alpha,\gamma)$, if $\zeta_{ij}^\diamond > 0$ as per (7.1v) for $\diamond = f^p, f^q$. Thus, for any $\zeta_i^q, \zeta_i^v, \zeta_{ij}^{f^p}, \zeta_{ij}^{f^q} = 0$ the dependency on the standard deviation would disappear. Finally, terms $\zeta_i^q, \zeta_i^v, \zeta_{ij}^{f^p}, \zeta_{ij}^{f^q}$ are given by (7.11b), (7.11e) and (7.11j). □

Similar to the result of Proposition 7.1, prices λ_i^p and λ_i^q do not explicitly depend on uncertainty and risk parameters. On the other hand, relative to (7.6), balancing reserve price χ depends on additional terms $y_i^q, y_i^v, y_i^{f^p}, y_i^{f^q}$, see (7.7), that relate the balancing reserve provided by each generator at node i to the risk of reactive power and voltage limits violation at every node $j \in \mathcal{N}$ and to the risk of power flow violations on every line $jk \in \mathcal{L}$. This risk awareness is not part of the generator decisions, which are only driven by its own production limits and cost, as indicated in (7.7). As a result of this incompleteness, given system-wide balancing price χ, generators may elect for balancing participation factors, which are sub-optimal from the system perspective. This can be overcome either by further completing the market in terms of transmission and voltage prices as proposed in [193], or by augmenting the system-wide balancing price to reflect location-specific constraints, e.g. $\tilde{\chi}_i := \chi + y_i^q + y_i^v + y_i^{f^p} + y_i^{f^q}$.

7.4 VARIANCE-AWARE PRICING

The risk-aware results of the EQV-CC in (7.1) yield solutions with a high variability (variance) of system state variables, which has been shown to complicate real-time operations, [142], [195]. The variances of reactive power generation, voltage magnitudes, and active and reactive flows can directly be computed from the standard deviations related to t_i^q, t_i^v, $t_{ij}^{f^p}$, $t_{ij}^{f^q}$, respectively. We introduce the metric $V(t_i^q, t_i^v, t_i^{f^p}, t_i^{f^q})$ that models a connection between the variances and system cost in the following variance-aware formulation:

$$\begin{aligned} \text{VA-CC}: \quad & \min_{\substack{p_G, q_G \\ v, \alpha, \theta}} \sum_{i \in \mathcal{N}} c_i(p_{G,i}) + \sum_{i \in \mathcal{N}} \frac{\alpha_i^2}{b_i} S^2 + V(t_i^q, t_i^v, t_{ij}^{f^p}, t_{ij}^{f^q}) \\ \text{s.t.} \quad & (7.1b)\text{–}(7.1w). \end{aligned} \tag{7.12}$$

Specifically, metric $V(\cdot)$ penalizes the variance of state variables and, thus, it can be used to trade-off the overall system variance and the expected operating cost in the system as discussed in [142]. We define metric $V(\cdot)$ as:

$$\begin{aligned} V(t_i^q, t_i^v, t_{ij}^{f^p}, t_{ij}^{f^q}) = & \sum_{i \in \mathcal{G}} (\Psi_i^q (t_i^q)^2) + \sum_{i \in \mathcal{N}} \Psi_i^v (t_i^v)^2 \\ & + \sum_{ij \in \mathcal{L}} (\Psi_{ij}^{f^p} (t_{ij}^{f^p})^2 + \Psi_i^{f^q} (t_{ij}^{f^q})^2), \end{aligned} \tag{7.13}$$

where Ψ_i^q, Ψ_i^v, $\Psi_{ij}^{f^p}$, $\Psi_{ij}^{f^q}$ are variance penalty factors in the units of [\$/MVAr^2], [\$/V^2], [\$/MW^2] and [\$/MVAr^2], respectively. Note that active power standard deviation t_i^p is already controlled by the generation cost and the constraints on α_i.

Proposition 7.4. *Consider the VA-CC in (7.12). Let λ_i^p, λ_i^q be dual multipliers of the nodal active and reactive power balance at node i as in (7.1b). Further, let χ be the dual multiplier of the balancing adequacy constraint in (7.1d). Then (i) λ_i^p and λ_i^q are given by (7.3) and (7.4) and (ii) χ is given as:*

$$\chi = \frac{1}{\sum_{i \in \mathcal{G}} b_i} \Big(S^2 + z_\epsilon S \sum_{i \in \mathcal{G}} b_i (\delta_i^+ + \delta_i^-) + \sum_{i \in \mathcal{G}} b_i (y_i^q + y_i^v + y^{f^p} + y^{f^q}) \Big), \tag{7.14}$$

where:

$$y_i^q = \sum_{j \in \mathcal{G}} [R_j^q]_i \zeta_j^q \frac{(R_j^q + X_j^q \operatorname{diag}(\gamma)) \Sigma e - R_j^q \alpha S^2}{\sigma_{q_{G,j}}(\alpha, \gamma)} \tag{7.15}$$

$$y_i^v = \sum_{j \in \mathcal{N}} [R_j^v]_i \zeta_j^v \frac{(R_j^v + X_j^v \operatorname{diag}(\gamma)) \Sigma e - R_j^v \alpha S^2}{\sigma_{v_j}(\alpha, \gamma)} \tag{7.16}$$

$$y_i^\diamond = 2 \sum_{jk \in \mathcal{L}} [R_{jk}^\diamond]_i \zeta_{ij}^\diamond \frac{(R_{jk}^\diamond + X_{jk}^\diamond \operatorname{diag}(\gamma)) \Sigma e - R_{jk}^\diamond \alpha S^2}{\sigma_{\diamond_{jk}}(\alpha, \gamma)} \tag{7.17}$$

$$\zeta_j^q = z_{\epsilon_q}(\delta_j^{q,+} + \delta_j^{q,-}) - 2\sigma_{q_{G_j}}(\alpha,\gamma)\Psi_j^q \tag{7.18}$$

$$\zeta_j^v = z_{\epsilon_v}(\mu_j^+ + \mu_j^-) - 2\sigma_{v_j}(\alpha,\gamma)\Psi_j^v \tag{7.19}$$

$$\zeta_{jk}^\diamond = z_{\epsilon_f/2.5}(\xi_{ij}^{\diamond,+} + \xi_{ij}^{\diamond,-}) + z_{\epsilon_f/5}\xi_{ij}^{\diamond,0} - 2\sigma_{\diamond_{jk}}(\alpha,\gamma)\Psi_j^\diamond \tag{7.20}$$

where $\diamond = f^p, f^q$.

Proof. The first-order optimality conditions of (7.12) for $p_{G,i}$, $q_{G,i}$, α_i, f_{ij}^p, f_{ij}^q and auxiliary variables are:

$$\begin{aligned}
&\text{(7.5a), (7.5b), (7.11c), (7.11d) and (7.11f)–(7.11i)}\\
(\alpha_i):\quad & z_{\epsilon_p}S(\delta_i^{p,+} + \delta_i^{p,-}) + \chi + \sum_{j\in\mathcal{G}} \nu_j^q [R_j^q]_i\\
&+ \sum_{j\in\mathcal{N}} \nu_j^v [R_j^v]_i + \sum_{jk\in\mathcal{L}} \nu_{jk}^\diamond [R_{jk}^\diamond]_i = (\frac{1}{b_i} + 2\Psi_i^p)\alpha_i S^2\\
&\qquad\qquad i\in\mathcal{G}, \diamond = f^p, f^q \qquad (7.21a)\\
(t_i^q):\quad & z_{\epsilon_p}(\delta_i^{q,+} + \delta_i^{q,-}) - \zeta_i^q = 2t_i^q\Psi_i^q \qquad i\in\mathcal{G} \qquad (7.21b)\\
(t_i^v):\quad & z_{\epsilon_v}(\mu_i^+ + \mu_i^-) - \zeta_i^v = 2t_i^v\Psi_i^v \qquad i\in\mathcal{N} \qquad (7.21c)\\
(t_{ij}^\diamond):\quad & z_{\epsilon_f/2.5}(\xi_{ij}^{\diamond,+} + \xi_{ij}^{\diamond,-}) + z_{\epsilon_f/5}\xi_{ij}^{\diamond,0} - \zeta_{ij}^\diamond = 2t_{ij}^\diamond\Psi_{ij}^\diamond\\
&\qquad\qquad ij\in\mathcal{L}, \diamond = f^p, f^q \qquad (7.21d)
\end{aligned}$$

The result (i) follows directly from the proof of Proposition 7.1. The result (ii) follows from re-arranging (7.21a) using (7.1d) to eliminate α_i. Note that terms ν_i^q, ν_i^v, $\nu_{ij}^{f^p}$, $\nu_{ij}^{f^q}$ are given by (7.11c), (7.11d) and (7.11h) and terms (7.18)–(7.20) follow from (7.21b)–(7.21d). Similarly to the proof of Proposition 7.3, $t_i^v = \sigma_{v_j}(\alpha,\gamma)$, if $\zeta_i^v > 0$ as per (7.1m), $t_{ij}^{f^p} = \sigma_{f^p_{jk}}(\alpha,\gamma)$, if $\zeta_{ij}^{f^p} > 0$ as per (7.1m), and $t_{ij}^{f^q} = \sigma_{f^p_{jk}}(\alpha,\gamma)$, if $\zeta_{ij}^{f^q} > 0$ as per (7.1v). □

Relative to the results of Proposition 7.3, terms y_i^q, y_i^v, $y_i^{f^p}$, $y_i^{f^q}$ now include an inherent trade-off between the risk of limit violation and the absolute standard deviations weighted by penalty factors Ψ_i^p, Ψ_i^q, Ψ_i^v, $\Psi_{ij}^{f^p}$, $\Psi_{ij}^{f^q}$, see (7.18)–(7.20). Since dual multipliers $\zeta_j^q, \zeta_j^v, \zeta_{jk}^{f^p}, \zeta_{jk}^{f^q}$ must be non-negative by definition, the scarcity rents of reactive power $\delta_j^{q,+}, \delta_j^{q,-}$, voltage magnitude μ_j^+, μ_j^-, active power flows $\xi_{ij}^{f^p,+}, \xi_{ij}^{p,-}, \xi_{ij}^{f^p,0}$ and reactive power flows $\xi_{ij}^{f^q,+}, \xi_{ij}^{f^q,-}, \xi_{ij}^{f^q,0}$ and risk parameters $z_{\epsilon_p}, z_{\epsilon_v}, z_{\epsilon_f}$ set an upper bound to the standard deviations $\sigma_{p_{G,j}}, \sigma_{v_j}, \sigma_{f^p_{jk}}, \sigma_{f^q_{jk}}$ weighted by the penalty factors.

7.5 ILLUSTRATIVE CASE STUDY

Table 7.1 compares the results of the deterministic, GEN-CC, EQV-CC and VA-CC cases for different values of ϵ and Ψ. As expected, the objective value and expected generation cost increase as we introduce additional chance constraints and increase the value of Ψ, thus internalizing the cost of re-dispatch to ensure larger security margins and lower variance of state variables. Similarly to the results in [142], which uses DC power flow assumptions, increasing variance penalty factor Ψ does not significantly raise the expected generation cost. This observation suggests that this reduction in state variable variances is achieved by adjustments to those variables, which are not limited by binding constraints in the optimal solution. In other words, this result shows that the variance of variables related to non-binding constraints can be controlled without significantly affecting the optimal values of other variables. Note that the variance of variables related to binding chance constraints is *a priori* controlled by the defined violation tolerance of these constraints.

Also, increasing conservatism of the model increases system-wide balancing reserve price χ for both values of ϵ. For example, in the GEN-CC, the value of χ is only driven by chance constraints on power output limits of generators, as per Proposition 7.2, while the EQV-CC and VA-CC introduce additional components (e.g. reactive power, voltage and flow variances) to price χ as per Propositions 7.3 and 7.4. Location-specific prices λ_i^p and λ_i^q for all network nodes are displayed in Fig. 7.1a), while Figs. 7.1b)–c) map the relative difference between λ_i^p for the VA-CC case with $\Psi = 100$ and $\epsilon = 0.01$ and the deterministic case. At the majority of nodes, prices λ_i^p (indicated by the box-plots in Fig. 7.1a) remain within 32–38 \$/MWh. Note that unlike χ, which significantly increases for more conservative models, prices for λ_i^p and λ_i^q do not vary as much as conservatism increases. This corresponds to our findings in Propositions 7.1–7.4, which show that active and reactive power prices do not explicitly depend on the uncertainty and risk parameters. However, at some nodes, prices λ_i^p and λ_i^q in the GEN-CC and VA-CC cases exhibit larger deviations, e.g. see λ_i^p at nodes 20 and 23, which are also in proximity of wind farms, as shown in Fig. 7.1c). A resulting high flow variance on the line between nodes 19 and 23 causes price differentiation at nodes 19, 20, 21 and 23, 24, 25.

7.5.1 *Analysis of Variance of State Variables*

Table 7.1 shows how the aggregated variance of state variables $\sum_i \sigma^2_{q_{G,i}}$, $\sum_i \sigma^2_{v_i}$, $\sum_i \sigma^2_{f^p_{ij}}$, $\sum_i \sigma^2_{f^q_{ij}}$ change relative to the EQV-CC case as penalty Ψ increases. Even if Ψ is set to a small value, the variance of state variables reduce significantly, without a large increase in the objective function, expected generation cost, and prices λ_i^p and λ_i^q. Furthermore, as the value of ϵ increases, the relative reduction in variances of all state variables slightly reduces. The effect of variance penalty Ψ on prices is two-fold. First, it does not affect prices λ_i^p and λ_i^q relative to the EQV-CC case. Second, system-wide balancing price

χ, which internalizes the variance penalties as per Proposition 7.4, increases with penalty Ψ.

7.6 CONCLUSION

This chapter described an approach to internalize RES stochasticity and risk parameters in electricity prices. Using SOC duality, these risk- and variance-aware prices are derived from a chance-constrained AC-OPF and are itemized in terms of active and reactive power, voltage support and power flow components. We proved that active and reactive power prices do not explicitly depend on uncertainty and risk parameters, while expressions for balancing reserve prices explicitly include these parameters. Further, introducing variance penalties on the system state variables has been shown to internalize the trade-off between variance, risk and system cost at a modest increase in the expected operating cost. The results have been demonstrated and analyzed on the modified IEEE 118-node testbed

Table 7.1: Optimal Solutions of the deterministic, GEN-CC, EQV-CC and VA-CC cases.

Risk Level	Model	Det	GEN-CC	EQV-CC	VA-CC ($\Psi = \Psi_i^p = \Psi_i^q = \Psi_i^v = \Psi_{ij}^{f^p} = \Psi_{ij}^{f^q}, \forall i, \forall ij$)				
	Ψ	–	–	–	0.1	1	10	100	1000
$\epsilon_p = \epsilon_q = \epsilon_v = \epsilon_f = 0.1$	Objective [$]	91103.22	91107.33	92237.67	92237.74	92238.30	92243.86	92296.91	92764.30
	Exp. Gen. Cost [$]	91103.22	91107.33	92237.67	92237.68	92237.68	92237.72	92239.70	92260.83
	Δ rel. to EQV-CC	98.770%	98.774%	100.000%	100.000%	100.000%	100.000%	100.002%	100.025%
	χ [$]	–	8.72	28.10	28.11	28.23	29.40	40.35	125.54
	$\Delta \sum_i \sigma^2_{q_{G,i}}$ [%]	–	–	100.0%	0.132%	0.103%	0.090%	0.087%	0.064%
	$\Delta \sum_i \sigma^2_{v_i}$ [%]	–	–	100.0%	3.459%	1.215%	0.349%	0.269%	0.225%
	$\Delta \sum_{ij} \sigma^2_{f^p_{ij}}$ [%]	–	–	100.0%	61.071%	60.458%	60.537%	59.798%	59.614%
	$\Delta \sum_{ij} \sigma^2_{f^q_{ij}}$ [%]	–	–	100.0%	55.808%	54.793%	54.925%	54.584%	54.313%
$\epsilon_p = \epsilon_q = \epsilon_v = \epsilon_f = 0.01$	Objective [$]	91103.22	91107.71	93744.95	93745.01	93745.57	93751.17	93805.19	94281.35
	Exp. Gen. Cost [$]	91103.22	91107.71	93744.95	93744.95	93744.94	93744.96	93747.04	93772.27
	Δ rel. to EQV-CC	97.182%	97.187%	100.000%	100.000%	100.000%	100.000%	100.002%	100.029%
	χ [$]	–	9.74	25.93	25.94	26.03	26.95	37.47	126.42
	$\Delta \sum_i \sigma^2_{q_{G,i}}$ [%]	–	–	100.0%	0.194%	0.188%	0.187%	0.163%	0.149%
	$\Delta \sum_i \sigma^2_{v_i}$ [%]	–	–	100.0%	25.384%	4.570%	1.073%	0.752%	0.650%
	$\Delta \sum_{ij} \sigma^2_{f^p_{ij}}$ [%]	–	–	100.0%	64.291%	64.526%	64.404%	62.879%	62.103%
	$\Delta \sum_{ij} \sigma^2_{f^q_{ij}}$ [%]	–	–	100.0%	54.022%	54.241%	54.193%	52.940%	52.626%

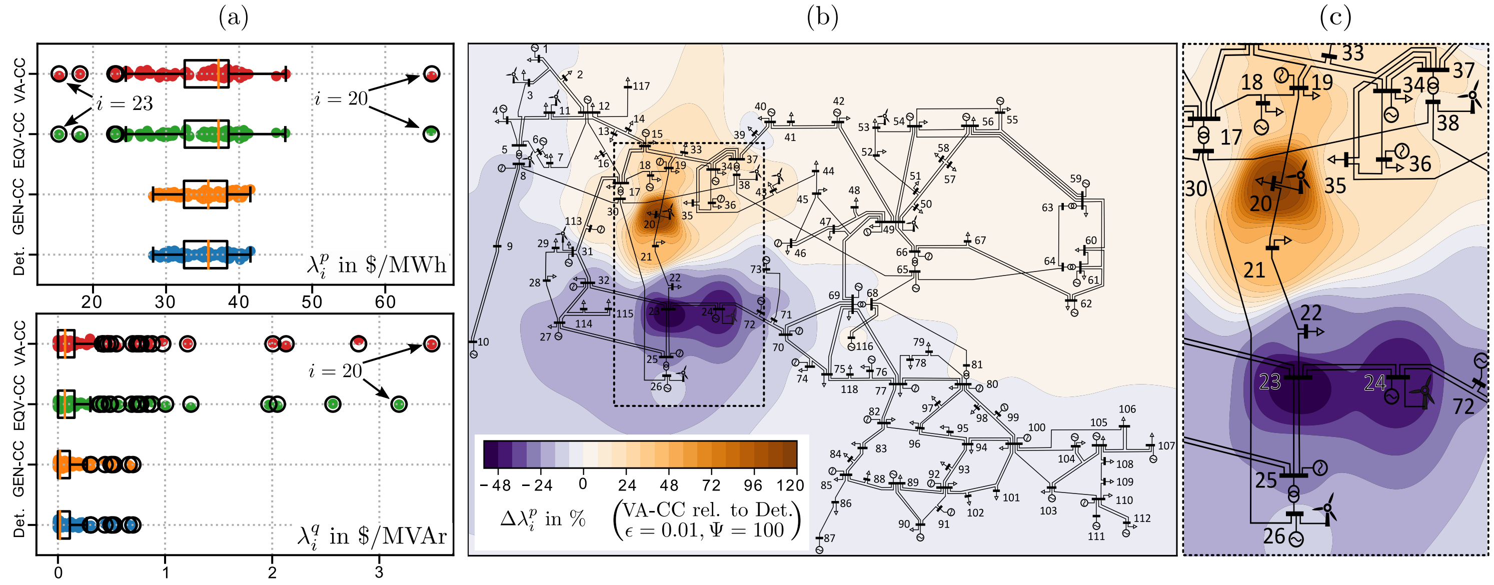

Figure 7.1: (a) Active and reactive power prices λ_i^p and λ_i^q for the deterministic, GEN-CC and EQV-CC cases and VA-CC with $\Psi = 100$ for risk level $\epsilon = 0.01$. The orange line within the blue box represents the median value, the left and right edges of the box represent the first and third quartiles and the outliers are plotted as circles. (b) Difference of active power prices λ_i^p in the VA-CC ($\Psi = 100$) relative to the deterministic case (in %). (c) Magnification of the area indicated by the doted rectangle in (b).

8 RISK-COMPLETE COORDINATION

This chapter extends the chance-constrained electricity market of [P3], [P4], [9] as discussed in previous Chapters 6 and 7, to enable risk-trading. For this purpose, we derive a risk-averse market-clearing model and introduce a financial security product modeled as an Arrow-Debreu Security (ADS) that can be traded among market participants. Further, the probability space of underlying uncertainty is discretized in a finite number of outcomes, which makes it possible to design practical risk contracts and to produce energy, balancing reserve and risk prices. Notably, although risk contracts are discrete, the model preserves the continuity of chance constraints. The case study illustrates the usefulness of the proposed risk-averse chance-constrained electricity market with risk trading.

The contents of this chapter have been published in 2020 as the article entitled "Risk trading in a chance-constrained stochastic electricity market" in the *IEEE Control System Letters*, [P5]. For this dissertation, the original article has been moderately adapted to ensure unified notation and connections to other chapters.

8.1 INTRODUCTION

Uncertain RES challenge the efficiency of existing wholesale electricity markets, which still lack risk-hedging financial instruments, [117]. As a result, electricity markets are incomplete with respect to uncertainty and risk, i.e. they do not provide market participants with a mechanism to secure their positions relative to all probable future states of the system. The CC-OPF-based electricity market design, as discussed in previous Chapters 6 and 7 and in [9], internalizes the RES uncertainty and produces uncertainty-aware electricity prices that support welfare efficiency, revenue adequacy and cost recovery. However, the previous designs assume (i) risk-neutrality and (ii) a single common belief on the system uncertainty. In reality, market participants are likely to trade (i) in a risk-averse manner and (ii) with different uncertainty beliefs. Thus, decisions are more conservative and lead to less efficient market outcomes, if there is no opportunity to compensate the risk of uncertain costs with financial securities, [129].

Although common in the fields of stochastic optimization and finance, [81], the notion of risk aversion has only recently gained attention in power system operations and electricity markets. For example, the work in [196] developed risk-averse control strategies for decentralized generation resources and [121] explored the effects of risk-averse electricity producers in a two-stage market equilibrium. However, while hedging uncertain cost against risk using the conditional-value-at-risk (CVaR), [121], [196] do not consider risk trading. On the other hand, building on the theoretical groundwork [129], [130], the work in [131] proposes a risk-complete, multi-stage, scenario-based stochastic energy market by introducing risk-trading via ADS. This risk completeness, i.e. risk trading via financial instruments parallel to all other traded assets and services, provably enabled the existence of a risk-averse competitive equilibrium, if all market participants are endowed with a coherent risk measure. In [197] the results from [131] are applied to a two-stage stochastic electricity market, showing that a risk-averse equilibrium might not be unique. In line with [131], [197], the work in [132] demonstrates that different risk perceptions of market participants may encourage them to act strategically, thus causing suboptimal market outcomes, which can be avoided in risk-complete electricity markets.

Departing from scenario-based stochastic programming used in market designs in [43], [73], [121], [124], [131], [197], this chapter explores risk trading via ADS in the chance-constrained electricity market proposed in [P3], [P4], [9], [127]. Unlike data-demanding scenario-based approaches, chance constraints only require statistical moments to internalize uncertainty in the market design using continuous probability distributions. Therefore, we first develop a general risk-complete chance-constrained electricity market with continuous, infinite-dimensional ADS. Second, we show that ADS can be discretized to enable practical risk contracts for a given set of uncertain outcomes. Finally, this chapter analyzes risk-averse market outcomes and investigates the effects of risk trading on market prices.

8.2 CHANCE-CONSTRAINED ELECTRICITY MARKET

Consider a centrally coordinated dispatch based on a CC-OPF formulation that we call chance-constrained electricity market. To better highlight relationships between probabilistic constraints and the effects of risk-averse objectives, this chapter will repeat a few necessary formulations to improve clarity. For detailed derivations of the CC-OPF see Chapter 3.

The market operator solves:

$$\min_{p_{G,i},\alpha_i} \quad \mathbb{F}_0\left[\sum_{i\in\mathcal{G}} c_i(p_{G,i}(\boldsymbol{\omega}))\right] \tag{8.1a}$$

$$\text{s.t.} \quad p_{U,i}(\boldsymbol{\omega}_i) = p_{U,i} + \boldsymbol{\omega}_i \qquad \forall i \in \mathcal{U} \tag{8.1b}$$

$$p_{G,i}(\boldsymbol{\omega}) = p_{G,i} - \alpha_i^\top \boldsymbol{\omega} \qquad \forall i \in \mathcal{G} \tag{8.1c}$$

$$(\delta_i^+): \quad \mathbb{P}[p_{G,i}(\boldsymbol{\omega}) \leqslant p_{G,i}^{\max}] \geqslant 1-\epsilon_p \qquad \forall i \in \mathcal{G} \tag{8.1d}$$

$$(\delta_i^-): \quad \mathbb{P}[p_{G,i}(\boldsymbol{\omega}) \geqslant p_{G,i}^{\min}] \geqslant 1-\epsilon_p \qquad \forall i \in \mathcal{G} \tag{8.1e}$$

$$(\theta): \quad \mathbb{P}[F(p_G(\boldsymbol{\omega}), p_U(\boldsymbol{\omega}), p_D) \in \mathcal{F}] \geqslant 1-\epsilon_f \tag{8.1f}$$

$$(\lambda_i): \quad p_{G,i} + p_{U,i} + p_i(F) = p_{D,i} \qquad \forall i \in \mathcal{N} \tag{8.1g}$$

$$(\chi_u): \quad \sum_{i \in \mathcal{G}} \alpha_{i,u} = 1 \qquad \forall u \in \mathcal{U}, \tag{8.1h}$$

where (8.1a) minimizes the system operating cost evaluated by measure $\mathbb{F}_0$ (e.g. expectation, if $\mathbb{F}_0 \equiv \mathbb{E}$) over the random vector of RES forecast errors $\boldsymbol{\omega} = [\boldsymbol{\omega}_i, i \in \mathcal{U}]$ and given the cost function of each generator $c_i(p_{G,i})$. Eq. (8.1b) models the uncertain RES power output $p_{U,i}(\boldsymbol{\omega}_i)$ at node i as the RES forecast $p_{U,i}$ plus the RES forecast error $\boldsymbol{\omega}_i$. Eq. (8.1c) defines the power output of conventional generators under uncertainty $p_{G,i}(\boldsymbol{\omega})$ using an affine control policy, where $p_{G,i}$ and $\alpha_i = [0 \leqslant \alpha_{i,u} \leqslant 1, u \in \mathcal{U}]$ are decisions for the scheduled power output and the vector of participation factors for balancing reserve of generator i. Here $\alpha_{i,u}$ denotes the participation factor of generator i in response to the RES forecast error at node $u \in \mathcal{U}$. Chance constraints (8.1d) and (8.1e) ensure that the power output of conventional generator i under uncertainty does not exceed the upper or lower limits $p^{\max}_{G,i}$ and $p^{\min}_{G,i}$ with a probability of $1 - \epsilon_p$. Similarly, (8.1f) ensures that DC power flows computed using function $F(p_{G,i}(\boldsymbol{\omega}), p_{U,i}(\boldsymbol{\omega}), p_{D,i})$, which maps net nodal injections to power flows, are contained in a convex set of feasible power flows given by $\mathcal{F}$ with a probability of $1 - \epsilon_f$. Finally, (8.1g) is the nodal power balance constraint given the nodal demand and power flow injections $p_{D,i}$ and $p_i(F)$. Eq. (8.1h) ensures that the procured balancing reserve is sufficient to mitigate $\boldsymbol{\omega}$. Greek letters in parentheses denote dual multipliers.

8.2.1 *Deterministic Reformulation*

Using the quadratic cost model from (3.4):

$$c_i(p_{G,i}(\boldsymbol{\omega})) = c_{2i}(p_{G,i}(\boldsymbol{\omega}))^2 + c_{1i} p_{G,i}(\boldsymbol{\omega}) + c_{0i},$$

where c_{2i}, c_{1i}, c_{0i} are cost coefficients, and using $\mathbb{F}_0 \equiv \mathbb{E}$ and $\boldsymbol{\omega} \sim \mathcal{N}(0, \Sigma)$, where Σ is the covariance matrix of $\boldsymbol{\omega}$, (8.1) has a tractable convex (conic) reformulation, see Chapter 3:

$$\min_{\substack{p_{G,i}, \alpha_i \\ s_{p_{G,i}}}} \quad \sum_{i \in \mathcal{G}} c_i(g_i) + c_{2i} \left\| \alpha_i^\top \Sigma^{1/2} \right\|_2^2 \tag{8.2a}$$

$$\text{s.t.} \quad (\zeta_i): \quad s_{p_{G,i}} \geqslant \left\| \alpha_i^\top \Sigma^{1/2} \right\|_2 \qquad \forall i \in \mathcal{G} \tag{8.2b}$$

$$(\delta_i^+): \quad p_{G,i} + z_{\epsilon_p} s_{p_{G,i}} \leqslant p^{\max}_{G,i} \qquad \forall i \in \mathcal{G} \tag{8.2c}$$

$$(\delta_i^i): \quad -p_{G,i} + z_{\epsilon_p} s_{p_{G,i}} \leqslant -p^{\min}_{G,i} \qquad \forall i \in \mathcal{G} \tag{8.2d}$$

$$(\theta): \quad \tilde{F}_{\epsilon_f}(p_G, p_U, p_D, \alpha) \leqslant 0 \tag{8.2e}$$

$$(\lambda_i): \quad p_{G,i} + p_{U,i} + p_i(\tilde{F}_{\epsilon_f}) = p_{D,i} \qquad \forall i \in \mathcal{N}, \tag{8.2f}$$

$$(\chi_u): \quad \sum_{i \in \mathcal{G}} \alpha_{i,u} = 1 \qquad \forall u \in \mathcal{U}, \tag{8.2g}$$

where $z_\epsilon = \Phi^{-1}(1-\epsilon)$ is the quantile function of the standard normal distribution and $s_{p_{G,i}}$ is an auxiliary decision variable modeling the standard deviation of $p_{G,i}(\omega)$. As explained in [P3], the reserve provided by each producer can then be computed as $z_{\epsilon_p} s_{p_{G,i}}$, where $s_{p_{G,i}}$ depends on participation factors α_i. (Note that this expression holds even for more general distribution assumptions on ω, see [9]). Function $\tilde{F}_{\epsilon_f}(\cdot)$ in (8.2e) maps the decision variables, parameters, statistical characteristics of ω and security threshold ϵ_f into a vector of power flows with security margins so that (8.2e) is equivalent to chance constraint (8.1f), see e.g. Section 3.3.

8.2.2 *Equilibrium Formulation*

The optimization problem in (8.1) and (8.2) represents a risk-neutral market operator and has been proven to yield energy and balancing reserve prices λ_i and χ_u, which solve the following equilibrium, [P3], [P4], [9], [127]:

$$\left\{ \begin{array}{ll} \max_{\substack{p_{G,i},\alpha_i \\ s_{p_{G,i}}}} & \lambda_i p_{G,i} + \chi^\top \alpha_i - \mathbb{E}[c_i(p_{G,i}(\omega))] \\ \text{s.t.} & (8.2b)\text{–}(8.2d) \end{array} \right\}, \ \forall i \in \mathcal{G} \quad (8.3a)$$

$$(8.2e)\text{–}(8.2g) \quad (8.3b)$$

where (8.3a) is a profit maximization solved by each conventional generator (producer) and (8.3b) are the market-clearing conditions. As shown in Chapters 6 and 7, λ_i and χ_u can be interpreted as equilibrium energy and reserve prices.

8.3 RISK AVERSE MARKET

The optimization in (8.3a) solved by each producer is risk neutral because it assumes average (expected) outcomes of random ω. In practice, however, producers are likely to hedge against the risk of uncertain costs based on their risk perception. This section considers risk-averse profit maximizing producers endowed with a *risk measure* $\mathbb{F}_i$.

8.3.1 *Coherent Measures of Risk*

Intuitively, a risk measure evaluates an uncertain outcome $\mathbf{Z}$ in terms of an equivalent deterministic outcome $\mathbb{F}[\mathbf{Z}]$ so that a producer endowed with risk measure $\mathbb{F}$ is indifferent between accepting uncertain $\mathbf{Z}$ or its certainty equivalent $\mathbb{F}[\mathbf{Z}]$. Additionally, a risk measure is called *coherent* if, [81], [90]:

(i) $\mathbb{F}[c] = c$, i.e. the certainty equivalent of a deterministic constant $c \in \mathbb{R}$ is equal to the constant,

(ii) $\mathbb{F}[c\mathbf{Z}] = c\,\mathbb{F}[\mathbf{Z}]$, i.e. an uncertain outcome $\mathbf{Z}$ scaled by some positive constant $c > 0$ is equal to the scaled certainty equivalent,

(iii) $\mathbb{F}[(1-c)\mathbf{Z} + c\mathbf{Y}] \leqslant (1-c)\,\mathbb{F}[\mathbf{Z}] + c\,\mathbb{F}[\mathbf{Y}]$ for $c \in [0,1]$, i.e. the risk measure is convex, and

(iv) $\mathbb{F}[\mathbf{Z}] \leqslant \mathbb{F}[\mathbf{Y}]$ if $\mathbf{Z} \preccurlyeq \mathbf{Y}$, i.e. the risk measure is monotone.

For example, the expectation operator $\mathbb{E}$ is a coherent measure of risk, [81], but neglects the volatility of outcomes, and is therefore associated with risk-neutrality.

Any coherent risk measure can be expressed as, [81]:

$$\mathbb{F}[\mathbf{Z}] = \sup_{\mathbb{P}\in\mathcal{P}} \mathbb{E}_{\mathbb{P}}[\mathbf{Z}] \tag{8.4}$$

where $\mathcal{P}$ denotes the *risk set* (risk envelope) of $\mathbb{F}$, i.e. a compact convex set of probability measures, and $\mathbb{E}_{\mathbb{P}}$ is the expectation over the probability measure $\mathbb{P}$. Risk set $\mathcal{P}$ uniquely defines $\mathbb{F}$ and can be structured such that $\sup_{\mathbb{P}\in\mathcal{P}} \mathbb{E}_{\mathbb{P}}[\mathbf{Z}]$ is identical to specific risk measures, e.g. CVaR, [81].

Remark 8.1. Defining a risk measure in terms of a worst-case probability distribution as in (8.4) is structurally identical to *distributionally robust optimization* that can be applied to chance constraints (8.1d)–(8.1f), see e.g. [P2], [P3], [9] and Chapters 4 and 5. This work, however, focuses on the evaluation of the objective, i.e. the reformulation of constraints in (8.2c)–(8.2e) remains unchanged.

8.3.2 *Risk-Averse Profit Maximization*

To derive a risk-averse modification of (8.2), we define a risk set using a moment ambiguity set, which generally yields tractable convex optimization problems, [154]. Thus, the risk set of each producer i is:

$$\mathcal{P}_i = \{\mathbb{P}(\omega) \in \mathcal{P} \mid \mathbb{E}_{\mathbb{P}}[\omega] = 0, \mathrm{Var}_{\mathbb{P}}[\omega] \in \mathcal{S}_i\}, \tag{8.5}$$

where $\mathcal{P}$ is the set of probability distributions and $\mathcal{S}_i = \{\Sigma_1, ..., \Sigma_K\}$ is the set of K covariance matrices $(\Sigma_1, ..., \Sigma_K)$, where K is the same for all producers. Set $\mathcal{S}_i$, and thus set $\mathcal{P}_i$, captures the belief of producers on the accuracy of RES forecast data and forecasting methods. Given that all producers are likely to have access to similar data providers, we make the assumption that risk sets $\tilde{\mathcal{P}}_i, i \in \mathcal{G}$ are non-disjoint, i.e. $\bigcap_{i\in\mathcal{G}} \tilde{\mathcal{P}}_i \neq \emptyset$, [130], [131]. Notably, $\mathcal{P}_i$ is a set of continuous distributions as opposed to discrete polyhedral probability measures in [131], [197], which rely on a set of pre-described scenarios. Using (8.4) and (8.5) yields:

$$\begin{aligned} &\min_{p_{G,i},\alpha_i} \sup_{\mathbb{P}\in\mathcal{P}_i} \mathbb{E}_{\mathbb{P}}[c_i(p_{G,i}(\omega))] \\ &\quad = \min_{p_{G,i},\alpha_i} c_i(p_{G,i}) + \sup_{k=1,...,K} c_{2i} \left\| \alpha_i^\top \Sigma_k^{1/2} \right\|_2^2 . \end{aligned} \tag{8.6}$$

Although $\mathcal{P}_i$ as defined in (8.5) is non-convex, solving (8.6) is equivalent to solving the following problem with convex polyhedral set $\tilde{\mathcal{S}}_i = \text{conv}(\mathcal{S}_i)$, [198, Section 6.4.2]:

$$\min_{p_{G,i},\alpha_i} \quad c_i(p_{G,i}) + \sup_{\Sigma_k \in \tilde{\mathcal{S}}_i} c_{2i} \left\| \alpha_i^\top \Sigma_k^{1/2} \right\|_2^2 \tag{8.7}$$

and we can define:

$$\tilde{\mathcal{P}}_i = \{\mathbb{P}(\omega) \in \mathcal{P} \mid \mathbb{E}_{\mathbb{P}}[\omega] = 0, \text{Var}_{\mathbb{P}}[\omega] \in \tilde{\mathcal{S}}_i\} \tag{8.8}$$

as the convex counterpart of $\mathcal{P}_i$, which yields the following coherent risk measure:

$$\mathbb{F}_i\left[c_i(p_{G,i}(\omega))\right] = \sup_{\mathbb{P} \in \tilde{\mathcal{P}}_i} \mathbb{E}_{\mathbb{P}}[c_i(p_{G,i}(\omega))]. \tag{8.9}$$

Using the epigraph form of (8.7), the cost minimization in (8.2) can be recast as the following risk-averse modification:

$$\min_{\substack{p_{G,i},\alpha_i\\ s_{p_{G,i}},t_i}} \quad \sum_{i \in \mathcal{G}} (c_i(p_{G,i}) + t_i) \tag{8.10a}$$

$$\text{s.t.} \quad \text{(8.2b)–(8.2g)} \tag{8.10b}$$

$$(\eta_{i,k}): \quad t_i \geqslant c_{2i} \left\| \alpha_i^\top \Sigma_k^{1/2} \right\|_2^2 \quad \forall \Sigma_k \in \mathcal{S}_i, \forall i. \tag{8.10c}$$

Similarly, the risk-averse modification of (8.3a) follows as:

$$\max_{\substack{p_{G,i},\alpha_i\\ s_{p_{G,i}},t_i}} \quad \lambda_i p_{G,i} + \chi^\top \alpha_i - c_i(p_{G,i}) - t_i \tag{8.11a}$$

$$\text{s.t.} \quad \text{(8.2b)–(8.2d) and (8.10c).} \tag{8.11b}$$

Note that Σ in (8.2b) remains unchanged, see Remark 8.1.

Remark 8.2. Unlike in (8.3a), the risk-averse profit maximization in (8.11) allows different producers to have different perceptions of the system uncertainty, which can be modeled as different risk attitudes drawn from producer-specific set $\mathcal{P}_i$.

8.4 RISK TRADING

If producer i is endowed with coherent risk measure $\mathbb{F}_i$ given by risk set $\mathcal{P}_i$ and seeks to maximizes its risk adjusted profit as in (8.11), its decision will be more conservative in the absence of risk-trading opportunities. Thus, a risk-incomplete market as in (8.10) will be less efficient and suffer welfare losses. This section describes an approach to complete the chance-constrained market with respect to risk by introducing ADS trading.

8.4.1 *Continuous Risk Trading*

ADS as introduced in [199] is a common security contract that depends on the outcome of an uncertain asset, which in the case of the chance-constrained electricity market in (8.10) is the RES forecast error given by ω. Thus, a buyer of the contract pays price $\mu(\omega)$ to receive a payment of 1 for a pre-defined realization of ω. Hence, if producer i seeks to receive a payment of $a_i(\omega)$ for all possible ω, it pays in advance:

$$\pi_{a_i} = \int_{\Omega} \mu(\omega) a_i(\omega) d\omega \tag{8.12}$$

where Ω is the space of all possible outcomes of ω. If $a_i(\omega) \leqslant 0$, then producer i sells ADS (i.e. provides security to the system) and receives the payment of $\pi_{a_i} \leqslant 0$. Otherwise, if $a_i(\omega) \geqslant 0$, producer i purchases ADS and pays $\pi_{a_i} \geqslant 0$. Further, the market must ensure revenue adequacy, i.e. that the amount of ADS purchased and sold match:

$$(\mu(\omega)) : \quad \sum_{i \in \mathcal{G}} a_i(\omega) = 0 \quad \forall \omega \in \Omega. \tag{8.13}$$

Given the risk trading model in (8.12) and (8.13), each profit-maximizing producer can be modeled as follows:

$$\max_{\substack{p_{G,i}, \alpha_i, a_i(\omega) \\ s_{p_{G,i}}, t_i}} \quad \lambda_i p_{G,i} + \chi^\top \alpha_i - t_i - \pi_{a_i} \tag{8.14a}$$

$$\text{s.t.} \quad \text{(8.2b)–(8.2d)} \tag{8.14b}$$

$$(\eta_{i,k}) : \ t_i \geqslant \mathbb{E}_{\mathbb{P}_k}[c_i(p_{G,i}(\omega))] - \mathbb{E}_{\mathbb{P}_k}[a_i(\omega)], \ \forall \mathbb{P}_k \in \mathcal{P}_i, \tag{8.14c}$$

where π_{a_i} reflects the additional cost or revenue due to risk trading, as given in (8.12), and $\mathbb{E}_{\mathbb{P}_k}[a_i(\omega)]$ in (8.14c) is the expected ADS cost or revenue over probability measure $\mathbb{P}_k$. Given (8.13) and (8.14), extending the risk-averse market-clearing in (8.10) with risk trading yields:

$$\min_{\substack{p_{G,i}, \alpha_i, a_i(\omega) \\ s_{p_{G,i}}, t_i}} \quad \sum_{i \in \mathcal{G}} (c_i(p_{G,i}) + t_i) \tag{8.15a}$$

$$\text{s.t.} \quad \text{(8.2b)–(8.2g), (8.13) and (8.14c),} \tag{8.15b}$$

where (8.13) enforces the market-clearing condition yielding dual multiplier $\mu(\omega)$. Using (8.15) and under the assumption that set $\mathcal{F}$ is sufficiently large to accommodate injections $p_G(\omega)$, $p_U(\omega)$, p_D without causing network congestion[1] (i.e. energy prices are uniform $\lambda = \lambda_i$), we prove:

1 This assumption simplifies derivations, but the result holds for the congested case if transmission assets and services are priced [192].

Proposition 8.1. *Let λ, χ, and $\mu(\omega)$ be equilibrium energy, balancing, and risk prices, respectively, so that $\{\lambda_i = \lambda; \chi_u; \mu(\omega); p_{G,i}, \forall i \in \mathcal{G}; \alpha_i, \forall i \in \mathcal{G}; a_i(\omega), \forall i \in \mathcal{G}\}$ solves (8.15). Then $\mu(\omega)$ can be interpreted as a probability measure that solves a risk-neutral equivalent of the risk-averse profit maximization with ADS trading.*

Proof. The market-clearing problem in (8.15) remains convex as long as $a_i(\omega)$ is convex in ω. Therefore, KKT conditions can be invoked. The Lagrangian function of the profit maximization of each producer in (8.14) can be written as:

$$\begin{aligned}\mathcal{L}_i = \lambda p_{G,i} + \chi^\top \alpha_i - t_i - \pi_{a_i} - \zeta_i\left(\left\|\alpha_i^\top \Sigma^{1/2}\right\|_2 - s_{p_{G,i}}\right) \\ - \delta_i^+(p_{G,i} + z_\epsilon s_{p_{G,i}} - p_{G,i}^{\max}) - \delta_i^-(-p_{G,i} + z_\epsilon s_{p_{G,i}} + p_{G,i}^{\min}) \\ - \sum_{k=1}^{K} \eta_{i,k}(\mathbb{E}_{\mathbb{P}_k}[c_i(p_{G,i}(\omega)) - a_i(\omega)] - t_i)\end{aligned} \tag{8.16}$$

Hence, the resulting optimality conditions for t_i, $a_i(\omega)$ are:

$$\frac{\partial \mathcal{L}_i}{\partial t_i} = -1 + \sum_{k=1}^{K} \eta_{i,k} = 0 \quad \Rightarrow \quad \sum_{k=1}^{K} \eta_{i,k} = 1 \tag{8.17}$$

$$\begin{aligned}\frac{\partial \mathcal{L}_i}{\partial a_i(\omega)} = -\mu(\omega) + \sum_{k=1}^{K} \eta_{i,k} f(\omega, \sigma_k) = 0 \\ \Rightarrow \quad \mu(\omega) = \sum_{k=1}^{K} \eta_{i,k} f(\omega, \Sigma_k),\end{aligned} \tag{8.18}$$

where $f(\omega, \Sigma_k)$ denotes the probability density function of a multivariate, zero-mean distribution with covariance Σ_k. Note that for the derivation of (8.18) we used:

$$\frac{\partial \pi_{a_i}}{a_i(\omega)} = \frac{\partial}{\partial a_i(\omega)} \int_\Omega \mu(\omega) a_i(\omega) d\omega = \mu(\omega), \tag{8.19}$$

$$\frac{\partial}{\partial a_i(\omega)} \mathbb{E}_{\mathbb{P}_k}[a_i(\omega)] = \frac{\partial}{a_i(\omega)} \int_\Omega a_i(\omega) f(\omega, \Sigma_k) d\omega = f(\omega, \Sigma_k). \tag{8.20}$$

Conditions (8.17) and (8.18) lead to two relevant observations:

(O1) Dual multiplier $\mu(\omega)$ in (8.13) is a probability measure as it is the weighted average of K probability density functions with zero means and covariance matrices $\Sigma_1, ..., \Sigma_k$. In other words, random $\mathbf{Z}(\omega) \sim \mu(\omega)$ has the expected value of $\mathbb{E}_\mu[\mathbf{Z}(\omega)] = 0$ and the variance of $\mathrm{Var}_\mu[\mathbf{Z}(\omega)] = \sum_{k=1}^{K} \eta_{i,k} \Sigma_k$.

(O2) Since $\tilde{S}_i$ is a convex set, condition (8.17) ensures that $\sum_{i=1}^{K} \eta_{i,k} \Sigma_k \in \tilde{S}_i$ and thus $\mu(\omega) \in \tilde{\mathcal{P}}_i$.

The set of optimal decisions $\{\lambda;\chi_u;\mu(\omega);p_{G,i},\forall i \in \mathcal{G};\alpha_i,\forall i \in \mathcal{G};a_i(\omega),\forall i \in \mathcal{G}\}$ maximize $\mathcal{L}_i$ given in (8.16). Using observation O1, the fifth term in (8.16) recasts as:

$$\begin{aligned}
&\sum_{k=1}^{K} \eta_{i,k}(\mathbb{E}_{\mathbb{P}_k}[c_i(p_{G,i}(\omega)) - a_i(\omega)]) \\
&\quad = \sum_{k=1}^{K} \eta_{i,k} \int_{\Omega} [c_i(p_{G,i}(\omega)) - a_i(\omega)] f(\omega, \Sigma_k) d\omega \\
&\quad = \int_{\Omega} [c_i(p_{G,i}(\omega)) - a_i(\omega)] \sum_{k=1}^{K} \eta_{i,k} f(\omega, \Sigma_k) d\omega \\
&\quad = \int_{\Omega} [c_i(p_{G,i}(\omega)) - a_i(\omega)] \mu(\omega) d\omega \\
&\quad = \mathbb{E}_{\mu}[c_i(p_{G,i}(\omega))] - \pi_{a_i}.
\end{aligned} \tag{8.21}$$

Substituting (8.21) in (8.16) leads to:

$$\mathcal{L}_i = p_{G,i} + \chi\alpha_i - \mathbb{E}_{\mu}[c_i(p_{G,i}(\omega))] - y_i^{\delta} - y_i^{\zeta}, \tag{8.22}$$

where y_i^{δ}, y_i^{ζ} denote the terms related to duals δ_i, ζ_i in (8.16). Hence, (8.22) is a risk-neutral equivalent, evaluated with respect to probability measure $\mu(\omega)$, of the risk-averse profit of producer i participating in risk trading with ADS. □

Given Proposition 8.1, the optimization of individual producers in (8.14) is related to the risk-averse chance-constrained electricity market with ADS trading in (8.15):

Proposition 8.2. *Let λ, χ_u, and $\mu(\omega)$ be equilibrium energy, balancing, and risk prices so that $\{\lambda_i = \lambda;\chi_u;\mu(\omega);p_{G,i},\forall i \in \mathcal{G};\alpha_i,\forall i \in \mathcal{G};a_i(\omega),\forall i \in \mathcal{G}\}$ solves problem (8.15). Given that $\bigcap_{i\in\mathcal{G}} \tilde{\mathcal{P}}_i \neq \emptyset$, then these prices and allocations solve the risk-averse chance-constrained market with risk trading with $\tilde{\mathcal{P}}_0 = \bigcap_{i\in\mathcal{G}} \tilde{\mathcal{P}}_i$ and worst case probability measure $\mu(\omega)$.*

Proof. Given the optimal solution for each producer, it follows from the complementary slackness of (8.14c):

$$\eta_{i,k}(\mathbb{E}_{\mathbb{P}_k}[c_i(p_{G,i}(\omega)) - a_i(\omega)] - t_i) = 0. \tag{8.23}$$

By summing (8.23) over all i and k, comparing with (8.21), and using (8.13) to eliminate π_{a_i}, we write:

$$\begin{aligned}
\sum_{i\in\mathcal{G}} t_i &= \sum_{i\in\mathcal{G}} \sum_{k=1}^{K} \eta_{i,k}(\mathbb{E}_{\mathbb{P}_k}[c_i(p_{G,i}(\omega)) - a_i(\omega)] \\
&= \mathbb{E}_{\mu}\Big[\sum_{i\in\mathcal{G}} c_i(p_{G,i}(\omega))\Big].
\end{aligned} \tag{8.24}$$

Also, since (8.14c) is a convex epigraph, we have

$$t_i = \max_{\mathbb{P}\in\tilde{\mathcal{P}}_i} \mathbb{E}_{\mathbb{P}_k}[c_i(p_{G,i}(\omega)) - a_i(\omega)]. \tag{8.25}$$

Given (8.25), term $\sum_{i \in \mathcal{G}} t_i$ in (8.24) can also be written as:

$$\begin{aligned}\sum_{i \in \mathcal{G}} t_i &= \sum_{i \in \mathcal{G}} \max_{\mathbb{P}_k \in \tilde{\mathcal{P}}_i} \mathbb{E}_{\mathbb{P}_k}[c_i(p_{G,i}(\omega)) - a_i(\omega)] \\ &\overset{\text{A}}{\geqslant} \max_{\mathbb{P} \in \bigcap_{i \in \mathcal{G}} \tilde{\mathcal{P}}_i} \mathbb{E}_{\mathbb{P}} \Big[\sum_{i \in \mathcal{G}} c_i(p_{G,i}(\omega)) - a_i(\omega) \Big] \\ &\overset{\text{B}}{=} \max_{\mathbb{P} \in \bigcap_{i \in \mathcal{G}} \tilde{\mathcal{P}}_i} \mathbb{E}_{\mathbb{P}} \Big[\sum_{i \in \mathcal{G}} c_i(p_{G,i}(\omega)) \Big],\end{aligned} \tag{8.26}$$

where transition A is due to the replacement of individual risk sets $\mathcal{P}_i$ with the intersection of all risk sets $\tilde{\mathcal{P}}_0 = \bigcap_{i \in \mathcal{G}} \tilde{\mathcal{P}}_i$ and transition B is due to the market-clearing ADS condition in (8.13). Since $\mu(\omega) \in \tilde{\mathcal{P}}_i, \forall i \in \mathcal{G}$ and $\tilde{\mathcal{P}}_0 \neq \emptyset$, due to observation O2 above, (8.24) and (8.26) yield:

$$\mathbb{E}_{\mu}\Big[\sum_{i \in \mathcal{G}} c_i(p_{G,i}(\omega))\Big] = \max_{\mathbb{P}_k \in \tilde{\mathcal{P}}_0} \mathbb{E}_{\mathbb{P}_k}\Big[\sum_{i \in \mathcal{G}} c_i(p_{G,i}(\omega))\Big], \tag{8.27}$$

showing that $\mu(\omega)$ is the worst-case probability measure for the risk-averse market with risk trading. □

8.4.2 *Discrete Risk Trading*

Recall that Section 8.4.1 defines ADS as continuous over ω, which leads to an infinite-dimensional problem in (8.15) and obstructs tractable computations and designing practical risk contracts. To overcome these caveats, the probability space of ω can be discretized to consider contracts for discrete events. Hence, consider the system-wide (aggregated) RES forecast error given as $\mathbf{O} = e^\top \omega$ with mean $\mathbb{E}_{\mathbb{P}_k}[\mathbf{O}] = 0$ and variance $\mathrm{Var}_{\mathbb{P}_k}[\mathbf{O}] = e^\top \Sigma_k e =: \sigma_k^2$, where e is the vector of ones of appropriate dimensions. The probability space of $\mathbf{O}$ can then be divided into W events $w = 1, ..., W$, where each event is a closed interval given by $\mathcal{W}_w = [l_w, u_w]$ so that $\bigcup_{w=1}^{W} \mathcal{W}_w = \mathbb{R}$. These intervals are sequential such that $l_1 = -\infty$, $u_W = \infty$ and $u_w = l_{w+1}, w = 1, ..., W-1$. Thus, the probability of each discrete outcome is defined by $\mathbb{P}_k$ as:

$$\begin{aligned}P_w(\sigma_k) := \mathbb{P}_k[\mathbf{O} \in \mathcal{W}_w] &= \mathbb{P}_k[(\mathbf{O} \leqslant u_w) \cap (\mathbf{O} \geqslant l_w)] \\ &= \int_{l_w}^{u_w} f(x, \sigma_k) dx\end{aligned} \tag{8.28}$$

and can be pre-computed for all $w = 1, ..., W$ and $k = 1, ..., K$. Using the discrete space notation, (8.12) recasts as:

$$\pi_{a_i} = \sum_{w=1}^{W} \mu_w a_{i,w}, \tag{8.29}$$

where $a_{i,w} \in \mathbb{R}$. Next, using (8.28), the expected cost or payment $a_i(\omega)$ under $\mathbb{P}_k$ can be computed as:

$$\mathbb{E}_{\mathbb{P}_k}[a_i(\omega)] = \sum_{w=1}^{W} a_{i,w} P_w(\sigma_k). \tag{8.30}$$

Finally, using (8.29) and (8.30) and the discrete-space equivalent of (8.18), i.e. the optimality condition for $a_{i,w}$, the discrete-space equivalent of $\mu(\omega)$ is computed as:

$$\begin{aligned}\mu_w &= \sum_{k=1}^{K} \eta_k P_w(\sigma_k) = \sum_{k=1}^{K} \eta_{i,k} \int_{l_w}^{u_w} f(x, \sigma_{i,k}) dx \\ &= \int_{l_w}^{u_w} \sum_{k=1}^{K} \eta_{i,k} f(x, \sigma_{i,k}) dx \quad \forall i \in \mathcal{G},\end{aligned} \tag{8.31}$$

where $\sigma_{i,k} = \left\| e^\top \Sigma_k^{1/2} \right\|_2$ with $\Sigma_k \in \mathcal{S}_i$. Hence, due to (8.31), μ_w retains the interpretation of $\mu(\omega)$ from observation O1 of Proposition 8.1. Indeed, a random variable with probability density function $\sum_{k=1}^{K} \eta_{i,k} f(x, \sigma_{i,k})$ has variance $\left\| e^\top (\sum_{k=1}^{K} \eta_{i,k} \Sigma_k)^{1/2} \right\|_2^2 = e^\top (\sum_{k=1}^{K} \eta_k \Sigma_k) e$, it follows that $\mathrm{Var}_\mu(\mathbf{O}) = e^\top (\sum_{k=1}^{K} \eta_{i,k} \Sigma_k) e$. Using this result and (8.28)–(8.31), a discrete modification of the risk-averse chance-constrained electricity market with risk trading in (8.15) is:

$$\min_{\substack{p_{G,i}, \alpha_i, a_{i,w} \\ s_{p_{G,i}}, t_i}} \quad \sum_{i \in \mathcal{G}} (c_i(p_{G,i}) + t_i) \tag{8.32a}$$

$$\text{s.t.} \quad (8.2b)\text{–}(8.2g) \tag{8.32b}$$

$$(\eta_{i,k}) : \quad t_i \geqslant c_{2i} \left\| \alpha_i^\top \Sigma_k^{1/2} \right\|_2^2 + \sum_{w=1}^{W} a_{i,w} P_w(\sigma_{i,k}), \quad \forall \Sigma_k \in \mathcal{S}_i, \forall i \tag{8.32c}$$

$$(\mu_w) : \quad \sum_{i \in \mathcal{G}} a_{i,w} = 0, \quad \forall\, w = 1, ..., W. \tag{8.32d}$$

Since the discrete representation of ADS contracts in (8.32) is a special case of the infinite-dimensional representation in (8.15), the results of Propositions 8.1 and 8.2 hold for (8.32).

8.4.3 *Price Analysis with Risk Trading*

Using the risk-averse chance-constrained electricity market with discrete risk trading in (8.32), this section analyzes resulting energy, balancing reserve and risk prices as follows:

Proposition 8.3. *Consider the risk-averse chance-constrained market with risk trading in* (8.32). *Let* λ_i, χ_u *and* μ_w *be the dual multipliers of the* *active power balance* (8.2f)*, the reserve sufficiency constraint* (8.2g) *and the ADS market-clearing constraint* (8.32d)*. Then μ_w is given by* (8.31) *and*

$$\lambda_i = 2c_{2i}p_{G,i} + c_{i1} + (\delta_i^+ - \delta_i^-) + y_{p_{G,i}}(\theta) \tag{8.33}$$

$$\chi_u = \frac{1}{|\mathcal{G}|}\sum_{i\in\mathcal{G}}\left(2c_{2i}\alpha_i^\top[\overline{\Sigma}_i]_u + z_{\epsilon_p}\delta_i\frac{\alpha_i^\top[\Sigma]_u}{s_{G,i}} + y_{\alpha_{i,u}}(\theta)\right), \tag{8.34}$$

where $y_{p_{G,i}}(\theta) := \theta^\top\frac{\partial\tilde{F}_{\epsilon_f}}{\partial p_{G,i}}$, $y_{\alpha_{i,u}}(\theta) := \theta^\top\frac{\partial\tilde{F}_{\epsilon_f}}{\partial\alpha_{i,u}}$, $\overline{\Sigma}_i := (\sum_{k=1}^K \eta_{i,k}\Sigma_k \mid \Sigma_k \in \mathcal{S}_i)$*,* $\delta_i := \delta_i^+ + \delta_i^-$*,* $[X]_u$ *is the vector of elements in the* u*-th column of matrix* X*, and* $s_{G,i} = \left\|\alpha_i^\top\Sigma^{1/2}\right\|_2$*, i.e. the standard deviation of* $p_{G,i}(\boldsymbol{\omega})$*.*

Proof. Let $\mathcal{L}$ be the Lagrangian function of (8.32), its first-order optimality conditions for $p_{G,i}$, $\alpha_{i,u}$, $s_{p_{G,i}}$ and $a_{i,w}$ are:

$$\begin{aligned}\frac{\partial\mathcal{L}}{\partial p_{G,i}} &= 2c_{2i}p_{G,i} + c_{i1} + (\delta_i^+ - \delta_i^-)\\ &\quad + y_{p_{G,i}}(\theta) - \lambda_i = 0,\ \forall i\in\mathcal{G}\end{aligned} \tag{8.35a}$$

$$\begin{aligned}\frac{\partial\mathcal{L}}{\partial \alpha_{i,u}} &= 2c_{2i}\alpha_i^\top[\overline{\Sigma}_i]_u + \zeta_i\frac{\alpha_i^\top[\Sigma]_u}{\left\|\alpha_i^\top\Sigma^{1/2}\right\|_2}\\ &\quad + y_{\alpha_{i,u}}(\theta) - \chi_u = 0,\ \forall i\in\mathcal{G},\ \forall u\in\mathcal{U}\end{aligned} \tag{8.35b}$$

$$\frac{\partial\mathcal{L}}{\partial s_{p_{G,i}}} = -\zeta_i + \delta_i^+ z_{\epsilon_p} + \delta_i^- z_{\epsilon_p} = 0,\ \forall i\in\mathcal{G} \tag{8.35c}$$

$$\frac{\partial\mathcal{L}}{\partial a_{i,w}} = \sum_{k=1}^K \eta_{i,k}P_w(\sigma_{k,i}) - \mu_w = 0 \tag{8.35d}$$

Expressions (8.33) and (8.34) follow immediately from (8.35d) and (8.35a), respectively. Expressing ζ_i from (8.35c) and summing over all $i\in\mathcal{G}$ in (8.35b) yields (8.34). □

Notably, energy prices in (8.33) are driven by cost coefficients of $c_i(\cdot)$ and do not explicitly depend on random $\boldsymbol{\omega}$, risk set $\mathcal{P}_i$ and tolerance to chance constraint violations ϵ_p. On the other hand, the balancing reserve price in (8.33) depends on $\boldsymbol{\omega}$ (via parameter Σ), $\mathcal{P}_i$ (via parameter $\overline{\Sigma}_i$) and ϵ_p. Finally, risk prices in (8.31) depends on the degree of discretization W, which affects interval limits l_w and u_w, and individual risk perception given by set $\mathcal{P}_i$ (via parameter $\sigma_{i,k}$).

8.5 ILLUSTRATIVE CASE STUDY

We conduct a case study to illustrate some of the theoretical results of this chapter by comparing the *ex ante* outcomes of the risk-averse chance-constrained electricity market without risk trading ("NO-RT"), as formulated in (8.10), and with risk trading ("RT"), as formulated in (8.32). We construct a data set that includes five conventional producers with parameters $c_{1i} = \{10, 7, 7, 15, 17\}$\$/MW,

Table 8.1: Power Outputs and Balancing Participation Factors

		$\alpha_{i,u}$ in the RT case					$\alpha_{i,u}$ in the NO-RT case				
	$p_{G,i}$	$u=1$	2	3	4	5	1	2	3	4	5
$i=1$	26.04	0.09	0.18	0.26	0.34	0.21	0.19	0.19	0.23	0.31	0.24
2	10.00	0.41	0.30	0.40	0.10	0.17	0.39	0.26	0.32	0.10	0.25
3	10.00	0.31	0.28	0.06	0.33	0.31	0.37	0.27	0.12	0.28	0.23
4	15.70	0.01	0.14	0.14	0.12	0.26	0.04	0.15	0.18	0.14	0.20
5	13.36	0.18	0.10	0.15	0.11	0.06	0.02	0.13	0.15	0.17	0.08
χ_u	–	1.24	1.54	0.72	0.69	1.31	0.91	1.47	1.31	1.34	1.11

(Indices i relate to producers, indices u relate to uncertain RES.)

$c_{2i} = 0.1c_{1i}, \forall i \in \mathcal{G}$, $p_{G,i}^{\max} = \{30, 10, 10, 25, 25\}$ MW and $p_{G,i}^{\min} = 0, \forall i \in \mathcal{G}$, and five undispatchable stochastic RES producers. The total system demand is $\sum_{i\in\mathcal{N}} p_{D,i} = 100$ MW and forecasted RES production is $p_{U,i} = 5$ MW, $\forall i \in \mathcal{U}$. The risk sets $\mathcal{P}_i$ defined by set $\mathcal{S}_i$, see (8.5), of the individual producers are constructed with $K = 10$ as follows. Each producer i has a set $\mathcal{S}_i$ of $K-1$ covariance matrices that reflect their individual risk perception. We randomly generate these sets with the standard deviation of $\boldsymbol{\omega}_i$ between 0 to $0.4p_{U,i}$ and the correlation between 0 to 0.5. Additionally, we assume there exists a "common" covariance defined such that all $\boldsymbol{\omega}_i$ have a standard deviation of $0.2p_{U,i}$ and no correlation. This common covariance matrix is added to all $\mathcal{S}_i$ and can, for example, reflect information provided by the market operator or some third-party forecast provider. We create eight ADS events by discretizing the probability space of $\mathbf{O}$ in eight intervals using breakpoints $[-0.2, -0.1, -0.05, 0, 0.05, 0.1, 0.2]$, as explained in Section 8.4.2 and shown on the x-axis of Fig. 8.1(a). The code and data is available in [200].

For this data set, the RT case reduces the risk-adjusted system cost by 0.2% relative to the NO-RT case. Notably, the energy cost component (4,656.50 \$) and energy prices (62.09 \$) are the same in both cases, but the balancing reserve cost component is reduced by 11 % (from 6.17 \$ to 5.52 \$). Similarly, generation levels $p_{G,i}$ remain unchanged for both cases (see Table 8.1). On the other hand, the introduction of ADS trading changes the balancing reserve provision ($\alpha_{i,u}$) and its prices (χ_u), as shown in Table 8.1, which is influenced by different risk beliefs of producers.

Fig. 8.1 summarizes the discrete events and resulting risk trades. Each column in Fig. 8.1 reflects one event, numbered on the x-axis of Fig. 8.1(b) and with the interval breakpoints shown on the x-axis of Fig 8.1(a). ADS trading outcomes are itemized in Fig. 8.1(b), where negative and positive values indicate ADS selling and purchasing pro-

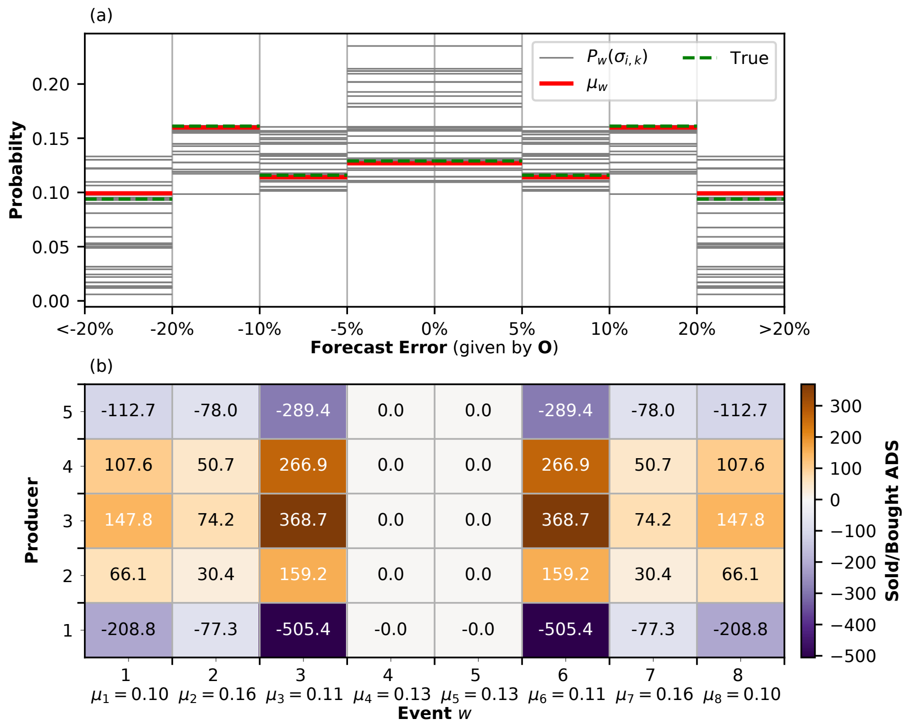

Figure 8.1: Risk trading results in the RT case: (a) itemizes the event probabilities $P_w(\sigma_{i,k})$, see (8.28), drawn from all individual risk sets (shown in thin gray lines) relative to the "common" distribution (dashed green line) and the ADS prices μ_w (solid red line); (b) itemizes the ADS trades, where negative (purple) values indicate a producer selling ADS and positive (orange) values indicate a producer buying ADS. The columns in both (a) and (b) reflect the events with breakpoints indicated on the x-axis of (a) and event numbers as indicated on the x-axis of (b).

ducers, respectively. Due to the symmetry of the RES uncertainty distributions, the ADS trading outcomes are also symmetric. Note that producers 1 and 5 are security providers and producers 2-4 are security takers. Specifically, in the NO-RT case, producer 5 expects to attain a greater profit by providing less balancing reserve to RES $u = 1$ than in the RT case. In other words, when producer 5 can hedge its risk via ADS trade, it is incentivized to procure more balancing reserve for RES $u = 1$. The risk-aversion also affects the ADS prices in Fig. 8.1(b) given by dual μ_w of the ADS market-clearing constraint (8.13) for each event. As shown in Fig. 8.1(a), the values of risk prices μ_w in Fig. 8.1(b), match the "common" event probabilities. That is, μ_w is indeed a probability measure, as in Proposition 8.1, and captures the risk perception at the intersection of all risk sets $\tilde{\mathcal{P}}_i$, as in Proposition 8.2.

8.6 Conclusion

This chapter has developed a risk-averse modification of the chance-constrained electricity market discussed in previous Chapters 6 and 7 by completing it with ADS-based risk trading. By discretizing the outcome space of the system uncertainty, we formulated practical ADS contracts that lead to a computationally tractable market-clearing optimization with risk trading. This optimization reduces the system operating cost relative to the case with no risk trading and produces energy, balancing reserve and risk prices. In particular, both qualitative and quantitative analyses indicate that system uncertainty and risk parameters do not explicitly affect the energy prices, but explicitly contribute to the formation of the balancing reserve and risk prices.

Part IV

CONCLUSIONS

9 CONCLUSION AND OUTLOOK

Realizing the necessity of modern power systems to host increasing numbers of stochastic renewable and distributed energy resources, this dissertation has emphasized the usefulness of risk-aware power system control, dispatch and market-coordination. The proposed set of methods enables system and market operators to internalize statistical properties of uncertain injections from renewable energy sources (RES) or distributed energy resources (DERs) into established decision making tools to mitigate uncertainty-related risk. As a result, evaluation of controllable generation, intermittent RES injection and reserve capacity in the context of physical system constraints improves and, thus, increases RES hosting capacity at a moderate increase of cost. Applications of these methods for active distribution system operation, AC-complete transmission system dispatch and risk-complete electricity markets have been studied.

9.1 SUMMARY

Specifically, we first derived tractable chance-constrained modifications of the optimal power flow (OPF) problem for transmission and distribution systems (CC-OPF). Then we proposed a data-driven approach to immunize the CC-OPF against errors in the uncertainty statistics using confidence bounds on the empirical moment estimations. This distributionally-robust modification of the CC-OPF has been applied to a distribution system with significant behind-the-meter RES generation and controllable DERs and showed improved robustness against out-of-sample uncertainty realizations. Extending on the analyses of distribution system operation, we then proposed a regression-based online-learning framework to co-optimize DER operation and incentive signals broadcast to flexible loads in a demand response (DR) program. We highlighted that neglecting system physics in DR price signals, as common in the related literature, may lead to power flow and voltage violations that impede a safe system operation. The effectiveness of the learning algorithm has been proved analytically and numerically via regret analyses.

Next, we used convex duality theory to obtain a risk-aware electricity market clearing with efficient energy and reserve prices from the CC-OPF formulation. We derived energy prices as distribution locational marginal prices (DLMPs) for low-voltage distribution networks and as AC-complete locational marginal prices (LMPs) for high-voltage transmission systems. Additionally, we showed that the CC-OPF formulations yield efficient prices for real-time balancing participation and procuring the necessary reserve capacity. Qualitative and quantitative analyses demonstrated that energy prices are not explicitly depending on system uncertainty. Reserve prices, on the other hand, include terms related to forecast error statistics and risk parameters. Additionally, these prices avoid a per-scenario trade-off by internalizing the continuous probability space of the underlying uncertainty via moment information (variance). Therefore, cost recovery and revenue adequacy can always be guaranteed. Finally, we presented a chance-constrained market-clearing with risk-averse market participants using coherent risk metrics. Here, we showed that the risk-averse market can retain an equilibrium if risk can be traded among market participants via suitable financial products, i.e. Arrow-Debreu Securitys (ADSs). A suitable discretization of the probability space of the uncertain parameter enabled the design of practical contracts and improved computational tractability.

9.2 RESEARCH OUTLOOK

The contributions of this dissertation are constrained by some specific modeling assumptions and the specific design of the studied problems. Future research may relax some of these constraints to unravel new improvements and enable new or generalized applications. A few potential pathways are outlined below.

ENERGY STORAGES Although energy storages (ESs) can be modeled as controllable generators or DERs that participate in energy and balancing reserve provisions, some features that are specific to ES obstruct a straight-forward implementation in the chance-constrained framework. First, ES operative constraints are usually “hard”, i.e. they do not allow any short-term violations, see discussion in Box 2 and [148]. However, possibilities to include these constraints of ES into future CC-OPF models may comprise (i) a mixed robust-risk-aware framework that ensures ES compliance for all possible outcomes, e.g. along the lines of [148], (ii) an explicit analysis of corrective actions in case of a constraint violation along the lines of [147] or (iii) using improved detailed models of ES operation to define optimal operation set-points that may be violated for a short period of time. Option (iii) may be the most promising, because detailed dynamic models of power-electronic interfaced chemical ES suggest possibilities of short-term and low-magnitude deviations from preferred states. For example, [201] suggests that the technically short-term feasible charging rate of certain battery system can be three to five times higher than the preferred long-term rate. These observations may be sufficient to enable a chance-constrained operational paradigm. Second, ES exhibit time-coupled constraints which raise some issues in the context of CC-OPF as discussed below.

TIME-COUPLED CONSTRAINTS Random variables with inter-temporal dependencies complicate an exact reformulation of the CC-OPF problem. Such dependencies may occur as time-correlations within the vector of uncertain parameters or time-coupled probabilistic constraints, e.g. from ES or generator ramping. Notably, expanding the variance-covariance matrix of the uncertain parameter vector to capture time-correlations may be possible using the formulations presented in this work. However, this neglects the possibility of time-to-time corrective actions after the outcome of the uncertainty has been observed. These multiperiod decisions warrant the use of methods from dynamic programming and model-predictive control. While these are promising approaches to generalize CC-OPF calculations, they may obstruct analytical reformulations to analyze price components and prove the existence of market equilibria.

FINANCIAL PRODUCTS This dissertation studied risk trading and financial risk hedging using generic ADSs. While this concept is useful for the theoretic analyses of risk-averse markets, it does not have an immediate real-world equivalent. Variance-based products, such as variance swaps or a more general variance-based pricing theory, [202], [203], may provide interesting pathways towards the implementation of efficient real-world stochastic electricity markets.

ASYMMETRIC DATA AVAILABILITY While centrally managed power system operations and electricity markets typically rely on forecasts from commercial providers, [204], the same data might not be available to all stakeholders in the system. Similarly, individual resource operators may have access to more divers data at higher resolution that is not shared externally. General information asymmetry may be included via coherent risk metrics as done in Chapter 8 or via iterative negotiation as proposed in recent work in [205]. However, these approaches neglect any cost of obtaining forecast data from third-party providers and, thus, the trade-off between additional cost of procuring more accurate forecasts and potentially increased profits from using such forecast. By designing suitable products or incentive schemes operators may be encouraged to invest in better forecast and share the resulting data with the system operator and other market participants. We expect that such data-products or data-markets will further mitigate adverse effects of stochastic RES and DERs.

Part V

APPENDIX

A PRIMER ON (CONVEX) OPTIMIZATION

This chapter provides a brief overview on some optimization concepts that are relevant for this dissertation. The main vocabulary and definitions are adapted from [198] and the section on conic optimization additionally follows [177].

A.1 DEFINITIONS

Consider the following generic constrained optimization problem:

$$\begin{aligned} \min_{x} \quad & f_0(x) && && \text{(A.1a)} \\ \text{s.t.} \quad & f_i(x) \leqslant 0 && i = 1, \ldots, m && \text{(A.1b)} \\ & h_i(x) = 0 && i = 1, \ldots, p, && \text{(A.1c)} \end{aligned}$$

where $x = [x_1, \ldots, x_n]^\top$ is the vector of decision variables. Problem (A.1) minimizes objective (A.1a) while enforcing *inequality constraints* in (A.1b) and *equality constraints* in (A.1c). Any point x that satisfies all constraints (A.1b) and (A.1c) is called *feasible point* and the set of all feasible points is called *feasible set*. If the feasible set is empty, i.e. the constraints contradict each other, the problem is *infeasible*. The *optimal value* of (A.1) is the smallest $p^* = f_0(x^*)$ that can be attained from the feasible set and the corresponding feasible point x^* is called *optimal point*. The pair (p^*, x^*) is typically referred to as *optimal solution*. It is worth pointing out that the function in the problem objective does not necessarily require a mathematically special treatment. In fact, the problem

$$\begin{aligned} \min_{x,t} \quad & t && && \text{(A.2a)} \\ \text{s.t.} \quad & f_0(x) \leqslant t && && \text{(A.2b)} \\ & f_i(x) \leqslant 0 && i = 1, \ldots, m && \text{(A.2c)} \\ & h_i(x) = 0 && i = 1, \ldots, p, && \text{(A.2d)} \end{aligned}$$

is exactly equivalent to (A.1), even though f_0 is now a constraint. Formulation (A.2) is called the *epigraph form* of problem (A.1). The mathematical properties of functions $f_0, \{f_i\}_{i=1,\ldots,n}, \{h_i\}_{i=1,\ldots,p}$ and the resulting feasible set, determine possible approaches to find an optimal solution. Ideally, the problem is *convex*

To set up a discussion on convex optimization, we first require some definitions of convexity in a more general sense.

Definition A.1 (Convex Set). *A set $\mathcal{C}$ is called* convex *if for any two points $x_1, x_2 \in \mathcal{C}$ and any $\theta \in [0, 1]$ the combination $\theta x_1 + (1-\theta)x_2 \in \mathcal{C}$.*

We call a combination $\theta_1 x_i + \ldots + \theta_k x_k$ of points $x_1, \ldots, x_k$ with $\theta_1 + \ldots + \theta_k = 1$ a *convex combination* and note that every convex set contains all convex combinations of all its elements.

Definition A.2 (Convex Hull)**.** *The* convex hull *of a set* $\mathcal{X}$*, i.e* $\operatorname{conv}(\mathcal{X})$*, is the set of all convex combinations in* $\mathcal{X}$*:*

$$\operatorname{conv}(\mathcal{X}) = \{\theta_1 x_i + \ldots + \theta_k x_k \mid x_i \in \mathcal{X},\ i=1,\ldots,k,\ \theta_1 + \ldots + \theta_k = 1\}.$$

For every convex set $\mathcal{C}$ we have $\mathcal{C} \equiv \operatorname{conv}(\mathcal{C})$ and for every non-convex set $\mathcal{X}$ we have $\mathcal{X} \subset \operatorname{conv}(\mathcal{X})$. We can now define

Definition A.3 (Convex Function)**.** *A function* $f : \mathbb{R}^n \to \mathbb{R}$ *is called* convex *if for all*[1] x_1, x_2 *with any* $\theta \in [0, 1]$ *we have*

$$f(\theta x_1 + (1-\theta)x_2) \leqslant \theta f(x_1) + (1-\theta) f(x_2).$$

The connection between convex sets and convex functions can be made through the epigraph $\operatorname{epi}(f)$ of function f.

Definition A.4 (Epigraph)**.** *The epigraph of a function* $f : \mathbb{R}^n \to \mathbb{R}$ *is*

$$\operatorname{epi}(f) = \{(x, t) \mid f(x) \leqslant t\}.$$

A function is convex if and only if its epigraph is a convex set. Further, assuming that f is differentiable[2], Definition A.3 implies that f is convex if and only if

$$f(x_2) \geqslant f(x_1) + \nabla f(x_1)^\top (x_2 - x_1). \tag{A.3}$$

See [198, Section 3.1.3] for the proof. If value $f(x_1)$ and gradient $\nabla f(x_1)$ of function f at point x_1 is known (local information) we can infer a relationship to the value of f at any other point x_2 (global information) through (A.3). This property enables most of the beneficial properties of convex optimization.

Definition A.5 (Convex Optimization)**.** *An optimization problem of the form* (A.1) *is called* convex *if the functions defining objective and inequality constraints* $f_0, \ldots, f_m$ *are convex and all functions defining equality constraints are affine, i.e.* $h_i(x) = a_i^\top x - b_i,\ i = 1, \ldots, p$.

Note that minimizing a convex objective f_0 is equivalent to maximizing the *concave*[3] objective $-f_0$.

Definition A.6 (Linear Optimization)**.** *A convex optimization problem is called* linear *if the functions defining objective and inequality constraints* $f_0, \ldots, f_m$ *are affine, i.e.* $f_i(x) = a_i^\top x - b_i,\ i = 0, \ldots, p$.

1 An explicit discussion of the *domains* is omitted given the limited impact on the required applications and the possibility of domain extension as $\tilde{f}(x) := \{f(x) \text{ if } x \in \operatorname{dom} f, \infty \text{ else}\}$.
2 As is assumed for all functions here throughout.
3 See Definition A.3, but reverse the inequality sign.

A.2 DUALITY AND OPTIMALITY

Property (A.3) of convex functions can be used to derive an optimality criterion based on the observation that any local minimum of convex f_0 will also be a global minimum: If $\nabla f_0(x_1) = 0$ for any x_1, then, given (A.3), $f_0(x_2) \geqslant f_0(x_1)$ for any x_2, thus identifying x_1 as a global minimizer. For a constrained optimization problem, however, the global minimizer of f_0 might not be an element of the problem's feasible set $\mathcal{X}$ and we get that $x_1 \in \mathcal{X}$ is optimal if and only if

$$\nabla f_0(x_1)^\top (x_2 - x_1) \geqslant 0 \qquad \forall x_2 \in \mathcal{X}. \tag{A.4}$$

See [198, Section 4.2.3] for the proof.

How to find such an optimal point is, however, unclear, which leads us to the introduction of *Lagrangian Duality*:

Definition A.7 (Lagrangian/Dual Function)**.** *Consider an optimization problem of the form* (A.1)*. Its* Lagrangian *is defined as:*

$$L(x, \lambda, \nu) \coloneqq f_0(x) + \sum_{i=1}^{m} \lambda_i f_i(x) + \sum_{i=1}^{p} \nu_i h_i(x),$$

and λ_i *and* ν_i *are called* Lagrangian multipliers *of their respective constraints and vectors* $\lambda = [\lambda_1, \ldots, \lambda_m]$ *and* $\nu = [\nu_1, \ldots, \nu_p]$ *are called* dual variables *of the optimization problem. The minimum of* L *over* x *is the defined as* Dual Function $g(\lambda, \nu)$*:*

$$g(\lambda, \nu) \coloneqq \min_x L(x, \lambda, \nu).$$

Notably, $g(\lambda, \nu)$ is an *unconstrained* optimization problem. Under condition $\lambda \geqslant 0$, dual function $g(\lambda, \nu)$ has the important property that it constitutes a lower bound for optimal value p^*, [198, Section 5.1.3]:

$$g(\lambda, \nu) \leqslant p^*. \tag{A.5}$$

Thus, the best lower bound on p^*, denoted d^*, is the optimal value of

$$\max_{\lambda,\nu} \quad g(\lambda, \nu) \tag{A.6a}$$

$$\text{s.t.} \quad \lambda \geqslant 0, \tag{A.6b}$$

which is called *dual problem* and is convex, even if (the so called *primal*) problem (A.1) is not, [198, Section 5.2]. Optimal value d^* of the dual problem is by definition the best lower bound of optimal value p^* and $d^* \leqslant p^*$ holds even for non-convex optimization problems. This property is called *weak duality*. If the primal problem is convex, and there exists a *strictly feasible point* x such that $f_i(x) < 0$, $i = 1, \ldots m$ and $h_i(x) = 0$, $i = 1, \ldots p$, also *strong duality* holds and $d^* = p^*$. This property is called *Slater's condition* and is extremely useful for finding (globally) optimal solutions, especially for numerical solvers: If $f_0(\tilde{x}) = g(\tilde{\lambda}, \tilde{\nu})$ for a set of candidate primal and dual points $\tilde{x}$ and $(\tilde{\lambda}, \tilde{\nu})$, then $\tilde{x}$ is primal optimal and $(\tilde{\lambda}, \tilde{\nu})$ is dual optimal. If $f_0(\tilde{x}) - g(\tilde{\lambda}, \tilde{\nu}) \leqslant \epsilon$, then it is guaranteed that the candidate solution is not more than ϵ suboptimal. Difference $f_0(\tilde{x}) - g(\tilde{\lambda}, \tilde{\nu})$ is called *duality gap*.

If strong duality can be assumed (e.g. when the problem of interest is convex and Slater's condition holds) we find the following important property:

Definition A.8 (Complementary Slackness)**.** *Given an optimization problem of the form* (A.1) *and assuming strong duality, for any primal optimal* x^* *and dual optimal* (λ^*, ν^*) *it holds that, [198, Section 5.5.2]:*

$$\lambda_i^* f_i(x^*) = 0, \qquad\qquad i = 1, \dots, m,$$

i.e. all inequality constraints and their dual multipliers are connected under complementary slackness *such that*

$$f_i(x^*) < 0 \;\Rightarrow\; \lambda_i^* = 0 \qquad\qquad \lambda_i^* > 0 \;\Rightarrow\; f_i(x^*) = 0.$$

Finally, we observe that for any primal optimal x^* and dual optimal (λ^*, ν^*) the (unconstrained) Lagrangian $L(x^*, \lambda^*, \nu^*)$ is minimized as per Definition A.7 so that

$$\nabla L(x^*, \lambda^*, \nu^*) = 0.$$

Definition A.9 (KKT Conditions)**.** *Given an optimization problem of the form* (A.1) *and assuming strong duality, the following* KKT-conditions *hold for any primal and dual optimal points* $x^*, (\lambda^*, \nu^*)$*:*

$$\begin{aligned} \nabla f_0(x^*) + \sum_{i=1}^{m} \lambda_i^* \nabla f_i(x^*) + \sum_{i=1}^{p} \nu_i \nabla h_i(x^*) = 0& \\ f_i(x^*) \leqslant 0,\; \lambda_i^* \geqslant 0,\; \lambda_i^* f_i(x^*) = 0& \quad i = 1, \dots, m \\ h_i(x^*) = 0& \quad i = 1, \dots, p. \end{aligned}$$

If the primal problem is convex, then the KKT-conditions are also sufficient, [198, Section 5.5.3], i.e. any $x, (\lambda, \nu)$ that fulfill the KKT-conditions are optimal with zero duality gap.

A.3 ADDITIONAL NOTES ON CONIC OPTIMIZATION

Conic programming constrains some decision variables of an optimization problem to be an element of one or more conic sets.

Definition A.10 (Cone, Convex Cone, Proper Cone, Dual Cone)**.** *A set* $\mathcal{C}$ *is called a* cone *if for every* $x \in \mathcal{C}$ *and* $\theta \geqslant 0$ *we have* $\theta x \in \mathcal{C}$*. If* $\mathcal{C}$ *is additionally convex it is a* convex cone *and for any* $x_1, x_2 \in \mathcal{C}$ *and* $\theta_1, \theta_2 \geqslant 0$ *we have* $\theta_1 x_1 + \theta_2 x_2 \in \mathcal{C}$*. A cone* $\mathcal{C}$ *is called* proper *if it is convex, closed, has a non-empty interior and is pointed, i.e. contains no line. The set* $\mathcal{C}^* = \{y \mid x^\top y \geqslant 0 \forall x \in \mathcal{C}\}$ *is called the* dual cone *of a cone* $\mathcal{C}$*.*

All cones that are of interest for this dissertation are proper. Proper cones allow the definition of the generalized inequality:

$$x \preceq_{\mathcal{C}} y \quad \Leftrightarrow \quad y - x \in \mathcal{C}. \tag{A.7}$$

Using (A.7) Problem (A.1) can be generalized by writing the inequality constraints in (A.1b) as

$$f_i(x) \preceq_{\mathcal{C}} 0, \qquad i = 1, \ldots, m, \tag{A.8}$$

which is equivalent to requiring $-f_i(x) \in \mathcal{C}$. Notably, all properties and concepts that have been derived in Section A.2 remain valid in the context of generalized inequality constraints with the exception that the non-negativity of dual λ_i also needs to be required in terms of a generalized inequality, $\lambda_i \succeq_{\mathcal{C}^*} 0$, [198, Section 5.9]. It follows that for any convex optimization problem with conic constraints of the form (A.8) (and especially any linear problem with conic constraints) the KKT conditions as in Definition A.9 are sufficient to identify the primal and dual optimal points $x^*, (\lambda^*, \nu^*)$.

Many non-linear or initially non-convex constraints can be expressed as conic constraints, see [177]. The remainder of this section briefly introduces quadratic cones as they are the most important for the formulations in this dissertation. Let $x \in \mathbb{R}^n$ be itemized as $x = [x_1, \ldots x_n]$ and we define:

Definition A.11 (Quadratic Cone/Second-Order Cone)**.** *The* $(1+n)$*-dimensional* quadratic cone *(or* second-order cone*) is defined as*

$$\begin{aligned} \mathcal{Q}^{1+n} &:= \left\{(t, x) \in \mathbb{R}^{1+n} \mid t \geqslant \sqrt{x_1^2 + \ldots + x_n^2}\right\} \\ &= \left\{(t, x) \in \mathbb{R}^{1+n} \mid t \geqslant \|x\|_2\right\}. \end{aligned}$$

Definition A.12 (Rotated Quadratic Cone)**.** *The* $(2+n)$*-dimensional* rotated quadratic cone *is defined as*

$$\begin{aligned} \mathcal{Q}_r^{2+n} &:= \left\{(t, h, x) \in \mathbb{R}^{2+n} \mid 2th \geqslant x_1^2 + \ldots + x_n^2,\ t, h \geqslant 0\right\} \\ &= \left\{(t, h, x) \in \mathbb{R}^{2+n} \mid 2th \geqslant \|x\|_2^2,\ t, h \geqslant 0\right\} \end{aligned}$$

Using Definitions A.11 and A.12, we find the following important reformulations (for an exhaustive list of conic reformulations of constraints see [177]).

SECOND-ORDER CONE CONSTRAINT A constraint on decision variable $x \in \mathbb{R}^n$ of the form

$$\|Ax + b\| \leqslant c^\top x + d, \tag{A.9}$$

with parameter matrix $A \in \mathbb{R}^{\times}$ and parameter vector $c \in \mathbb{R}^n$ is called *second-order cone constraint*. Using Definition A.11 and introducing auxiliary variables $t \in \mathbb{R}^m$ and $h \in \mathbb{R}$, constraint (A.9) is equivalent to the set of constraints

$$t = Ax + b \tag{A.10a}$$
$$h = c^\top x + d \tag{A.10b}$$
$$(t, h) \in \mathcal{Q}^{m+1}. \tag{A.10c}$$

Constraints (A.10a) and (A.10b) are affine and constraint (A.10c) is conic convex. Therefore, if the remainder of the problem is convex, the KKT-conditions can be applied.

CONVEX QUADRATIC SET Consider the quadratic constraint on decision variables $x \in \mathbb{R}^n$ and $t \in \mathbb{R}$ of the form

$$\frac{1}{2}x^\top Qx + c^\top x \leqslant t, \tag{A.11}$$

with positive semidefinite parameter matrix $Q \in \mathbb{R}^{n \times n}$ and parameter vector $c \in \mathbb{R}^n$. First, because Q is positive semidefinite, $x^\top Qx$ is a convex set and allows the following epigraph form of (A.11):

$$h + c^\top x \leqslant t \tag{A.12a}$$
$$x^\top Qx \leqslant 2h. \tag{A.12b}$$

Second, due to Q being positive semidefinite there exists a decomposition $Q = (Q^{1/2})^\top (Q^{1/2})$ that allows the following reformulation of (A.12b) based on Definition A.12:

$$(t, 1, (Q^{1/2})x) \in \mathcal{Q}_r^{2+n}. \tag{A.13}$$

Enforcing (A.12a) and (A.13) is equivalent to enforcing (A.11).

B A PRIMER ON (OPTIMAL) POWER FLOW

This chapter recalls some fundamentals of modeling power flows and shows the derivation of the standard power flow equations, their connection to OPF, as well as their common approximations and relaxations used in transmission and distribution system analyses. As outlined in Section 1.2, the scope of this dissertation is restricted to balanced system operation in a steady state. The derivations in this chapter reflect this restriction and mostly follow the logic of [8], [50]. The derivations in Section B.4 are adapted from [50] and those in Section B.5 follow [185].

B.1 COMPLEX POWER INJECTIONS

With very few exceptions, power systems rely on power transmission via AC, meaning that the functions describing the temporal evolution of current and voltages, $i(t)$ and $v(t)$, respectively, are *harmonic* functions characterized by their spectrum of magnitudes and frequencies. In steady state, these functions can be assumed *sinusoidal* with frequency ω (typically 50 or 60 Hz).[1] Thus, the voltage $v_k(t)$ at bus k and the current $i_k(t)$ injected into the system at bus k can be written as:

$$v_k(t) = V_k^{\max}\cos(\omega t + \theta_k^V), \quad i_k(t) = I_k^{\max}\cos(\omega t + \theta_k^V), \tag{B.1}$$

where $V_k^{\max}$ and $I_k^{\max}$ are constant[2] *amplitudes* of voltage and current, respectively, and θ_k^V and θ_k^I are the voltage and current *phases* (or phase angles). The resulting *instantaneous power* $p_k(t)$ injected at bus i is

$$\begin{aligned} p_k(t) = v_k(t)i_k(t) &= V_k^{\max}I_k^{\max}\cos(\omega t + \theta_k^V)\cos(\omega t + \theta_k^I) \\ &= \frac{1}{2}V_k^{\max}I_k^{\max}\cos(\theta_k^V - \theta_k^I) + \cos(2\omega t + \theta_k^V + \theta_k^I), \end{aligned} \tag{B.2}$$

and the resulting *average power* p_k over one period $2\pi/\omega$ is

$$p_k = \frac{\omega}{2\pi}\int_0^{2\pi/\omega} p_k(t) = \frac{1}{2}V_k^{\max}I_k^{\max}\cos(\theta_k^V - \theta_k^I). \tag{B.3}$$

1 Note that the angular frequency and its common notation ω is only used in this chapter. In all other chapter ω refers to uncertainty.

2 In steady state the amplitudes can be considered constant. To capture dynamics and state transitions, time-depended amplitudes have to be modeled. See e.g. [51] for more details.

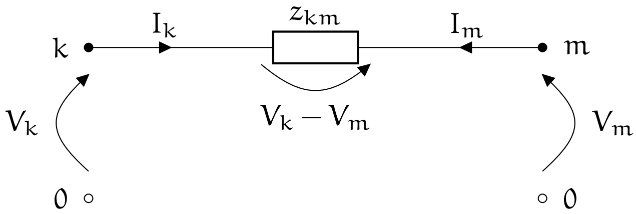

Figure B.1: Power flow over a complex impedance.

The harmonic properties of $v_k(t)$ and $i_k(t)$ allow a more compact expression in terms of (effective) *phasors*. Recalling Euler's identity $e^{\pm j\theta} = \cos\theta \pm j\sin\theta$, where $j := \sqrt{-1}$ (to avoid confusion with the notation for current), we can write $v(t)$ and $i(t)$ as

$$v_k(t) = V_k^{max}\Re(e^{j(\omega t+\theta_k^V)}) = \Re(V_k^{max}e^{j\theta_k^V}e^{j\omega t}) \tag{B.4}$$

$$i_k(t) = I_k^{max}\Re(e^{j(\omega t+\theta_k^I)}) = \Re(I_k^{max}e^{j\theta_k^I}e^{j\omega t}), \tag{B.5}$$

where $\Re(e^{j\theta}) = \cos(\theta)$, i.e. the real part of the exponential function. We define the effective voltage and current phasors at bus k as

$$V_k = \frac{V_k^{max}}{\sqrt{2}}e^{j\theta_k^V}, \quad I_k = \frac{I_k^{max}}{\sqrt{2}}e^{j\theta_k^I}, \tag{B.6}$$

where $e^{j\omega t}$, i.e. information on (constant) frequency and time have been dropped. Using (B.6) we can now express average power p_k as defined in (B.3) as:

$$\begin{aligned} p_k &= \frac{V_k^{max}}{\sqrt{2}}\frac{I_k^{max}}{\sqrt{2}}\cos(\theta_k^V - \theta_k^I) \\ &= |V_k||I_k|\cos(\theta_k^V - \theta_k^I) \\ &= \Re(V_k I_k^*), \end{aligned} \tag{B.7}$$

where the asterisk * denotes the complex conjugate. We call $p_k = \Re(V_k I_k^*)$ *active power*. Further, equation (B.7) suggests the definition of the quantities

$$q_k = \Im(V_k I_k^*) = |V_k||I_k|\sin(\theta_k^V - \theta_k^I), \tag{B.8}$$

where $\Im(e^{j\theta}) = \cos(\theta)$, i.e. the imaginary part of the exponential function, and

$$s_k = p_K + jq_k = V_k I_k^*, \tag{B.9}$$

i.e. the complex number composed from p_k and q_k. We call q_k *reactive power* and s_k *apparent power*. Phase difference $\theta_k^V - \theta_k^I$ is typically denoted ϕ_k, and $\cos\phi_k$, as in (B.7), is called the *power factor* at bus k. Notably, if $\theta_k^V - \theta_k^I = \phi_k = 0$ then $\cos\phi_k = 1$ and $S_k = p_k$, i.e. at unity power factor bus k only injects active power into the system.

Consider the simple circuit in Figure B.1. The (complex AC) current $I_k = -I_m$ flowing from k to m is related to the (complex AC) voltage difference $V_k - V_m$ through the complex *impedance* z_{km}, which is defined in terms of its real and imaginary parts:

$$z_{km} = r_{km} + jx_{km}. \tag{B.10}$$

We call r_{km} and x_{km} *resistance* and *reactance*, respectively. It holds that

$$V_k - V_m = z_{km} I_k. \tag{B.11}$$

The inverse $\frac{1}{z_{km}} = y_{km}$ is called *admittance* and it holds that:

$$I_k = y_{km}(V_k - V_m), \tag{B.12}$$

and

$$\begin{aligned} y_{km} = \frac{1}{z_{km}} &= \frac{r_{km}}{r_{km}^2 - x_{km}^2} + j\frac{-x_{km}}{r_{km}^2 + x_{km}^2} \\ &= g_{km} + jb_{km}, \end{aligned} \tag{B.13}$$

where we call g_{km} and b_{km} *conductance* and *susceptance*.

Box 3 – On missing phases.

All derivations in this section rely on single phase representations of all parts of the studied power system. Notably, AC power is generated and transmitted on *three-phases* that are ideally *balanced*. The (balanced) three-phase system ensures a more efficient power transmission and reduces the necessary amount of conducting material, e.g. by avoiding the use of a neutral conductor, [8].

For any three phase signal (e.g. voltage or current) in a balanced three-phase AC systems it holds that the components on each phase only differ by a phase angle shift of $\frac{2\pi}{3}$ (120 degree). Therefore, for any balanced three-phase signal $x_{abc}(t)$ we have:

$$x_{abc}(t) = \begin{bmatrix} x_a(t) \\ x_b(t) \\ x_c(t) \end{bmatrix} = X^{max} \begin{bmatrix} \cos(\omega t) \\ \cos(\omega t - \frac{2\pi}{3}) \\ \cos(\omega t + \frac{2\pi}{3}) \end{bmatrix}.$$

Notably, $x_{abc}(t)$ is fully defined by its amplitude X^{max} and frequency ω, allowing us to only consider one phase in all derivations of such a system.

B.2 POWER FLOW EQUATIONS

Consider a power system with n buses collected in set $\mathcal{N}$ connected by l lines collected in set $\mathcal{L}$. The electrical characteristics of (non-transforming) transmission equipment (e.g. overhead transmission lines) between two busses $k \in \mathcal{N}$ and $m \in \mathcal{N}$ can be modeled using the Π-*model* as shown in Figure B.2. In addition to the (series) impedance $z_{km} = 1/y_{km}$ the model is endowed with the *shunt admittance* $y_{km}^{sh} =$

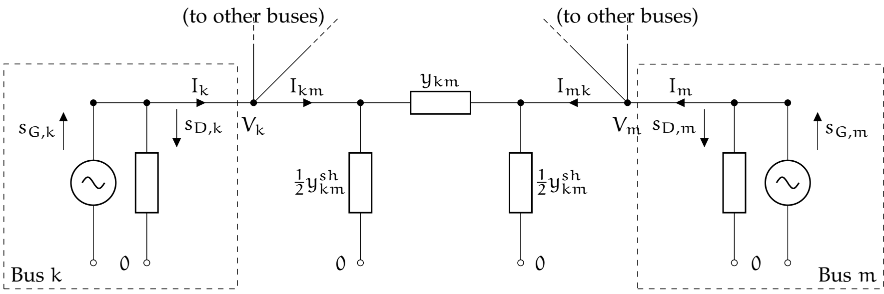

Figure B.2: Non-transforming Π-model of bus interconnection.

$g^{sh}_{km} + jb^{sh}_{km}$. The impedance mainly captures the branches inductive characteristics and, in fact, resistance r_{km} is typically an order of magnitude smaller than reactance x_{km} and ignored in some models, see Section B.4. The shunt admittance mainly captures capcitative effects and typically b^{sh}_{km} dominates g^{sh}_{km}.

Consider the schematic in Figure B.2. Here, for every bus $k \in \mathcal{N}$ we differentiate between the net power injection $s_k = s_{G,k} - s_{D,k}$, i.e. generation minus load, carried by current I_k at voltage V_k, and currents I_{km} flowing over the branch between k and any other bus $m \in \mathcal{N}_k$, where $\mathcal{N}_k$ is the set of all buses connected to bus k. For all $k \in \mathcal{N}$ and $km : m \in \mathcal{N}_k$ current I_{km} satisfies

$$I_{km} = y_{km}(V_k - V_m) + \frac{1}{2}y^{sh}_{km}V_k, \tag{B.14}$$

and

$$I_k = \sum_{km:m\in\mathcal{N}_k} I_{km}. \tag{B.15}$$

Let vectors $I = [I_k,\ k \in \mathcal{N}]^\top \in \mathbb{C}^n$ and $V = [V_k,\ k \in \mathcal{N}]^\top \in \mathbb{C}^n$ collect the (complex) current injections and voltages of all buses. Using (B.14) and (B.15) we can construct a *bus admittance matrix* $Y \in \mathbb{C}^{n\times n}$ so that

$$I = YV, \text{ and } I_k = \sum_{m\in\mathcal{N}} Y_{km}V_m. \tag{B.16}$$

Matrix Y with elements Y_{km} is constructed as

$$Y_{km} = \begin{cases} \sum_{ko:o\in\mathcal{N}_k} y_{ko} + \frac{1}{2}y^{sh}_{ko}, & \text{if } m = k \\ -y_{km}, & \text{if } m \in \mathcal{N}_k \\ 0, & \text{else.} \end{cases} \tag{B.17}$$

From $Y \in \mathbb{C}^n$ follows the possible decomposition

$$Y = G + jB \tag{B.18}$$

with $G \in \mathbb{R}^n$ and $B \in \mathbb{R}^n$.

We can now create a useful and compact formulation. First, we define $v_k := |V_k|$ and $\theta_{km} = \theta_k - \theta_m$ (where we have dropped the V superscript) for more concise notation and to obtain consistency with the main text of this dissertation. Next, using (B.9) and (B.16), power s_k injected by bus k is given as

$$\begin{aligned} s_k &= V_k I_k^* = V_k \Big(\sum_{m \in \mathcal{N}} Y_{km} V_m \Big)^* = V_k \sum_{m \in \mathcal{N}} Y_{km}^* V_m^* \\ &= \sum_{m \in \mathcal{N}} v_k v_m (\cos\theta_{km} + j \sin\theta_{km})(G_{km} - jB_{km}), \end{aligned} \tag{B.19}$$

from which we get

$$p_k = \Re(s_k) = \sum_{m \in \mathcal{N}} v_k v_m (G_{km} \cos\theta_{km} + B_{km} \sin\theta_{km}) \tag{B.20}$$

$$q_k = \Im(s_k) = \sum_{m \in \mathcal{N}} v_k v_m (G_{km} \sin\theta_{km} - B_{km} \cos\theta_{km}). \tag{B.21}$$

For power flow analysis it is useful to decompose (B.20) and (B.21) into power flow and injection components such that:

$$f^p_{km} = v_k v_m (G_{km} \cos\theta_{km} + B_{km} \sin\theta_{km}) \tag{B.22a}$$

$$f^q_{km} = v_k v_m (G_{km} \sin\theta_{km} - B_{km} \cos\theta_{km}) \tag{B.22b}$$

$$p_k = v_k^2 G_{kk} + \sum_{km: m \in \mathcal{N}_k} f^p_{km} \tag{B.22c}$$

$$q_k = -v_k^2 B_{kk} + \sum_{km: m \in \mathcal{N}_k} f^q_{km}, \tag{B.22d}$$

where f^p_{km} and f^q_{km} denote the active and reactive power injected by bus k into line km. Equations (B.22) are referred to as the *(AC) power flow equations*. Notably, $f^p_{km} \neq -f^p_{mk}$ and $f^q_{km} \neq -f^q_{mk}$. The differences $f^p_{km} + f^p_{mk}$ and $f^q_{km} + f^q_{mk}$ capture the active and reactive *power losses* in the system.

Remark B.1. (Including transformer branches) A transformer between k and m with admittance y^{tx}_{km} and a normalized turn ratio of $a : 1$, $a \geqslant 0$, such that current I_{km} and voltage V_k are transformed to aI_{km} and $\frac{1}{a}V_k$, can be modeled in terms of the Π-model setting the shunt admittance at bus k to $\frac{1-a}{a^2} y^{tx}_{km}$, the series admittance $\frac{1}{a} y^{tx}_{km}$, and the shunt admittance at bus m to $\frac{a-1}{a} y^{tx}_{km}$. See [8, Example 9.3] or, for more detailed model derivations, [50, Appendix B].

B.3 THE POWER FLOW PROBLEM AND OPTIMAL POWER FLOW

The *power flow problem* summarizes the task of finding a solution to (B.22) for given injections from generation and loads, as well as voltage requirements. The *optimal power flow (OPF) problem* extends the power flow problem to finding the *optimal* decision of available (constrained) decision variables, such as generation and voltage levels, that solve (B.22).

Each bus is described by its active and reactive net injection, $p_k = p_{G,k} - p_{D,k}$ and $q_k = q_{G,k} - q_{D,k}$, as well as its voltage magnitude and angle, v_k and θ_k, i.e. a set of four variables or parameters. However, for each bus there are only two independent equations in (B.22). To render the problem well-defined, each bus is assigned a type:

- At "PV" buses, active power injection and voltage magnitudes are fixed as parameters, i.e. are considered *controlled*. PV buses are typically busses with connected generators.
- At "PQ" buses, active and reactive power injections are fixed. PQ buses are typically load busses.
- Finally, the reference bus, or θV bus, has fixed voltage angle (typically zero) and magnitude. The θV accounts for the fact that (B.22) rely on voltage *differences* and compensate for power losses in the system (which are unknown before the solution of the problem.)

Power flow equations (B.22) are non-linear and non-convex. While the power flow problem can be solved efficiently with iterative approaches such as the Newton-Raphson method, [8], or more advanced algorithms, e.g. [206], ACOPF requires additional effort to ensure optimality and feasibility. For many practical purposes (B.22) can be approximated, e.g. via linearization or neglecting weak couplings between active power and voltage magnitudes, and reactive power and voltage angles, or replaced with a convex relaxation, e.g. second-order conic or semidefinite, [167], [207], [208]. The remainder of this chapter shows two common modifications of the power flow equations for OPF analyses in transmission (Section B.4) and distribution (Section B.5) systems.

B.4 DC POWER FLOW APPROXIMATION

In high-voltage transmission systems, the electrical properties of any transmission line km is typically dominated by its reactance x_{km} and, thus, resistance r_{km} as well as shunt admittance y^{sh}_{km} can be neglected. Further, under normal operating conditions, $v_k \approx 1$ p.u., i.e. all voltage magnitudes are very close to the nominal system voltage, and voltage angle differences $|\theta_{km}|$ for all connection k to m are small. (See Box 4 for a brief description of the unit p.u.) This gives the following set of approximations, [S3], [7], [44]:

$$r_{km} \approx 0, \quad y^{sh}_{km} \approx 0 \tag{B.23a}$$
$$v_k v_m \approx 1 \tag{B.23b}$$
$$\sin\theta_{km} \approx \theta_{km}, \quad \cos\theta_{km} \approx 0. \tag{B.23c}$$

Using (B.23) we get for active power injections and flows from (B.22)

$$f^p_{km} = B_{km}\theta_{km} = B_{km}(\theta_k - \theta_m) \tag{B.24a}$$

$$p_k = \sum_{km:m\in\mathcal{N}_k} f^p_{km}. \tag{B.24b}$$

Equations (B.24) are typically called *DC power flow equations* because the linear relation (B.24a) is loosely reminiscent of Ohm's law for DC circuits. Note that using (B.23) on reactive power flows and injections from (B.22) eliminates them and they are ignored in the DC power flow formulation. Also, due to $r_{km} \approx 0$ active power losses are not accounted for and $f^p_{km} = f^p_{mk}$ for all $km \in \mathcal{N}$.

For all B_{km} in (B.24) we now have:

$$B_{km} = \begin{cases} \sum_{ko:o\in\mathcal{N}_k} \frac{1}{x_{ko}}, & \text{if } m = k \\ -\frac{1}{x_{km}}, & \text{if } m \in \mathcal{N}_k \\ 0, & \text{else,} \end{cases} \tag{B.25}$$

and matrix B is called *bus susceptance matrix*. The vector of active power injections $p = [p_k,\ k \in \mathcal{N}]^\top \in \mathbb{R}^n$ and the vector of voltage angles $\theta = [\theta_k,\ k \in \mathcal{N}]^\top \in \mathbb{R}^n$ are now related via the *linear* relationship

$$p = B\theta. \tag{B.26}$$

A similar formulation can be found for the vector of active power flows $f^p = [f_{km},\ km \in \mathcal{L}] \in \mathbb{R}^l$. Let $A \in \{-1, 0, 1\}^{l\times n}$ be the arc-node incidence matrix of the arbitrarily oriented graph $\Gamma(\mathcal{N}, \mathcal{L})$ describing the studied network, such that all entries A_{km} are zero except $A_{km} = 1$ and $A_{mk} = -1$ if there exits an arc (line) between nodes (buses) k and m that is pointing from k to m. Further, let $b = [b_{km},\ km \in \mathcal{L}] \in \mathbb{R}^l$ be the vector of line susceptances, then we can write

$$f^p = \operatorname{diag}(b)A\theta = B^{(f)}\theta, \tag{B.27}$$

where $B^{(f)} := \operatorname{diag}(b)A$ is the so called *line susceptance matrix*. Note that $B = A^\top \operatorname{diag}(b)A$. Denoting $B = B^{(n)}$ for clarity, we can now formulate the linear DCOPF problem as used in Section 3.2 on page 33.

Vector p of active power injections and vector f^p of active power flows are directly connected through vector θ of voltage angles as per (B.26) and (B.27) so that $f^P = B^{(f)}(B^{(n)})^{-1}p$. However, because (B.26) and (B.27) rely on voltage angle *differences* matrix $B^{(n)}$ is not directly invertible. Instead, we need to define a reference (or "slack" bus, see also Section B.3) with fixed voltage angles. Without loss of generality we choose the index of the slack node to be $i_{\text{slack}} = 1$. This allows the following definition of a pseudo-inverse $\hat{B}^{(n)}$ of $B^{(n)}$ as

$$\hat{B}^{(n)} := \begin{bmatrix} 0 & 0 \\ 0 & \left(\tilde{B}^{(n)}\right)^{-1} \end{bmatrix}, \tag{B.28}$$

where $\tilde{B}^{(n)} \in \mathbb{S}^{N-1}$ is the bus susceptance matrix without the row and column associated with the slack bus (first row and first column in our case). We can now write

$$f^P = B^{(f)}\hat{B}^{(n)}p =: B^{(p)}p, \tag{B.29}$$

where we call $B^{(p)}$ the *power transfer distribution factor (PTDF) matrix*.

Box 4 – On the per-unit system

Power system analyses commonly applies the so called per-unit system to relate parameter and variable values to a fixed base value. Typical base quantities are base (apparent) power s^{base} and base voltage (magnitude) V^{base}. Base power s^{base} is used to scale power flows, generator outputs and loads (i.e. all power related quantities) and is fixed throughout the system. Base voltage V^{base}, in analogy, scales voltage related quantities and is fixed throughout the same voltage level of the system. Other base quantities that are used to scale current, impedance and susceptance can be obtained from s^{base} and V^{base}:

$$\begin{aligned} I^{\text{base}} &= \frac{s^{\text{base}}}{V^{\text{base}}} \\ z^{\text{base}} &= \frac{V^{\text{base}}}{I^{\text{base}}} = \frac{(V^{\text{base}})^2}{s^{\text{base}}} \\ y^{\text{base}} &= \frac{1}{Z^{\text{base}}}. \end{aligned}$$

All base quantities have the value of 1 p.u.:

$$s^{\text{base}} = V^{\text{base}} = I^{\text{base}} = z^{\text{base}} = y^{\text{base}} = 1\,\text{p.u.}.$$

The per unit value of real quantities can be obtained as:

$$a^{\text{p.u.}} = \frac{a^{\text{real}}}{a^{\text{base}}}.$$

The per-unit system has various advantages. It avoids explicit calculations of voltage and current on either side of transformers, it allows an immediate intuition of whether or not the system is operating at nominal values and it enables the DC approximation where we use $V_k V_m \approx 1$ p.u..

B.5 BRANCH FLOW AND LINDISTFLOW

The so called *branch flow model* is an approximation of the AC power flow equations for *radial* networks and has initially been introduced in [115], [209]. A network is called radial if the network graph $\Gamma(\mathcal{N}, \mathcal{L})$ is a tree. Further, without loss of generality we define Γ as a directed graph such that all arcs are pointing away from the root node, indexed as 0, and we call this direction *downstream*, see Figure B.5. Because Γ is a tree, each node $k \neq 0$ has exactly one parent node $\mathcal{A}_k$ and a, potentially empty, set of children nodes $\mathcal{C}_k$.

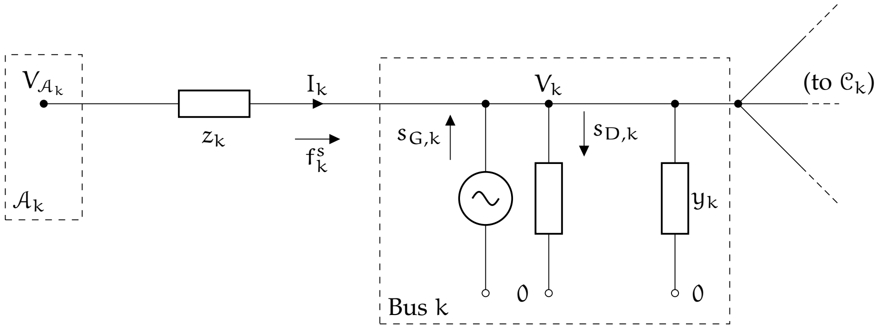

Figure B.3: Branch flow model notations

B.5.1 *Branch Flow and Relaxations*

While we maintain the line model introduced in Figure B.2 above, we slightly change its notation as shown in Figure B.3. First we note that each line from k to m is uniquely defined by its downstream node and we can resort to using a single index $k \in \mathcal{N}^+$, where $\mathcal{N}^+ = \mathcal{N} \setminus \{0\}$, to define line-specific variables (flow, current, impedance). Next, with each line $k \in \mathcal{N}^+$ we only associate its series impedance $z_k = r_k + jx_k$. Shunt admittance $y_k = g_k + b_k$ is attributed to the network's *buses*. We drop the sh superscript and note that shunt admittance is always expressed as admittances and series impedance is always expressed as impedance.

Introducing f^s_k as the apparent power flowing *into* bus k, see Figure B.3, we can set up the *branch flow equations* directly as:

$$V_{\mathcal{A}_k} - V_k = z_k I_k \tag{B.30a}$$
$$f^s_k = V_k I^*_k \tag{B.30b}$$
$$f^s_k + s_k = \sum_{m \in \mathcal{C}_k} (f^s_m + z_m i^2_m) + y_k v^2_k. \tag{B.30c}$$

Equation (B.30c) sets the power balance for each node including line losses $I_m(V_k - V_m) = z_m i^2_m$ and shunt losses $y_k v^2_k$. We now define $u_k = v^2_k$ and $l_k = i^2_k$ to simplify notations. From (B.30a) and (B.30b) and noting that $u_{\mathcal{A}_k} = |V_{\mathcal{A}_k}|^2 = V_{\mathcal{A}_k} V^*_{\mathcal{A}_k}$ we get

$$\begin{aligned} & V_{\mathcal{A}_k} = V_k + z_k I_k = V_k + z_k \frac{f^s_k}{V_k} \\ \Rightarrow \quad & u_{\mathcal{A}_k} = u_k + |z_k|^2 l_k + (z_k f^*_k + z^*_k f_k). \end{aligned} \tag{B.31}$$

Next, by noting that (B.30b) implies $|f^s_k|^2 = |V_k|^2 |I_k|^2$ and splitting (B.30c) into its active and reactive components, we obtain the *relaxed branch flow equations*

$$f^p_k + p_k = \sum_{m \in \mathcal{C}_k} (f^p_m + r_m l_m) + g_k u_k \tag{B.32a}$$

$$f_k^q + q_k = \sum_{m \in \mathcal{C}_k} (f_m^q + x_m l_m) + b_k u_k \tag{B.32b}$$

$$u_{\mathcal{A}_k} = u_k + 2(r_k f_k^p + x_k f_k^q) + (r_k^2 + x_k^2) l_k \tag{B.32c}$$

$$l_k = \frac{(f_k^p)^2 + (f_k^q)^2}{u_k}. \tag{B.32d}$$

Equations (B.32) are dubbed "relaxed" due to the elimination of any dependence from current or voltage phase angles, thus relaxing points to circles on the convex plane. However, the resulting solution allows the recovery of voltage angles and thus the recovery of the solution to the original problem in (B.30b), [167].

From an OPF perspective, the only non-linear equation (constraint) in (B.32) is (B.32d). The equality (B.32d) can be relaxed to an inequality such that

$$l_k \geqslant \frac{(f_k^p)^2 + (f_k^q)^2}{u_k}. \tag{B.33}$$

If used as a constraint in an OPF problem, (B.33) can be formulated as the following *convex* SOC constraint

$$l_k + v_k \geqslant \left\| [2f_k^p, 2f_q^p, l_k - v_k] \right\|_2. \tag{B.34}$$

(See Appendix A.3 for more information on second-order cones.) This relaxed constraint has been shown to be tight in the optimal solution of an radial OPF and thus provides an optimal solution to the original branch flow model, [167]. A OPF formulation for a radial distribution grid using the SOC relaxed branch flow model is presented in Section 6.2.2 on page 95.

B.5.2 *LinDistFlow*

The so called LinDistFlow model is a common linear approximation of the relaxed branch flow model (B.32). We obtain this approximation by dropping terms related to losses so that (i) $y_k \approx 0$, (ii) $|z_k|^2 \approx 0$, and (iii) $r_m l_m \approx 0$, $x_m l_m \approx 0$. As a result, active and reactive power flows are decoupled and current square l_k can be removed from the set of equations. The resulting *LinDistFlow equations* are thus given as

$$f_k^p + p_k = \sum_{m \in \mathcal{C}_k} f_m^p \tag{B.35a}$$

$$f_k^q + q_k = \sum_{m \in \mathcal{C}_k} f_m^q \tag{B.35b}$$

$$u_{\mathcal{A}_k} = u_k + 2(r_k f_k^p + x_k f_k^q). \tag{B.35c}$$

These linear equations are the basis for the CC-OPF formulations for radial systems as presented in Chapters 4,5 and 6.

C A PRIMER ON (ELECTRICITY) MARKET THEORY

This chapter recalls some fundamentals of (micro)economic theory in the context of electricity markets and derives the marginal-cost-based pricing concept. The derivations of this chapter mainly follow [34], [117], [118]. An interesting discussion on electricity markets from the perspective of control theory is given in [40]. This chapter relies on some concepts of convex optimization introduced in Appendix A.

To not exceed the scope of this dissertation, this chapter does not provide a discussion of the fundamental philosophy of market-based coordination or the underlying assumptions of economic theory. The author recommends [210].

C.1 PRODUCER DECISIONS

We first introduce the concept of marginal cost and establish a relation to prices in a competitive market. Then, we discuss other cost components and short- and long-run profits.

Proposition C.1 (Marginal Cost). *Let $c_i(p_{G,i})$ be the cost function of a generator i describing the cost for operating at production level $p_{G,i}$ and let π^p be the payment (price) for each produced unit $p_{G,i}$ which is independent of $p_{G,i}$ (i.e. generator i is a* price-taker*). The optimal (profit maximizing) production level $p^*_{G,i}$ is attained when the* marginal cost *of production $\frac{\partial c_i(p_{G,i})}{\partial p_{G,i}}$ are equal to price π^p, i.e.:*

$$\frac{\partial c_i(p^*_{G,i})}{\partial p_{G,i}} = \pi^p. \tag{C.1}$$

Proof. If π^p is fixed, the only decision variable of generator i is $p_{G,i}$. The profit maximization problem is thus given as

$$p^*_{G,i} = \arg\max_{p_{G,i}} (\pi^p p_{G,i} - c_i(p_{G,i})). \tag{C.2}$$

Equation (C.2) can be solved as:

$$\frac{\partial}{\partial p_{G,i}} (\pi^p p_{G,i} - c_i(p_{G,i})) = 0, \tag{C.3}$$

which immediately leads to the result in (C.1). □

Corollary C.1 (Upper Production Limits). *Consider Proposition C.1. If optimal production $p^*_{G,i}$ given price π^p is larger than the generators capacity $p^{max}_{G,i}$, then price π^p is equal to the generators marginal cost $\left.\frac{\partial c_i(p_{G,i})}{\partial p_{G,i}}\right|_{p_{G,i}=p^{max}_{G,i}}$ plus a margin δ_i that is the shadow price of the capacity constraint.*

Proof. The capacity-constrained profit maximization problem of generator i with respect to price π^p is given as

$$\max_{p_{G,i}} \quad \pi^p p_{G,i} - c_i(p_{G,i}) \tag{C.4a}$$

$$\text{s.t.}$$

$$(\delta_i): \quad p_{G,i} \leqslant p_{G,i}^{max}, \tag{C.4b}$$

where δ_i is the Lagrangian dual multiplier (see Appendix A) of constraint (C.4b). The Lagrangian function of (C.4) is

$$\mathcal{L}_i(p_{G,i}, \delta_i) = -(\pi^p p_{G,i} - c_i(p_{G,i}) + \delta_i^+(p_{G,i} - p_{G,i}^{max}). \tag{C.5}$$

From solving $\frac{\partial}{\partial p_{G,i}}\mathcal{L} = 0$ we obtain

$$\pi^p = \frac{\partial c(p_{G,i})}{\partial p_{G,i}} + \delta_i^+. \tag{C.6}$$

If constraint (C.4b) is binding, then $\delta_i^+ > 0$ and (C.6) is the result of Corollary C.1; Otherwise we recover the result of Proposition C.1 □

Multiplier δ_i captures the value of an additional unit from this generator if it could extend its capacity. This term is referred to as *scarcity rent*, because it describes payments made to this generator beyond its marginal cost due to its, scarcity, [118]. This term, however, is unique to power system economics and has no rigorous counterpart in microeconomics.

Corollary C.2 (Lower Production Limits)**.** *Consider Proposition C.1. If optimal production $p_{G,i}^*$ given price π^p is lower than the generators minimum generation capacity $p_{G,i}^{min}$, then the generator will not produce.*

Proof. If $p_{G,i}^{min} = 0$, then proof is analogous to Corollary C.1. If $p_{G,i}^{min} > 0$ we nee to add a binary option $u_i \in \{0, 1\}$ of not producing:

$$\max_{p_{G,i}} \quad u_i(\pi^p p_{G,i} - c_i(p_{G,i})) \tag{C.7a}$$

$$\text{s.t.}$$

$$(\delta_i): \quad u_i p_{G,i}^{min} \leqslant p_{G,i}. \tag{C.7b}$$

$$u_i \in \{0, 1\}. \tag{C.7c}$$

If $\pi^p < \frac{\partial c_i(p_{G,i})}{\partial p_{G,i}}\Big|_{p_{G,i}=p_{G,i}^{min}}$, then the maximum profit is 0 with $u_i = 0$. Otherwise we recover the result of Proposition C.1. □

If a generator produces at marginal cost and does not receive a scarcity rent, it is called *marginal unit*. In this case, payment $\pi^p p_{G,i}$ will cover immediate *variable cost*, e.g. fuel. *Fixed cost*, e.g. capital cost, that occur even when the generator is not in use, are recovered over time on average in a competitive market, because time dependent price fluctuations will create sufficient scarcity rents, [118, Sections

1-5.3, 2–2]. Additionally, production at marginal cost is a *short-run* profit optimization strategy, i.e. the generator cost function is fixed and cost depend only on the chosen level of production. In the *long-run*, the generator might be able to alter the parametrization of its cost-function, e.g. by investments in new equipment, supply-chain adaptations or leaving the market.

C.2 COMPETITIVE EQUILIBRIUM

If a market is competitive, i.e. no individual participant can execute market power to influence the price, all participants are profit-maximizing and share necessary information, then there exists a *competitive equilibrium* in which supply meets demand and the price equals the marginal cost of production. The existence of this "equilibrium" implies the existence of some form of "dynamics". These dynamics are related to price and quantity adjustments that lead to an *efficient* market clearing, [118, Section 1-5]. Quantity adjustments refer to the profit-maximizing behavior of price taking producers derived in Section C.1 above. If the price is higher than the marginal cost, generators will increase production and vice versa. Price adjustments occur at quantity mismatches. If demand exceeds supply producers will increase their asking price and vice versa.

When all market participants can observe market prices and traded quantities, a sequence of quantity and price adjustments will eventually reach an equilibrium state as shown in the classic supply-and-demand graphic in Figure C.1. The red graph plots the *aggregated* profit-maximizing production level of all generators in the market, i.e. their marginal cost. The blue graph plots the total demand p_D as a function of the price. If demand is inelastic it resembles a vertical line and thus fixes the required production quantity. At equilibrium all marginal units have the same marginal cost, i.e. there are no saving opportunities by reducing the production of one generator and increasing the production of another, thus rendering it efficient [118, Section 1-5].

Aggregated scarcity rents, i.e. differences between marginal production cost and price π^p, are called *producer surplus* and are shown as the striped area in Figure C.1. The aggregated differences between price π^p and the customers' willingness to pay are called *consumer surplus* and are shown as the dotted area in Figure C.1. The sum of producer and customer surplus is called *social welfare*. The market is efficient when welfare is maximized. If demand is fixed and inelastic, consumer surplus is infinite (or can not be reasonably defined). In this case, the market is efficient if it maximizes producer surplus, which is identical to minimizing production cost because producers with lowers marginal cost will produce "first".

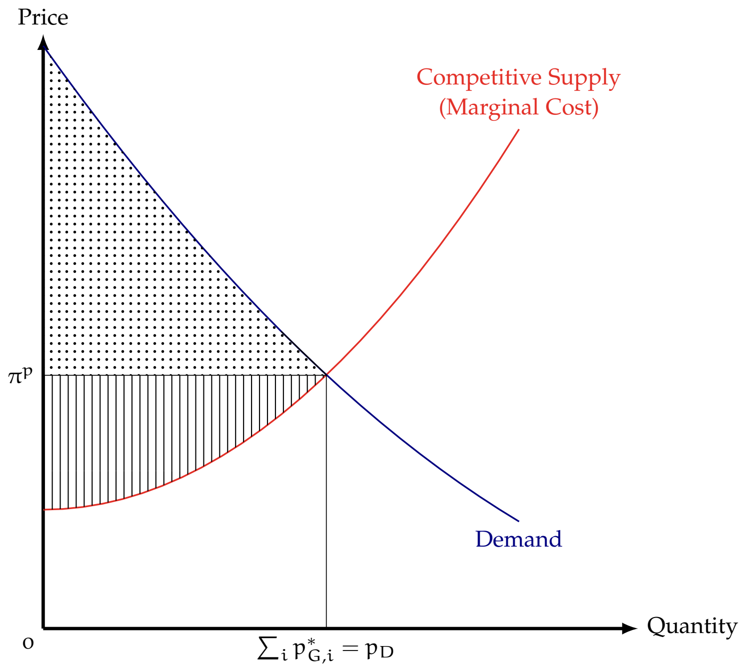

Figure C.1: Competitive Equilibrium. Dotted area is consumer surplus, striped area is producer surplus.

In theory, the competitive equilibrium will occur "naturally" from free trading between producers and consumers. In practice, supply and demand is settled in some form of institutional context. Heavily regulated electricity markets are centrally manged by a market operator and typically implement complex auction processes, [S6], [34], [118]. Thus, the remaining sections of this chapter show how prices that yield a competitive equilibrium can be obtained from a cost minimization problem and what effect physical system requirements have on the resulting prices.

C.3 MARGINAL PRICING

Consider an electricity market that is centrally cleared by a market operator, who collects bids from producers in the form of cost functions c_i, $i \in \mathcal{G}$ and production limits $p_{G,i}^{\max}$ and seeks to minimize the cost to supply demand p_D. If all cost functions are convex, the following proposition holds. A brief discussion on non-convex markets is provided in Box 5.

Proposition C.2 (System Marginal Pricing). *Consider a convex market clearing problem of the form*

$$\min \sum_{i \in \mathcal{G}} c_i(p_{G,i}) \tag{C.8a}$$

s.t.

$$(\lambda): \quad \sum_{i \in \mathcal{G}} p_{i,G} = p_D \tag{C.8b}$$

$$(\delta^+): \quad p_{i,G} \leqslant p_{G,i}^{max} \qquad \forall i \in \mathcal{G}. \tag{C.8c}$$

Let $(\{p_{G,i}^*, \delta_i^{+*}\}_{i \in \mathcal{G}}, \lambda^*)$ *be the primal-dual optimal solution to* (C.8). *Then* λ^* *and* $\sum_{i \in \mathcal{G}} p_{G,i}^*$ *are the price and quantity corresponding to the competitive equilibrium of this market.*

Proof. The Lagrangian function of (C.8) is:

$$\mathcal{L} = \sum_{i \in \mathcal{G}} c_i(p_{G,i}) + \lambda(p_D - \sum_{i \in \mathcal{G}} p_{G,i}) + \sum_{i \in \mathcal{G}} (\delta_i^+ - p_{G,i}^{max}). \tag{C.9}$$

Solving

$$\frac{\partial \mathcal{L}}{\partial p_{G,i}} = 0 \tag{C.10}$$

for all $i \in \mathcal{G}$ leads to

$$\lambda^* = \left. \frac{\partial c_i(p_{G,i})}{\partial p_{G,i}} \right|_{p_{G,i} = p_{G,i}^*} + \delta_i^+ \qquad \forall i \in \mathcal{G}. \tag{C.11}$$

The result in (C.11) recovers the optimal producer decision of Corollary C.1 exactly when we set $\pi^p = \lambda^*$. Thus, when all producers are confronted with price $\pi^p = \lambda^*$, their optimal production $p_{G,i}^*$ satisfies $\sum_{i \in \mathcal{G}} p_{G,i}^* = p_D$ as per (C.8b), and their marginal cost of production is equal to π^p. We can now show that requirements of a competitive equilibrium are met:

1. The market is *cleared* as per (C.8b).
2. The market is cleared efficiently, i.e. at minimal cost, as per (C.8a).
3. Generators produce such that the price equals their marginal cost of production plus a scarcity rent, as per (C.11), i.e. the price is *incentive compatible* and producers will bid truthfully.

□

The price obtained as dual of the market clearing constraint (C.8b) is called *system marginal price*.

Box 5 – On non-convexities.

System and locational marginal pricing through dual multipliers requires a convex optimization problem that allows to invoke the KKT optimality conditions as discussed in Appendix A. Two sources of non-convexities that often arise in electricity markets are binary decision variables and non-convex power flow equations.

Binary decision variables arise when generator cost functions and physical limits require considerations of their *status* to capture, e.g. no-load cost, minimum generation levels, start-up or shut-down cost. (An OPF problem that includes binary variables to account for the on- or off-states of generators is typically called *unit commitment problem*.) The AC power flow equations are non-convex per se and require some effort to allow a feasible solution in an optimization problem, see Appendix B.

To enable marginal pricing, these non-convexities have to be mitigated via convex approximations, relaxations or reformulations. A common technique involves a two-stage solution process that first solves the non-convex problem ("dispatch run") and then uses the solution as a basis for the second "pricing run" by either fixing the optimal binary variables, [88], or linearizing the problem around the first stage solution, [193],[P4].

If no suitable convexification is possible, out-of-market uplift payments to ensure cost recovery or revenue adequacy may be necessary,[211], [212].

C.4 LOCATIONAL MARGINAL PRICES

A theory on how to establish an efficient market clearing mechanisms in the context of a power network with physical constraints was proposed in the 1988 edition of [120] as *locational marginal prices (LMPs)*. Consider a power network with a set of nodes (buses) $\mathcal{N}$. To simplify notations assume that each bus $i \in \mathcal{N}$ hosts a generator with cost function c_i and generation limit $p_{G,i}^{\max}$ and has a total load of $p_{D,i}$. The buses are connected by a set of arbitrarily oriented arcs (lines) $\mathcal{L}$ and the power flow f_l^p, $\forall l \in \mathcal{L}$ is determined by a linear mapping such that $f_l^p = \sum_{i\in\mathcal{N}} B_{li}(p_{G,i} - p_{D_i})$. (This linear mapping is derived from the DC power flow equations as shown in Appendix B.) Each line $l \in \mathcal{L}$ is characterized by a maximum capacity $f_l^{p,\max}$.

Proposition C.3. *(Locational Marginal Pricing) Consider the convex market clearing problem from Proposition C.2 with the additional requirement, that the physical power flow does not exceed feasible transmission limits:*

$$\min \quad \sum_{i\in\mathcal{G}} c_i(p_{G,i}) \tag{C.12a}$$

s.t.

$$(\lambda): \quad \sum_{i\in\mathcal{N}} p_{G,i} = \sum_{i\in\mathcal{N}} p_{D,i} \tag{C.12b}$$

$$(\mu_l^-, \mu_l^+): \quad -f_l^{p,\max} \leqslant \sum_{i\in\mathcal{N}} B_{li}(p_{G,i} - p_{D,i}) \leqslant f_l^{p,\max} \quad \forall l \in \mathcal{L} \tag{C.12c}$$

$$(\delta^+): \quad p_{i,G} \leqslant p_{G,i}^{\max} \quad \forall i \in \mathcal{G}. \tag{C.12d}$$

Let $(\{p_{G,i}^*, \lambda_i^*, \delta_i^{+*}\}_{i\in\mathcal{N}}, \{\mu_l^{+*}, \mu_l^{-*}\}_{l\in\mathcal{L}})$ *be the primal-dual optimal solution to* (C.12) *and define* $\lambda_i^* := \lambda - \sum_{l\in\mathcal{L}} B_{li}(\mu_l^{+*} - \mu_l^{-*})$, $\forall i \in \mathcal{N}$. *Then* $\{\lambda_i^*\}_{i\in\mathcal{N}}$ *and* $\{p_{G,i}^*\}_{i\in\mathcal{N}}$ *are sets of prices and quantities that constitute a competitive equilibrium.*

Proof. The Lagrangian function of (C.12) is:

$$\begin{aligned}\mathcal{L} = &\sum_{i\in\mathcal{G}} c_i(p_{G,i}) + \lambda(p_D - \sum_{i\in\mathcal{N}} p_{G,i}) + \sum_{i\in\mathcal{N}} (\delta_i^+ - p_{G,i}^{\max}) \\ &+ \sum_{l\in\mathcal{L}} \mu_l^+ (\sum_{i\in\mathcal{N}} B_{li}(p_{G,i} - p_{D,i}) - f_l^{\max}) \\ &+ \sum_{l\in\mathcal{L}} \mu_l^- (f_l^{\max} - \sum_{i\in\mathcal{N}} B_{li}(p_{G,i} - p_{D,i}))\end{aligned} \tag{C.13}$$

Solving

$$\frac{\partial \mathcal{L}}{\partial p_{G,i}} = 0 \tag{C.14}$$

for all $i \in \mathcal{G}$ leads to

$$\lambda^* - \sum_{l\in\mathcal{L}} B_{li}(\mu_l^{+*} - \mu_l^{-*}) = \left.\frac{\partial c_i(p_{G,i})}{\partial p_{G,i}}\right|_{p_{G,i}=p^*_{G,i}} + \delta_i^+ \quad \forall i \in \mathcal{G}. \tag{C.15}$$

The result in (C.15) recovers the optimal producer decision of Corollary C.1 exactly when we set $\pi_i^p = \lambda_i^* = \lambda^* - \sum_{l\in\mathcal{L}} B_{li}(\mu_l^{+*} - \mu_l^{-*})$. Thus, when all producers are confronted with price $\pi_i^p = \lambda_i^*$, their optimal production $p^*_{G,i}$ satisfies (C.12b) and (C.12c), and their marginal cost of production is equal to π_i^p. This meets the requirements of a competitive equilibrium as shown in the proof of Proposition C.2. □

Problem (C.12) is a DCOPF problem (see Appendix B) and prices $\{\lambda_i^*\}_{i\in\mathcal{N}}$ are called *locational marginal price*. Note that λ_i^* depends on duals (μ_l^+, μ_l^-) of transmission capacity constraint (C.12c). If $\mu_i^+ = \mu_i^- = 0$, $\forall l \in \mathcal{L}\}$, i.e. transmission limits are not restrictive to the solution of (C.12), then $\lambda_i^* = \lambda^*$, $\forall i \in \mathcal{N}$.

BIBLIOGRAPHY

References [P1]–[P5] and [S1]–[S6] are listed in the author's bibliography on page vii.

[1] H.-p. Chao, S. Oren, and R. Wilson, «Reevaluation of vertical integration and unbundling in restructured electricity markets,» in *Competitive electricity markets*, Elsevier, 2008, pp. 27–64 (cit. on pp. 3, 7, 19).

[2] E. Van der Vleuten and V. Lagendijk, «Transnational infrastructure vulnerability: The historical shaping of the 2006 European "Blackout",» *Energy Policy*, vol. 38, no. 4, pp. 2042–2052, 2010 (cit. on p. 3).

[3] Y. Tang, G. Bu, and J. Yi, «Analysis and lessons of the blackout in Indian power grid on July 30 and 31, 2012,» in *Zhongguo Dianji Gongcheng Xuebao(Proceedings of the Chinese Society of Electrical Engineering)*, Chinese Society for Electrical Engineering, vol. 32, 2012, pp. 167–174 (cit. on p. 3).

[4] D. Griggs, M. Stafford-Smith, O. Gaffney, *et al.*, «Sustainable development goals for people and planet,» *Nature*, vol. 495, no. 7441, pp. 305–307, 2013 (cit. on p. 3).

[5] F. Frei, A. Loder, and C. R. Bening, «Liquidity in green power markets–An international review,» *Renewable and Sustainable Energy Reviews*, vol. 93, pp. 674–690, 2018 (cit. on p. 3).

[6] F. D. Munoz, B. F. Hobbs, J. L. Ho, *et al.*, «An engineering-economic approach to transmission planning under market and regulatory uncertainties: WECC case study,» *IEEE Transactions on Power Systems*, vol. 29, no. 1, pp. 307–317, 2013 (cit. on p. 3).

[7] D. Bienstock, M. Chertkov, and S. Harnett, «Chance-constrained optimal power flow: Risk-aware network control under uncertainty,» *Siam Review*, vol. 56, no. 3, pp. 461–495, 2014 (cit. on pp. 3, 7, 12, 14, 16, 17, 25, 31–35, 51–53, 68, 89, 91, 115, 164).

[8] A. R. Bergen, *Power systems analysis*. Pearson Education India, 2009 (cit. on pp. 3, 7, 11–13, 19, 33, 159, 161, 163, 164).

[9] Y. Dvorkin, «A chance-constrained stochastic electricity market,» *IEEE Transactions on Power Systems*, vol. 35, no. 4, pp. 2993–3003, 2020 (cit. on pp. 4, 7, 8, 20, 22, 23, 25, 26, 32, 89–91, 115–118, 129, 130, 132, 133).

[10] P. Jahangiri and D. C. Aliprantis, «Distributed Volt/VAr control by PV inverters,» *IEEE Transactions on power systems*, vol. 28, no. 3, pp. 3429–3439, 2013 (cit. on p. 5).

[11] P. M. Carvalho, P. F. Correia, and L. A. Ferreira, «Distributed reactive power generation control for voltage rise mitigation in distribution networks,» *IEEE transactions on Power Systems*, vol. 23, no. 2, pp. 766–772, 2008 (cit. on p. 5).

[12] M. Caramanis, E. Ntakou, W. W. Hogan, *et al.*, «Co-optimization of power and reserves in dynamic T&D power markets with distributed energy resources,» *Proceedings of the IEEE*, vol. 104, no. 4, pp. 807–836, 2016 (cit. on pp. 5, 6, 19, 21, 24, 89, 91).

[13] P. Andrianesis and M. Caramanis, «Distribution Network Marginal Costs: Enhanced AC OPF Including Transformer Degradation,» *IEEE Transactions on Smart Grid*, vol. 11, no. 5, pp. 3910–3920, 2020. DOI: 10.1109/TSG.2020.2980538 (cit. on p. 5).

[14] C. Liu, K. Chau, D. Wu, *et al.*, «Opportunities and challenges of vehicle-to-home, vehicle-to-vehicle, and vehicle-to-grid technologies,» *Proceedings of the IEEE*, vol. 101, no. 11, pp. 2409–2427, 2013 (cit. on p. 5).

[15] Y. Dvorkin, R. Fernandez-Blanco, D. S. Kirschen, *et al.*, «Ensuring profitability of energy storage,» *IEEE Transactions on Power Systems*, vol. 32, no. 1, pp. 611–623, 2016 (cit. on p. 5).

[16] S. W. Alnaser and L. F. Ochoa, «Optimal sizing and control of energy storage in wind power-rich distribution networks,» *IEEE Transactions on Power Systems*, vol. 31, no. 3, pp. 2004–2013, 2015 (cit. on p. 5).

[17] Y. V. Makarov, P. Du, M. C. Kintner-Meyer, *et al.*, «Sizing energy storage to accommodate high penetration of variable energy resources,» *IEEE Transactions on sustainable Energy*, vol. 3, no. 1, pp. 34–40, 2011 (cit. on p. 5).

[18] A. Oudalov, R. Cherkaoui, and A. Beguin, «Sizing and optimal operation of battery energy storage system for peak shaving application,» in *2007 IEEE Lausanne Power Tech*, IEEE, 2007, pp. 621–625 (cit. on p. 5).

[19] E. Dall'Anese, S. V. Dhople, B. B. Johnson, *et al.*, «Decentralized optimal dispatch of photovoltaic inverters in residential distribution systems,» *IEEE Transactions on Energy Conversion*, vol. 29, no. 4, pp. 957–967, 2014 (cit. on p. 5).

[20] W. Lin and E. Bitar, «Decentralized stochastic control of distributed energy resources,» *IEEE Transactions on Power Systems*, vol. 33, no. 1, pp. 888–900, 2017 (cit. on pp. 5, 92).

[21] M. Farivar, R. Neal, C. Clarke, *et al.*, «Optimal inverter VAR control in distribution systems with high PV penetration,» in *2012 IEEE Power and Energy Society general meeting*, IEEE, 2012, pp. 1–7 (cit. on p. 5).

[22] P. Šulc, S. Backhaus, and M. Chertkov, «Optimal distributed control of reactive power via the alternating direction method of multipliers,» *IEEE Transactions on Energy Conversion*, vol. 29, no. 4, pp. 968–977, 2014 (cit. on p. 5).

[23] R. Li, Q. Wu, and S. S. Oren, «Distribution locational marginal pricing for optimal electric vehicle charging management,» *IEEE Transactions on Power Systems*, vol. 29, no. 1, pp. 203–211, 2014 (cit. on pp. 5, 24, 89, 90).

[24] US DOE, «Benefits of demand response in electricity markets and recommendations for achieving them,» *Tech. Rep*, 2006 (cit. on pp. 6, 61).

[25] P. Siano, «Demand response and smart grids—A survey,» *Renewable and sustainable energy reviews*, vol. 30, pp. 461–478, 2014 (cit. on pp. 6, 61).

[26] S. Koch, J. L. Mathieu, and D. S. Callaway, «Modeling and control of aggregated heterogeneous thermostatically controlled loads for ancillary services,» in *Proc. PSCC*, Citeseer, 2011, pp. 1–7 (cit. on p. 6).

[27] ConEd, conedsmartac.com (cit. on pp. 6, 61).

[28] F. E. R. C. (FERC). (2017). «Assessment of Demand Response and Advance Metering,» [Online]. Available: ferc.gov/legal/staff-reports/2017/DR-AM-Report2017.pdf (cit. on pp. 6, 61, 66).

[29] S. Acharya, Y. Dvorkin, H. Pandžić, *et al.*, «Cybersecurity of Smart Electric Vehicle Charging: A Power Grid Perspective,» *IEEE Access*, 2020 (cit. on p. 6).

[30] N. Tucker, A. Moradipari, and M. Alizadeh, «Constrained thompson sampling for real-time electricity pricing with grid reliability constraints,» *IEEE Transactions on Smart Grid*, vol. 11, no. 6, pp. 4971–4983, 2020 (cit. on p. 6).

[31] P. Li, H. Wang, and B. Zhang, «A distributed online pricing strategy for demand response programs,» *IEEE Transactions on Smart Grid*, vol. 10, no. 1, pp. 350–360, 2017 (cit. on pp. 6, 25, 62, 63, 75, 81).

[32] K. Khezeli and E. Bitar, «Risk-sensitive learning and pricing for demand response,» *IEEE Transactions on Smart Grid*, vol. 9, no. 6, pp. 6000–6007, 2017 (cit. on pp. 6, 25, 62, 63, 65, 82).

[33] B. Wealer, S. Bauer, L. Göke, *et al.*, «High-priced and dangerous: Nuclear power is not an option for the climate-friendly energy mix,» *DIW Weekly Report*, vol. 9, no. 30, pp. 235–243, 2019 (cit. on p. 7).

[34] D. S. Kirschen and G. Strbac, *Fundamentals of power system economics*. John Wiley & Sons, 2018 (cit. on pp. 7, 19, 20, 34, 169, 172).

[35] R. H. Wiser and M. Bolinger, «2018 Wind Technologies Market Report,» 2019 (cit. on p. 7).

[36] IEA, «Renewable energy market update,» IEA, Tech. Rep., 2020. [Online]. Available: www.iea.org/reports/renewable-energy-market-update (cit. on p. 7).

[37] F. Capitanescu, J. M. Ramos, P. Panciatici, *et al.*, «State-of-the-art, challenges, and future trends in security constrained optimal power flow,» *Electric Power Systems Research*, vol. 81, no. 8, pp. 1731–1741, 2011 (cit. on p. 7).

[38] B. F. Hobbs and S. S. Oren, «Three waves of US reforms: Following the path of wholesale electricity market restructuring,» *IEEE Power and Energy Magazine*, vol. 17, no. 1, pp. 73–81, 2019 (cit. on pp. 7, 8, 21, 22).

[39] P. Joskow and J. Tirole, «Reliability and competitive electricity markets,» *The Rand Journal of Economics*, vol. 38, no. 1, pp. 60–84, 2007 (cit. on p. 7).

[40] G. Wang, A. Kowli, M. Negrete-Pincetic, *et al.*, «A control theorist's perspective on dynamic competitive equilibria in electricity markets,» *IFAC Proceedings Volumes*, vol. 44, no. 1, pp. 4933–4938, 2011 (cit. on pp. 8, 169).

[41] J. L. Sweeney, «The California electricity crisis: Lessons for the future,» *Bridge*, vol. 32, no. 2, pp. 23–31, 2002 (cit. on p. 8).

[42] J. C. Smith, S. Beuning, H. Durrwachter, *et al.*, «The wind at our backs,» *IEEE Power and Energy magazine*, vol. 8, no. 5, pp. 63–71, 2010 (cit. on p. 8).

[43] J. Kazempour, P. Pinson, and B. F. Hobbs, «A stochastic market design with revenue adequacy and cost recovery by scenario,» *IEEE Transactions on Power Systems*, vol. 33, no. 4, pp. 3531–3545, 2018 (cit. on pp. 8, 14, 20–23, 89–91, 115, 116, 130).

[44] A. J. Wood, B. F. Wollenberg, and G. B. Sheblé, *Power generation, operation, and control*. John Wiley & Sons, 2013 (cit. on pp. 11–13, 17, 32, 164).

[45] B. Stott and E. Hobson, «Power system security control calculations using linear programming, Part I,» *IEEE Transactions on Power Apparatus and Systems*, no. 5, pp. 1713–1720, 1978 (cit. on p. 11).

[46] B. Stott and E. Hobson, «Power system security control calculations using linear programming, Part II,» *IEEE Transactions on Power Apparatus and Systems*, no. 5, pp. 1721–1731, 1978 (cit. on p. 11).

[47] J. Carpentier, «Optimal power flows,» *International Journal of Electrical Power & Energy Systems*, vol. 1, no. 1, pp. 3–15, 1979 (cit. on p. 11).

[48] S. Wang, S. Shahidehpour, D. S. Kirschen, *et al.*, «Short-term generation scheduling with transmission and environmental constraints using an augmented Lagrangian relaxation,» *IEEE Transactions on Power Systems*, vol. 10, no. 3, pp. 1294–1301, 1995 (cit. on p. 11).

[49] E. Dall'Anese and A. Simonetto, «Optimal power flow pursuit,» *IEEE Transactions on Smart Grid*, vol. 9, no. 2, pp. 942–952, 2016 (cit. on p. 11).

[50] D. Bienstock, *Electrical transmission system cascades and vulnerability: an operations research viewpoint*. SIAM, 2015 (cit. on pp. 11, 12, 35, 159, 163).

[51] P. Kundur, N. J. Balu, and M. G. Lauby, *Power system stability and control*. McGraw-hill New York, 1994, vol. 7 (cit. on pp. 12, 33, 159).

[52] B. Xu, Y. Dvorkin, D. S. Kirschen, *et al.*, «A comparison of policies on the participation of storage in US frequency regulation markets,» in *2016 IEEE Power and Energy Society General Meeting (PESGM)*, IEEE, 2016, pp. 1–5 (cit. on p. 12).

[53] M. Paolone, T. Gaunt, X. Guillaud, *et al.*, «Fundamentals of power systems modelling in the presence of converter-interfaced generation,» *Electric Power Systems Research*, vol. 189, p. 106 811, 2020 (cit. on p. 12).

[54] F. Milano, F. Dörfler, G. Hug, *et al.*, «Foundations and challenges of low-inertia systems,» in *2018 Power Systems Computation Conference (PSCC)*, IEEE, 2018, pp. 1–25 (cit. on p. 12).

[55] J. Fang, Y. Tang, H. Li, *et al.*, «The role of power electronics in future low inertia power systems,» in *2018 IEEE International Power Electronics and Application Conference and Exposition (PEAC)*, IEEE, 2018, pp. 1–6 (cit. on p. 12).

[56] Y. G. Rebours, D. S. Kirschen, M. Trotignon, *et al.*, «A survey of frequency and voltage control ancillary services—Part I: Technical features,» *IEEE Transactions on power systems*, vol. 22, no. 1, pp. 350–357, 2007 (cit. on pp. 12, 13).

[57] Y. G. Rebours, D. S. Kirschen, M. Trotignon, *et al.*, «A survey of frequency and voltage control ancillary services—Part II: Economic features,» *IEEE Transactions on power systems*, vol. 22, no. 1, pp. 358–366, 2007 (cit. on p. 12).

[58] N. G. Hingorani, «FACTS technology-state of the art, current challenges and the future prospects,» in *IEEE Power Engineering Society General Meeting*, vol. 2, 2007 (cit. on p. 12).

[59] W. H. Kersting, *Distribution system modeling and analysis*. CRC press, 2012 (cit. on p. 13).

[60] N. G. Singhal, N. Li, and K. W. Hedman, «A reserve response set model for systems with stochastic resources,» *IEEE Transactions on Power Systems*, vol. 33, no. 4, pp. 4038–4049, 2017 (cit. on pp. 13, 14).

[61] N. Li, N. Singhal, and K. Hedman, «An enhanced security-constrained unit commitment model with reserve response set policies,» in *Proceedings of the 50th Hawaii International Conference on System Sciences*, 2017 (cit. on p. 13).

[62] NYISO, *Manual 12 -Transmission and Dispatch Operations Manual*, 2020. [Online]. Available: `nyiso.com/manuals-tech-bulletins-user-guides` (cit. on p. 14).

[63] S. Sharma, «2019 Methodology for Determining Minimum Ancillary Service Requirements,» ERCOT, Tech. Rep., 2019. [Online]. Available: `www.ercot.com/` (cit. on pp. 14, 115).

[64] NREL, «Western Wind and Solar Integration Study, National Renewable Energy,» Tech. Rep., 2010. [Online]. Available: `www.nrel.gov` (cit. on pp. 14, 115).

[65] ENSTO-E, *Verfahren zur dynamischen Bestimmung des Bedarfs für Sekundärregel- und Minutenreserve*, 2018. [Online]. Available: `www.regelleistung.net/ext/tender/remark/news/345` (cit. on p. 14).

[66] D. Chattopadhyay and R. Baldick, «Unit commitment with probabilistic reserve,» in *2002 IEEE Power Engineering Society Winter Meeting. Conference Proceedings (Cat. No. 02CH37309)*, IEEE, vol. 1, 2002, pp. 280–285 (cit. on p. 14).

[67] A. Papavasiliou, S. S. Oren, and R. P. O'Neill, «Reserve requirements for wind power integration: A scenario-based stochastic programming framework,» *IEEE Transactions on Power Systems*, vol. 26, no. 4, pp. 2197–2206, 2011 (cit. on pp. 14, 20).

[68] M. Lubin, Y. Dvorkin, and L. Roald, «Chance constraints for improving the security of AC optimal power flow,» *IEEE Transactions on Power Systems*, vol. 34, no. 3, pp. 1908–1917, 2019 (cit. on pp. 14, 18, 25, 31, 32, 39, 40, 44, 52, 94, 115).

[69] E. Dall'Anese, K. Baker, and T. Summers, «Chance-constrained AC optimal power flow for distribution systems with renewables,» *IEEE Transactions on Power Systems*, vol. 32, no. 5, pp. 3427–3438, 2017 (cit. on pp. 14, 18, 19, 32, 53, 68, 89, 90).

[70] T. Yong and R. Lasseter, «Stochastic optimal power flow: formulation and solution,» in *2000 Power Engineering Society Summer Meeting*, IEEE, vol. 1, 2000, pp. 237–242 (cit. on p. 14).

[71] P. Carpentier, G. Gohen, J.-C. Culioli, *et al.*, «Stochastic optimization of unit commitment: a new decomposition framework,» *IEEE Transactions on Power Systems*, vol. 11, no. 2, pp. 1067–1073, 1996 (cit. on p. 14).

[72] J. M. Morales, A. J. Conejo, K. Liu, *et al.*, «Pricing electricity in pools with wind producers,» *IEEE Transactions on Power Systems*, vol. 27, no. 3, pp. 1366–1376, 2012 (cit. on pp. 14, 21, 23, 89, 90, 115, 116).

[73] S. Wong and J. D. Fuller, «Pricing energy and reserves using stochastic optimization in an alternative electricity market,» *IEEE Transactions on Power Systems*, vol. 22, no. 2, pp. 631–638, 2007 (cit. on pp. 14, 20–23, 89, 90, 115, 116, 130).

[74] L. Wu, M. Shahidehpour, and T. Li, «Stochastic security-constrained unit commitment,» *IEEE Transactions on power systems*, vol. 22, no. 2, pp. 800–811, 2007 (cit. on pp. 14, 15).

[75] L. Xie, P. M. Carvalho, L. A. Ferreira, *et al.*, «Wind integration in power systems: Operational challenges and possible solutions,» *Proceedings of the IEEE*, vol. 99, no. 1, pp. 214–232, 2010 (cit. on pp. 14, 15).

[76] Q. P. Zheng, J. Wang, and A. L. Liu, «Stochastic optimization for unit commitment—A review,» *IEEE Transactions on Power Systems*, vol. 30, no. 4, pp. 1913–1924, 2014 (cit. on pp. 14, 15).

[77] A. Tuohy, P. Meibom, E. Denny, *et al.*, «Unit commitment for systems with significant wind penetration,» *IEEE Transactions on power systems*, vol. 24, no. 2, pp. 592–601, 2009 (cit. on pp. 14, 15).

[78] P. A. Ruiz, C. R. Philbrick, E. Zak, *et al.*, «Uncertainty management in the unit commitment problem,» *IEEE Transactions on Power Systems*, vol. 24, no. 2, pp. 642–651, 2009 (cit. on pp. 14, 15).

[79] H. Pandžić, Y. Dvorkin, T. Qiu, *et al.*, «Toward cost-efficient and reliable unit commitment under uncertainty,» *IEEE Transactions on Power Systems*, vol. 31, no. 2, pp. 970–982, 2015 (cit. on pp. 14, 15).

[80] R. J. Wets *et al.*, «Stochastic programming,» *Handbooks in operations research and management science*, vol. 1, pp. 573–629, 1989 (cit. on p. 14).

[81] R. T. Rockafellar, «Coherent approaches to risk in optimization under uncertainty,» in *OR Tools and Applications*, Informs, 2007, pp. 38–61 (cit. on pp. 14, 24, 36, 129, 132, 133).

[82] A. Papavasiliou, S. S. Oren, and B. Rountree, «Applying high performance computing to transmission-constrained stochastic unit commitment for renewable energy integration,» *IEEE Transactions on Power Systems*, vol. 30, no. 3, pp. 1109–1120, 2014 (cit. on p. 15).

[83] J. M. Morales, S. Pineda, A. J. Conejo, *et al.*, «Scenario reduction for futures market trading in electricity markets,» *IEEE Transactions on Power Systems*, vol. 24, no. 2, pp. 878–888, 2009 (cit. on pp. 15, 22).

[84] J. Dupacová, N. Gröwe-Kuska, and W. Römisch, *Scenario reduction in stochastic programming: An approach using probability metrics*. Humboldt-Universität zu Berlin, Mathematisch-Naturwissenschaftliche Fakultät . . ., 2000 (cit. on p. 15).

[85] Y. Dvorkin, Y. Wang, H. Pandzic, *et al.*, «Comparison of scenario reduction techniques for the stochastic unit commitment,» in *2014 IEEE PES General Meeting | Conference & Exposition*, IEEE, 2014, pp. 1–5 (cit. on p. 15).

[86] L. Wu and M. Shahidehpour, «Accelerating the Benders decomposition for network-constrained unit commitment problems,» *Energy Systems*, vol. 1, no. 3, pp. 339–376, 2010 (cit. on p. 15).

[87] C. Zhao, J. Wang, J.-P. Watson, *et al.*, «Multi-stage robust unit commitment considering wind and demand response uncertainties,» *IEEE Transactions on Power Systems*, vol. 28, no. 3, pp. 2708–2717, 2013 (cit. on p. 15).

[88] R. P. O'Neill, P. M. Sotkiewicz, B. F. Hobbs, *et al.*, «Efficient market-clearing prices in markets with nonconvexities,» *European journal of operational research*, vol. 164, no. 1, pp. 269–285, 2005 (cit. on pp. 15, 174).

[89] R. A. Jabr, «Adjustable robust OPF with renewable energy sources,» *IEEE Transactions on Power Systems*, vol. 28, no. 4, pp. 4742–4751, 2013 (cit. on pp. 15, 17).

[90] P. Artzner, F. Delbaen, J.-M. Eber, *et al.*, «Coherent measures of risk,» *Mathematical finance*, vol. 9, no. 3, pp. 203–228, 1999 (cit. on pp. 16, 132).

[91] R. T. Rockafellar, S. Uryasev, *et al.*, «Optimization of conditional value-at-risk,» *Journal of risk*, vol. 2, pp. 21–42, 2000 (cit. on pp. 16, 36, 37).

[92] A. Charnes and W. W. Cooper, «Chance-constrained programming,» *Management science*, vol. 6, no. 1, pp. 73–79, 1959 (cit. on p. 16).

[93] B. L. Miller and H. M. Wagner, «Chance constrained programming with joint constraints,» *Operations Research*, vol. 13, no. 6, pp. 930–945, 1965 (cit. on p. 16).

[94] A. Prekopa, «On probabilistic constrained programming,» in *Proceedings of the Princeton symposium on mathematical programming*, Citeseer, vol. 113, 1970, p. 138 (cit. on p. 16).

[95] U. A. Ozturk, M. Mazumdar, and B. A. Norman, «A solution to the stochastic unit commitment problem using chance constrained programming,» *IEEE Transactions on Power Systems*, vol. 19, no. 3, pp. 1589–1598, 2004 (cit. on p. 16).

[96] H. Yu, C. Chung, K. Wong, *et al.*, «A chance constrained transmission network expansion planning method with consideration of load and wind farm uncertainties,» *IEEE Transactions on Power Systems*, vol. 24, no. 3, pp. 1568–1576, 2009 (cit. on p. 16).

[97] H. Zhang and P. Li, «Chance constrained programming for optimal power flow under uncertainty,» *IEEE Transactions on Power Systems*, vol. 26, no. 4, pp. 2417–2424, 2011 (cit. on p. 16).

[98] M. Vrakopoulou, J. L. Mathieu, and G. Andersson, «Stochastic optimal power flow with uncertain reserves from demand response,» in *2014 47th Hawaii International Conference on System Sciences*, IEEE, 2014, pp. 2353–2362 (cit. on p. 16).

[99] R. T. Rockafellar and S. Uryasev, «Conditional value-at-risk for general loss distributions,» *Journal of banking & finance*, vol. 26, no. 7, pp. 1443–1471, 2002 (cit. on p. 16).

[100] A. Nemirovski and A. Shapiro, «Convex approximations of chance constrained programs,» *SIAM Journal on Optimization*, vol. 17, no. 4, pp. 969–996, 2007 (cit. on p. 17).

[101] T. Summers, J. Warrington, M. Morari, *et al.*, «Stochastic optimal power flow based on convex approximations of chance constraints,» in *2014 Power Systems Computation Conference*, IEEE, 2014, pp. 1–7 (cit. on p. 17).

[102] L. Roald, S. Misra, T. Krause, *et al.*, «Corrective control to handle forecast uncertainty: A chance constrained optimal power flow,» *IEEE Transactions on Power Systems*, vol. 32, no. 2, pp. 1626–1637, 2016 (cit. on pp. 17, 31, 52, 115).

[103] L. Roald, S. Misra, M. Chertkov, *et al.*, «Optimal power flow with weighted chance constraints and general policies for generation control,» in *2015 54th IEEE conference on decision and control (CDC)*, IEEE, 2015, pp. 6927–6933 (cit. on pp. 17, 34).

[104] M. Carrión, Y. Dvorkin, and H. Pandžić, «Primary frequency response in capacity expansion with energy storage,» *IEEE Transactions on Power Systems*, vol. 33, no. 2, pp. 1824–1835, 2017 (cit. on p. 17).

[105] M. Lubin, Y. Dvorkin, and S. Backhaus, «A robust approach to chance constrained optimal power flow with renewable generation,» *IEEE Transactions on Power Systems*, vol. 31, no. 5, pp. 3840–3849, 2015 (cit. on pp. 17, 52).

[106] L. Roald, F. Oldewurtel, B. Van Parys, *et al.*, «Security constrained optimal power flow with distributionally robust chance constraints,» *arXiv preprint 1508.06061*, 2015 (cit. on pp. 17, 32, 52, 57, 91).

[107] Y. Zhang, S. Shen, and J. L. Mathieu, «Distributionally robust chance-constrained optimal power flow with uncertain renewables and uncertain reserves provided by loads,» *IEEE Transactions on Power Systems*, vol. 32, no. 2, pp. 1378–1388, 2016 (cit. on p. 18).

[108] K. Lehmann, A. Grastien, and P. Van Hentenryck, «AC-feasibility on tree networks is NP-hard,» *IEEE Transactions on Power Systems*, vol. 31, no. 1, pp. 798–801, 2015 (cit. on pp. 18, 62).

[109] M. Vrakopoulou, M. Katsampani, K. Margellos, *et al.*, «Probabilistic security-constrained AC optimal power flow,» in *2013 IEEE Grenoble Conference*, IEEE, 2013, pp. 1–6 (cit. on p. 18).

[110] X. Bai, L. Qu, and W. Qiao, «Robust AC optimal power flow for power networks with wind power generation,» *IEEE Transactions on Power Systems*, vol. 31, no. 5, pp. 4163–4164, 2015 (cit. on p. 18).

[111] R. Louca and E. Bitar, «Robust AC optimal power flow,» *IEEE Transactions on Power Systems*, vol. 34, no. 3, pp. 1669–1681, 2018 (cit. on p. 18).

[112] L. Roald and G. Andersson, «Chance-constrained AC optimal power flow: Reformulations and efficient algorithms,» *IEEE Transactions on Power Systems*, vol. 33, no. 3, pp. 2906–2918, 2017 (cit. on p. 18).

[113] M. Bragin, Y. Dvorkin, and A. Darvishi, «Toward coordinated transmission and distribution operations,» in *2018 IEEE Power & Energy Society General Meeting (PESGM)*, IEEE, 2018, pp. 1–5 (cit. on p. 18).

[114] C. W. Gellings, M. Samotyj, and B. Howe, «The future's smart delivery system [electric power supply],» *IEEE Power and Energy Magazine*, vol. 2, no. 5, pp. 40–48, 2004 (cit. on pp. 18, 51).

[115] M. E. Baran and F. F. Wu, «Optimal capacitor placement on radial distribution systems,» *IEEE Transactions on power Delivery*, vol. 4, no. 1, pp. 725–734, 1989 (cit. on pp. 19, 166).

[116] K. Turitsyn, P. Sulc, S. Backhaus, *et al.*, «Options for control of reactive power by distributed photovoltaic generators,» *Proceedings of the IEEE*, vol. 99, no. 6, pp. 1063–1073, 2011 (cit. on p. 19).

[117] S. Bose and S. H. Low, «Some emerging challenges in electricity markets,» in *Smart Grid Control*, Springer, 2019, pp. 29–45 (cit. on pp. 19, 20, 22, 129, 169).

[118] S. Stoft, *Power System Economics: Designing Markets for Electricity*, 1st. Wiley-IEEE Press, 2002, ISBN: 0471150401 (cit. on pp. 20, 169–172).

[119] A. L. Ott, «Experience with PJM market operation, system design, and implementation,» *IEEE Transactions on Power Systems*, vol. 18, no. 2, pp. 528–534, 2003 (cit. on p. 20).

[120] F. C. Schweppe, M. C. Caramanis, R. D. Tabors, *et al.*, *Spot pricing of electricity*. Springer Science & Business Media, 2013 (cit. on pp. 21, 89, 116, 174).

[121] S. J. Kazempour and P. Pinson, «Effects of risk aversion on market outcomes: A stochastic two-stage equilibrium model,» in *2016 PMAPS International Conference*, 2016, pp. 1–6 (cit. on pp. 21, 129, 130).

[122] E. Ela, C. Wang, S. Moorty, *et al.*, «Electricity markets and renewables: A survey of potential design changes and their consequences,» *IEEE Power and Energy Magazine*, vol. 15, no. 6, pp. 70–82, 2017 (cit. on p. 21).

[123] B. Wang and B. F. Hobbs, «Real-time markets for flexiramp: A stochastic unit commitment-based analysis,» *IEEE Transactions on Power Systems*, vol. 31, no. 2, pp. 846–860, 2015 (cit. on p. 21).

[124] S. Martin, Y. Smeers, and J. A. Aguado, «A stochastic two settlement equilibrium model for electricity markets with wind generation,» *IEEE Transactions on Power systems*, vol. 30, no. 1, pp. 233–245, 2014 (cit. on pp. 21, 23, 89, 90, 130).

[125] G. Zakeri, G. Pritchard, M. Bjorndal, *et al.*, «Pricing wind: A revenue adequate, cost recovering uniform price auction for electricity markets with intermittent generation,» *INFORMS Journal on Optimization*, vol. 1, no. 1, pp. 35–48, 2019 (cit. on pp. 21–23).

[126] G. Pritchard, G. Zakeri, and A. Philpott, «A single-settlement, energy-only electric power market for unpredictable and intermittent participants,» *Operations Research*, vol. 58, no. 4-part-2, pp. 1210–1219, 2010 (cit. on p. 22).

[127] X. Kuang, Y. Dvorkin, A. J. Lamadrid, *et al.*, «Pricing Chance Constraints in Electricity Markets,» *IEEE Transactions on Power Systems*, vol. 33, no. 4, pp. 4634–4636, 2018 (cit. on pp. 22, 23, 90, 115, 130, 132).

[128] A. Ratha, J. Kazempour, A. Virag, *et al.*, «Exploring market properties of policy-based reserve procurement for power systems,» in *58th IEEE Conference on Decision and Control*, IEEE, 2019 (cit. on p. 23).

[129] D. Ralph and Y. Smeers, «Pricing risk under risk measures: an introduction to stochastic-endogenous equilibria,» *SSRN 1903897*, 2011 (cit. on pp. 24, 129, 130).

[130] D. Ralph and Y. Smeers, «Risk trading and endogenous probabilities in investment equilibria,» *SIAM J. Optim.*, vol. 25, no. 4, pp. 2589–2611, 2015 (cit. on pp. 24, 89, 101, 130, 133).

[131] A. Philpott, M. Ferris, and R. Wets, «Equilibrium, uncertainty and risk in hydro-thermal electricity systems,» *Mathematical Programming*, vol. 157, no. 2, pp. 483–513, 2016 (cit. on pp. 24, 89, 130, 133).

[132] R. Cory-Wright and G. Zakeri, «On stochastic auctions in risk-averse electricity markets with uncertain supply,» *arXiv preprint 1804.08815*, 2018 (cit. on pp. 24, 130).

[133] R. A. Verzijlbergh, L. J. De Vries, and Z. Lukszo, «Renewable energy sources and responsive demand. Do we need congestion management?» *IEEE Transactions on Power Systems*, vol. 29, no. 5, pp. 2119–2128, 2014 (cit. on pp. 24, 89).

[134] P. M. Sotkiewicz and J. M. Vignolo, «Nodal pricing for distribution networks: efficient pricing for efficiency enhancing DG,» *IEEE Transactions on Power Systems*, vol. 21, no. 2, pp. 1013–1014, 2006 (cit. on pp. 24, 89, 90).

[135] G. Heydt, B. H. Chowdhury, M. L. Crow, *et al.*, «Pricing and control in the next power distribution system,» *IEEE Transactions on Smart Grid*, vol. 3, no. 2, pp. 907–914, 2012 (cit. on pp. 24, 89, 90).

[136] L. Bai, J. Wang, C. Wang, *et al.*, «Distribution locational marginal pricing (DLMP) for congestion management and voltage support,» *IEEE Transactions on Power Systems*, vol. 33, no. 4, pp. 4061–4073, 2018 (cit. on pp. 24, 89, 90, 94, 95).

[137] S. Huang, Q. Wu, S. S. Oren, *et al.*, «Distribution locational marginal pricing through quadratic programming for congestion management in distribution networks,» *IEEE Transactions on Power Systems*, vol. 30, no. 4, pp. 2170–2178, 2015 (cit. on pp. 24, 89, 90).

[138] J. Zhao, Y. Wang, G. Song, *et al.*, «Congestion Management Method of Low-Voltage Active Distribution Networks Based on DLMP,» *IEEE Access*, 2019 (cit. on pp. 24, 89, 90).

[139] A. Papavasiliou, «Analysis of distribution locational marginal prices,» *IEEE Transactions on Smart Grid*, vol. 9, no. 5, pp. 4872–4882, 2018 (cit. on pp. 24, 57, 60, 75, 76, 89, 90, 98, 106).

[140] Z. Yuan, M. R. Hesamzadeh, and D. R. Biggar, «Distribution locational marginal pricing by convexified ACOPF and hierarchical dispatch,» *IEEE Transactions on Smart Grid*, vol. 9, no. 4, pp. 3133–3142, 2018 (cit. on pp. 24, 89).

[141] Y. Ding, S. Pineda, P. Nyeng, *et al.*, «Real-time market concept architecture for EcoGrid EU,» *IEEE Transactions on Smart Grid*, vol. 4, no. 4, pp. 2006–2016, 2013 (cit. on pp. 24, 89).

[142] D. Bienstock and A. Shukla, «Variance-aware optimal power flow: Addressing the tradeoff between cost, security, and variability,» *IEEE Transactions on Control of Network Systems*, vol. 6, no. 3, pp. 1185–1196, 2019 (cit. on pp. 26, 116, 122, 124).

[143] M. Lubin, Y. Dvorkin, and S. Backhaus, «A robust approach to chance constrained optimal power flow with renewable generation,» *IEEE Transactions on Power Systems*, vol. 31, no. 5, pp. 3840–3849, 2016 (cit. on pp. 32, 91, 115).

[144] W. Xie and S. Ahmed, «Distributionally robust chance constrained optimal power flow with renewables: A conic reformulation,» *IEEE Transactions on Power Systems*, vol. 33, no. 2, pp. 1860–1867, 2018 (cit. on p. 32).

[145] Y. Dvorkin, M. Lubin, S. Backhaus, *et al.*, «Uncertainty sets for wind power generation,» *IEEE Transactions on Power Systems*, vol. 31, no. 4, pp. 3326–3327, 2015 (cit. on pp. 32, 52, 57, 91).

[146] T. Nesti, J. Nair, and B. Zwart, «Temperature overloads in power grids under uncertainty: A large deviations approach,» *IEEE Transactions on Control of Network Systems*, vol. 6, no. 3, pp. 1161–1173, 2019 (cit. on p. 34).

[147] R. Kannan, J. R. Luedtke, and L. A. Roald, «Stochastic DC optimal power flow with reserve saturation,» *Electric Power Systems Research*, vol. 189, p. 106 566, 2020 (cit. on pp. 34, 148).

[148] D. Bienstock, G. Muñoz, S. Yang, *et al.*, «Robust linear control of storage in transmission systems, and extensions to robust network control problems,» in *2017 IEEE 56th Annual Conference on Decision and Control (CDC)*, IEEE, 2017, pp. 799–806 (cit. on pp. 35, 148).

[149] M. Lubin, D. Bienstock, and J. P. Vielma, «Two-sided linear chance constraints and extensions,» *arXiv preprint arXiv:1507.01995*, 2015 (cit. on pp. 43, 44).

[150] S. Wang, S. Chen, L. Ge, *et al.*, «Distributed generation hosting capacity evaluation for distribution systems considering the robust optimal operation of OLTC and SVC,» *IEEE Transactions on Sustainable Energy*, vol. 7, no. 3, pp. 1111–1123, 2016 (cit. on p. 49).

[151] A. Hassan, Y. Dvorkin, D. Deka, *et al.*, «Chance-constrained ADMM approach for decentralized control of distributed energy resources,» in *2018 Power Systems Computation Conference (PSCC)*, IEEE, 2018, pp. 1–7 (cit. on p. 52).

[152] P. M. Esfahani and D. Kuhn, «Data-driven distributionally robust optimization using the Wasserstein metric: Performance guarantees and tractable reformulations,» *Mathematical Programming*, vol. 171, no. 1-2, pp. 115–166, 2018 (cit. on p. 52).

[153] J. Blanchet, Y. Kang, and K. Murthy, «Robust Wasserstein profile inference and applications to machine learning,» *Journal of Applied Probability*, vol. 56, no. 3, pp. 830–857, 2019 (cit. on p. 52).

[154] E. Delage and Y. Ye, «Distributionally robust optimization under moment uncertainty with application to data-driven problems,» *Operations research*, vol. 58, no. 3, pp. 595–612, 2010 (cit. on pp. 52, 133).

[155] Y. Guo, K. Baker, E. Dall'Anese, *et al.*, «Data-based distributionally robust stochastic optimal power flow—Part I: Methodologies,» *IEEE Transactions on Power Systems*, vol. 34, no. 2, pp. 1483–1492, 2018 (cit. on p. 52).

[156] J. D. Taft, P. De Martini, and L. Kristov, «A reference model for distribution grid control in the 21st century,» Pacific Northwest National Laboratory (PNNL), Richland, WA (United States), Tech. Rep., 2015 (cit. on p. 52).

[157] W. R. Pestman, *Mathematical statistics: an introduction*. Walter de Gruyter, 1998, vol. 1 (cit. on p. 54).

[158] A. Ben-Tal, L. El Ghaoui, and A. Nemirovski, *Robust optimization*. Princeton University Press, 2009, vol. 28 (cit. on p. 56).

[159] I. Dunning, J. Huchette, and M. Lubin, «JuMP: A Modeling Language for Mathematical Optimization,» *SIAM Review*, vol. 59, no. 2, pp. 295–320, 2017. DOI: 10.1137/15M1020575 (cit. on pp. 57, 77).

[160] R. Mieth and Y. Dvorkin. (2018). «Code Supplement - DR-AC-CCOPF,» [Online]. Available: github.com/korpuskel91/distribution_grid_analysis (cit. on p. 57).

[161] K. P. Schneider, B. Mather, B. C. Pal, *et al.*, «Analytic Considerations and Design Basis for the IEEE Distribution Test Feeders,» *IEEE Transactions on Power Systems*, 2017 (cit. on p. 60).

[162] R. Deng, Z. Yang, M.-Y. Chow, *et al.*, «A survey on demand response in smart grids: Mathematical models and approaches,» *IEEE Transactions on Industrial Informatics*, vol. 11, no. 3, pp. 570–582, 2015 (cit. on pp. 62, 64).

[163] M. R. Sarker, M. A. Ortega-Vazquez, and D. S. Kirschen, «Optimal coordination and scheduling of demand response via monetary incentives,» *IEEE Transactions on Smart Grid*, vol. 6, no. 3, pp. 1341–1352, 2015 (cit. on p. 62).

[164] A. J. Conejo, J. M. Morales, and L. Baringo, «Real-time demand response model,» *IEEE Transactions on Smart Grid*, vol. 1, no. 3, pp. 236–242, 2010 (cit. on p. 62).

[165] V. Gø'mez, M. Chertkov, S. Backhaus, *et al.*, «Learning price-elasticity of smart consumers in power distribution systems,» in *2012 IEEE SmartGridComm Conference*, 2012, pp. 647–652 (cit. on pp. 62, 63).

[166] L. Jia, Q. Zhao, and L. Tong, «Retail pricing for stochastic demand with unknown parameters: An online learning approach,» in *51st IEEE Conference on Comm., Cntr., and Comp.*, 2013, pp. 1353–1358 (cit. on pp. 62, 63).

[167] S. H. Low, «Convex relaxation of optimal power flow—Part I: Formulations and equivalence,» *IEEE Transactions on Control of Network Systems*, vol. 1, no. 1, pp. 15–27, 2014 (cit. on pp. 62, 164, 168).

[168] C. Coffrin and P. Van Hentenryck, «A linear-programming approximation of AC power flows,» *INFORMS Journal on Computing*, vol. 26, no. 4, pp. 718–734, 2014 (cit. on p. 62).

[169] A. V. den Boer and B. Zwart, «Simultaneously learning and optimizing using controlled variance pricing,» *Management science*, vol. 60, no. 3, pp. 770–783, 2014 (cit. on pp. 63, 74, 82).

[170] N. B. Keskin and A. Zeevi, «Dynamic pricing with an unknown demand model: Asymptotically optimal semi-myopic policies,» *Operations Research*, vol. 62, no. 5, pp. 1142–1167, 2014 (cit. on pp. 63, 74, 75).

[171] O. Besbes and A. Zeevi, «On the (surprising) sufficiency of linear models for dynamic pricing with demand learning,» *Management Science*, vol. 61, no. 4, pp. 723–739, 2015 (cit. on p. 65).

[172] S. Huang, J. Lian, H. Hao, *et al.*, «Transactive Control Design for Commercial Buildings to Provide Demand Response,» *IFAC-PapersOnLine*, vol. 51, no. 34, pp. 151–156, 2019 (cit. on p. 65).

[173] K. Bruninx, Y. Dvorkin, E. Delarue, *et al.*, «Valuing demand response controllability via chance constrained programming,» *IEEE Transactions on Sustainable Energy*, vol. 9, no. 1, pp. 178–187, 2017 (cit. on pp. 65, 90).

[174] A. V. Oppenheim and G. C. Verghese, *Signals, systems and inference*. Pearson, 2015 (cit. on p. 66).

[175] S. Chatterjee and J. S. Simonoff, *Handbook of regression analysis*. Wiley Online Library, 2013, vol. 5 (cit. on p. 68).

[176] S. Zymler, D. Kuhn, and B. Rustem, «Distributionally robust joint chance constraints with second-order moment information,» *Mathematical Programming*, vol. 137, no. 1-2, pp. 167–198, 2013 (cit. on p. 71).

[177] *The MOSEK Modeling Cookbook*, 2018. [Online]. Available: docs.mosek.com/modeling-cookbook/index.html (cit. on pp. 72, 118, 153, 157).

[178] R. Mieth and Y. Dvorkin. (). «Code Supplement - DR Online Learning,» [Online]. Available: github.com/korpuskel91/DROnlineLearning_CodeSupplement (cit. on pp. 77, 107).

[179] H. Khodr, F. Olsina, P. De Oliveira-De Jesus, *et al.*, «Maximum savings approach for location and sizing of capacitors in distribution systems,» *El. Pwr. Syst. Res.*, vol. 78, no. 7, pp. 1192–1203, 2008 (cit. on p. 83).

[180] H. Ye, Y. Ge, M. Shahidehpour, *et al.*, «Uncertainty marginal price, transmission reserve, and day-ahead market clearing with robust unit commitment,» *IEEE Transactions on Power Systems*, vol. 32, no. 3, pp. 1782–1795, 2017 (cit. on p. 90).

[181] K. Baker and A. Bernstein, «Joint Chance Constraints in AC Optimal Power Flow: Improving Bounds through Learning,» *IEEE Transactions on Smart Grid*, 2019 (cit. on p. 90).

[182] H. Wu, M. Shahidehpour, Z. Li, *et al.*, «Chance-constrained day-ahead scheduling in stochastic power system operation,» *IEEE Transactions on Power Systems*, vol. 29, no. 4, pp. 1583–1591, 2014 (cit. on p. 91).

[183] Next Kraftwerke. (2019). «Balancing Markets,» [Online]. Available: www.next-kraftwerke.be/en/knowledge-hub/balancing-markets/ (cit. on p. 92).

[184] H. Yuan, F. Li, Y. Wei, *et al.*, «Novel linearized power flow and linearized OPF models for active distribution networks with application in distribution LMP,» *IEEE Transactions on Smart Grid*, vol. 9, no. 1, pp. 438–448, 2018 (cit. on p. 94).

[185] M. Farivar and S. H. Low, «Branch flow model: Relaxations and convexification—Part I,» *IEEE Transactions on Power Systems*, vol. 28, no. 3, pp. 2554–2564, 2013 (cit. on pp. 95, 159).

[186] L. Wood, R. Hemphill, J. Howat, *et al.*, «Recovery of utility fixed costs: Utility, consumer, environmental and economist perspectives,» Lawrence Berkeley National Lab.(LBNL), Berkeley, CA (United States), Tech. Rep., 2016 (cit. on p. 100).

[187] M. E. Initative, *Utility of the Future*, 2016. [Online]. Available: `energy.mit.edu/research/utility-future-study/` (cit. on p. 100).

[188] M. Farsi, M. Filippini, *et al.*, «A Benchmarking analysis of electricity distribution utilities in Switzerland,» *Centre for Energy Policy and Economics Working Paper*, no. 43, 2005 (cit. on p. 100).

[189] Z. Wang, D. S. Kirschen, and B. Zhang, «Accurate semidefinite programming models for optimal power flow in distribution systems,» *arXiv preprint arXiv:1711.07853*, 2017 (cit. on p. 112).

[190] L. Roald, F. Oldewurtel, T. Krause, *et al.*, «Analytical reformulation of security constrained optimal power flow with probabilistic constraints,» in *2013 IEEE Grenoble Conference*, IEEE, 2013, pp. 1–6 (cit. on pp. 115, 117).

[191] W. Xie and S. Ahmed, «Distributionally robust chance constrained optimal power flow with renewables: A conic reformulation,» *IEEE Transactions on Power Systems*, vol. 33, no. 2, pp. 1860–1867, 2017 (cit. on p. 115).

[192] R. P. O'Neill, E. B. Fisher, B. F. Hobbs, *et al.*, «Towards a complete real-time electricity market design,» *J. of Regulatory Econ.*, vol. 34, no. 3, pp. 220–250, 2008 (cit. on pp. 116, 135).

[193] P. Lipka, S. S. Oren, R. P. O'Neill, *et al.*, «Running a more complete market with the SLP-IV-ACOPF,» *IEEE Transactions on Power Systems*, vol. 32, no. 2, pp. 1139–1148, 2016 (cit. on pp. 116, 121, 174).

[194] A. Ben-Tal and A. Nemirovski, *Lectures on modern convex optimization: analysis, algorithms, and engineering applications*. SIAM, 2001 (cit. on p. 118).

[195] S. S. Baghsorkhi and I. A. Hiskens, «Impact of wind power variability on sub-transmission networks,» in *2012 IEEE Power and Energy Society General Meeting*, IEEE, 2012, pp. 1–7 (cit. on p. 122).

[196] C. A. Hans, P. Sopasakis, J. Raisch, *et al.*, «Risk-averse model predictive operation control of islanded microgrids,» *IEEE Transactions on Control Systems Technology*, 2019 (cit. on pp. 129, 130).

[197] H. Gérard, V. Leclère, and A. Philpott, «On risk averse competitive equilibrium,» *Oper. Res. Lett.*, vol. 46, no. 1, pp. 19–26, 2018 (cit. on pp. 130, 133).

[198] S. Boyd and L. Vandenberghe, *Convex optimization*. Cambridge univ. press, 2004 (cit. on pp. 134, 153–157).

[199] K. J. Arrow, «The role of securities in the optimal allocation of risk-bearing,» in *Readings in Welfare Econ.* Springer, 1973, pp. 258–263 (cit. on p. 135).

[200] (2020). «Code Supplement - Risk Trading in CC-EM,» [Online]. Available: github.com/korpuskel91/risk_trading_CCMarket (cit. on p. 141).

[201] J. Wang, P. Liu, J. Hicks-Garner, *et al.*, «Cycle-life model for graphite-LiFePO4 cells,» *Journal of power sources*, vol. 196, no. 8, pp. 3942–3948, 2011 (cit. on p. 148).

[202] A. V. Swishchuk, «Variance and volatility swaps in energy markets,» *Available at SSRN 1628178*, 2010 (cit. on p. 149).

[203] L. Dierks and S. Seuken, «The Competitive Effects of Variance-based Pricing,» *arXiv preprint arXiv:2001.11769*, 2020 (cit. on p. 149).

[204] PJM, *Manual 12: Balancing Operations*, 2012 (cit. on p. 149).

[205] V. Dvorkin, J. Kazempour, and P. Pinson, «Chance-Constrained Equilibrium in Electricity Markets With Asymmetric Forecasts,» *arXiv preprint arXiv:2005.11749*, 2020 (cit. on p. 149).

[206] T. J. Overbye, «Computation of a practical method to restore power flow solvability,» *IEEE Transactions on Power Systems*, vol. 10, no. 1, pp. 280–287, 1995 (cit. on p. 164).

[207] M. B. Cain, R. P. O'neill, A. Castillo, *et al.*, «History of optimal power flow and formulations,» *Federal Energy Regulatory Commission*, vol. 1, pp. 1–36, 2012 (cit. on p. 164).

[208] D. K. Molzahn and I. A. Hiskens, «A Survey of Relaxations and Approximations of the Power Flow Equations,» 2019 (cit. on p. 164).

[209] M. Baran and F. F. Wu, «Optimal sizing of capacitors placed on a radial distribution system,» *IEEE Transactions on power Delivery*, vol. 4, no. 1, pp. 735–743, 1989 (cit. on p. 166).

[210] T. Piketty, «About capital in the twenty-first century,» *American Economic Review*, vol. 105, no. 5, pp. 48–53, 2015 (cit. on p. 169).

[211] C. Ruiz, A. J. Conejo, and S. A. Gabriel, «Pricing non-convexities in an electricity pool,» *IEEE Transactions on Power Systems*, vol. 27, no. 3, pp. 1334–1342, 2012 (cit. on p. 174).

[212] R. Weinhold and S. A. Gabriel, «Discretely constrained mixed complementary problems: Application and analysis of a stylised electricity market,» *Journal of the Operational Research Society*, vol. 71, no. 2, pp. 237–249, 2020 (cit. on p. 174).

COLOPHON

Written between August and December 2020 in New York City during the Coronavirus Pandemic.

This document was typeset using the typographical look-and-feel `classicthesis` developed by André Miede. `classicthesis` is available for both LaTeX and LyX: https://bitbucket.org/amiede/classicthesis/.

Final Version as of May 22, 2021 (`classicthesis` version 4.2).